TESIS DE LA UNIVERSIDAD
DE ZARAGOZA

2014

44

Ana Pérez Sanz

# Holoceno climate, vegetation and human aimpact in the Western Mediterranean inferred from Pyrenean lake records and climate models

Departamento
Ciencias de la Tierra

Director/es
González Sampériz, Penélope
Valero Garcés, Blas



ISSN 2254-7606

Prensas de la Universidad
Universidad Zaragoza

Universidad Zaragoza
1542

Tesis Doctoral

# HOLOCENO CLIMATE, VEGETATION AND HUMAN AIMPACT IN THE WESTERN MEDITERRANEAN INFERRED FROM PYRENEAN LAKE RECORDS AND CLIMATE MODELS


Autor

Ana Pérez Sanz

Director/es

González Sampériz, Penélope
Valero Garcés, Blas

**UNIVERSIDAD DE ZARAGOZA**
Ciencias de la Tierra


2014

# Holocene
# climate, vegetation and human impact
# in the Western Mediterranean
# inferred from
# Pyrenean lake records and
# climate models

**Ana Pérez Sanz**

PhD Thesis

Instituto Pirenaico de Ecología. Consejo Superior de Investigaciones Científicas

Departamento de Ciencias de la Tierra. Facultad de Ciencias. Universidad de Zaragoza

2014

This dissertation is submitted to the Faculty of Science of the University of Zaragoza for the degree of Doctor of Philosophy.

Memoria presentada para optar al grado de Doctor en Geología por la Universidad de Zaragoza.

**Title**

Holocene climate, vegetation and human impact in the Western Mediterranean inferred from Pyrenean lake records and climate models.

Reconstrucción holocena de la dinámica del clima, vegetación y acción humana en el Mediterráneo Occidental a partir de registros lacustres pirenaicos y modelos climáticos.

**PhD Student**

Ana Pérez Sanz

**Supervisors**

Penélope González Sampériz
Blas Lorenzo Valero Garcés

**Institutions**

Instituto Pirenaico de Ecología, IPE-CSIC
Pyrenean Institute of Ecology, IPE-CSIC

Departamento de Ciencias de la Tierra. Facultad de Ciencias. Universidad de Zaragoza

Department of Earth Sciences. Faculty of Sciences. University of Zaragoza

*A mis padres*

*Moví los hilos de mi destino,*

*fui el dueño de mi libertad.*

Evaristo

IPE
INSTITUTO PIRENAICO DE ECOLOGÍA
CSIC

Comisión de Doctorado

Departamento de Ciencias de la Tierra

Universidad de Zaragoza

Los doctores Penélope González Sampériz y Blas Lorenzo Valero Garcés, investigadores del Instituto Pirenaico de Ecología (IPE-CSIC), en calidad de co-directores de tesis de doctorado de Ana Pérez Sanz

Certifican:

Que Ana Pérez Sanz ha realizado bajo nuestra dirección el trabajo que, para optar al grado de Doctor en Geología, presenta con el título: "*Holocene climate, vegetation and human impact in the Western Mediterranean inferred from Pyrenean lake records and climate models*" (Reconstrucción holocena de la dinámica del clima, vegetación y acción humana en el Mediterráneo Occidental a partir de registros lacustres pirenaicos y modelos climáticos)

Que el trabajo se adapta a los objetivos establecidos en el Proyecto de Tesis Doctoral, aprobado el 9 de septiembre del 2013 por el Departamento de Ciencias de la Tierra y ratificado por la Comisión de Doctorado el 16 de septiembre del 2013

Y para que así conste, firmamos la presente Certificación en Zaragoza el 17 de febrero de 2014 para los efectos que sean oportunos.

Fdo. Penélope González-Sampériz

Fdo. Blas Lorenzo Valero-Garcés

# CONTENTS

## AGRADECIMIENTOS / ACKNOLEDGEMENTS

Me siento especialmente afortunada por la etapa doctoral que me ha tocado vivir. Han sido pocas las dificultades y muchas las alegrías que he pasado durante estos años. Esto es, sin duda, debido al increíble grupo de personas que me rodean y me han rodeado a lo largo de este periodo. Con estas líneas me gustaría recordar y agradecer a todas esas personas que durante estos años han contribuido de manera profesional y personal a la elaboración de este proyecto tan importante.

La presente tesis doctoral no hubiera sido posible, ni siquiera imaginable, sin la guía, el trabajo, los consejos y el apoyo de mis directores Penélope González Sampériz y Blas Valero Garcés. Lo que he aprendido a su lado está más allá de lo que podría haber imaginado. Esto es aplicable no sólo al plano científico, sino también humano. A su lado he madurado científica y personalmente.

Los agradecimientos son extensibles a mis compañeros de grupo de investigación cuya calidad humana ha hecho que las pequeñas dificultades científicas que han podido aparecer a lo largo de esta tesis se diluyan y pierdan en la memoria de estos cinco años de trabajo. Me gustaría agradecer en particular a Ana Moreno y Graciela Gil que han contribuido de manera determinante al contenido científico de esta tesis, así como al resto del equipo que han participado física o moralmente a la consecución de este trabajo: Josu, Edu, Fernando, Matias, Miguel Sevilla, Miguel Bartolomé, María y Carlos. Y a otros que ya no forman parte del equipo oficial pero que han sido parte imprescindible en este proyecto: Mario, Pablo, Mayte, Carlos Sancho, Ánchel, Belén, Bea, Aida, Raquel, Pol y Laura Lasheras.

Durante mi etapa investigadora en el Instituto Pirenaico de Ecología he tenido la fortuna de haber podido compartir impresiones con investigadores de otros grupos de investigación. Estoy especialmente orgullosa de haber podido ampliar mis horizontes científicos de la mano de los doctores José María García, Teodoro Lasanta, Chechu Camarero, Gabriel Montserrat y en especial Nacho López que se involucró y me ayudó en lo personal.

I would like to give special thanks to Prof. Sandy Harrison for hosting me and supervising me at the Macquarie University in Sydney and introducing me in the model world. I am very grateful for the opportunity to have met her and to have worked closely with her. I will never forget the invitation to the Sydney Opera House!

Si algo voy a echar de menos de mi etapa en el IPE son las conversaciones sobre lo humano y lo divino de los almuerzos junto con Pili, Hugo, María, Javi, Jesús, Nacho y Fergus como núcleo duro. No ha habido tema que se haya escapado de las garras críticas de este grupo de jóvenes investigadores: ciencia, política, religión, economía, recortes, austeridad,

educación… ¡además de haber solucionado la crisis un millón de veces! Conversaciones que garantizaron una dosis bien alta de risa diaria.

Por supuesto, me gustaría agradecer también al resto de compañeros del IPE con los que he compartido momentos especiales: Edu, Josu, Fabi, Enrique, Jorge, Cecilia, Paloma, Iker, Sam y Jesus V.

Además, me llevo a una amiga para toda la vida: Pili. Tenerla como compañera de despacho ha sido lo mejor que me podría haber pasado. Gracias por todas las confidencias, tu buen humor y la complicidad. Y por haber hecho de esta etapa una experiencia inolvidable.

Mi familia es parte fundamental de lo que soy como persona. Tengo la suerte de contar con una familia que da valor al significado de la palabra familia. Si a alguien admiro en esta vida, esos son mi madre, mi padre y mi hermano. Y sobre todo a mi yaya, Pilar Franco, que me ha enseñado que no hay nada imposible si uno se lo propone y que es el ejemplo de cómo hay que ser en la vida. A mis tíos Pili, Ibán y Susana y a mis primos Adrián y Paula, que me hacen reír tanto y siempre tienen palabras de apoyo; y a mis primitos Bruno y Claudia que alegran a cualquiera con su presencia. Me siento inmensamente orgullosa y feliz de formar parte de una familia así.

Además tengo una familia no consanguínea que también es parte fundamental de lo que soy. Mis amigas de Logroño me han acompañado en todos los momentos importantes de mi vida. Es más, hacen importante cualquier momento. Miro hacia atrás y no hay ni un solo instante en el que no hayan estado presentes. No necesariamente físicamente, a veces hemos puesto distancias geográficas muy grandes de por medio, pero siempre moral y anímicamente. Siempre arrancando una sonrisa. Más bien una carcajada. Muchas gracias por todo Yvonne, Sandra, Marta, Marina, Laura V, Laura U, Bea y Ana. Me alegro muchísimo de que forméis parte de mi vida.

Hace ya muchos años que salí de mi casa para llegar a la ciudad del cierzo. Aquí he encontrado otra gran familia con la que he compartido grandes experiencias. Alberto, Anika, Edu, Isabel, Juli, Marcos, Navarro, Raúl y Rubén. Por supuesto también quiero dedicar un agradecimiento especial a Moreno, Sebas, José Manuel, Hernando y demás integrantes de un grupo de cuyo nombre no quiero acordarme, que me hacen partirme de risa con sus comentarios afilados, desternillantes y mordaces. Sois la razón por la que me considero totalmente zaragozana y por la que he echado raíces aquí.

Quiero agradecer a Raúl todos los buenos momentos de los últimos meses. Es increíble lo que me puedo llegar a reír a su lado. Gracias por darme unos martes de lujo.

No puedo olvidarme de Alberto que ha hecho que mi vuelta a tierras mañas haya sido la mejor de las posibles y que junto con David han sido los mejores compañeros de piso del mundo haciéndome sentir como en mi propia casa.

Durante seis meses he vivido en la ciudad más excitante del mundo, pero también la más lejana: Sidney. Me gustaría dedicar un agradecimiento muy especial a Álvaro y Catherine que me recibieron con las puertas de su casa abiertas y me hicieron olvidar la distancia que me separaba de mi mundo. Nunca podré olvidar lo que habéis hecho por mí. Vuestra ayuda y apoyo lo han significado todo. Muchísimas gracias por todo. It has been the most life-changing experience.

I would also like to give special thanks to Li. I am very honored that I got to meet him. I cannot forget your help and support.

Quiero agradecer a Saúl todo su apoyo y ánimo constante durante gran parte de este largo camino.

¡Gracias a todos!

## RESUMEN

La presente Tesis Doctoral aborda una detallada reconstrucción paleoclimática en el Pirineo Central durante el Holoceno a partir del estudio palinológico de dos secuencias lacustres localizadas a diferentes altitudes y que representan dos pisos de vegetación muy bien diferenciados: en primer lugar, la Basa de la Mora, localizado en el piso subalpino y, en segundo lugar, en el lago de Estaña, en piso basal del Pre-Pirineo. Además, se ha seleccionado el Holoceno Medio para estudiar la fiabilidad de los modelos climáticos a la hora de reconstruir los climas del pasado en el Mediterráneo, a partir del análisis de la expresión estacional de los climas en las simulaciones del Coupled Model Intercomparison Project (CMIP5).

El estudio multiproxy (polen, sedimentología, geoquímica, quironómidos y microcarbón) de alta resolución de la secuencia de la Basa de la Mora (BSM) (42º32' N, 0º19' E, 1914 m s.n.m) muestra una marcada variabilidad ambiental en el Pirineo Central durante el Holoceno. El robusto modelo de edad, basado en 15 dataciones radiocarbónicas, respalda la primera reconstrucción precisa de cambios climáticos rápidos durante el Holoceno en esta área. En el Holoceno temprano se registra una cuenca altamente arbolada, con unos niveles lacustres altos y procesos intensos de run-off en la cuenca favoreció la existencia de comunidad de quironómidos dominados por taxones no lacustres (Orthocladiinae) relacionados con la entrada de arroyos fluviales. Este escenario es coherente con la alta estacionalidad en latitudes medias en el Hemisferio Norte causada por la configuración de los parámetros orbitales durante el Holoceno Temprano, que provocaría un aumento en la acumulación de nieve en las cumbres pirenaicas durante el invierno así como unas altas tasas de fusión de la nieve durante el verano. Entre 9.8 y 8.1 cal yr BP, se reconoce una gran inestabilidad climática debido al registro de profundos cambios en la cubierta vegetal y de una alta fluctuación en los procesos de erosión en la cuenca. Las variaciones entre coníferas y mesofitos has revelado la ocurrencia de al menos cuatro eventos rápidos y de corta duración registrados aproximadamente a 9.7, 9.3, 8.8 y 8.3 cal Ka BP. Entre 8.1 y 5.7, durante el Holoceno Medio, un clima más estable con abundante precipitación dio lugar a los máximos niveles lacustres, la expansión del bosque de caducifolios, la retirada de las coníferas y la intensificación de los fuegos. Hacia el 5.7 cal Ka BP un cambio climático hacia condiciones más secas contribuyó al declive regional de los arboles caducifolios, la expansión de los pinos y *Juniperus* y un descenso notable de los niveles del lago. A pesar de las condiciones más secas, la actividad del fuego se redujo debido a una disminución de la biomasa disponible. Dos intervalos especialmente áridos tuvieron lugar entre 2.9 y 2.4 cal Ka BP y entre 1.2 y 0.7 cal Ka BP (800-1300 AD). El segundo coincide con la Anomalía Climática Medieval y en la secuencia BSM se registra como unos de los periodos más áridos del Holoceno. La actividad antrópica es escasa e incluso nula durante la mayor parte del Holoceno, hasta al menos los últimos 700 años, cuando se reconocen los primeros signos de deforestación. La Pequeña Edad de Hielo se registra por un aumento de los niveles lacustres

y por lun abandono de las actividades humanas debido a las condiciones frías en las cumbres pirenaicas.

El registro palinológico del lago de Estaña (EST) (670 m s.n.m., 42°02’N, 0°32’E) proporciona la primera reconstrucción Holocena de la vegetación en piso basal de los Pirineos. La presente Tesis Doctoral presenta una comparación de la secuencia de Estaña con otras secuencias polínicas pirenaicas localizadas en pisos de vegetación más altos, permitiendo ilustrar el papel de los cambios en temperatura y precipitación que dieron lugar a un ajuste vertical de los pisos de vegetación en los Pirineos durante el Holoceno. Durante el comienzo del Holoceno, una estacionalidad alta y unas condiciones extremadme áridas dieron lugar a un paisaje estépico en Estaña, impidiendo las expansión del bosque en altitud. Entre 9.2 y 8.2 cal Ka BP, un aumento de las temperaturas de invierno junto a una mayor disponibilidad hídrica permitieron la expansión de los taxones arbóreos, principalmente *Corylus*, en Estaña. Este paisaje dominado por taxones mesófilos sugiere una distribución uniforme de la precipitación a lo largo del año en el piso basal de los Pirineos. Sin embargo, contrasta con un patrón de precipitación con una estación seca establecido en cotas más altas del Pirineo, indicando la existencia de un patrón hidrológico muy complejo en la región durante este periodo. Entre 8.2 y 6 cal Ka BP, la ocurrencia de inviernos cálidos y condiciones muy húmedas con una distribución de la precipitación uniforme, dio lugar al desarrollo de un bosque de tipo Mediterráneo, formado por *Quercus* semi-caducifolios, en Estanya y favoreció la expansión en altitud del bosque de caducifolios, el cual pudo establecerse en el piso subalpino. El periodo entre 6 y 4.8 cal Ka BP fue una fase de transición a nivel regional en el que se empezó a establecer una estacionalidad en la precipitación caracterizada por la existencia de una estación árida. Dado el carácter mediterráneo de la vegetación en Estaña, este cambio en el patrón de la vegetación sólo afecto a la vegetación mesófila del piso subalpino. El establecimiento final de unas condiciones áridas en torno al 4.8 cal Ka BP, causó la desaparición de importantes masas de árboles caducifolios en el área y favoreció la expansión de *Quercus* semi-caucifolio y perennifolio en Estaña y la expansión de *Pinus* a mayores altitudes. Los primeros signos de actividad antrópico en Estaña se registran hacia el años 3.1 cal Ka BP con la ocurrencia de la primera fase de deforestación y la aparición de polen de tipo *Cerealia*. El aumento del manejo del paisaje se produjo en torno al 0.8 cal ka BP debido a la expansión de las actividades agrícolas y ganaderas.

Además, en la presente Tesis Doctoral también se ha analizado la expresión estacional de los climas del Mediterráneo y norte de África en las simulaciones del Coupled Model Intercomparison Project (CMIP5) para el Holoceno-Medio y el periodo Pre-Industrial. Las observaciones climáticas actuales muestran cuatro tipos distintos de regímenes de precipitación caracterizados por una distribución estacional y una cantidad total de precipitación diferente: una banda ecuatorial, caracterizada por un pico doble en la precipitación; la zona del Monzón, caracterizada por la concentración de la lluvia en verano; el desierto, caracterizado por una baja estacionalidad y cantidad total de lluvia; y la zona del

Mediterráneo, caracterizado por sequía estival. En las simulaciones para el periodo Pre-Industrial, la mayoría de los modelos simulan adecuadamente la posición de los climas del Mediterráneo y del ecuador pero sobrestiman la extensión de la influencia del monzón y subestiman la expansión del desierto. Sin embargo, la mayoría de los modelos fallan a la hora de reproducir la cantidad total de precipitación en cada zona. En las simulaciones para el Holoceno-Medio, los modelos simulan una reducción de la precipitación de invierno en la zona ecuatorial, y una expansión hacia el norte del monzón con un aumento significativo de la precipitación de verano y otoño. La precipitación aumenta ligeramente en el desierto, principalmente en verano y otoño, debido a una expansión hacia el norte del monzón. Por su parte los cambios en el Mediterráneo son muy pequeños, aunque hay un ligero aumento de la precipitación en primavera consistente con los datos paleoclimáticos que muestran una expansión de los arboles caducifolios y por tanto un aumento de la precipitación en la estación de crecimiento durante el Holoceno Medio. La comparación con las reconstrucciones también sugieren que la mayoría de los modelos subestiman los cambios anuales en precipitación durante el Holoceno Medio en todas las zonas salvo en la banda ecuatorial.

## SUMMARY

The present PhD Thesis addresses a detailed paleo-climate reconstruction for the Central Pyrenees during the Holocene through the study of two lacustrine sequences placed at different altitudes, representing two marked different vegetation belts:Lake Basa de la Mora located in the subalpine belt and Lake Estaña placed in the basal belt of the Pre-Pyrenean Ranges. Additionally, this Thesis has also analyzed the simulations from the fifth phase of the Coupled Model Intercomparison Project (CMIP5) of Mediterranean climates for the mid-Holocene (*midHolocene*, 6 ka) and compare with available pollen-based climate reconstructions.

High resolution multiproxy data (pollen, sedimentology, geochemistry, chironomids and charcoal) from the Basa de la Mora (BSM) lake sequence (42º32′ N, 0º19′ E, 1914 m a.s.l.) show marked climate variability in the central southern Pyrenees throughout the Holocene. A robust age model based on 15 AMS radiocarbon dates underpins the first precise reconstruction of rapid climate changes during the Holocene from this area. During the Early Holocene, increased winter snowpack and high snowmelt during summer, as a consequence of high seasonality, led to higher lake levels, a chironomid community dominated by non-lacustrine taxa (Orthocladiinae) related to higher inlet streams, and a forested landscape with intense run-off processes in the watershed. From 9.8 to 8.1 cal ka BP, climate instability is inferred from rapid and intense forest shifts and high fluctuation in surface run-off. Shifts among conifers and mesophytes reveal at least four short-lived dry events at 9.7, 9.3, 8.8 and 8.3 cal ka BP. Between 8.1 and 5.7 cal ka BP a stable climate with higher precipitation favoured the highest lake levels and a forest expansion, with spread of mesophytes, withdrawal of conifers and intensification of fires, coinciding with the Holocene Climate Optimum. At 5.7 cal ka BP a major change leading to drier conditions contributed to a regional decline in mesophytes, expansion of pines and junipers, and a significant lake level drop. Despite drier conditions, fire activity decreased as a consequence of biomass reduction. Two arid intervals occurred between 2.9 and 2.4 cal ka BP and at 1.2-0.7 cal ka BP (800-1300 AD). The latter coincides with the Medieval Climate Anomaly and is one of the most arid phases of the Holocene in BSM sequence.

The Holocene palynological record from Lake Estanya (EST) (670 m a.s.l., 42°02′N, 0°32′E) provides the first Holocene vegetation reconstruction from the basal belt of the southern Pyrenees. The present Thesis presents a comparison of the Estanya sequence with other Pyrenean pollen sequences placed at higher altitudes that illustrates the role of temperature and precipitation changes as main drivers of the altitudinal vegetation shifts in the southern Pyrenees during the Holocene. High continentality and dry conditions during the onset of the Holocene (11.4 and 9.8 cal ka BP) resulted in a landscape dominated by steppe vegetation in Estanya and a limited forest expansion in altitude. Between 9.2 and 8.2 cal ka BP, increase in winter temperature and in moisture conditions allowed the expansion of the arboreal taxa,

mainly *Corylus*, in Estanya. This deciduous-dominated landscape suggests an evenly-distributed precipitation pattern in the basal level of the Pyrenees. However, it contrasts with the well-established dry season at higher altitudes and underlines a complex hydrological pattern in the region during this period. Between 8.2 and 6 cal ka BP, warm winters and more humid conditions with evenly-distributed precipitation led to the establishment of a well-developed Mediterranean forest in Estanya and favoured the upward expansion of the deciduous forest, which reached the subalpine belt. The period between 6 and 4.8 was a regional transition phase characterized by a shift in the precipitation seasonality with the establishment of a dry season. Given the Mediterranean-nature of the vegetation of Estanya, this shift affected exclusively the higher vegetation belts characterized by a larger presence of mesophytes. The final establishment of drier conditions at 4.8 cal ka BP caused the disappearance of important deciduous masses in the area and favoured the spread of semi-deciduous and evergreen *Quercus* in Estanya and *Pinus* at higher altitudes. The first signs of anthropogenic activity in Estanya are recorded at 3.1 cal ka BP with the occurrence of a deforestation phase and the appearance of *Cerealia* type. Increasing landscape management took place at 0.8 cal ka BP through the spread of grazing and farming practices.

Additionally, this Thesis has also analyzed the spatial expression of seasonal climates of the Mediterranean and northern Africa in pre-Industrial (*piControl*) and mid-Holocene (*midHolocene*, 6 ka) simulations from the fifth phase of the Coupled Model Intercomparison Project (CMIP5). Modern observations show four distinct precipitation regimes characterized by differences in the seasonal distribution and total amount of precipitation: an equatorial band characterized by a double peak in rainfall, the monsoon zone characterized by summer rainfall, the desert characterized by low seasonality and total precipitation, and the Mediterranean zone characterized by summer drought. Most models correctly simulate the position of the Mediterranean and the equatorial climates in the *piControl* simulations, but over-estimate the extent of monsoon influence and underestimate the extent of desert. However, most models fail to reproduce the amount of precipitation in each zone. Model biases in the simulated magnitude of precipitation are unrelated to whether the models reproduce the correct spatial patterns of each regime. In the *midHolocene*, the models simulate a reduction in winter rainfall in the equatorial zone, and a northward expansion of the monsoon with a significant increase in summer and autumn rainfall. Precipitation is slightly increased in the desert, mainly in summer and autumn, with northward expansion of the monsoon. Changes in the Mediterranean are small, although there is an increase in spring precipitation consistent with palaeo-observations of increased growing-season rainfall. Comparison with reconstructions shows most models under-estimate the mid-Holocene changes in annual precipitation, except in the equatorial zone. Biases in the *piControl* have only a limited influence on *midHolocene* anomalies in ocean-atmosphere models; carbon-cycle models show no relationship between *piControl* bias and *midHolocene* anomalies. Biases in the prediction of the *midHolocene* monsoon expansion are unrelated to how well the models simulate changes in Mediterranean climate.

# 1

# Introduction

## Outline

Knowledge of Earth's past climates is essential to understand modern variability and forecast future Earth's climate. The window to past climate reconstruction is paleoenvironmental and paleoclimate analyses. The Pyrenees is a unique region to study past climate environments in north-eastern Iberia and the western Mediterranean because its geographic location and detailed, high-resolution reconstructions provide a regional framework to test climate models.

## 1.1. SCIENTIFIC CONTEXT

### 1.1.1. Looking back to look forward

The current climate change as a result of the increasing atmospheric greenhouse gases and particularly $CO_2$ levels caused by anthropogenic emissions is one of the most relevant scientific issues of our times (IPCC 2001, 2007). The atmospheric $CO_2$ concentration has increased from 270 ppm (parts per million) in the Pre-Industrial Age (late 19$^{th}$ century) to 393.66 ppm in October 2013 (http://co2now.org). At geological scales, the $CO_2$ concentration reached levels similar to present about 3 Myr ago (Beerling and Royer, 2011) but since then, atmospheric $CO_2$ levels have remained lower and never had such a high increase rate as during the last centuries (Pearson and Palmer, 2000). Consequently, scientific and social concerns about the short- and long-term consequences of the current change of the atmosphere composition have grown during the last decades.

The effects of climate change are particularly worrying in the Mediterranean -southern Europe and northern Africa-, characterized by the typical Mediterranean summer drought and annual water deficit. The frequency of drought events has increased over recent times in this region (European Environmental Agency, 2012; Hoerling et al., 2012) and is expected to intensify in the near future (Meehl et al., 2007; Nikulin et al., 2011), posing a direct threat to population living in the region, which relies on water availability for all human-related activities such as agriculture, industry, tourism or urbanization. A large number of climate simulations try to assess the hydrological consequences of climate change and to design the adaptation to the likely long-term imbalance between supply and demand in the Mediterranean region (Giorgi and Lionello, 2008; Ducrocq et al., 2013).

The General Circulation Models (GCM) are the essential tool to simulate and predict the short- and long-term climate evolution resulting from the current atmosphere modification (Donner et al., 2011). Climate models are based on mathematic equations that represent the physic-chemical processes governing the coupled atmospheric-ocean circulation. They are able to simulate important aspects of the current climate at large-scales, but in general they still need improving their resolution at smaller scales where regional geographic features along with biological and chemical processes determine high spatial variability in regional and local climates (Hewitson and Crane, 1996; Gutiérrez et al., 2013). This is particularly evident in the precipitation projections for the Mediterranean region, where rainfall is linked to a number of climate component, such as the strength of the Afro-Asian monsoon system, the North Atlantic Oscillation Index (NAO), the Mediterranean Sea Surface Temperature, or the mean annual temperature -especially the summer temperature-, resulting in a high year-to-year variability hard to predict by climate models (Rodwell and Hoskins, 2001; Trigo et al., 2002; López-Moreno et al., 2011; Gaetani et al., 2011).

To assess the reliability of climate models to reproduce accurately the climate system and, subsequently, to predict the expected climate change, models are evaluated according to their ability to reproduce the distant past, when climate features were significantly different from present conditions (Braconnot et al., 2012). Thus, detailed and quantified past changes in temperature and precipitation are crucial to test climate models. The knowledge of past climates results from the study of archives of past ecosystems, which contain information about past temperatures and precipitation conditions under which they developed. In this regard, lakes provide a unique opportunity to obtain continuous records of environmental changes in terrestrial areas (Last and Smol, 2001). Lacustrine records from Mediterranean lakes play a central role to understand the nature and evolution of the Mediterranean climate with a longer perspective than that provided by the instrumental records (Moreno and Valero-Garcés, 2011; Lionello, 2012).

### 1.1.2. Paleoclimate data

#### 1.1.2.1. Holocene Pyrenean sequences as past climate windows

The study of Holocene sequences in the Pyrenees is of particular interest for paleo-climate research because of several reasons, related to the unique characteristics of the Holocene and also the geographic location of the Pyrenees.

The Holocene is a highly interesting period in Earth´s climate history because of its uniqueness:

- In the first place, it provides the temporal framework to study variations in temperature and precipitation during the most recent past when boundary conditions have not changed dramatically compared to glacial stages. Although the Holocene's climate has been traditionally believed to be fairly stable compared to the previous glacial era, marked climate shifts have occurred, some of which have been particularly fast and abrupt (Bond, 1997; Mayewski et al., 2004). At a millennial scale, the Holocene climate evolution has been greatly determined by changes in the incoming energy -solar insolation- resulting from fluctuations in the orbital parameters (Bond et al., 2001). Orbitally-derived changes in the latitudinal temperature gradient determine the ocean-atmosphere circulation, which is the main earth's climate driver (Bridgman et al., 2006). However, at centennial and decadal scales and super-imposed to the long-term climate trend, the Holocene has undergone fast and short climate shifts, sometimes as brief as decades, known as Abrupt Climate Changes (Mayewski et al., 2004; Steffense et al., 2008). Although the causes of these climate shifts have not been clearly established (National Academies Press, 2002), changes in the currents caused by internal oceanic dynamics, disruption or at least weakening of the Atlantic Meridional Overturning Circulation (AMOC), as a consequence of large inputs of freshwater into the North Atlantic from partial melting of the Ice Sheets, millennial - scale changes in insolation among other have been recognized as important triggers (Wanner et al., 2008). .

- The second reason is that the Mid-Holocene time interval from 8.2 to 6 ka represents a key period to compare paleo-climate simulations with paleo-data (Steig, 1999). At around 6 ka BP the ice-land-ocean configuration was similar to today but the climate was significant different (Braconnot et al., 2007) – e.g., more humid condition across the Mediterranean region (Prentince and Jolly., 2000) - suggesting that the atmosphere-ocean circulation patterns were different (Shin et al., 2006) Therefore, Mid-Holocene palaeo-data provide an opportunity to check the ability of models to simulate past precipitation scenarios resulting from different configuration in the atmospheric-ocean coupling (Braconnot et al., 2012). This information is crucial to evaluate the ability of climate models to simulate past climates and therefore provide a frame to measure our confidence in models to forecast future climate scenarios.

- A third reason for Holocene´s interest is that climate changes are intrinsically related with our own history as human beings. Since the development of agricultural and grazing techniques and the widespread use of fire to open the landscape, ancient cultures were able to manage their immediate environment for their own benefit. Nevertheless, the degree of human disturbance on the vegetation since the first Neolithic settlements is still controversial. In the Iberian Peninsula, many authors support that from the Mid-Holocene, even at the end of the Early Holocene in some cases, a more continuous fire-use and land-management determined, along with the climate, the evolution of the vegetation in many places giving rise to "cultural landscapes" (Burjachs et al., 1997; Riera et al., 2004; Vannière et al., 2008; Sadori et al., 2011; Magyari et al., 2012; Gassiot et al., 2012; Berrocal et al., 2012). Conversely, in other cases, the vegetation seems to adapt mainly to climatic conditions until the most recent times when anthropogenic activities turned into the most important control (Carrión et al., 2001: Villaverde sequence; Aranbarri et al., 2014: Villarquemado palaeolake; Morales-Molino and García-Antón, 2013: Ayoó de Vidriales). Actually, past climate shifts were responsible of relevant human migrations in search of better conditions (Cullen et al., 2000; Hoelzmann et al., 2001; Nuñez et al., 2002; González-Sampériz et al., 2009) illustrating how human populations have been largely subjected to weather. The Holocene sequences provide information to assess the human landscape management history and its subordination or not to climate factors during the last 11,700 years.

The Pyrenees is a compelling region for paleo-climate studies because of its unique geographic location. The Pyrenees are a high mountain range placed in mid-latitudes and situated between the Eurosiberian and the Mediterranean biogeographic regions of Europe (fig.1.1). These particular geographical features made them extremely sensitive to changes in:

- Temperature. As a consequence of its location in mid-latitudes and their steep altitudinal gradient, the Pyrenees are characterized by a high temperature gradient from lowlands to highlands (fig. 1.2a) that results in a highly diverse altitudinal zonation of the vegetation (fig. 1.3b) (see Appendix for a detailed vegetation map of the Pyrenees). A recent study has demonstrated that some cold-adapted plant species are being outcompeted by more warm-adapted species in high altitudes as a result of the current global warming (Gottfried et al., 2013). This thermophilization process, as called by the authors, points out the high sensitivity and the fast response of the vegetation in the Pyrenees to temperature changes.

- Precipitation. The Pyrenees are bounded by the Mediterranean Sea to the east and the Atlantic Ocean to the west. The precipitation regime, mostly linked to the strength of the Atlantic fronts (fig. 1.2b), determines the east-west limit between the Atlantic humid forest and the Mediterranean dry forest (fig. 1.3b; supplementary material). This feature occurs exclusively in the southern slopes of the Pyrenees, which is not affected by the Foehn winds.

- Anthropogenic activities. In mountainous regions such as the Pyrenees, low altitude areas are much more prone to have been continually occupied than high altitude zones, where climate is more severe and could hinder temporally the presence of human settlements and activities. The comparison and integration of sequences placed at different altitudes provides information about how humans have interacted with their environment, to what extent anthropogenic activities are responsible for large vegetation shifts and, whether the occupation patterns are somehow influenced by environmental stress.

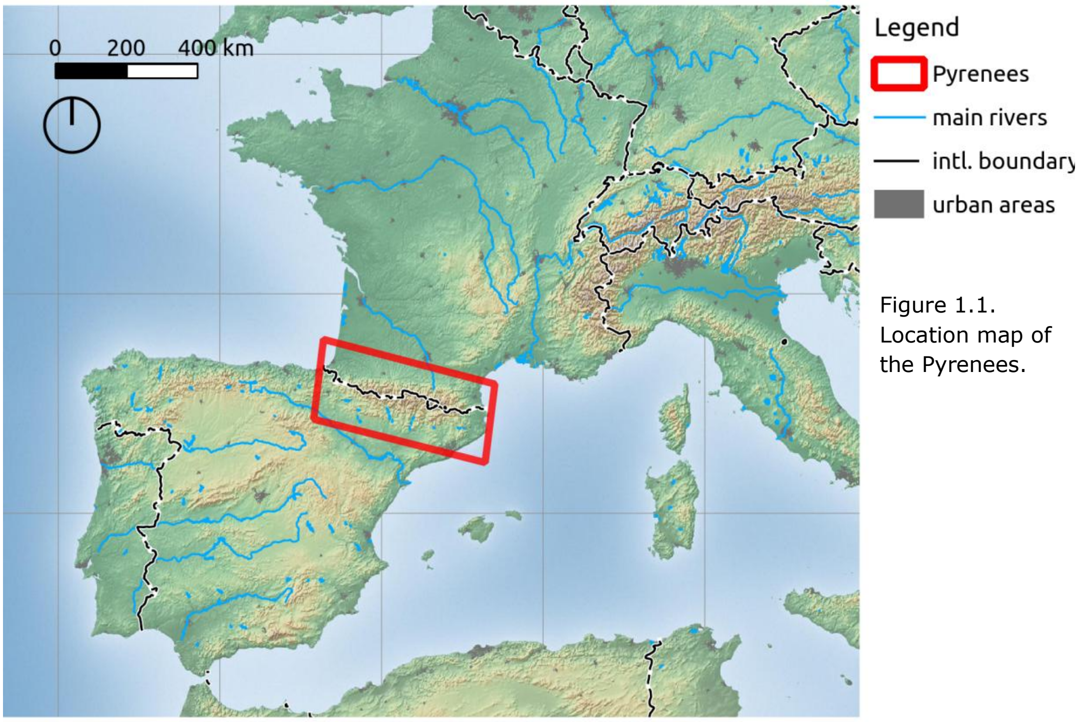


**Figure 1.1**. Location map of the Pyrenees. Map plotted by Miguel Sevilla Callejo.

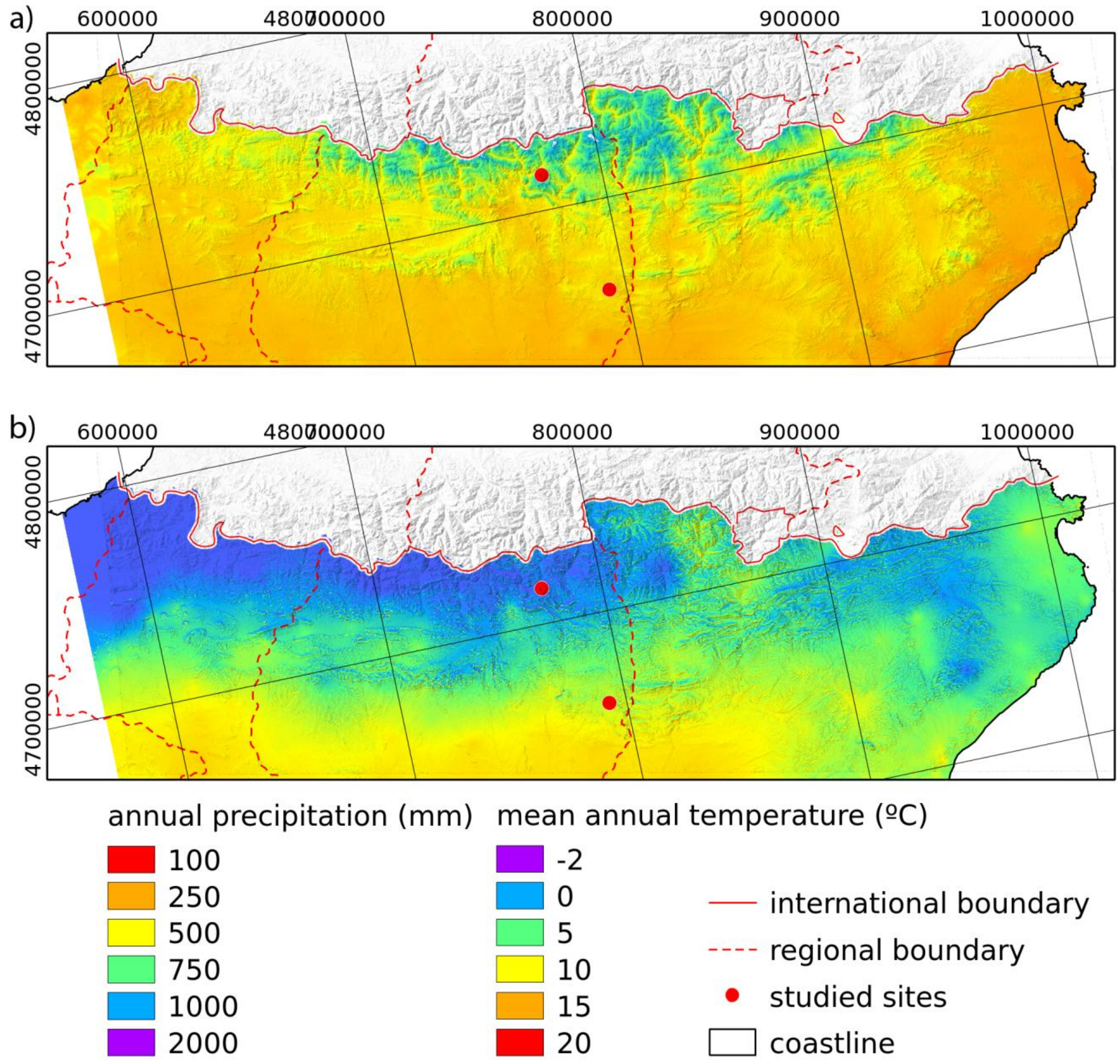


**Figure 1.2**. a) Temperature map of the Pyrenees. b) Precipitation map of the Pyrenees. Source: Atlas Climático Digital de la Península Ibérica. Map plotted by Miguel Sevilla Callejo.

#### 1.1.2.2. Previous studies: what we know and what is missing

Our knowledge of Holocene vegetation dynamics in the Pyrenees has greatly improved during the last decade, as many studies based on lake sediments have been published (Aubert et al., 2004; Guiter et al., 2005; Pla and Catalan, 2005; González-Sampériz et al., 2006; Miras et al., 2007, 2010; Pèlachs et al., 2007; Ejarque et al., 2009, 2010; Morellón et al., 2009; Bal et al., 2011; Corella et al., 2010; Rull et al., 2011; Pérez-Obiol et al., 2012; Rius et al., 2012; Cunill et al., 2013).

Most of these studies have focused mainly on palynological reconstructions that have documented the evolution of the vegetation. But they have also provided sedimentological and biological proxies about the evolution of the limnological systems and the watersheds, the paleohydrology, and reconstructions of different aspects of past climate dynamics.

Palaeo-environmental studies available in the southern face of the Pyrenees are summarized in figure 1.3. According to these studies the expansion of the forest in altitude was delayed at least ca. 1000 since the beginning of the Holocene due to yet severe climate conditions (Miras et al., 2007; Cunill et al., 2012), although the forest spread easily afterwards. During the Early Holocene increase in humidity was much pronounced in the Atlantic-influenced area, where it took place a large expansion of mesophytes (Montserrat-Martí, 1992; González-Sampériz et al., 2006), than in the Mediterranean-influenced area, where pine was the main forest component (Miras et al., 2007; Pérez-Obiol et al., 2012). Nevertheless, during the Mid Holocene, even the highest and most eastern sequences recorded some increase in mesophytes due to more humid environmental conditions (Miras et al., 2007; Pèlachs et al., 2007). Approximately after ca 5 cal ka BP, deciduous trees decreased probably as a result of the onset of a trend to drier conditions that, in general, has continued until the present (Miras et al., 2007). Conversely, at this time *Abies* expanded considerably, although whether this expansion was climate-driven or, responded to migratory paths from the glacial refugia is controversial (Montserrat-Martí, 1992; Pèlachs et al., 2009, 2011). Another subject of much debate is the spread of *Fagus* from ca 4 cal ka BP (Montserrat-Martí, 1992; Pèlachs et al., 2009). The expansion of this tree coincides with an increasing presence of anthropogenic signals, indicating that beech spread could be favored by humans (Miras et al., 2007, Pèlachs et al., 2011). In general terms, the impact of the anthropogenic activities rose during the Roman Times and gained momentum during the middle ages.

Although we know the main vegetation pattern changes during the Holocene, there is still an important lack of information regarding:

- Shifts in vegetation belts as a result of changes in temperature.
  Most of the sites are located at altitudes above 1600 m. a.s.l., hindering the comparison of migration and time-evolution of the vegetation belts (fig. 1.3a). Up to now, there are only two sequences located below 1200 m. a.s.l.: Paul the Bubal, but it only has one radiocarbon date for the Holocene (Montserrat-Martí, 1992); and Montcortés, but the published pollen record only covers the last 1000 years (Rull et al., 2011). Consequently, there is a shortage of data from the low altitude vegetation belts in the Pyrenees that could complete the altitudinal transects and shed light about changes in species distributions related to temperatures shifts during the Holocene.

- Vegetation dynamics as a result of changes in precipitation.
  Most palynological studies are located in the Eastern Pyrenees while fewer sites are from the Western area (fig. 1.3a). In general, the eastern lacustrine sequences are the most recent studies, achieving better resolution and chronological control. Conversely, the scarce western-central sequences either lack a good temporal framework (Montserrat-Martí, 1992) or do not cover the whole Holocene (González-Sampériz et al., 2006). As a result, detailed comparisons between eastern and western areas in order to investigate variations in the limit of the Atlantic and Mediterranean forests related to changes in the precipitation regimen, are not possible. Furthermore, the eastern sequences are placed

too far from the Atlantic influence to have recorded more oceanic conditions even during past periods of stronger westerlies.

- The relationship between climate and hydrological balance
  Palynological studies from Pyrenean sites have not been systematically integrated with sedimentological and paleolimnological studies (Pla and Catalan, 2005; Miras et al., 2007, 2010; Ejarque et al., 2010; Pérez-Obiol et al., 2012), missing an opportunity to integrate regional vegetation dynamics with local environmental conditions in order to capture common climate signals. The reconstruction of past lake level changes can characterize or constrain the features of the precipitation patterns inferred from the vegetation composition. The Quaternary Global Change research team from the Pyrenean Institute of Ecology (IPE-CSIC, http://www.ipe.csic.es/cambios-globales/) has been a pioneer team in Spain that systematically applies a multiproxy strategy to paleoclimate studies based on lake sediments.

- Rapid and abrupt changes during the Holocene.
  Because of the low sample resolution or/and because of their location in a more stable environment, available palaeo-environmental sequences from the Pyrenees do not provide evidence of the forest response to the abrupt climate changes occurred during the Holocene.

- Differences in patterns of human occupation between lowlands and highlands.
  Evidence of anthropogenic activities in the Pyrenees is ancent. Signs of human activity in the subalpine belt of central and eastern Pyrenees can be traced back to ca 8 cal ka BP (Miras et al., 2007; Ejarque et al., 2010) and can be recognised sporadically through the whole Neolithic period (Pèlachs et al., 2007; Miras et al., 2010; Cunill et al., 2012; Pérez-Obiol et al., 2012). On the other hand, in spite of the accessibility of the central Pyrenean lowlands and their more suitable climate than the highlands, there is a completely lack of information of human activities in these areas from sedimentary archives (fig. 3a). Up to now, there are only two lacustrine sequences located under 1200 m a.s.l in this region: Paul the Bubal (Montserrat-Martí, 1992) and Montcortés, (Rull et al., 2011). Some archaeological sites have provided pollen data too but they only cover short chronological periods (González-Sampériz, 2004).

**Figure 1.3**. a) Schematic representation of the vegetation zones of the Southern Pyrenees including the location and altitude of all the paleoenvironmental sequences available in the area. Portalet: González-Sampériz et al., 2006; Paul de Bubal: Montserrat-Martí, 1992; Tramacastilla: Montserrat-Martí, 1992; BSM (Basa de la Mora): present study; Estanya: present study; Morellón, 2009; Redo: Pla and Catalan, 2005; Montcortés: Corella et al., 2010; Rull et al., 2011; Burg: Pèlachs et al., 2007; Estanilles: Pérez-Obiol et al., 2012; Pradell: Ejarque et al., 2009; BDE (Bosc dels Estanyons): Miras et al., 2007; PDP (Planells de Perafita): Miras et al., 2010; RDO (Rius del Orris): Ejarque et al., 2010. b) Vegetation description of the different vegetation belt of the Pyrenees. The definition of the vegetation belts are based on Villar, 1997, Domínguez-Llovería and Puente-Cabeza, 2003 and Ninot et al., (2007). The description includes the main trees, shrubs and herbs that for each belt, sorted out by order of abundance. Main species are highlighted in bold.

a)

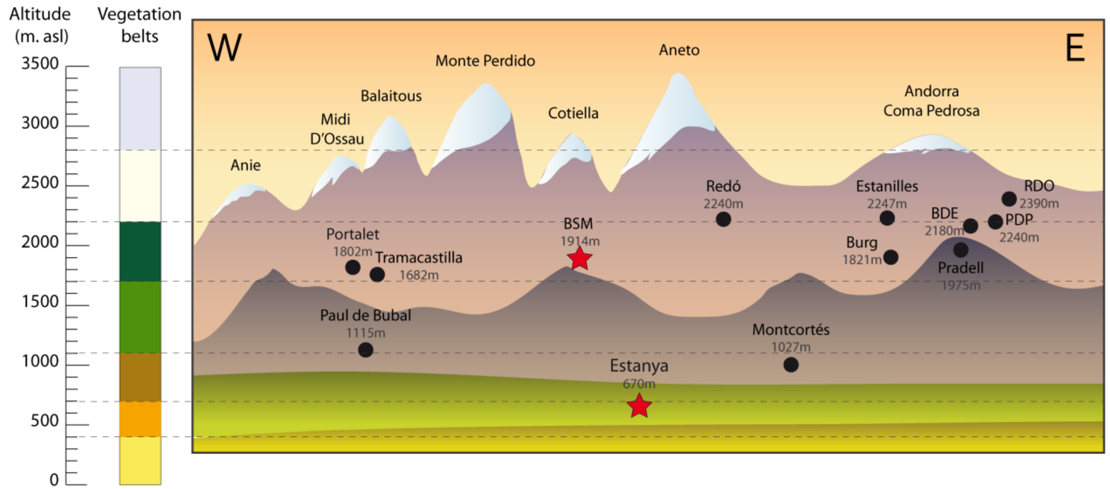


b)

| Belt Name | Altitude (m) | Trees | Shrubs/Bushes | Herbs |
|---|---|---|---|---|
| Nival | 2800-upwards | Absence of vegetation | | |
| Alpine | 2200-2800 | | | *Festuca gautieri, Elyna myosuroides, Festuca eskia, Nardus stricta, Dryas octopetala* |
| Sub-Alpine | 1700-2200 | ***Pinus uncinata**, Abies alba, Betula pendula* | *Juniperus communis* subsp. *alpina, Rhododendron ferrugineum, Vaccinium myrtillus, Sorbus aucuparia, S. chamaemespilus* | *Festuca scoparia, Helicotrichon sedenense, Thymelaeae nivalis* |
| Montane | 1100-1700 | ***Pinus sylvestris**, Abies alba, Fagus sylvatica, Corylus avellana, Betula pendula, Fraxinus excelsior, Tilia platyphyllos* | *Buxus sempervirens, Rhamnus alpina, Echinospartum horridum, Veronica officinalis, Arctostaphylos uva-ursi* | *Primula veris, Aquilegia vulgaris, Ranunculus tuberosus, Lilium pyrenaicum* |
| Sub-Montane | 700-1100 | ***Quercus faginea**, **Q. rotundifolia**, Q. pubescens, Q. humilis, Pinus sylvestris, P. nigra,* | *Buxus sempervirens, Juniperus communis, J. oxycedrus, J. phoenicea, Genista scorpius, Phillyrea angustifolia, Lonicera etrusca* | *Carex hallerana, Coronilla emerus, Rubia peregrina* |
| Basal | 400-700 | ***Quercus rotundifolia**, Pinus halepensis* | *Quercus coccifera, Juniperus phoenicea, J. oxycedrus, Pistzacia lentiscus, Rhamnus alaternus, Arbutus unedo, Genista scorpius* | *Salvia officinalis, Stipa pennata, S. offneri, Convolvulus lanuginosus* |
| Semi-Arid | up to 400 | *Pinus halepensis* | ***Juniperus thurifera, J. phoenicea**, J. communis, J. oxycedrus, Retama sphaerocarpa, Ephedra sp.* | *Lygeum spartum, Brachypodium retusum, Artemisia herba-alba* |
| Riparian forest | | *Populus nigra, Corylus avellana, Betula pendula, Salix alba, Populus tremula, Fraxinus excelsior, F. angustifolia* | *Clematis vitalba, C. recta, Frangula alnus* | *Saponaria officinalis, Polygonum persicaria, P. lapathifolium,* |

#### 1.1.3. Paleoclimate models for the Mediterranean region

The Mid-Holocene (8.2 - 6 ka BP) provides an opportunity to examine climate-model performance in the Mediterranean region. Palaeo-environmental evidence suggests that during the Mid-Holocene the Mediterranean region was wetter than today. A more positive balance and a change in rainfall seasonality during this period is supported by the rise in lake levels (Kohfeld and Harrison, 2000; Magny et al., 2002; Roberts et al., 2008) and the expansion of deciduous trees (Prentice et al., 1996; Roberts et al., 2004; Carrión et al., 2010) recorded across the region.

However, given the high complexity of interactions involved in the Mediterranean climate (Xoplaki et al., 2003; Luterbacher et al., 2006; Lionello, 2012), models have been unable to reproduce the observed MH patterns of rainfall in the Mediterranean during the Holocene. This was identified as a problem in the atmosphere-only simulations made during the first phase of the Palaeoclimate Modelling Intercomparison Project (PMIP1: see e.g. Masson et al., 1999; Guiot et al., 1999; Bonfils et al., 2004), coordinated by the Working Group on Coupled Modeling (WGCM), and also in the coupled ocean-atmosphere simulations made during PMIP2, where the spatial extent and the magnitude of the changes were not well captured (Brewer et al., 2007)

A new suite of climate simulations from Coupled Model Intercomparison Project (CMIP5, Taylor et al., 2012) has been launched recently and are being analyzed as part of the third phase of the Palaeoclimate Modelling Intercomparison Project (PMIP3: Braconnot et al., 2012). The CMIP5 experiments represent a new opportunity to assess the ability of the climate models to reproduce past and present precipitation changes in the Mediterranean region in a better way.

## 1.2. OBJECTIVES

The present PhD dissertation hast three overarching objectives.

Given the high potential of the Holocene Pyrenean sequences to provide past environmental informations, this PhD dissertation aims:

- to investigate past precipitation and temperature changes in the Pyrenees based on vegetation dynamics and lake level variations through multi-dimensional and multi-proxy studies from sequences placed at different altitudes, in order to get a thorough understanding of the long-term climate evolution and the impact of the abrupt climate changes in the Western Mediterranean during the Holocene.

Additionally, given the concerns of the precipitation over the Mediterranean region, the present thesis also aims:

- to check the ability of climate models from the CMIP5 to simulate the reconstructed more humid conditions in the Mediterranean region during the Mid-Holocene in order to measure their reliability on future climate scenarios.

Finally, given the presence of human populations in the area since at least the Early Holocene, the last objective of this work is:

- to describe the timeline of the human activities in the Pyrenees in order to find out patterns of occupation, landscape modifications and effects of climate events on populations.

## 1.3. OUTLINE

This PhD dissertation embraces two different research fields with specific methodologies: i) reconstruction of paleoclimates and palaeo-environments based on field and laboratory work and ii) evaluation of models analyses, based on mathematical calculations. For these reasons, methodology is described in each chapter instead of constituting an independent section.

The present PhD thesis is divided in 6 chapters. The first one is the Introduction where the scientific context of the study and the main goals of the research are described Chapters 2 and 3 cover the first objective (climate reconstruction in the Pyrenees from two lake sequences). Chapter 4 includes the second objective (evaluation of Mid-Holocene model simulations). Each of them includes an introduction to the subject, the methodology, the results obtained, a general discussion of the results, and some conclusions.

Chapter 5 comprises a summary and a brief discussion of all the results accomplished in previous chapters. The third objective is accomplished in this chapter.

Finally, chapter 6 summarizes the main conclusions of this thesis.

Next, there is an explanation of the road map followed to achieve the objectives of the present thesis.

### 1. First objective

To study the past precipitation-temperature interactions in the Pyrenees, two lake sequences placed at two different altitudinal vegetation zones in the central part of the Pyrenees and Pre-Pyrenees were selected. The main reasons for the particular location of the sequences were:

- An altitude gradient. Different altitude means different climate conditions and, consequently, different vegetation composition. The comparison between vegetation dynamics in highlands and lowlands allows inferences on the evolution of the altitudinal belts as a response to a common change in temperature. In addition, the comparison between lake levels evolution at different altitudes provide a regional understanding of paleo-hydrological evolution.

- Atlantic and Mediterranean influences. The central part of the Pyrenees is close to the present limit between the Atlantic and Mediterranean climate boundary. The evolution of the Atlantic- and Mediterranean-related taxa allowed to investigate past changes in the precipitation regimen related to strengthening or weakening of the Atlantic humid fronts.

The selected sequences are the following:

- Basa de la Mora (BSM) (42º32′N, 0º19′E), at 1914 m. a.s.l. in the subalpine belt, was selected because likely would report changes in the treeline as a result of temperature variations. In addition, it is also located half-way between the Atlantic Ocean and the Mediterranean Sea, so that it is particularly sensitive to changes in precipitation regimen as a result of shifts in the strength of the Atlantic fronts.

- Estaña (EST) (42º02′N, 0º32′E), at 670 m. a.s.l., in the Pre-Pyrenean Range, provides the first Holocene vegetation reconstruction in the basal belt. In addition, it is located in direct contact with the semi-desert regimen of the Central Ebro Basin, so that it is rather susceptible to variability in water availability as a result of changes either in direct precipitation or in supplies from the Pyrenees.

Both sequences fill a relevant palaeo-climate gap in the Pyrenees, as shown in figure 3a.

**Methods**

The study of the BSM sequence included pollen, sedimentology, geochemistry, charcoal and chironomid analyses, and it is the first multiproxy high-resolution study to provide climate reconstructions in the sub-alpine belt of the Pyrenees. Charcoal and chironomids data have been obtained in collaborations with other researchers from the Pyrenean Institute of Ecology and University of Barcelona respectively(Dr. Graciela Gil Romera, Laura Lasheras, Dr. Maria Rieradevall and Pol Tarrats). They have been used to support and put in a context the rest of analyses, but they are not a direct contribution from this thesis.

The study of the EST sequence included exclusively pollen but a previous palaeo-hydrological reconstruction based on sedimentological and geochemical indicators carried out by Dr. Morellón, (2009) was used to integrate vegetation dynamics and lake evolution.

Each sequence is described in a different chapter. In chapter 2 we focus on the sequence located in the highlands (Basa de la Mora), while in chapter 3 we discuss the sequence located in the lowlands (Estaña). These chapters are the base of the climate reconstruction achieved in this work and hence constitute the main body of the present thesis.

## 2. Second objective

The achievement of the first objective made it clearer the different climate conditions that prevailed during the Mid-Holocene in the Central Pyrenees in terms of humidity.. This inspired the investigation on climate simulations for the Mid-Holocene. We focused on precipitation simulations because it is the most characteristic factor of Mediterranean climate, and water availability is a growing concern with large social implications.

**Area of interest**

The area analyzed to assess the reliability of the precipitation simulations over the Mediterranean during the Mid-Holocene included not only the Pyrenees, but the whole southern Europe and North Africa. The reason is that the position of the Inter Tropical Convergence Zone (ITCZ) may influence the position of the NAO centers -Azores High and Iceland Low- (Marshal et al., 2001; Souza and Cavalcanti, 2009). Given that the ITCZ is the main responsible for the monsoon precipitation over north Africa and the position of the NAO centers determines the strength of the North Atlantic westerlies -and consequently the precipitation over Europe-, the models will explore how changes in humid conditions over the Mediterranean region during the Mid-Holocene may be related to changes in the African monsoon and teleconnections with North Atlantic dynamics.

**Methods**

We analysed outputs from 12 General Circulation Models from the fifth phase of the Coupled Modelling Intercomparison Project (CMIP5) (Taylor et al., 2012). Analyses included firstly, Mid-Holocene simulations and comparison with palaeo-data recollected across the whole studied region and, secondly, simulations for present climate in order to explore whether past simulations are somewhat influenced or linked to the ability of models to simulate modern conditions. We want to know if some climate models are more reliable than others for the Mediterranean region.

The second objective is accomplished in chapter 4.

3. Third objective

After a thorough reconstruction of vegetation dynamics in an altitudinal transect in the Pyrenees was completed as part of the first objective, we explored trends in land uses through the analyses of indicators related to human activities in the BSM and EST sequences. In addition, having done a detailed and multiproxy palaeo-climate reconstruction in chapters 2 and 3, we explored whether vegetation changes could have been somewhat influenced by anthropogenic pressure, or whether, conversely, climate events may have challenged or changed human activities.

**Approach to study human activities in the Pyrenees**

Agriculture, grazing and deforestation are the three main human activities able to change the landscape since long time ago. In sedimentary sequences, agricultural activities are recorded through the presence of cultivated taxa such as cereal, olive tree, vine or cannabis; grazing activities are recorded through the presence of pastoral-related taxa such as nitrophilous plants; and, finally, deforestation phases are recognized through marked drops in the arboreal component (Li et al., 2008). We examined the evolution of these three main indicators in BSM and EST sequences in order to find differences in time and use of the landscape regarding the altitude and climate conditions.

The details of vegetation dynamics related to human activities are described in chapters 2 and 3 along with the general description and interpretation of pollen taxa. The main results and a general discussion about this third objective is accomplished in the Discussion part (chapter 5) but it does not constitute an independent chapter of the present thesis.

## 1.4. REARCH WOK AND CONTRIBUTIONS

The present PhD dissertation is based on the following research work:

**Research papers**

Pérez-Sanz, A., González-Sampériz, P., Morellón, M., Valero-Garcés, B.L., Gil-Romera, G., Fontaneda-Ríos, S. Holocene altitudinal vegetation shifts at the Southern Central Pyrenees (Spain): the mid-montane site Lake Estanya. To be submitted.

Pérez-Sanz, A., Li, G., González-Sampériz, P., Harrison, S.P. Evaluation of modern and Mid-Holocene seasonal precipitation of the Mediterranean and Northern Africa in the CMIP5 simulations. Clim. Past., 2014.

Pérez-Sanz, A., González-Sampériz, P., Moreno, A., Valero-Garcés, B., Gil-Romera, G., Rieradevall, M., Tarrats, P., Lasheras-Álvarez, L., Morellón, M., Belmonte, A., Sancho, C., Sevilla-Callejo, M., Navas, A. Holocene climate variability, vegetation dynamics and fire regime in the central Pyrenees: the Basa de la Mora sequence (NE Spain). Quat. Sci. Rev. 73, 149–169, 2013.

Pérez-Sanz, A., González-Sampériz, P., Valero-Garcés, B., Moreno, A., Morellón, M., Sancho, C., Belmonte, A., Gil-Romera, G., Sevilla, M., Navas, A. Clima y actividades humanas en la dinámica de la vegetación durante los últimos 2000 años en el Pirineo central: el registro palinológico de la Basa de la Mora (Macizo de Cotiella). Zubía 23, 17–38, 2011.

**Congress contributions**

Pérez-Sanz, A., et al., Paleoenvironmental reconstruction of Basa de la Mora glacial lake (Central Pyrenees) during the last 13 ka cal yr. BP: a high resoluton palynological study. XVIII INQUA Meeting, Bern. Quaternary International 279-280, 375, 2012 (poster contribution).

Pérez-Sanz, A., et al., Reconstrucción paleoambiental de la Basa de la Mora (Pirineo Central): estudio multiproxy de alta resolución. XIII Iberian Quaternary Meeting (AEQUA), Andorra la Vella. Abstract book 91-92, 2011. (poster contribution).

Pérez-Sanz, A. et al., Palaeoenvironmental reconstruction of Basa de la Mora glacial lake (Central Pyrenees) during the Holocene: preliminary results from palynological analyses. EGU General Assembly. Geophysical Research Abstracts 12, EGU2010-8076, 2010 (poster contribution).

Pérez-Sanz, A., et al., Reconstrucción paleoambiental del Ibón de la Basa de la Mora (Pirineos centrales, NE Iberia): primeros resultados del análisis palinológico. VII Iberian Quaternary Meeting (AEQUA), Faro. Abstract book 255-258, 2009 (poster contribution).

**Research stays**

Jan. 2013 – Jul. 2013: Maquarie University, Sydney, Australia.
Supervisor: Prof. Sandy Harrison.

In addition, data from the present Thesis has also contributed to the next research works:

Lasheras-Álvarez, L., **Pérez-Sanz, A.**, Gil-Romera, G., González-Sampériz, P., Sevilla-Callejo, M., Valero-Garcés, B.L., 2013. Historia del fuego y la vegetación en una secuencia holocena del Pirineo central: la Basa de la Mora. Cuad. Investig. Geográfica 39, 77–95.

Morellón, M., **Pérez-Sanz, A.**, Corella, J.P., Büntgen, U., Catalán, J., González-Sampériz, P., González-Trueba, J.J., López-Sáez, J.A., Moreno, A., Pla-Rabes, S., Saz-Sánchez, M. á., Scussolini, P., Serrano, E., Steinhilber, F., Stefanova, V., Vegas-Vilarrúbia, T., Valero-Garcés, B., 2012. A multi-proxy perspective on millennium-long climate variability in the Southern Pyrenees. Clim. Past 8, 683–700.

Moreno, A., Morellon, M., Martín-Puertas, C., Firgola, J., Canals, M., Cacho, I., **Pérez, A.**, Belmonte, Á., Vegas-Vilarrúbia, T., González-Sampériz, P., Valero-Garcés, B., 2011. Was there a common hydrological pattern in the Iberian Peninsula region during the Medieval Climate Anomaly? PAGES News 19, 16–18.

Moreno, A., **Pérez, A.**, Frigola, J., Nieto-Moreno, V., Rodrigo-Gámiz, M., Martrat, B., González-Sampériz, P., Morellón, M., Martín-Puertas, C., Corella, J.P., Belmonte, Á., Sancho, C., Cacho, I., Herrera, G., Canals, M., Grimalt, J.O., Jiménez-Espejo, F., Martínez-Ruiz, F., Vegas-Vilarrúbia, T., Valero-Garcés, B.L., 2012. The Medieval Climate Anomaly in the Iberian Peninsula reconstructed from marine and lake records. Quat. Sci. Rev. 43, 16–32.

Valero-Garcés, B., Morellón, M., Moreno, A., Corella, J.P., Martín-Puertas, C., Barreiro, F., **Pérez, A.**, Giralt, S., Mata-Campo, M.P., 2014. Lacustrine carbonates of Iberian Karst Lakes: Sources, processes and depositional environments. Sediment. Geol. 299, 1–29.

## References


Aranbarri, J., González-Sampériz, P., Valero-Garcés, B., Moreno, A., Gil-Romera, G., Sevilla-Callejo, M., García-Prieto, E., Di Rita, F., Mata, M.P., Morellón, M., Magri, D., Rodríguez-Lázaro, J., Carrión, J.S., 2014. Rapid climatic changes and resilient vegetation during the Lateglacial and Holocene in a continental region of south-western Europe. Glob. Planet. Change 114, 50–65.

Aubert, S., Belet, J.-M., Bouchette, A., Otto, T., Dedoubat, J.-J., Fontugne, M., Jalut, G., 2004. Dynamique tardiglaciaire et holocène de la végétation à l'étage montagnard dans les Pyrénées centrales. C. R. Biol. 327, 381–388.

Bal, M.-C., Pelachs, A., Perez-Obiol, R., Julia, R., Cunill, R., 2011. Fire history and human activities during the last 3300cal yr BP in Spain's Central Pyrenees: The case of the Estany de Burg. Palaeogeogr. Palaeoclimatol. Palaeoecol. 300, 179–190.

Beerling, D.J., Royer, D.L., 2011. Convergent Cenozoic CO2 history. Nat. Geosci. 4, 418–420.

Berrocal, M., Sebastián López, M., Uriarte González, A., López-Sáez, J.A., 2012. Landscape Construction and Long-Term Economic Practices: an Example from the Spanish Mediterranean Uplands Through Rock Art Archaeology. J. Archaeol. Method Theory.

Bond, G., 1997. A Pervasive Millennial-Scale Cycle in North Atlantic Holocene and Glacial Climates. Science 278, 1257–1266.

Bond, G., Kromer, B., Beer, J., Muscheler, R., Evans, M.N., Showers, W., Hoffmann, S., Lotti-Bond, R., Hajdas, I., Bonani, G., 2001. Persistent Solar Influence on North Atlantic Climate During the Holocene. Science 294, 2130 –2136.

Bonfils, C., de Noblet-Ducoudré, N., Guiot, J., Bartlein, P., 2004. Some mechanisms of mid-Holocene climate change in Europe, inferred from comparing PMIP models to data. Clim. Dyn. 23, 79–98.

Braconnot, P., Harrison, S.P., Kageyama, M., Bartlein, P.J., Masson-Delmotte, V., Abe-Ouchi, A., Otto-Bliesner, B., Zhao, Y., 2012. Evaluation of climate models using palaeoclimatic data. Nat. Clim. Change 2, 417–424.

Braconnot, P., Otto-Bliesner, B., Harrison, S., Joussaume, S., Peterchmitt, J.-Y., Abe-Ouchi, A., Crucifix, M., Driesschaert, E., Fichefet, T., Hewitt, C.D., Kageyama, M., Kitoh, A., Loutre, M.-F., Marti, O., Merkel, U., Ramstein, G., Valdes, P., Weber, L., Yu, Y., Zhao, Y., 2007. Results of PMIP2 coupled simulations of the Mid-Holocene and Last Glacial Maximum – Part 2: feedbacks with emphasis on the location of the ITCZ and mid- and high latitudes heat budget. Clim. Past 3, 279–296.

Brewer, S., Guiot, J., Torre, F., 2007. Mid-Holocene climate change in Europe: a data-model comparison. Clim. Past 3, 499–512.

Bridgman, H., Glantz, M.H., Oliver, J.E., 2006. The Global climate system: patterns, processes, and teleconnections. Cambridge University Press, Cambridge.

Burjachs, F., Giralt, S., Roca, J.R., Seret, G., Julià, R., 1997. Palinología holocénica y desertización en el Mediterráneo occidental, in: Ibáñez, J.J., Valero, B.L., Machado, C. (Eds.), Burjachs. Geoforma Ediciones, Logroño.

Carrión, J.S., Fernández, S., González-Sampériz, P., Gil-Romera, G., Badal, E., Carrión-Marco, Y., López-Merino, L., López-Sáez, J.A., Fierro, E., Burjachs, F., 2010. Expected trends and surprises in the Lateglacial and Holocene vegetation history of the Iberian Peninsula and Balearic Islands. Rev. Palaeobot. Palynol. 162, 458–475.

Carrión, J.S., Munuera, M., Dupré, M., Andrade, A., 2001. Abrupt vegetation changes in the Segura Mountains of southern Spain throughout the Holocene. J. Ecol. 89, 783–797.

Corella, J.P., Moreno, A., Morellón, M., Rull, V., Giralt, S., Rico, M.T., Pérez-Sanz, A., Valero-Garcés, B.L., 2010. Climate and human impact on a meromictic lake during the last 6,000 years (Montcortès Lake, Central Pyrenees, Spain). J. Paleolimnol. 46, 351–367.

Cullen, H.M., deMenocal, P.B., Hemming, S., Brown, F.H., Guilderson, T., Sirocko, F., 2000. Climate change and the collapse of the Akkadian empire: Evidence from the deep sea. Geology 28, 379–382.

Cunill, R., Soriano, J.-M., Bal, M.-C., Pèlachs, A., Pérez-Obiol, R., 2012. Holocene treeline changes on the south slope of the Pyrenees: a pedoanthracological analysis. Veg. Hist. Archaeobotany 21, 373–384.

Cunill, R., Soriano, J.M., Bal, M.C., Pèlachs, A., Rodriguez, J.M., Pérez-Obiol, R., 2013. Holocene high-altitude vegetation dynamics in the Pyrenees: A pedoanthracology contribution to an interdisciplinary approach. Quat. Int. 289, 60–70.

Domínguez-Llovería, J.A., Puente-Cabeza,, J., 2003. La vegetación de la cuenca del Ebro. Heraldo de Aragón, [Zaragoza.

Donner, L.J., Schubert, W.H., Somerville, R., 2011. The development of atmospheric general circulation models: complexity, synthesis, and computation. Cambridge University Press, Cambridge; New York.

Ducrocq, V., Drobinski, P., Lambert, D., Molinié, G., Llasat, C., 2013. Preface: Forecast and projection in climate scenario of Mediterranean intense events: uncertainties and propagation on environment (the MEDUP project). Nat. Hazards Earth Syst. Sci. 13, 3043–3047.

Ejarque, A., Julià, R., Riera, S., Palet, J.M., Orengo, H.A., Miras, Y., Gascón, C., 2009. Tracing the history of highland human management in the eastern Pre-Pyrenees: an interdisciplinary palaeoenvironmental study at the Pradell fen, Spain. The Holocene 19, 1241 –1255.

Ejarque, A., Miras, Y., Riera, S., Palet, J.M., Orengo, H.A., 2010. Testing micro-regional variability in the Holocene shaping of high mountain cultural landscapes: a palaeoenvironmental case-study in the eastern Pyrenees. J. Archaeol. Sci. 37, 1468–1479.

European Environment Agency, 2012. Climate change, impacts and vulnerability in Europe 2012: an indicator-based report. European Environment Agency, Copenhagen.

Gaetani, M., Pohl, B., Douville, H., Fontaine, B., 2011. West African Monsoon influence on the summer Euro-Atlantic circulation. Geophys. Res. Lett., L09705 38, n/a–n/a.

Gassiot, E., Rodríguez-Antón, D., Burjachs, F., Antolín, F., Ballesteros, A., 2012. Poblamiento, explotación y entorno natural de los estadios alpinos y subalpinos del Pirineo Central durante la primera mitad del Holoceno. Cuaternario Geomorfol. 26, 29–45.

Giorgi, F., Lionello, P., 2008. Climate change projections for the Mediterranean region. Glob. Planet. Change 63, 90–104.

González-Sampériz, P., 2004. Evolución paleoambiental del sector central de la cuenca del Ebro durante el Pleistoceno superior y Holoceno. Universidad de Zaragoza, Departamento de Ciencias de la Antigüedad Instituto Pirenaico de Ecología, Zaragoza.

González-Sampériz, P., Utrilla, P., Mazo, C., Valero-Garcés, B., Sopena, M., Morellón, M., Sebastián, M., Moreno, A., Martínez-Bea, M., 2009. Patterns of human occupation during the early Holocene in the Central Ebro Basin (NE Spain) in response to the 8.2 ka climatic event. Quat. Res. 71, 121–132.

González-Sampériz, P., Valero-Garcés, B.L., Moreno, A., Jalut, G., García-Ruiz, J.M., Martí-Bono, C., Delgado-Huertas, A., Navas, A., Otto, T., Dedoubat, J.J., 2006. Climate variability in the Spanish Pyrenees during the last 30,000 yr revealed by the El Portalet sequence. Quat. Res. 66, 38–52.

Gottfried, M., Pauli, H., Futschik, A., Akhalkatsi, M., Barančok, P., Benito Alonso, J.L., Coldea, G., Dick, J., Erschbamer, B., Fernández Calzado, M.R., Kazakis, G., Krajči, J., Larsson, P., Mallaun, M., Michelsen, O., Moiseev, D., Moiseev, P., Molau, U., Merzouki, A., Nagy, L., Nakhutsrishvili, G., Pedersen, B., Pelino, G., Puscas, M., Rossi, G., Stanisci, A., Theurillat, J.-P., Tomaselli, M., Villar, L., Vittoz, P., Vogiatzakis, I., Grabherr, G., 2012. Continent-wide response of mountain vegetation to climate change. Nat. Clim. Change 2, 111–115.

Guiot, J., Boreux, J.J., Braconnot, P., Torre, F., 1999. Data-model comparison using fuzzy logic in paleoclimatology. Clim. Dyn. 15, 569–581.

Guiter, F., Andrieu-Ponel, V., Digerfeldt, G., Reille, M., Beaulieu, J.-L., Ponel, P., 2005. Vegetation history and lake-level changes from the Younger Dryas to the present in Eastern Pyrenees (France): pollen, plant macrofossils and lithostratigraphy from Lake Racou (2000 m a.s.l.). Veg. Hist. Archaeobotany 14, 99–118.

Gutiérrez, J.M., San-Martín, D., Brands, S., Manzanas, R., Herrera, S., 2013. Reassessing Statistical Downscaling Techniques for Their Robust Application under Climate Change Conditions. J. Clim. 26, 171–188.

Hewitson, B.C., Crane, R.G., 1996. Climate downsacling: techniques and application. Clim. Res. 7, 85–95.

Hoelzmann, P., Keding, B., Berke, H., Kröpelin, S., Kruse, H.-J., 2001. Environmental change and archaeology: lake evolution and human occupation in the Eastern Sahara during the Holocene. Palaeogeogr. Palaeoclimatol. Palaeoecol. 169, 193–217.

Hoerling, M., Eischeid, J., Perlwitz, J., Quan, X., Zhang, T., Pegion, P., 2012. On the Increased Frequency of Mediterranean Drought. J. Clim. 25, 2146–2161.

IPCC, 2001. The Scientific Basis. Contribution of Working Group I to the Third Assessment Report of the Intergovernmental Panel on Climate Change, Houghton, J.T., Y. Ding, D.J. Griggs, M. Noguer, P.J. van der Linden, X. Dai, K. Maskell, and C.A. Johnson. ed. Cambridge University Press, Cambridge, Uniited Kingdom and New York.

IPCC, 2007. Climate Change 2007: impacts, adaptation and vulnerability., Contribution of working group II to the fourth assessment report of the intergovernmental panel on cliamte change. ed. Cambridge University Press, Reino Unido.

Kohfeld, K.E., Harrison, S.P., 2000. How well can we simulate past climates? Evaluating the models using global palaeoenvironmental datasets. Quat. Sci. Rev. 19, 321–346.

Last, W.M., Smol, J.P., 2001. Tracking Environmental Change using Lake Sediments, Developments in Paleoenvironmental Research Series. Kluwer Academic Publishers, Norwell, MA, U.S.A.

Li, Z., Zhang, Z., Li, J., Zhang, Y., Li, Z., Liu, L., Fan, H., Li, G., 2008. Pollen distribution in surface sediments of a mangrove system, Yingluo Bay, Guangxi, China. Rev. Palaeobot. Palynol. 152, 21–31.

Lionello, P., 2012. The climate of the Mediterranean Region from the past to the future. Elsevier Science, Burlington.

López-Moreno, J.I., Vicente-Serrano, S.M., Morán-Tejeda, E., Lorenzo-Lacruz, J., Kenawy, A., Beniston, M., 2011. Effects of the North Atlantic Oscillation (NAO) on combined temperature and precipitation winter modes in the Mediterranean mountains: Observed relationships and projections for the 21st century. Glob. Planet. Change 77, 62–76.

Luterbacher, J., Xoplaki, E., Casty, C., Wanner, H., Pauling, A., Kuttel, M., Rutishauser, T., Bronnimann, S., Fischer, E., Fleitmann, D., 2006. Chapter 1 Mediterranean climate variability over the last centuries: A review, in: Developments in Earth and Environmental Sciences. Elsevier, pp. 27–148.

Magny, M., Miramont, C., Sivan, O., 2002. Assessment of the impact of climate and anthropogenic factors on Holocene Mediterranean vegetation in Europe on the basis of palaeohydrological records. Palaeogeogr. Palaeoclimatol. Palaeoecol. 186, 47–59.

Magyari, E.K., Jakab, G., Bálint, M., Kern, Z., Buczkó, K., Braun, M., 2012. Rapid vegetation response to Lateglacial and early Holocene climatic fluctuation in the South Carpathian Mountains (Romania). Quat. Sci. Rev. 35, 116–130.

Marshall, J., Kushnir, Y., Battisti, D., Chang, P., Czaja, A., Dickson, R., Hurrell, J., McCartney, M., Saravanan, R., Visbeck, M., 2001. North Atlantic climate variability: phenomena, impacts and mechanisms. Int. J. Climatol. 21, 1863–1898.

Masson, V., Cheddadi, R., Braconnot, P., Joussaume, S., Texier, D., 1999. Mid-Holocene climate in Europe: what can we infer from PMIP model-data comparisons? Clim. Dyn. 15, 163–182.

Mayewski, P.A., Rohling, E.E., Curt Stager, J., Karlén, W., Maasch, K.A., David Meeker, L., Meyerson, E.A., Gasse, F., van Kreveld, S., Holmgren, K., Lee-Thorp, J., Rosqvist, G., Rack, F., Staubwasser, M., Schneider, R.R., Steig, E.J., 2004. Holocene climate variability. Quat. Res. 62, 243–255.

Meehl, G.A., Stocker, T.F., Collins, W.D., Friedlingstein, P., Gaye, A.T., Gregory, J.M., Kitoh, A., Knutti, R., Murphy, J.M., Nodas, A., Raper, S.C.B., Watterson, I.G., Weaver, A.J., Zhao, Z.C., 2007. Global Climate Projections, in: Solomon, S., Quin, D., Manning, M., Chen, Z., Marquis, M., Averyt, K.B., Tignor, M., Miller, H.L. (Eds.), Climate Change 2007: The Physical Science Basis. Contribution of Working Group I to the Fourth Assessment Report of the Intergovernmental Panel on Climate Change. Cambridge University Press, Cambridge, UK and New York, USA.

Miras, Y., Ejarque, A., Orengo, H., Mora, S.R., Palet, J.M., Poiraud, A., 2010. Prehistoric impact on landscape and vegetation at high altitudes: An integrated palaeoecological and archaeological approach in the eastern Pyrenees (Perafita valley, Andorra). Plant Biosyst. - Int. J. Deal. Asp. Plant Biol. 144, 924–939.

Miras, Y., Ejarque, A., Riera, S., Palet, J.M., Orengo, H., Eubab, I., 2007. Dynamique holocène de la végétation et occupation des Pyrénées andorranes depuis le Néolithique ancien, d'après l'analyse pollinique de la tourbière de Bosc dels Estanyons (2180 m, Vall del Madriu, Andorre). Comptes Rendus Palevol 6, 291–300.

Montserrat-Martí, J., 1992. Evolución glaciar y postglaciar del clima y la vegetación en la vertiente sur del Pirineo: estudio palinológico., Monografías del Instituto Pirenaico de Ecología-CSIC. Zaragoza.

Morales-Molino, C., García-Antón, M., 2013. Vegetation and fire history since the last glacial maximum in an inland area of the western Mediterranean Basin (Northern Iberian Plateau, NW Spain). Quat. Res.

Morellón, M., 2009. Paleohidrología y cambios climáticos abruptos en el Noreste de la Península Ibérica durante los últimos 20.000 años: el registro lacustre de Estanya (Huesca). Universidad de Zaragoza, Departamento de Ciencias de la Tierra, Zaragoza.

Morellón, M., Valero-Garcés, B., Vegas-Vilarrúbia, T., González-Sampériz, P., Romero, Ó., Delgado-Huertas, A., Mata, P., Moreno, A., Rico, M., Corella, J.P., 2009. Lateglacial and Holocene palaeohydrology in the western Mediterranean region: The Lake Estanya record (NE Spain). Quat. Sci. Rev. 28, 2582–2599.

National Research Council Staff, National Academies Press, 2002. Abrupt Climate Change. Inevitable Surprises. National Academies Press, Washington.

Nikulin, G., KjellströM, E., Hansson, U., Strandberg, G., Ullerstig, A., 2011. Evaluation and future projections of temperature, precipitation and wind extremes over Europe in an ensemble of regional climate simulations. Tellus A 63, 41–55.

Ninot, J.M., Carrillo, E., Font, X., Carreras, J., Ferré, A., Masalles, R.M., Soriano, I., Vigo, J., 2007. Altitude zonation in the Pyrenees. A geobotanic interpretation. Phytocoenologia 37, 371–398.

Nuñez, L., Grosjean, M., Caratajena, I., 2002. Human Occupations and Climate Change in the Puna de Atacama, Chile. Science 298, 821–824.

Pearson, P.N., Palmer, M.R., 2000. Atmospheric carbon dioxide concentrations over the past 60 million years. Nature 406, 695–699.

Pèlachs, A., Julià, R., Pérez-Obiol, R., Soriano, J.M., Bal, M.-C., Cunill, R., Catalan, J., 2011. Potential influence of Bond events on mid-Holocene climate and vegetation in southern Pyrenees as assessed from Burg lake LOI and pollen records. The Holocene 21, 95 –104.

Pèlachs, A., Pérez-Obiol, R., Ninyerola, M., Nadal, J., 2009. Landscape dynamics of Abies and Fagus in the southern Pyrenees during the last 2200 years as a result of anthropogenic impacts. Rev. Palaeobot. Palynol. 156, 337–349.

Pèlachs, A., Soriano, J.M., Nadal, J., Esteban, A., 2007. Holocene environmental history and human impact in the Pyrenees. Contrib. Sci. 3, 421–429.

Pérez-Obiol, R., Bal, M.-C., Pèlachs, A., Cunill, R., Soriano, J.M., 2012. Vegetation dynamics and anthropogenically forced changes in the Estanilles peat bog (southern Pyrenees) during the last seven millennia. Veg. Hist. Archaeobotany 21, 385–396.

Pla, S., Catalan, J., 2005. Chrysophyte cysts from lake sediments reveal the submillennial winter/spring climate variability in the northwestern Mediterranean region throughout the Holocene. Clim. Dyn. 24, 263–278.

Prentice, C., Guiot, J., Huntley, B., Jolly, D., Cheddadi, R., 1996. Reconstructing biomes from palaeoecological data: a general method and its application to European pollen data at 0 and 6 ka. Clim. Dyn. 12, 185–194.

Prentice, I.C., Jolly, D., 2000. Mid-Holocene and glacial-maximum vegetation geography of the northern continents and Africa. J. Biogeogr. 27, 507–519.

Riera, S., Wansard, G., Julià, R., 2004. 2000-year environmental history of a karstic lake in the Mediterranean Pre-Pyrenees: the Estanya lakes (Spain). CATENA 55, 293–324.

Rius, D., Vannière, B., Galop, D., 2012. Holocene history of fire, vegetation and land use from the central Pyrenees (France). Quat. Res. 77, 54–64.

Roberts, N., Jones, M.D., Benkaddour, A., Eastwood, W.J., Filippi, M.L., Frogley, M.R., Lamb, H.F., Leng, M.J., Reed, J.M., Stein, M., Stevens, L., Valero-Garcés, B., Zanchetta, G., 2008. Stable isotope records of Late Quaternary climate and hydrology from Mediterranean lakes: the ISOMED synthesis. Quat. Sci. Rev. 27, 2426–2441.

Roberts, N., Stevenson, T., Davis, B., Cheddadi, R., Brewster, S., Rosen, A., 2004. Holocene climate, environment and cultural change in the circum-Mediterranean region, in: Battarbee, R.W., Gasse, F., Stickley, C.E. (Eds.), Past Climate Variability through Europe and Africa. Springer Netherlands, Dordrecht, pp. 343–362.

Rodwell, M.J., Hoskins, B.J., 2001. Subtropical Anticyclones and Summer Monsoons. J. Clim. 14, 3192–3211.

Rull, V., González-Sampériz, P., Corella, J.P., Morellón, M., Giralt, S., 2011. Vegetation changes in the southern Pyrenean flank during the last millennium in relation to climate and human activities: the Montcortès lacustrine record. J. Paleolimnol. 46, 387–404.

Sadori, L., Jahns, S., Peyron, O., 2011. Mid-Holocene vegetation history of the central Mediterranean. The Holocene 21, 117–129.

Shin, S.-I., Sardeshmukh, P.D., Webb, R.S., Oglesby, R.J., Barsugli, J.J., 2006. Understanding the Mid-Holocene Climate. J. Clim. 19, 2801–2817.

Souza, P., Cavalcanti, I.F.A., 2009. Atmospheric centres of action associated with the Atlantic ITCZ position. Int. J. Climatol. 29, 2091–2105.

Steffensen, J.P., Andersen, K.K., Bigler, M., Clausen, H.B., Dahl-Jensen, D., Fischer, H., Goto-Azuma, K., Hansson, M., Johnsen, S.J., Jouzel, J., Masson-Delmotte, V., Popp, T., Rasmussen, S.O., Röthlisberger, R., Ruth, U., Stauffer, B., Siggaard-Andersen, M.-L., Sveinbjörnsdóttir, Á.E., Svensson, A., White, J.W.C., 2008. High-Resolution Greenland Ice Core Data Show Abrupt Climate Change Happens in Few Years. Science 321, 680–684.

Steig, E.J., 1999. PALEOCLIMATE:Mid-Holocene Climate Change. Science 286, 1485–1487.

Taylor, K.E., Stouffer, R.J., Meehl, G.A., 2012. An Overview of CMIP5 and the Experiment Design. Bull. Am. Meteorol. Soc. 93, 485–498.

Trigo, R., Osborn, T., Corte-Real, J., 2002. The North Atlantic Oscillation influence on Europe: climate impacts and associated physical mechanisms. Clim. Res. 20, 9–17.

Vannière, B., Colombaroli, D., Chapron, E., Leroux, A., Tinner, W., Magny, M., 2008. Climate versus human-driven fire regimes in Mediterranean landscapes: the Holocene record of Lago dell'Accesa (Tuscany, Italy). Quat. Sci. Rev. 27, 1181–1196.

Villar, L., Sesé Franco, J.A., Ferrández, J.V., 1997. Atlas de la flora del Pirineo aragonés. Consejo de Protección de la Naturaleza de Aragón, Instituto de Estudios Altoaragoneses, [Spain].

Wanner, H., Beer, J., Bütikofer, J., Crowley, T.J., Cubasch, U., Flückiger, J., Goosse, H., Grosjean, M., Joos, F., Kaplan, J.O., Küttel, M., Müller, S.A., Prentice, I.C., Solomina, O., Stocker, T.F., Tarasov, P., Wagner, M., Widmann, M., 2008. Mid- to Late Holocene climate change: an overview. Quat. Sci. Rev. 27, 1791–1828.

Xoplaki, E., González-Rouco, F., Luter, J., Wanner, H., 2003. Mediterranean summer air temperature variability and its connection to the large-scale atmospheric circulation and SSTs. Clim. Dyn. 20, 723–739.

## APPENDIX

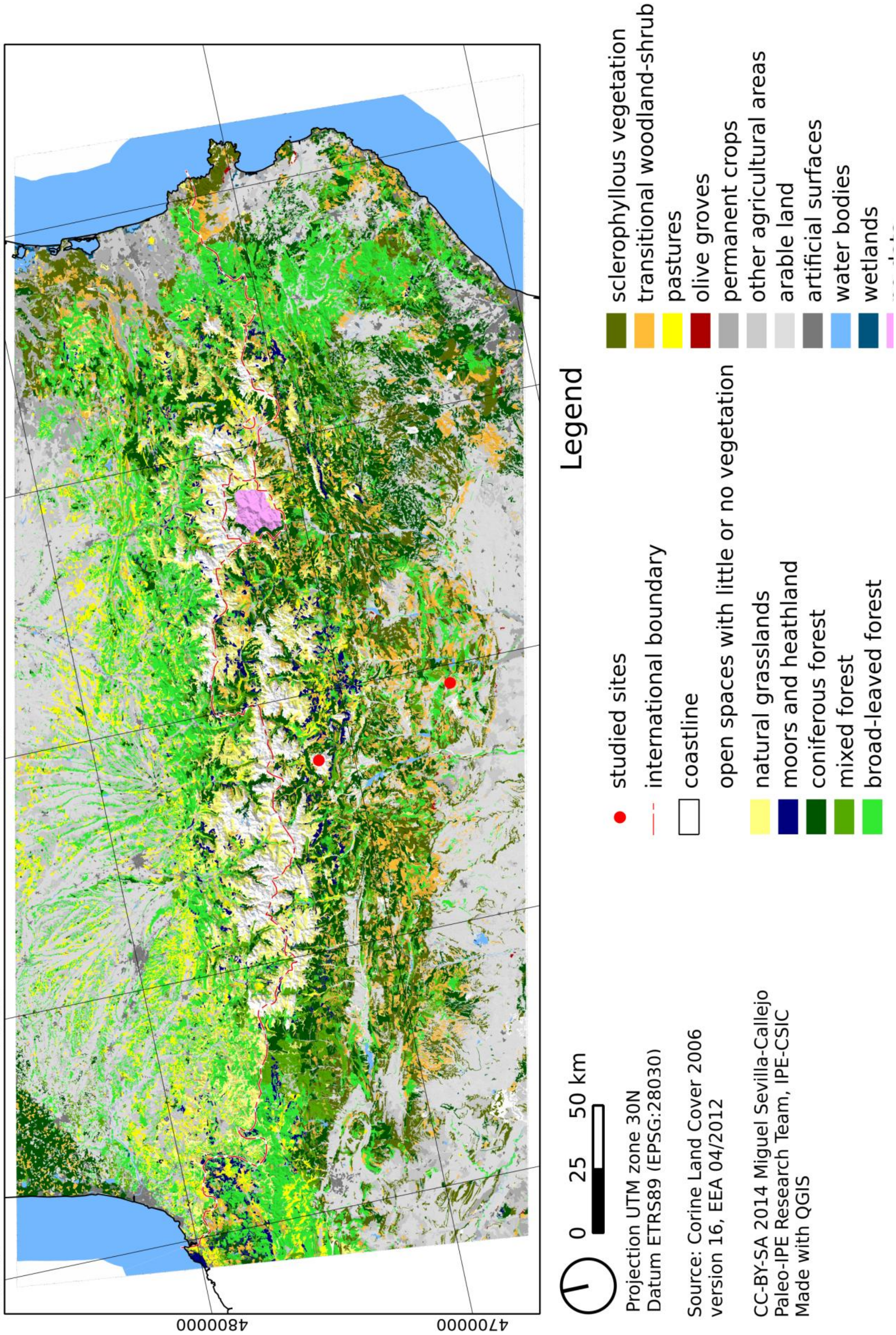


**Figure A1.1**. Vegetation map of the Pyrenees.

# 2

# La Basa de la Mora sequence. Climate at high altitudes

## Outline

The Basa de la Mora sequence provides the most robust and complete Holocene palaeo-environmental reconstruction carried out in the Pyrenees up to now. Placed in the sub-alpine belt of the Central Pyrenees at 1914 m a.s.l., this lake has witnessed relevant climate changes throughout the last 10,000 yr cal BP. Its sediments reveal a fascinating history of vegetation and lake-level changes that proves the high sensitivity of the Pyrenees to climate changes.

## 2.1. INTRODUCTION

Long-term climate evolution during the Holocene has been strongly modulated by orbitally-forced insolation trends which determine heat distribution throughout the planet. In the northern Hemisphere, summer insolation sets limits on the position and strength of the Inter Tropical Convergence Zone (ITCZ), which controls the position of the north-hemisphere cell atmospheric system (Wanner and Brönnimann et al. 2012). In particular, the location of the Azores High and the Iceland Low pressure centres determines the latitudinal position and intensity of the North Atlantic Westerlies and the storm tracks, which largely govern rainfall distribution in the Western Mediterranean area (Greatbatch, 2000, Marhsall et al. 2002). During the Early Holocene, the maximum summer insolation in the Northern Hemisphere led to a rapid northward displacement in the ITCZ and its associated rain belt (Fleitmann et al., 2007). This northern position of the ITCZ was responsible for bringing moisture to the current world-largest desert in North Africa (Sahara and Sahel) (deMenocal et al., 2000). As the summer insolation decreased the ITCZ displaced southward, the monsoon system weakened and in south-western Europe the climate followed a general trend to an increasingly aridity since the Mid Holocene that led to decreased lake levels (Magny et al., 2007, 2011; Valero-Garcés and Moreno, 2011) and major shifts in the vegetation composition (Fletcher and Zielhofer, 2011; Roberts et al., 2011).

However, beyond this general climate trend, many recent studies have documented the existence of rapid climate variability during the Holocene (Bond et al., 1997, 2001; Mayewski et al., 2004). Although the nature and mechanisms of these abrupt climate changes still remain unclear, weakening in the thermohaline circulation as consequence of meltwater inputs in the North Atlantic or changes in the Ocean´s dynamics has been recognised as one of the most important triggers (Renssen et al., 2007; Wanner et al., 2008). Furthermore, fluctuations in solar activity have also been responsible for climate shifts (Wanner et al., 2011). These short-living episodes of climate variability had a large impact over most of Europe, as it has been recorded in many continental palaeoclimate archives as lacustrine sediments (Magny et al., 2007), glacial deposits (Davis et al., 2009), and pollen records (Bordon et al., 2009; Magyari et al., 2012).

Holocene climate reconstructions for the North Atlantic region involve mainly changes in temperature (Brooks and Birks, 2001). However, in the Mediterranean area Holocene variability is mostly related to changes in water availability as it is documented in vegetation distribution (Jalut et al., 2009; Sadori et al., 2011), lake levels (Magny et al., 2011) and stalagmite growth (Fleitmann et al., 2007; Spötl et al., 2010).

The Iberian Peninsula climate integrates subtropical, Mediterranean and Atlantic influences due to its geographical location between the Mediterranean Sea and the Atlantic Ocean (Lionello et al., 2006). Moreover, the Iberian Peninsula has proven to be particularly sensitive to short-term climate shifts during the Holocene (Moreno et al., 2012a). Lakes experienced noteworthy variations in response to precipitation and evaporation shifts during the Holocene (Valero-Garcés et al., 2000; González-Sampériz et al., 2008; Martín-Puertas et al., 2008; Morellón et al., 2009). Changes in sea surface temperatures (Cacho et al., 2001) and deepwater formation (Frigola et al., 2007) in the Western Mediterranean show a fast response to the North Atlantic dynamics. Other Iberian continental records highlight large Holocene variability. For example, the isotope record in the Kaite Cave stalagmite (Domínguez-Villar et al., 2008) reflects variations in the amount of precipitation related to North Atlantic dynamics and fluctuations in palaeoflood activity of Tagus River, in Central Spain have been related to changes in prevailing atmospheric circulation patterns (Benito et al., 2003). Although vegetation is a very good indicator of past climate variability, there are only a few high-resolution pollen studies from the Iberian Peninsula (e.g. Carrión et al., 2010; Fletcher et al., 2013a, Jiménez-Moreno and Anderson, 2012), documenting the fast response of vegetation to abrupt climate changes (decadal- to centennial-scale) during the Holocene.

A recent study has proved the high-sensitivity to current global warming of middle-latitude high mountain ranges in general, and the Pyrenees in particular, documenting an speeding up of the replacement of cold-adapted plants by thermophilic species (Gottfried et al., 2012). Past climate changes during the Holocene should have also affected the flora and landscape of the Pyrenees. Furthermore, the southern slopes of the Pyrenees are not affected by Foehn winds, and the present climate is rather complex, influenced by a progressive west-to-east decrease in precipitation, due to weakening of the Atlantic humid fronts inland. Thus, the southern Pyrenees experience both Atlantic and Mediterranean climate regimes within a relatively short distance of less than 450 Km between the Cantabrian and Mediterranean seas. The Pyrenean vegetation reflects these climate conditions, varying from humid-Atlantic forests, dominated by oak and beech, in the west, to Mediterranean forests, dominated by mainly pine and drought-resistant taxa, in the central and eastern regions. Due to these particular geographical features the Central Pyrenees play a key role in providing information about past E-W shifts of the boundary between both regimes as a result of shifts in the atmospheric components and, particularly, shifts in the Westerlies strength.

In Western Europe, human disturbances in the landscape can be traced back to the Neolithic period and the climate signal is often masked by anthropogenic activities during the most recent times (Olfield, 2005; Carrión et al., 2007). Discriminating anthropogenic from natural forcings in landscape evolution has been subject of much debate during recent years (Carrión et al., 2010; Catalán et al., 2013). High-altitude sites are more useful than low-altitude sites for detecting climate signals, since more inhospitable climate conditions limit intense human landscape intervention.

### 2.1.1. Objectives

The main objective is to obtain a paleo-environmental reconstruction of climate, vegetation and fire dynamics from a lacustrine sequence located in the central part of the southern Pyrenees: the Basa de la Mora sequence. With this reconstruction we will tackle questions concerning: i) how the Atlantic and Mediterranean regimes have progressed along the

Holocene in the Pyrenees, ii) identification and timing of rapid episodes of climate change, and iii) elucidation of high mountain land-use system during last millennia.

## 2.2. STUDY AREA

### 2.2.1. Geological and geomorphological setting

Lake Basa de la Mora (BSM) (42º 32′ N, 0º 19′ E, 1914 m a.s.l.) is a small, shallow glacial lake located on the north-facing slope of the Cotiella Peak (2912 m a.s.l.), the highest summit of the Cotiella Massif in the central southern Pyrenees (fig.2.1). The Cotiella Massif belongs to the homonymous *nappe*, located in the western part of the South Pyrenean Central Unit (Seguret, 1972).

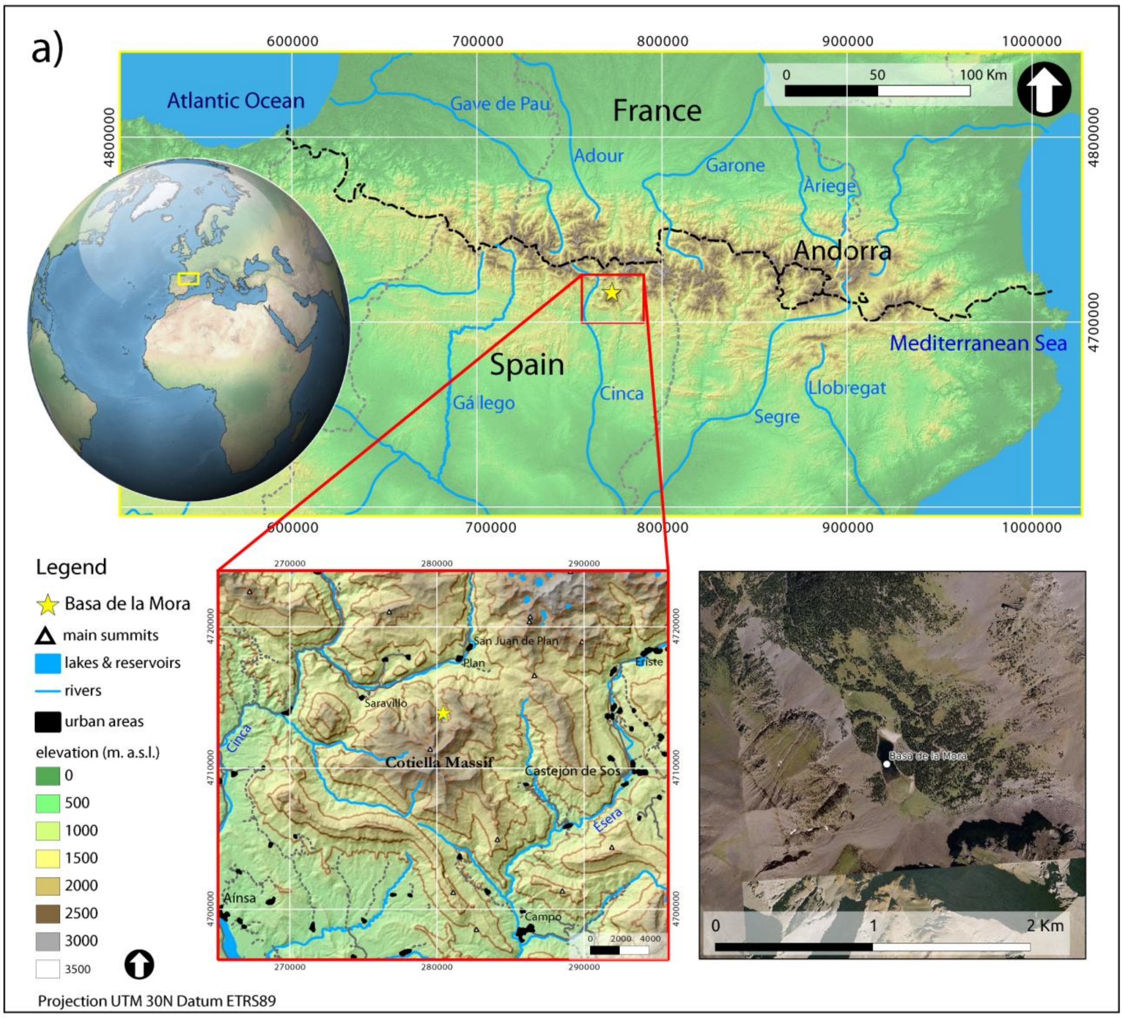


**Figure 2.1**. Location map of Lake Basa de la Mora in the Central Pyrenees (Spain). Map plotted by Miguel Sevilla Callejo.

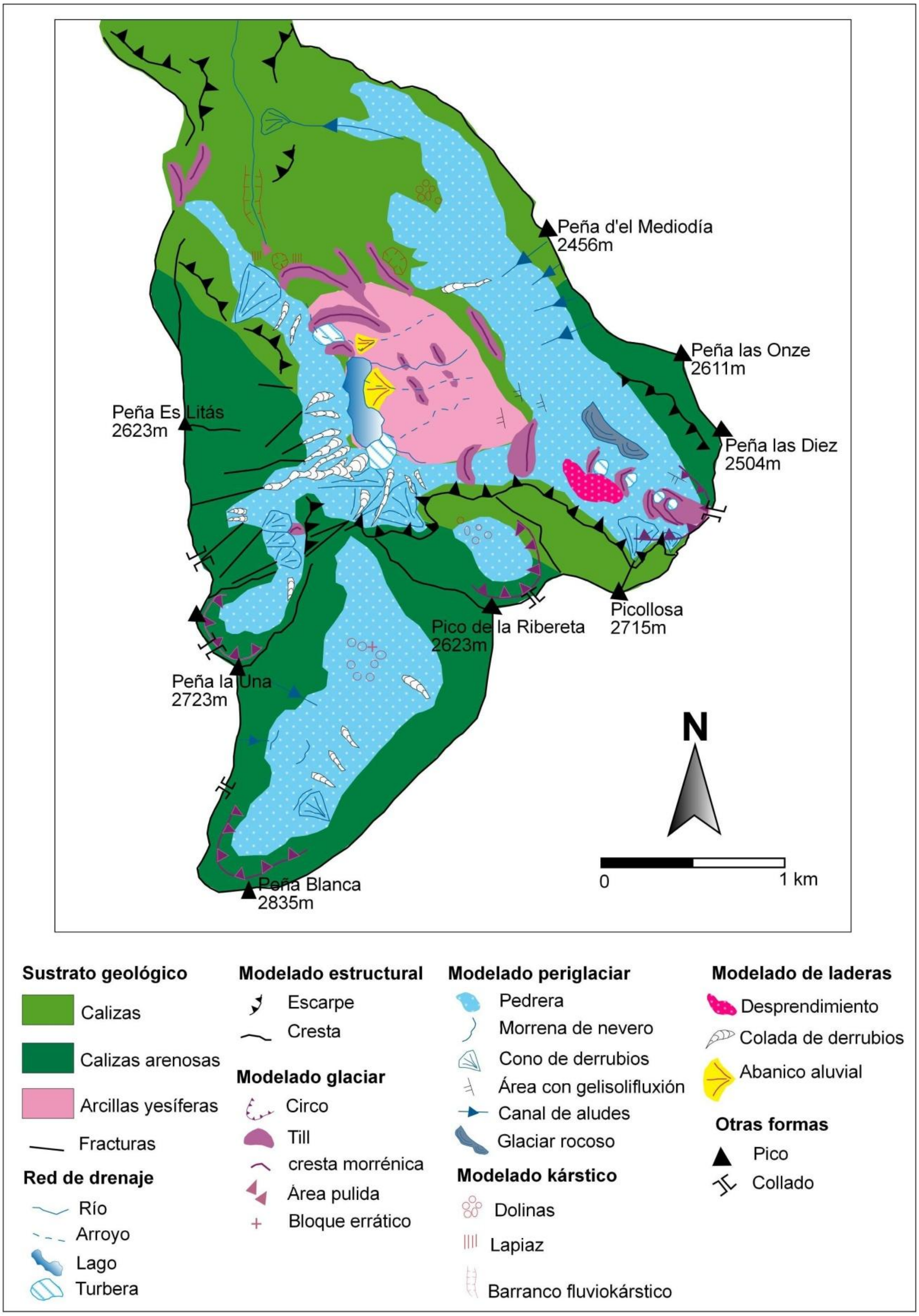


Figure 2.2. Geomorphological map of Lake Basa de la Mora in the Central Pyrenees (Spain). From Belmonte, in prep.

The landscape surrounding the lake results from intense karstic and glacial activity. Lake Basa de la Mora occupies a glacial over-deepened basin enclosed by a frontal moraine (Belmonte, 2004) and surrounded by steep limestone walls (fig. 2.2). The catchment consists of Mesozoic limestones and sandy limestones affected by several thrust sheets (reverse faults). Triassic marl and evaporite formations crop out at the base of the thrust sheets, providing a hydrological seal for the lake and favouring localized surface drainage into the lake along some creeks. Triassic ophite formations in the watershed are the source of highly characteristic sediments (hematite and other Fe- mineral with high magnetic susceptibility) within the lake deposits.

The Basa de la Mora basin belongs to the watershed of the Cinca River, one of the main tributaries of the Ebro River. The lake has smooth margins, a relatively small watershed (209 ha) and a total lake surface of ca. 3 ha (fig. 2.3). It is characterized by large seasonal water-level fluctuations: the maximum depth varies from ca. 2.5 to 4.5 m seasonally. The lake is fed by precipitation, surface runoff, ephemeral creeks and several small springs located on the southern margin. Water losses take place through a surface outlet to the north and evaporation. The substrate, made up of non-permeable Triassic material, greatly restricts groundwater losses.

**Figure 2.3**. Lake Basa de la Mora panoramic view.

### 2.2.2. Climate and vegetation

The Pyrenees is a mountain range in south-western Europe that extends from the Atlantic Ocean in the west to the Mediterranean Sea in the east, leading to a diverse climate and plant community along a W-E transect. The precipitation in the Pyrenees results from two different mechanisms: precipitation in the east is linked to cold fronts and some summer convection storms, while precipitation in the west comes from Atlantic frontal systems (Millán et al., 2005). The Atlantic influence extends as far as the Ordesa Valley (García-Ruiz et al., 2001), ca. 150 km from the Atlantic coast and 22 km west of the BSM. Both systems are directly related to the North Atlantic Oscillation (NAO) that principally determines winter precipitation in western Europe (Trigo et al., 2002).

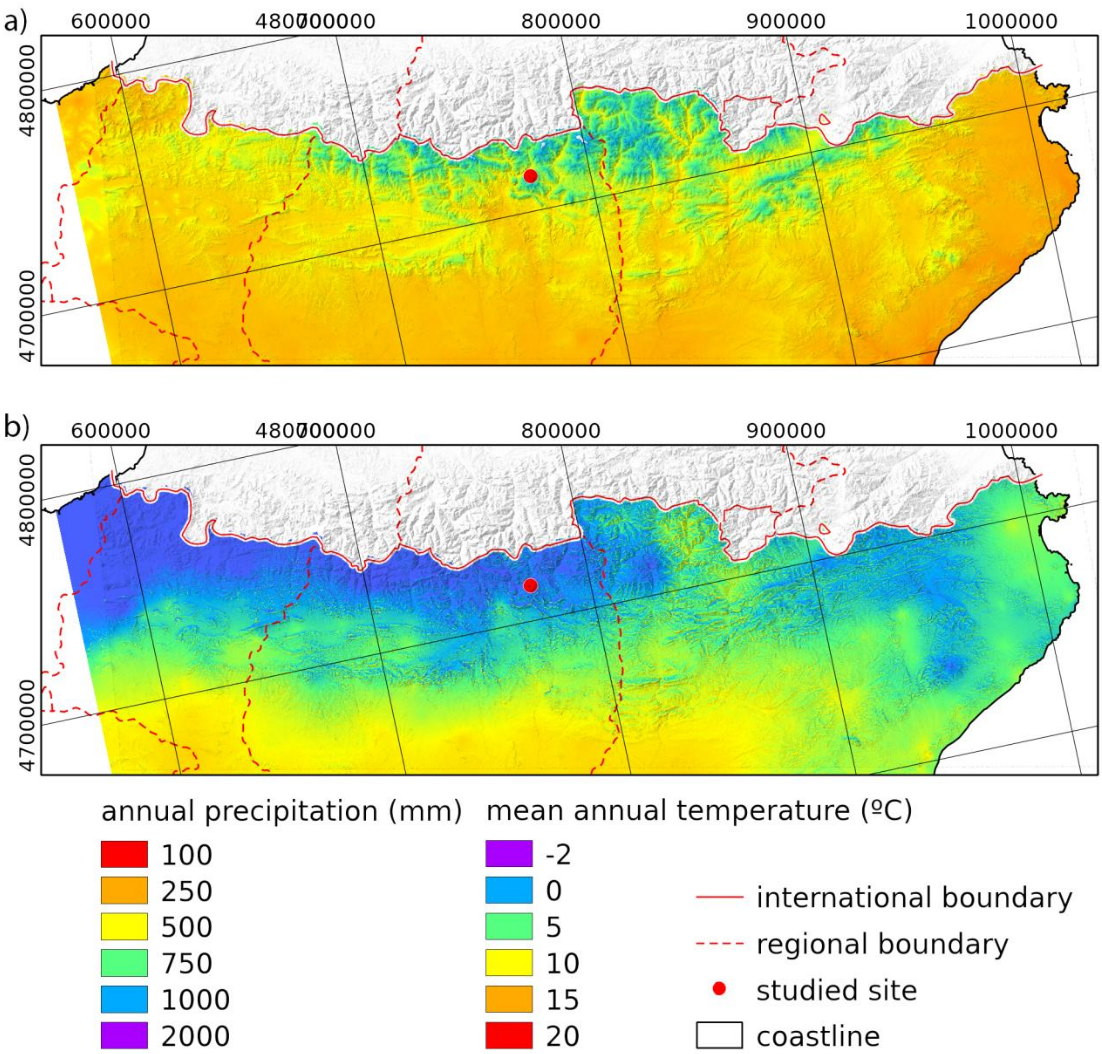


**Figure 2.4**. a) Temperature map of the Pyrenees. b) Precipitation map of the Pyrenees. Source: Atlas Climático Digital de la Península Ibérica. Map drawn by Miguel Sevilla Callejo.

The climate of the study area is sub-Mediterranean with continental features. Rainfall (annual average = 1360 mm) peaks during spring and autumn, following the Mediterranean pattern (García-Ruiz et al., 1985). However, summers are not as dry as is typical of the

Mediterranean because of frontal and convective precipitation which affects the mountainous areas in July and August. Mean air temperatures range from 0.5 to 15ºC between the coldest (January) and warmest (July) months, respectively (fig. 2. 4).

The vegetation cover shows a characteristic contrast between south and north facing slopes: the southern slopes are characterised by mediterranean-type components with sclerophyllous shrubland and evergreen *Quercus* communities, while the northern slopes have mixed conifer/deciduous taxa forests, including *Pinus sylvestris*, *Pinus uncinata*, *Abies alba*, *Betula alba*, *Corylus avellana*, *Fagus sylvatica*, *Quercus faginea* and *Quercus petraea* (fig. 2.5).

The altitudinal gradient between the valley bottoms and the Cotiella Peak, from 550 to 2900 m a.s.l., gives rise to an altitudinal distribution of vegetation, typical of mountain environments. Lowlands are occupied by crops and valley bottoms by riparian corridors (*Fraxinus excelsior*, *Populus* spp., and *Salix* spp.). Forests occur from the base of the foothills up to ~ 2000 m a.s.l. Below 1700 m a.s.l., the dominant species are determined by moisture availability and temperature range, mostly controlled by the slope orientation. From 1700 to 2000 m a.s.l. the forest is mainly composed of *Pinus uncinata* mixed with *Juniperus communis* shrubland and *Rhododendron ferrugineum* at the treeline. Above 2000 m a.s.l., steep rock formations and harsh climate prevent forest development, leading to a scrub-dominated landscape formed by dwarf junipers (*Juniperus communis sbsp. nana*), and alpine grassland (*Nardus stricta, Festuca eskiae, Caricion davallianae* and *Cynosurus cristatus*). Lake Basa de la Mora (BSM) is located in the subalpine belt, near the treeline, so the vegetation surrounding the lake is alpine grassland, *Pinus uncinata* forest and *Juniperus communis-Rhododendron ferugineum* shrublands.

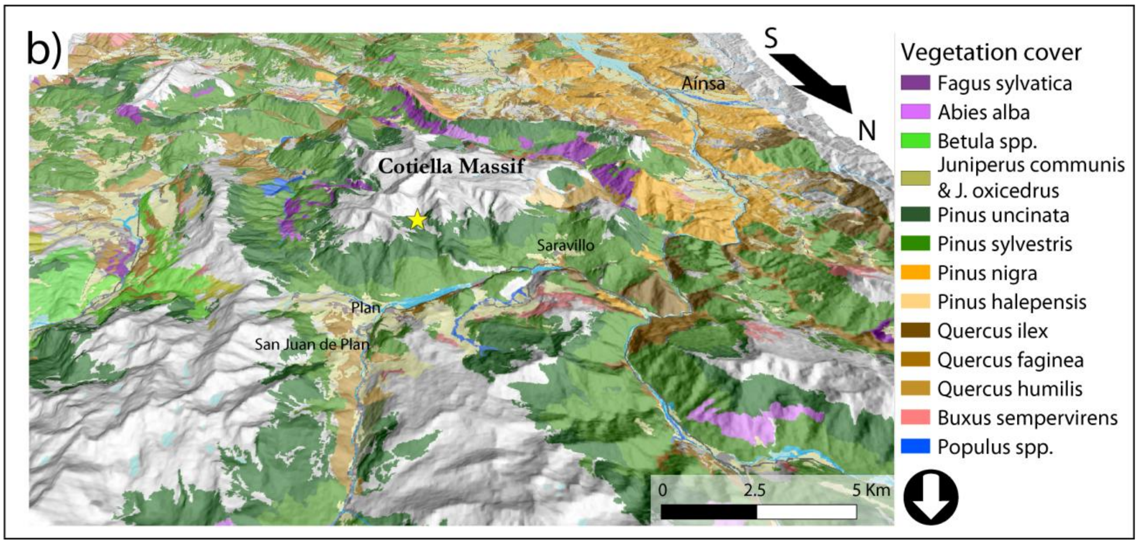


**Figure 2.5.** 3D regional vegetation map. In order to better discern the topography, the North is plotted at the bottom of the figure. The star marks the location of the Lake Basa de la Mora. Map plotted by Miguel Sevilla Callejo.

## 2.3. METHODOLOGY

The composite sequence of Basa de la Mora (BSM08-1A-1U) is based on two parallel cores retrieved from the deepest part of the lake (fig. 2.6) in summer 2008 (fig. 2.7). The longest core was taken with an Uwitec coring system and platform from the Pyrenean Institute of Ecology (IPE-CSIC). Two gravity cores were taken to recover the uppermost part of the sequence and the sediment/water interface. One of the short cores (BSM08-1A-1G) was sub-sampled every 1 cm in the field for $^{210}$Pb and $^{137}$Cs analyses and the other core (BSM08-1B-1G) was used to complete the upper part of the sequence. The cores were correlated applying sedimentological and geochemical criteria. The total length of the composite sequence is 12.10 meters. An additional littoral core (BSM-2A-1U) was taken in order to compare lacustrine depositional environments (fig. 2.5).

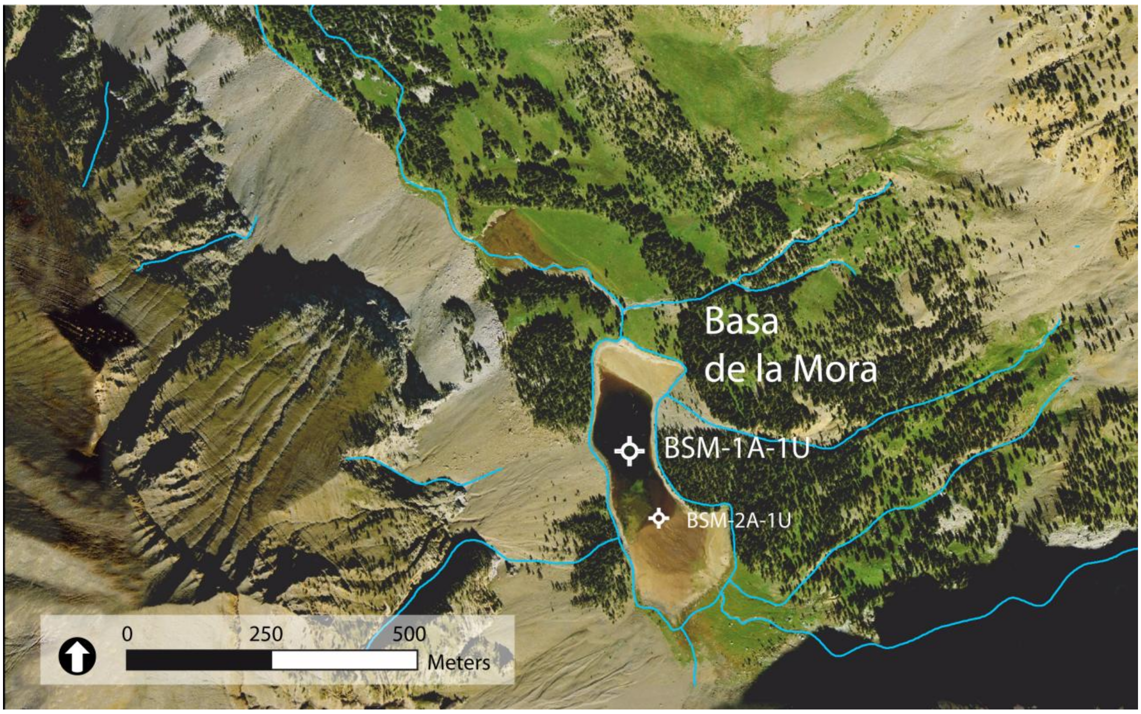


Figure 2.6. Location of cores BSM08-1A-1U and BSM08-2A-1U.

The cores were split lengthwise into two halves, imaged with a DMT Core Scanner and analyzed with a Geotek Multi-Sensor Core Logger (MSCL) at 5 mm intervals to characterise the sediment physical properties at the Limnological Research Center at the University of Minnesota (USA). Elemental geochemical composition was analyzed using the Itrax XRF Core Scanner at the Large Lakes Observatory (LLO) at the University of Minnesota (USA) at 0.5 cm resolution using 30-s count times, 30 kV X-ray voltage, and an X-ray current of 20 mA. These measurements provide estimates of relative element concentrations. The cores were sub-sampled at 2 cm resolution for Total Organic Carbon (TOC) and Total Inorganic Carbon (TIC) and analysed with a LECO144DR elemental analyser at the IPE-CSIC laboratory of Zaragoza (Spain). Sedimentary facies were defined by macroscopic characteristics including colour, grain-size, sedimentary structures, fossil content and by microscopic smear slide observations (Schnurrenberger et al., 2003). The sedimentological descriptions are supported by Scanning Electronic Microscopic (SEM) observations of selected samples made at the University of Zaragoza (Spain). Up to 11 samples representing the main facies were analysed for grain size distributions using a Malvern Laser Sizer (Mastersizer 2000) after removing the organics by $H_2O_2$ and using a dispersant agent to disaggregate the samples. Additionally, 36 samples were analysed for their mineralogical content by X-Ray Diffraction using an automatic Siemens D-500 X-ray diffractometer: Cu ka, 40 kV, 30mA and graphite monochromator. Identification and quantification of the different mineralogical species present in the crystalline fraction were carried out following a standard procedure (Chung, 1974). Sedimentary facies and physical properties (density, magnetic susceptibility) were also obtained for the littoral core (BSM-2A-1U).

**Figure 2.7**. Core drilling campaign in Lake Basa de la Mora (2008).

Samples for pollen analyses were obtained every 5 cm on both the BSM08-1A-1U and BSM08-1B-1G cores. This record covers the whole sedimentary record, except the base of the sequence (1209 - 1165.5 cm depth), which was sampled at higher resolution (1 cm) since the sedimentation rate was extremely low (see below). Sediment samples were prepared following the standard protocol described by Faegri and Iversen (1964) or Moore and Webb (1978), with some modifications (Dupré, 1988) including HCl, and KOH, mineral-organic particles separation with Thoulet solution (2.0 gr/cm$^3$ density) and sieving with 212 and 10µm mesh. *Lycopodium* spores in a known concentration were added in order to calculate the pollen concentration in the sediment and to test the laboratory procedures (Stockmarr, 1971). Pollen was identified using an optical microscope, with help of the reference collection of the IPE-CSIC and identification keys (Moore et al., 1991; Reille and Lowe, 1995). Counts were made to obtain a pollen sum, excluding aquatics and exotics, of at least 300 grains from a minimum of 20 taxa (fig. 2.8). The results have been plotted using PSIMPOLL 4.27 (Bennett, 2009). Additionally, 19 fresh moss samples were collected in order to analyse the current pollen rain. Samples were selected across a distant transect from the lake shore up to 1km-distance, in order to test differences in pollen rain with distance to the lake (fig. 2.9). Only 8 samples of them have been analysed in the present work. Samples were prepared following a similar process that fossil pollen samples but including acetolysis method as a first step.

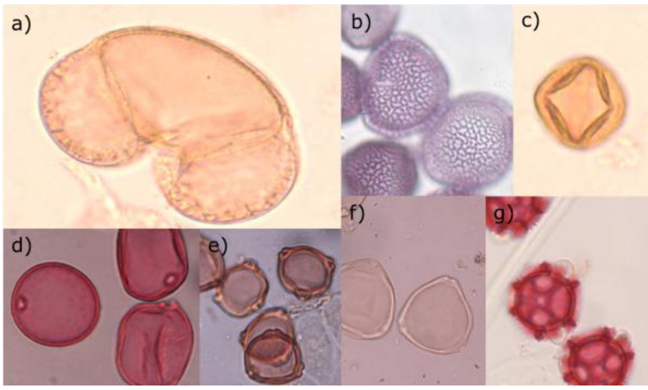


**Figure 2.8**. Photomicrographs of pollen grains. From left to right: a) *Pinus*, b) *Olea europaea*, c) *Quercus* sp., d) Poaceae, e) *Betula* sp., f) *Corylus* and g) Chichorioideae.

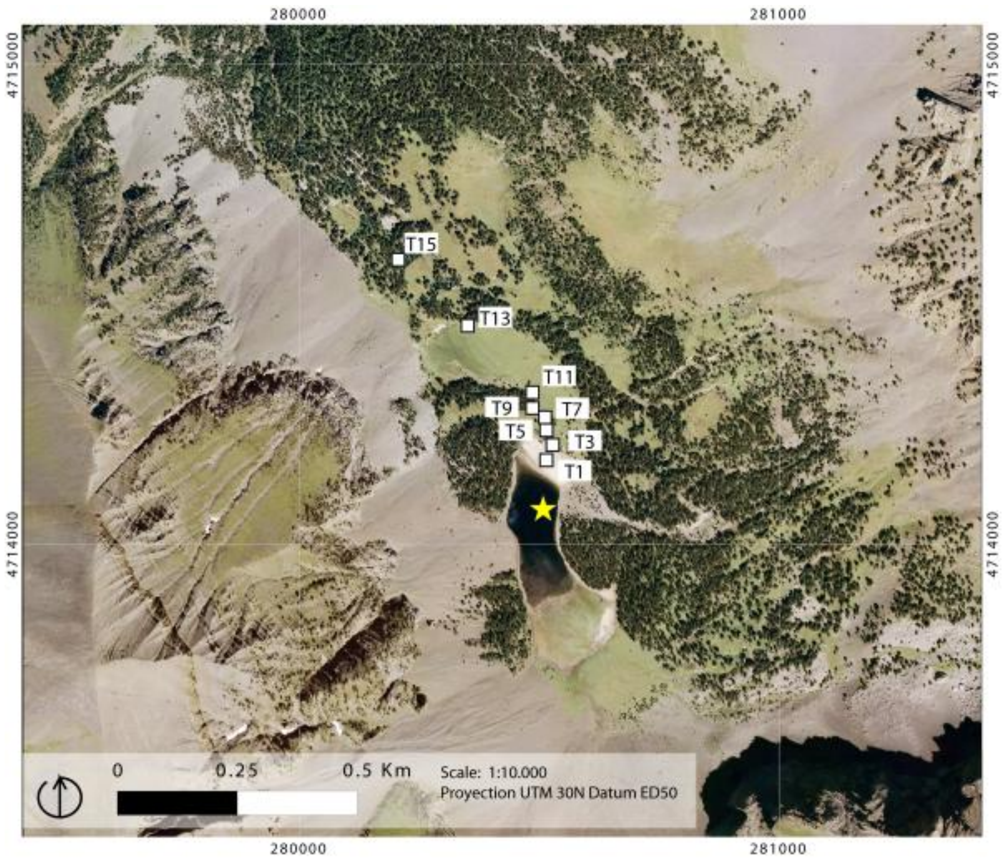


**Figure 2.9**. Location of the moss samples recolected through a transect from Lake Basa de la Mora. Only 8 of them (T1, T3, T5, T7, T9, T11 and T13) have been analyzed in this work.

Correlation analyses were made on smoothed data, after testing for normality (Shapiro-Wilk), using Pearson or Spearman correlation tests. Analysis have been performed by the R software package (Venables et al., 2008). Pairwise comparison was performed between MS and geochemical parameters, to help in the facies description, and then between MS (as a high-resolution sedimentological proxy) and the pollen data, to assess possible links between sedimentary changes and vegetation.


**Figure 2.10**. Photomicrograph of pollen and microcharcoal slides of representative samples. 1: Pinus grain; 2: Microcarcoal particle.

Sedimentary micro-charcoal particles were identified on pollen slides by optical microscopy (fig. 2.10). Only charcoal particles over 10 µm were counted in the same smear-slides than pollen grains and these were easily identified as black, angular and opaque particles (Clark, 1988). Charcoal influx ($mm^2/cm^3$) was estimated after Tinner and Hu (2003). No *Lycopodium* spores were found in some of the slides, so charcoal influx values were obtained by linear interpolation between the adjacent samples.

**Figure 2.11**. Photomicrograph Chironomus larvae head from BSM samples.

Chironomid samples were collected every 20 cm along the entire core, except at the top of the sequence (2.5-50 cm depth) where the sample interval was increased to 5 cm. The samples were processed following the standard procedure (Hofmann, 1986): 10% KOH digestion at 70º and 300 rpm for 20 minutes, followed by sediment sieving (90 µm). *Chironomidae* larvae head capsules (fig. 2.11) were examined under stereo microscope using a Bolgorov tray, picked out manually and dehydrated in 96% ethanol, before being mounted ventral side upwards in Euparal® as permanent slides. Taxonomic identification was carried out using an optical microscope (Olympus CX41) at 40x magnification and Cell B Imaging Software for Life Science Microscopy (Olympus). The larval head capsules were identified to the lowest taxonomic level possible using several specialized guides (Wiederholm, 1983; Rieradevall and Brooks, 2001; Brooks et al., 2007).

The chronology of the sequence is based on 15 calibrated AMS radiocarbon dates from the long core BSM08-1A-1U and $^{137}Cs$ and $^{210}Pb$ dating from the short core BSM08-1B-1G (fig. 2.12). Most of radiocarbon dates are based on terrestrial macrofossils and charcoal and they were analysed at Poznan Laboratory (Poland) (table 2.1). Bulk sediment and pollen concentrates were dated in the lowermost part of the sequence because of the paucity of organic remains. Dates have been calibrated using CALIB 6.0 software and the INTCAL09 curve (Reimer et al., 2009). The 2σ probability distribution interval was chosen. The age model was constructed by linear interpolation between the median ages of the probability distribution of adjacent calibrated dates. The $^{210}Pb_{ex}$ and $^{137}Cs$ activity in the upper samples was measured by gamma-ray spectrometry, using a high-resolution low-energy coaxial HPGe detector coupled to an amplifier at the Estación Experimental de Aula Dei. The chronology based on $^{210}Pb_{ex}$ was estimated by applying the constant rate of supply (CRS) model by Appleby (2001). The resulting age model provides a robust chronological framework for the high resolution paleo-environmental reconstruction presented in this work.

## 2.4. RESULTS

### 2.4.1. Chronology

Despite the existence of 15 AMS radiocarbon dates (table 2.1, fig. 2.12), the final age-depth model has been made with only 13 of them because the two lowermost dates (at 11.98 and 12.06 m depth) were not considered reliable. These basal samples are the only ones not based on terrestrial macrofossils (table 2.1). When these two dates (12628 ± 100 and 15828 ± 600 cal yr BP) are included in the age model, they force a change from consistently high sedimentation rates (1.2 mm/yr) between 0-11.67 m depth to extremely low rates (0.064 mm/yr) at the base (11.67-12.09 m depth). Given that these basal dates point out to the Late Glacial period, we attempted to characterize this zone by increasing the pollen sampling resolution. However, the pollen record did not show changes indicative of the last glacial-interglacial transition (LGIT, see section 4.3, zone BSM-0). Since there is no sedimentary evidence for a depositional hiatus, and no major change in the vegetation composition has been recorded, these two dates and the sediment interval in between were not used in the final age model.

The age model excluding the two basal dates indicates that the 11.67 m long record spans the last ca. 9.8 cal yr BP (fig. 2.12). Thus, the final age-depth model is based on 13 calibrated AMS radiocarbon dates, 11 on macrofossils and two on charcoal remains.

The short core, that includes the most recent period, has been dated by $^{210}$Pb and $^{137}$Cs activities. Two well-defined $^{137}$Cs peaks are recorded at the uppermost part of the sequence providing markers for the 1954-1959 and the 1963 maximum atmospheric nuclear bomb testing. The chronology based on $^{210}Pb_{ex}$ compares fairly well with the $^{137}$Cs peaks (fig. 2.10).

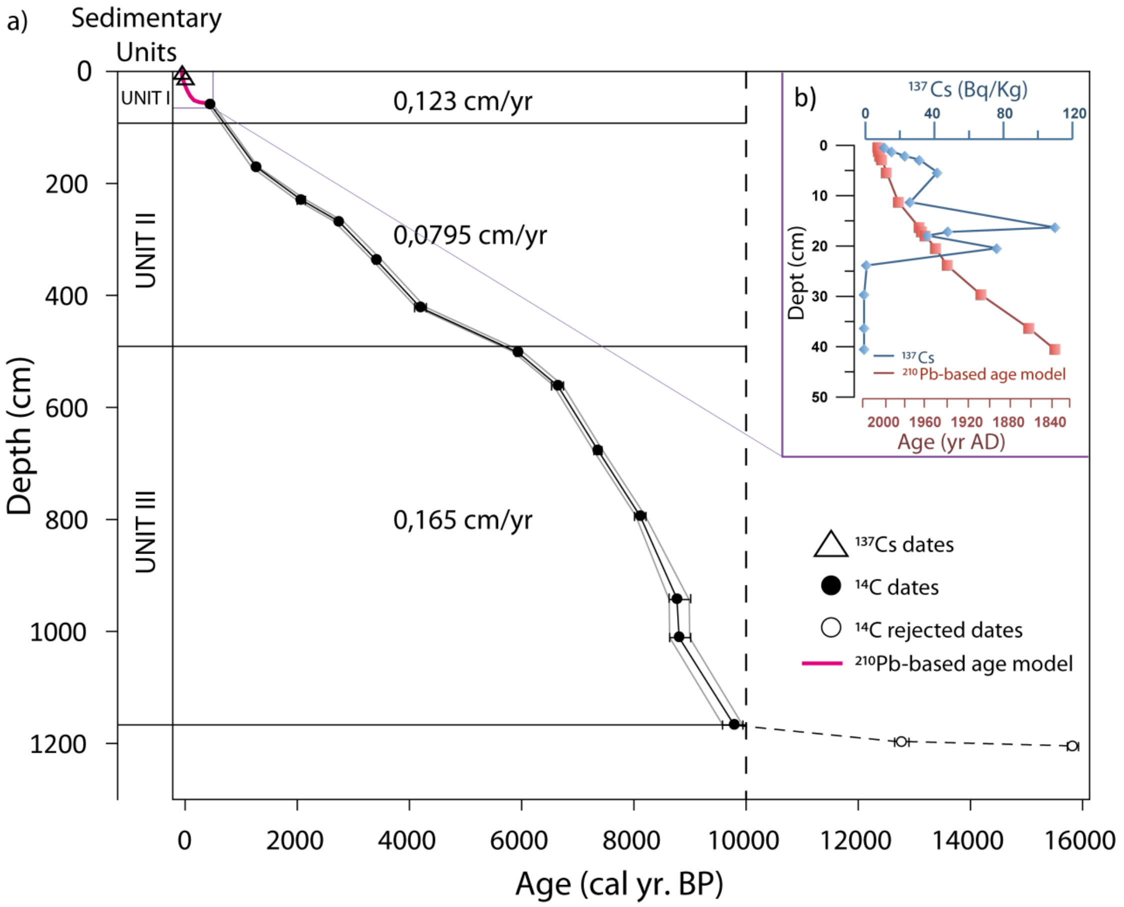


**Figure 2.12**. a) Age-depth model for the composite sequence of Basa de la Mora based on 15 AMS $^{14}$C dates and $^{210}$Pb and $^{137}$Cs activity at top. b) $^{210}$Pb-based age model and $^{137}$Cs profile obtained for the top 50 cm.

### 2.4.2. Sedimentary facies, geochemistry and lithological units

Six sedimentary facies were identified based on visual description, microscopic observations, grain-size data and mineralogical and geochemical composition (table 2.2). The sediments consist of either: i) carbonate – poor (< 2 % TIC), with lower TOC and high MS, organized in laminated or banded intervals, or ii) carbonate-rich (2 – 7 % TIC) with variable, but higher organic matter content (1-3 %) and low magnetic susceptibility, arranged in massive to banded deposits. The grain-size data indicates finer (mode at 6-7 μm) and better-sorted sediments in the silicate-rich, carbonate- poor facies, and coarser and more poorly sorted material in the carbonate-rich sediments.

| (b) Lab Code | Depth (cm) | Sample type | $^{14}C$ age (yr BP) | Calibrated age, 2σ (yr cal BP) | Median probability (yr cal BP) |
|---|---|---|---|---|---|
| Poz-29744 | 60 | Terrestrial macrorest | 385 ± 30 | 426-507 | 456 |
| Poz-35854 | 172 | Terrestrial macrorest | 1335 ± 30 | 1231-1304 | 1276 |
| Poz-29745 | 230 | Terrestrial macrorest | 2100 ± 30 | 1995-2146 | 2072 |
| Poz-35853 | 269 | Terrestrial macrorest | 2615 ± 30 | 2718-2777 | 2749 |
| Poz-35852 | 337 | Terrestrial macrorest | 3200 ± 30 | 3368-3469 | 3419 |
| Poz-35804 | 422 | Terrestrial macrorest | 3815 ±35 | 4089-4299 | 4206 |
| Poz-29743 | 502 | Terrestrial macrorest | 5185 ± 35 | 5893-6002 | 5942 |
| Poz-35803 | 562 | Terrestrial macrorest | 5840 ± 40 | 6533-6745 | 6657 |
| Poz-35802 | 677 | Terrestrial macrorest | 6450 ± 40 | 7288-7430 | 7367 |
| Poz-29746 | 795 | Charcoal | 7330 ± 50 | 8014-8214 | 8125 |
| Poz-35801 | 943 | Terrestrial macrorest | 7930 ± 50 | 8628-8983 | 8778 |
| Poz-29747 | 1011 | Charcoal | 7950 ± 50 | 8640-8990 | 8817 |
| Poz-29779 | 1167 | Terrestrial macrorest | 8780 ± 50 | 9581-9941 | 9798 |
| *Poz-35856* | *1198* | *Bulk sediment* | *10710 ± 60* | *12547-12743* | *12627* |
| *152235* | *1206* | *Pollen concentrates* | *13080 ± 100* | *15181-16476* | *15828* |

**Table 2.1**. AMS radiocarbon dates from core BSM08-1A-1U. Rejected dates are shown in brown and italics.

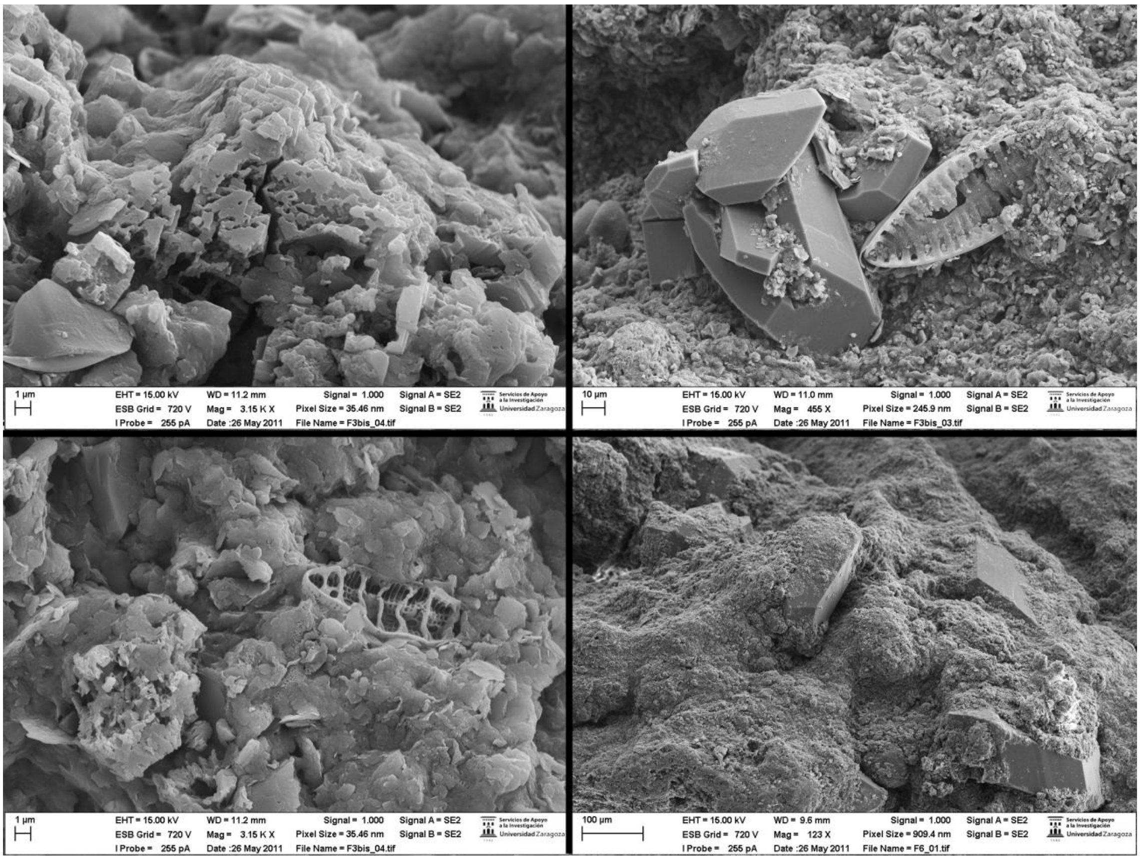

**Figure 2.13**. SEM image from Facies 5 of the BSM sediment core. A) authigenic crystals of carbonate partially disolved. B) authigenic crystals of gypsum and a diatom . C) detrital carbonate grains and diatom remains. D) detrital carbonate grains and authigenic grains of carbonate and gypsum.

The first group of sediments (Facies 1, 2 and 3) are banded to laminated silicate and carbonate fine silts dominated by clay minerals (20-30 %) and quartz (5-15 %) with minor amounts of calcite (< 25 %) and with presence of hematite, pyrite and clinochlorite. Facies 3 has the highest MS, and relatively high carbonate content. Facies 1 and 2 are more silicate-rich, but Facies 2 is finer, with lower MS, better-defined lamination and higher TOC content than Facies 1. The second group (Facies 4, 5 and 6) is dominated by massive carbonates (ca. 6% TIC; 60-80% calcite). Facies 5 and 6 have mottled textures and abundant gastropods, indicating littoral deposition. These facies dominate the littoral core (BSM-2A) almost entirely. Facies 4 has a higher TOC content (up to 3%) dominated by macrophyte and terrestrial remains. Facies 5 contains authigenic crystals of carbonate and gypsum, partially dissolved, pointing to deposition in ephemeral lake conditions with rapid fluctuations of lake level and salinity (fig. 2.13). Diatoms (pennate, benthic) only occur in the carbonate-rich Facies 5. Facies 6 has a slightly banded texture and lower TOC content than the other carbonate facies.

The BSM sequence has been divided into three main sedimentary units according to sedimentary facies, MS, TIC and TOC percentages and the mineralogical and geochemical composition (XRF) (fig. 2.14).

i. Unit 3 (1168-491 cm depth; 9800-5700 cal yr BP) corresponds to the lowermost part of the sequence and it is characterized by banded carbonate – poor sediments with high values of MS and relatively low TOC percentages (Facies 1, 2 and 3). TIC percentages and Ca, Sr and S values are low throughout Unit 3 while Si, K, Ti values (and particularly Fe and Mn) are high. The lowermost Sub-unit 3b (1168-690 cm depth, 9800-7450 cal yr BP) is composed of laminated Facies 1 and a thin interval of Facies 3. Magnetic Susceptibility (MS) reach the highest values of the sequence and are positively correlation with Mn (table 2.3). The high MS values are related to the presence of paramagnetic minerals eroded from ophite outcrops. Values of Ca and TIC are relatively low, but also display a strong positive correlation with MS. TOC percentages are the lowest in the sequence while TOC/N ratios are the highest. Sub-unit 3a (690-491 cm depth, 7450-5700 cal yr BP) is composed of Facies 2 and has finer lamination, lower MS and higher TIC and TOC values. Sub-unit 3a MS values are still high but decrease progressively. MS is significantly positively correlated with Mn and Fe (table 2.3). Ca values are very low and not significantly correlated with MS. TOC percentages increase, showing a significant negative correlation with MS, while TOC/N ratios decreases.

ii. Unit 2 (491-93 cm depth; 5700-680 cal yr BP) is made up of carbonate-rich Facies 5 and 6 with intercalations of organic-rich Facies 4. Thus, Unit 2, although highly variable, is characterized by the lowest values of MS and the highest content in TIC of the whole sequence. The high values of TIC in Unit 2 (up to 8%) are related to precipitation of authigenic carbonates. Sr and S elements increase considerably in this unit. TOC percentages also vary greatly during this period but, in general, they are relatively high and increase upwards. Relatively low TOC/TN values (< 12) indicate the dominance of lacustrine organic matter (Meyers, 2003). Si, Ti, Fe and Mn show parallel trends to MS (table 2.3). Unit 2 can be subdivided into three sub-units, following the facies association. Thus, *BSM 2c* (491-350 cm depth; 5700-3540

| Facies | Facies description |
|---|---|
| **Clastic, laminated facies** | |
| **1** | Gray banded to laminated quartz and carbonate silts. Mostly composed by clay minerals (45 %), calcite (17 %) and, quartz (7 %) and low organic matter (<1%). High MS (100 SI). Laminated intervals are composed of up to 1 cm thick couplets of (1) black, carbonate silty-sands with high quartz content, abundant hematites, chlorite and maphic minerals and occasional terrestrial and macrophyte remains and (2) gray carbonate silts with lower silicate minerals content and rare organic matter. |
| **2** | Dark gray laminated carbonate silts. Mineralogical composition similar to Facies 1, but better laminated higher organic content (1-2 %) and lower MS (average 40 SI). Couplets composed of mm- thick laminae of (1) black, carbonate silty-sands with abundant terrestrial and macrophyte remains and (2) brown carbonate silts with less siliciclastic minerals and lower organic matter. |
| **3** | Light gray banded carbonate silts. Dominant carbonate content (TIC, X %; calcite, 40 %); quartz (6 %) and significant amounts of hematites, pyrite, clinochlorite, other maphic. Low organic matter (1%). Very high MS (>150 SI). |
| ***Interpretation*** | Clastic dominated deposition in distal, deeper setting. Laminated facies reflect flooding episodes reaching the centre of the lake. More abundant carbonate (Facies 3) or organic matter (Facies 2) reflects changes in watershed and littoral environments. |
| **Carbonate and organic-rich facies** | |
| **4** | Black, massive, carbonate silts. Composition is dominated by calcite (45 %), quartz (10 %), clay minerals (10 %) and organic matter (>2%) of terrestrial and macrophyte origin. Abundant pyrite and rare hematites. Low MS (25 SI). Occasional presence of pennate diatoms. |
| **5** | Light gray, massive, carbonate silts. Composition is dominated by calcite (70 %), with relatively low quartz and clay minerals (7 %) and organic matter (<2%); occasional pyrite and rare hematites. Low MS (25 SI). Organic matter is terrestrial, macrophyte and lacustrine origin. Mottling is common. Abundant gastropods and presence of pennate diatoms. |
| **6** | Light brown, banded, carbonate silts. Composition is dominated by calcite (30 %), clay minerals (15 %) and relatively low quartz (9 %) and organic matter (<2%) mostly terrestrial and macrophyte remains. |
| ***Interpretation*** | Carbonate dominated deposition in littoral environments with higher carbonate and organic productivity (Facies 5) deeper, with more frequent anoxic conditions (Facies 4) and transitional (Facies 6). |

**Table 2.2**. Facies description and interpreted depositional environment of BSM sequence.

cal yr BP) is constituted by the alternation of cm-thick intervals of Facies 4 and 6 and displays an upward TIC increase (up to 8%). TOC percentages are highly variable but generally low (1-2 %). *BSM 2b* (350-240 cm depth; 3540-2200 cal yr BP) represents a 1 m-thick interval of Facies 5 with the highest TIC, Ca and calcite values and the lowest TOC and MS of the sequence (fig. 2.14). Higher Sr values occur as a result of more abundant biogenic aragonite. Finally, *BSM 2a* (240-93 cm depth; 2200-700 cal yr BP) comprises rhythmic sequences of about 20 cm-thick composed of thin layers of Facies 1->, Facies 4 -> Facies 5 (detrital- organic-carbonate).

| | **Unit 1 (0-93 cm)** | | **Unit 2 (93-491 cm)** | | **Sub-unit 3a (491-690 cm)** | | **Sub-unit 3b (690-1168)** | |
|---|---|---|---|---|---|---|---|---|
| | MS | | MS | | MS | | MS | |
| | r | p | r | p | r | p | r | p |
| **Si** | 0.726 | < 0.001 | 0.546 | < 0.001 | 0.146 | 0.148 | -0.346 | < 0.001 |
| **Ti** | 0.699 | < 0.001 | 0.688 | < 0.001 | 0.280 | 0.005 | -0.388 | < 0.001 |
| **Mn** | 0.688 | < 0.001 | 0.545 | < 0.001 | 0.543 | <0.001 | 0.451 | < 0.001 |
| **Fe** | 0.806 | < 0.001 | 0.582 | < 0.001 | 0.643 | < 0.001 | 0.162 | 0.013 |
| **Ca** | -0.660 | < 0.001 | -0.564 | < 0.001 | 0.179 | 0.075 | 0.671 | < 0.001 |
| **TIC** | -0.700 | < 0.001 | -0.591 | < 0.000 | 0.404 | <0.001 | 0.689 | < 0.001 |
| **TOC** | -0.746 | < 0.001 | -0.409 | < 0.001 | -0.609 | < 0.001 | -0.494 | < 0.001 |

**Table 2.3**. Correlation values between Magnetic Susceptibility and other geochemical parameters in the different sedimentary units.

iii. Unit 1 (93-0 cm depth; 698 cal yr BP-2007 AD) comprises carbonate – poor Facies 1 and organic-rich Facies 4. As a consequence, all geochemical indicators show high variability. Facies 1 lamination is less well defined than in Unit 3. MS values increase again and show strong positive correlation with Si, Ti, Mn and Fe, while the correlation with Ca and TIC and TOC is strongly negative (table 2.3). TOC/N ratios increase at the base of the unit and decrease towards the top: TOC percentages show the opposite pattern.

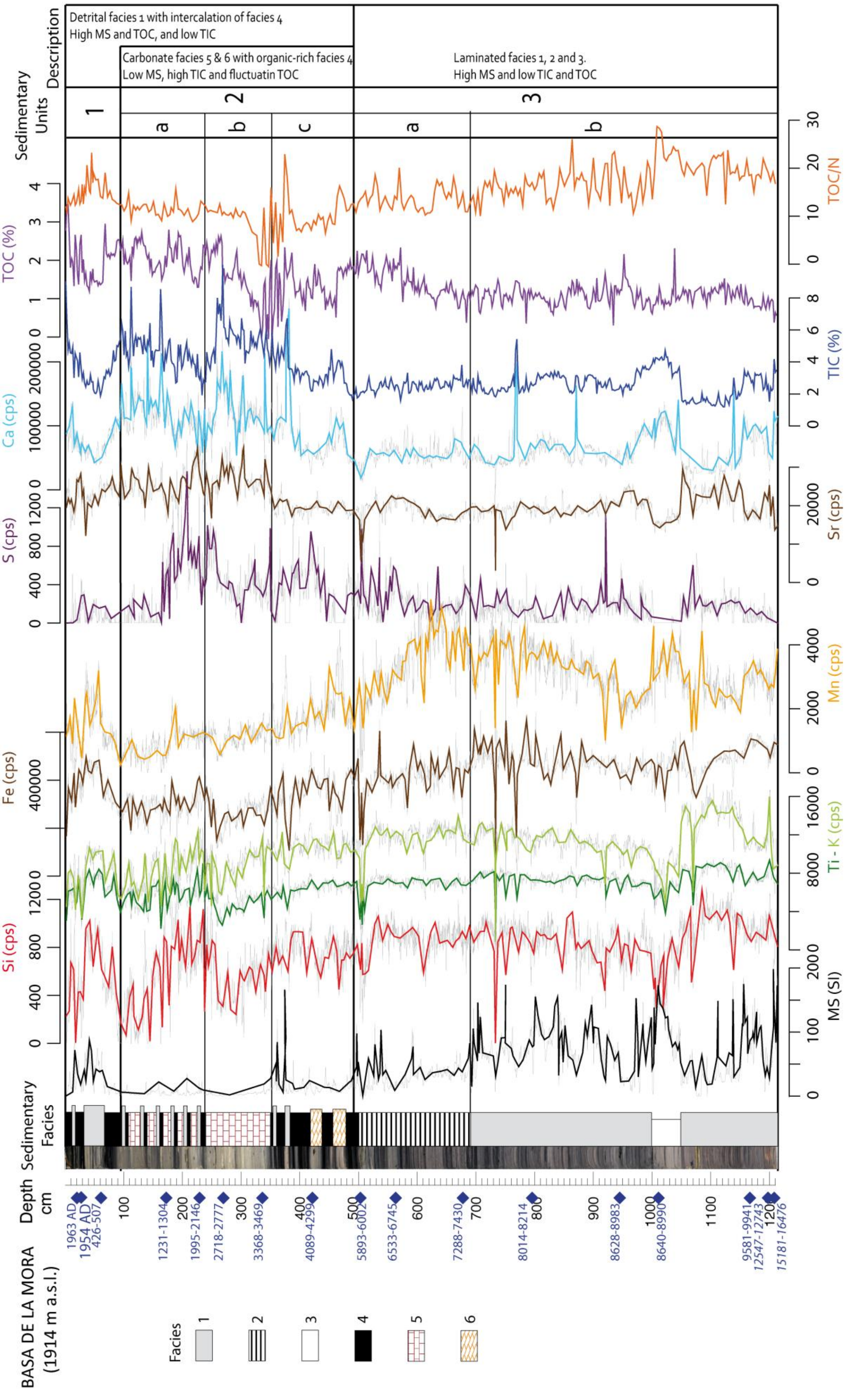


**Figure 2.14.** Main sedimentological features, geochemical and physical properties of the BSM sequence plotted in depth, indicating the location and results of radiocarbon dates.

### 2.4.3. Modern pollen rain

The modern pollen rain results agree largely with the regional vegetation around the Lake BSM. Despite the different distance to the lake (from 0 to 500 m), 7 out of 8 samples present stunning similar percentages of pollen highlighting the homogeneity of the pollen rain composition and its dispersal. Furthermore, the mean values of the modern pollen-rain samples compares fairly well with pollen percentages from the core-topmost sample (BSM08-1B-1G-1,12-13) (fig. 2.15). The AP values represent around 70% of the total, with *Pinus* accounting from approximately 60% in agreement with the dominance of this tree in the area and its high pollen productivity. Despite the distance of current formations to the lake (more than 5 km) (fig. 2.5 and Appendix I, fig A2.1), all types of *Quercus* are present in the pollen rain with values up to 5%. The mesophytes (*Betula*, *Corylus* and other Mesophytes grouo) show very low values or are even absent in some samples in agreement with their position in the bottom of the valleys. Regarding the main anthropogenic species it is

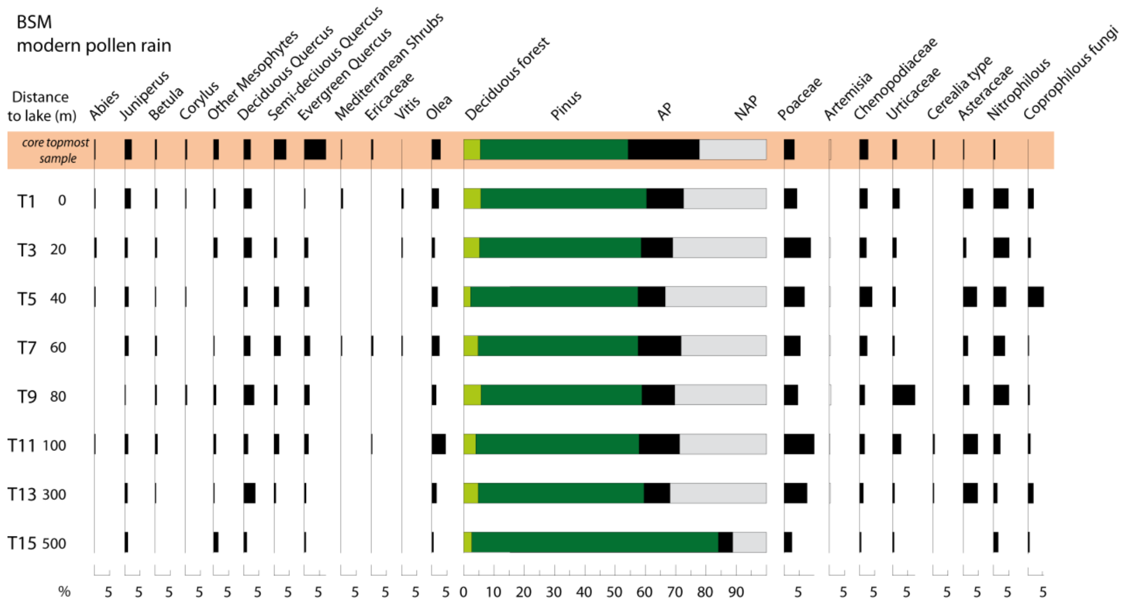


**Figure 2.15**. Modern pollen rain from 8 mosses samples collected across a distant transect from the lake shore to up 500 m. Sample highlighted in orange represents the core-topmost sample. *Other Mesophytes* group includes: *Alnus*, *Carpinus*, *Salix*, *Ulmus*, *Populus*, *Acer*, *Fraxinus* and *Juglans*. *Deciduous forest* group includes: *Betula*, *Corylus,* deciduous *Quercus Alnus*, *Carpinus*, *Salix*, *Ulmus*, *Populus*, *Acer*, *Fraxinus*, *Fagus*, *Tilia* and *Juglans*. *Nitrophilous* group includes: *Plantago* and *Rumex*.

remarkable the presence of *Olea*, with values ranging from 1 to 5%, and the occasional appearance of *Vitis*, in spite of the distance of the olive and wine fields to the lake, indicating the long-distance transport of these two species, particularly Olea (Cañellas-Boltá et al., 2009). Conversely, there is a large underestimation of all herbaceous species. The spare sample (T15) shows an overrepresentation of *Pinus*, reaching almost 85%, and an underrepresentation of the rest of trees. Nevertheless, this sample is located the farthest from the lake (500 m) and in any case, those values disguise the real vegetation composition. Despite the current grazing activity recognized in the area, only Urticaceae, *Rumex* and *Plantago* proportions (nitrophilous taxa) appear significant, while *Artemisia* values are remarkably low or even absent. This taxon is usually considered as anthropogenic indicator also in Late Holocene records, but in the case of the BSM sequence it seem not be related to the occurrence ofrecent human pressure given that, depite the current moderate grazing activities in the area, it is absent in current vegetation formations. Additionally, coprophilous fungi, other usual indicator of human pressure in pollen diagrams (López-Merino et al., 2011; Morales-Molino, 2013) are not a relevant component of the modern pollen rain.

In general, these results suggest that in the BSM sequence, tree values around 5% seem represent middle distance presence while tree values under 5% represent long-distance presence. They also suggest that the grazing activity cannot be directly related to the presence of *Artemisia* nor coprophilous fungi as often used in palynological interpretations, but to the presence of nitrophilous (like *Rumex* or *Plantago*) plants instead.

The matching values between the modern pollen rain and the vegetation present in the area validate the fossil pollen rain as representative of local, nearby and relatively regional past vegetation landscapes.

### 2.4.4. Pollen and charcoal data

The pollen record can be divided into six zones (BSM-0 to BSM-V: fig. 2.16). In BSM-I to BSM-V (9.8 ka cal BP-present), the 5 cm-resolution pollen analyses provide a temporal resolution of 22 to 150 years per sample. Statistical results for pairwise comparison between vegetation and geochemical parameters are shown in table 2.4. The maximum number of charcoal particles counted was 3098, with a mean of 307 and a SD of 453. The patterns of charcoal influx are consistent with the pollen zones. Appendix I (figs A.2.2, A2.3 and A2.4), located at the end of the thesis, shows all taxa found for the BSM sequence.

BSM-0 (1209-1167.5 cm depth; before 9800 cal yr BP)

This zone is characterised by scarce representation of the herbaceous component (NAP) and particularly the steppe taxa group (*Artemisia*, Chenopodiaceae, *Helianthemum, Plantago, Rumex*, which rarely exceed 5-10 %), and abundant representation of arboreal pollen (AP), dominated by conifers (mainly *Pinus*) and deciduous forest taxa (*Betula*, *Corylus*, *Alnus*, *Salix*, *Ulmus*, *Populus*, *Acer*, *Fraxinus*, *Fagus*, *Tilia* and deciduous *Quercus*), with values around 25-30 % (fig. 2.16). Representation of Poaceae and aquatics (Cyperaceae, *Ranunculus, Myriophyllum* and *Potamogeton*) in this zone is not significantly different to the rest of the sequence. The pollen spectra of this zone are not consistent with a pre-Holocene deposit as would be inferred from the two dates (15.8 cal ka BP and 12.6 cal ka BP) from this interval. Pollen content, together with the lack of sedimentological evidences for a hiatus, indicates that these dates are too old, due to a possible reservoir effect. Both palynological and sedimentological data suggest these are Holocene sediments, but given the absence of chronological control the record from this zone is not further considered in this study.

BSM-I (1167.5-815 cm depth; 9800-8200 cal yr BP)

Arboreal pollen varies between 60 and 80% of the total pollen abundance, and in some cases it exceeds 85%. *Pinus* is the main arboreal taxon, but deciduous taxa are well represented by *Betula*, *Corylus* and deciduous *Quercus,* with some significant fluctuations in *Betula*. *Juniperus* is also present with percentages above 6%. Evergreen *Quercus* and Mediterranean shrubs (*Pistacia*, *Rhamnus*, *Phillyrea*, *Buxus*, *Sambucus*, *Ephedra fragilis* and *E. distachya*) are present in relatively low but continuous percentages. The first *Tilia* appearance is recorded at 870 cm depth (8500 cal yr BP); this timing is consistent with other records from the region (Montserrat-Martí 1992; González-Sampériz et al., 2006; Miras et al., 2007; Pèlachs et al., 2007). Poaceae dominates the herbaceous stratum, while the abundance of *Helianthemum* significantly declines and *Artemisia* decreases in importance. *Myriophyllum* is the dominant aquatic. A significant change is found towards at the end of the zone (860 - 815 cm depth; 8400-8200 cal yr BP) characterized by a sharp decline in *Betula*, *Corylus* and deciduous *Quercus*, the virtual disappearance of Other Mesophytes (fig. 2.16) and the total absence of *Tilia*. *Pinus* increases to its maximum in the whole sequence, reaching 75%, and *Helianthemum* reappears at this time. This is a phase of high variability in fire activity, although charcoal counts are very low. *Pinus* and *Juniperus* show a positive correlation with MS within this zone, while *Betula*, *Corylus*, *Quercus faginea*, evergreen *Quercus* and *Myriophyllum* are negatively correlated with MS (table 2.4). Thus, MS is correlated negatively with moisture-adapted and temperate taxa, but positively with more drought-resistant taxa such as *Pinus* and *Juniperus*.

BSM-II (815-491 cm depth; 8200-5700 cal yr BP)

After the short, abrupt vegetation change previously described, forest contracts slightly but there is considerable compositional variability. *Pinus* decreases to 35% and *Juniperus* is also highly reduced in abundance. Deciduous taxa, mainly *Betula*, *Corylus* and deciduous *Quercus,* show large and more continuous expansion reaching their maximum values in the sequence (fig. 2.16). *Tilia* reappears and is constantly present at moderate levels throughout the zone. Evergreen *Quercus* declines to its minimum values, while Mediterranean Shrubs fluctuate in abundance. The first isolated appearance of *Abies* occurs at 646 cm (7200 cal yr BP). The NAP is mainly composed by Poaceae, *Artemisia* and Lamiaceae, as in the rest of the record. Aquatic plants are well represented by Cyperaceae, *Pedicularis, Ranunculus* and *Potamogeton,* although *Myriophyllum* is dominant and reaches its highest values in the sequence. Deciduous *Quercus* and *Tilia* abundances show a strong negative correlation with MS (table 2.4). There is an increasing trend of fire activity, although the variability is high (Lasheras et al., 2013).

BSM-III (491-389 cm depth; 5700-3900 cal yr BP)

The beginning of this zone is characterized by a steep decline in deciduous forest taxa, mainly *Betula* (abruptly reduced by nearly 60%) and deciduous *Quercus*. In contrast, *Pinus* expands rapidly and *Juniperus* and evergreen *Quercus* increase slightly (fig. 2.16). *Fagus* appears for the first time, chronologically fitting the regional expansion (Montserrat-Martí, 1992; Pla and Catalán, 2005). The base of the zone is characterised by the permanent presence of *Abies* in the area, after its initial appearance shortly before. Poaceae, *Artemisia,* Lamiaceae and Chenopodiaceae are still the main NAP taxa and *Rumex* rises. No significant changes are recorded on the aquatic component except a decrease in *Myriophyllum* and a short-term disappearance of *Potamogeton* at the base of the zone. The conifer/mesophyte ratio is inverted at the top of the zone, just before the transition from Sub-unit 2c into Sub-unit 2b. Fire activity reaches a maximum towards the end of this zone.

| | **BSM III & BSM IV (93-491 cm)** | | **BSM II(491-815 cm)** | | **BSM I (815-1168 cm)** | |
|---|---|---|---|---|---|---|
| | MS | | MS | | MS | |
| | r | p | r | p | r | p |
| ***Pinus*** | 0.453 | 0.003 | 0.444 | 0.006 | 0.464 | 0.001 |
| ***Juniperus*** | 0.351 | 0.023 | — | — | 0.339 | 0.021 |
| ***Betula*** | -0.573 | < 0.001 | — | — | -0.517 | < 0.001 |
| ***Corylus*** | — | — | — | — | -0.292 | 0.049 |
| ***Tilia*** | — | — | -0.537 | 0.002 | — | — |
| **Dec. *Quercus*** | — | — | -0.528 | 0.001 | — | — |
| ***Quercus* fag.** | -0.401 | 0.009 | — | — | -0.373 | 0.018 |
| **Ever. *Quercus*** | -0.378 | 0.014 | — | — | -0.505 | < 0.001 |
| ***Artemisia*** | — | — | -0.433 | 0.007 | — | — |
| **Cyperaceae** | — | — | 0.414 | 0.017 | — | — |
| ***Myriophyllum*** | — | — | — | — | -0.592 | < 0.001 |

**Table 2.4**. Correlation between MS and pollen taxa in the different pollen zones.

BSM-IV (389-93 cm depth; 3900-700 ca yr BP)

The beginning of this zone is characterized by a change in forest composition. *Pinus* recovers and becomes the dominant arboreal taxon, *Abies* reaches its maximum abundance and *Betula* exhibits its minimum values (fig. 2.16). *Juniperus* and evergreen *Quercus* increase, but *Corylus* and Other Mesophytes only experience a slight increase. *Tilia* decreases progressively and disappears at top of the zone. In contrast, *Fagus* reaches its highest levels, at a time consistent with other records from the region (Pla and Catalán, 2005; Pérez-Obiol et al., 2012). A sudden and abrupt rise of *Artemisia* and further decrease in mesophyte taxa accompany the *Pinus*-dominant landscape. The NAP, of which Poaceae and *Artemisia* constitute the main elements, accounts for 40% of the pollen sum. There are two peaks of *Artemisia* in this zone, the most modern (ca. 1000-1300 A.D) of which (when *Artemisia* reaches its maximum value in the whole sequence) coincides with the disappearance of *Abies* and *Tilia*. The aquatic component is markedly reduced in abundance, with low values of *Myriophyllum* and the absence of *Potamogeton* during the most of the zone contrasting with an increase in Cyperaceae. Cultivated taxa like *Olea*, *Vitis*, *Castanea* and *Cerealia* type appear more continuously. Although there are some marked peaks of *Pinus* in this zone, the general trend is for relatively stable pine forest during the last phase of sedimentary Sub-units 2b and 2a. An abrupt decrease in charcoal concentration lasting several centuries was followed by a new abrupt increase in fire activity at the end of the zone.

BSM-V (93-0 cm depth; 700 cal yr BP-present, 1250-2008 cal AD)

This zone is characterized by important changes in both pollen and sedimentological records (Unit 1). The most relevant feature is the increase in *Olea* and *Fraxinus. Pinus* increases up to the 70%, but with very short episodes of were abundance is much lower (40%). The expansion of pine is coincident with the decline of *Abies*, *Betula, Corylus* and Other Mesophytes (fig. 2.16). Deciduous *Quercu*s and, especially evergreen *Quercus* increase in abundance in the topmost part of the sequence. The NAP is still dominated by Poaceae, but *Artemisia* drops dramatically while Asteraceae and Chenopodiaceae reach their maximum values. *Myriophyllum* becomes less important and Cyperaceae dominates the aquatic assemblage. Variations in MS at this time are not correlated with vegetation composition changes. Fire activity is very high during most of the zone, but ceases in the top part of the record.

### 2.4.5. Chironomids

A total of 6422 chironomid head capsules were picked up, individually mounted and identified from 71 samples of the core BSM08-1A by Pol Tarrats and Maria Rieradeval (Universidad de Barcelona) (Tarrats, 2011). Total chironomid biodiversity was represented by 18 taxa (up to 9 taxa per sample), belonging to three chironomid subfamilies: *Tanypodinae, Orthocladiinae* and *Chironominae. Tanytarsus* gr. *lugens* was the most abundant all through the core, followed by *Procladius*, *Chironomus* and *Paratanytarsus*. *Chironomus* or *Paratanytarsus* are not shown in the diagram (fig. 2.17) because they are present through the entire sequence and show no clear pattern of changes through the Holocene. The chironomid assemblage indicates that the lake has been always relatively shallow and oligotrophic, although relatively rich in organic matter. Quantitative analysis of the *Chironomidae* allows the sequence to be divided into 4 zones:

CHZ-1: Chironomid Zone 1 (1168.5-491 cm depth; 9895 - 5700 cal yr BP)

Low values characterize this zone. *Tanytarsus* gr. *lugens* abundance is relatively low although with some fluctuations. *Procladius* reaches its maximum relative abundance within the core (30-60%), whereas *Pentaneurini* tribe appears through the entire zone although with a highly fluctuating distribution. The *Orthocladiinae* tribe is quite diverse, with an early representation of *Psectrocladius* gr. *limbatellus* and *Corynoneura* and a moderate representation of *Orthocladiinae* indet. (5-7%), which include several taxa related to water runoff and seepages (e.g. *Smittia*).

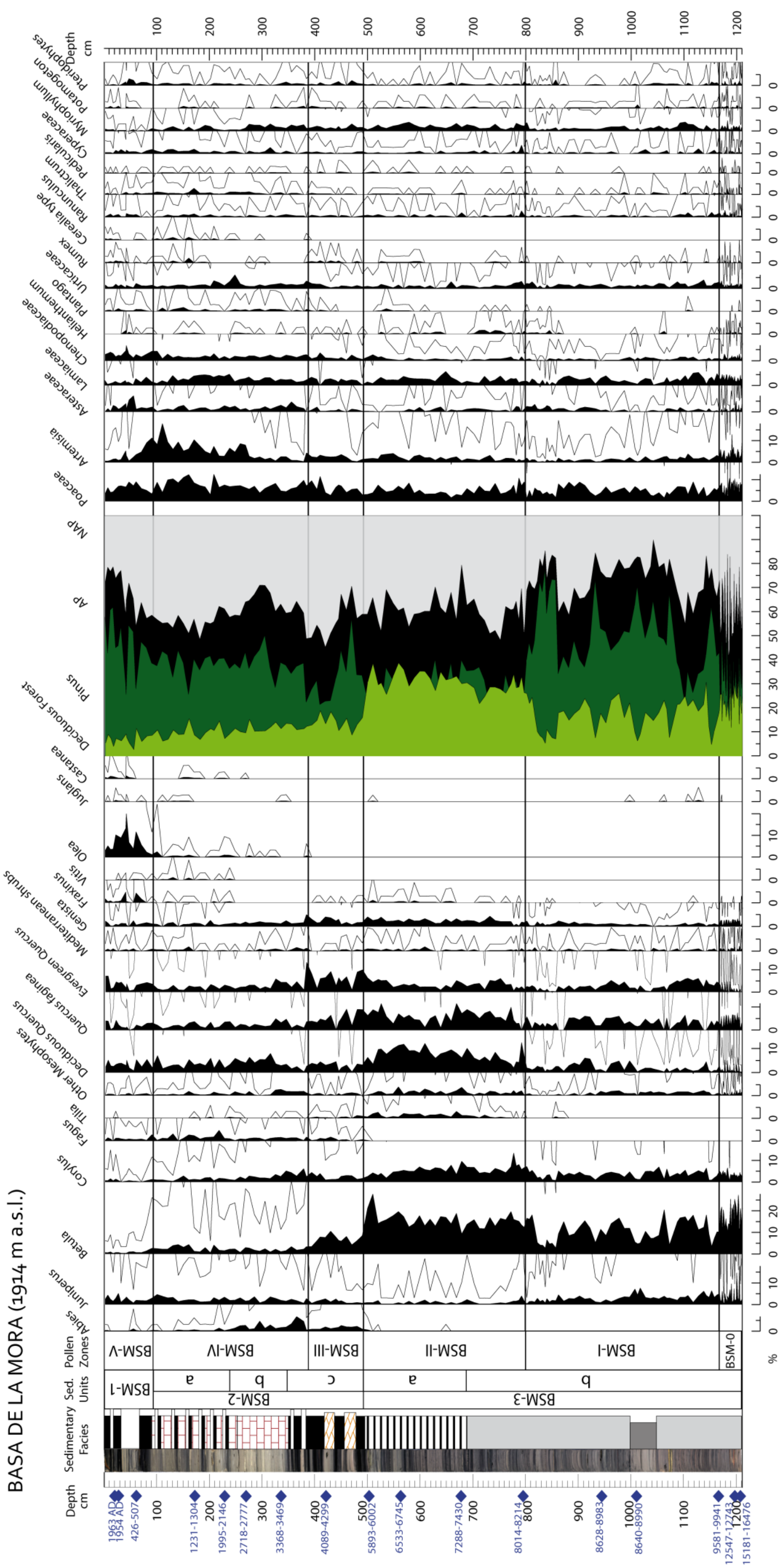


**Figure 2.16.** Pollen diagram of selected taxa from Basa de la Mora sequence, plotted in depth. Other Mesophytes curve groups *Alnus*, *Salix*, *Ulmus*, *Populus* and *Juglans* pollen types; Mediterranean shrubs groups *Pistacia*, *Rhamnus*, *Phillyrea*, *Buxus*, *Sambucus*, *Ephedra fragilis* and *E. distachya* pollen types; and Deciduous forest curve groups *Betula*, *Corylus*, *Fagus*, *Tilia*, deciduous *Quercus* and *Other Mesophytes* pollen types. As usually, AP includes all the arboreal taxa (trees and shrubs) and NAP the herbaceous component excluding aquatics and ferns.

CHZ-2: Chironomid Zone 2 (491-357 cm depth; 5700 - 3600 cal yr BP)

The abundance of *Tanypodinae* subfamily taxa (*Procladius* and *Pentaneurini*) reduced, whereas *Tanytarsus* gr. *lugens* increase and remains relatively high values throughout the zone (50-60%). Chironomid content values increase, although 3 samples from the base of the zone were almost sterile.

CHZ-3: Chironomid Zone 3 (357-56 cm depth; 3600 - 350 cal yr BP)

High chironomid content occur, although decreases towards the top of the zone. The main difference from the previous zone is the presence of *Psectrocladius* gr. *limbatellus* throughout the zone with relatively high abundances (up to 20%). *Procladius* reaches relatively high abundance (10-20%), although it does not reach previous values.

CHZ-4: Chironomid Zone 4 (56-0 cm depth; 350 cal yr BP - present; 1600 - 2008 AD)

The uppermost zone is characterized by a strong increase of *Psectrocladius* gr. *limbatellus,* together with *Pentaneurini* and *Corynoneura,* and a reduction in *Tanytarsus* gr. *lugens*. Percentage values, particularly of *Procladius,* fluctuate, although its abundance is similar to the previous zone.

## 2.5. DISCUSSION

### 2.5.1. The Early Holocene (9800-8150 cal yr BP): strong Mediterranean influence and high climate variability

During the Early Holocene, the Atlantic regions of Iberia were dominated by deciduous broadleaf trees (Santos et al., 2000; Muñoz-Sobrino et al., 2005, 2007; Moreno et al., 2011) while the Mediterranean, mountain and inland areas were covered mainly by dense pine forest (Carrión et al., 2010; Franco-Múgica et al., 2000; Rubiales et al., 2010 Morales-Molino et al., 2012). The southern Pyrenees record both climate regimes in a relative small area: the Atlantic climate to the west and the Mediterranean climate to the east. These particular geographical features led to some marked differences in plant communities between the two regions at the onset of the Holocene. Increasing humidity was much pronounced in the Atlantic-influenced area, with a large expansion of mesophytes (Montserrat-Martí 1992; González-Sampériz et al., 2006), while pine was the main tree taxon in the Mediterranean-influenced region (Miras et al., 2007; Pérez-Obiol et al., 2012). This suggests a stronger W-E precipitation gradient in the southern Pyrenees at the onset of the Holocene, with stronger influence of humid fronts in the west and persistent summer drought in the east.

In the BSM sequence, located at the modern transition between the Atlantic and Mediterranean climate regimes, the Early Holocene is characterized by the dominance of conifers over mesophytes (BSM-I) (fig. 2.17). High values of pines and *Juniperus* reflect a continental Mediterranean-climate influence during this period. The fire regime is not characterised by either frequent or virulent fires, probably because of fuel limitation as pine-dominated forests are less flammable than broadleaf woodlands. The dominance of *Pinus* over deciduous taxa suggests the existence of extreme seasonal temperatures and marked summer drought during the Early Holocene. However, deposition of carbonate-poor laminated Facies 1 and 3 indicates permanent and relatively high lake levels with abundant sediment delivery by run-off. High values of MS are related to the presence of paramagnetic minerals eroded from ophite outcrops and are consistent with high-energy transport to the lake. High correlation between MS and Ca and TIC is indicative of the detrital origin of carbonate minerals and supports high erosion rates during this period. The high abundance of non-lacustrine *Orthocladiinae* taxa, related to inlet streams, in this zone supports the idea of increased runoff due to high rainfall. The *Procladius* genus has been reported to be important in the Early Holocene in other European regions (Heiri et al., 2003) and its high abundance is consistent with higher lake levels because it inhabits fine sediments in the profundal zones of lakes (Saether, 1979; Prat et al., 1992).

The Early Holocene maximum in seasonality in the Northern Hemisphere may have been responsible for particularly cold winters and hot summers in mid latitudes. In the southern Pyrenees, this would have led to increased snow accumulation in winter and subsequent large snowpack melt during the warmer summer months leading to higher run-off. Evapotranspiration and low precipitation during summer drought periods would be largely compensated by increased melting water, leading to higher lake levels. The negative correlation between moisture-adapted taxa and MS supports the idea that run-off would be likely linked to melt processes rather than direct precipitation. Furthermore, positive correlation between MS and drought-resistant taxa such as *Juniperus* and *Pinus* confirms that run-off is related to increased continentality during this period.

The relatively dry and cold Early-Holocene climate of the Basa de la Mora (BSM) is in agreement with many studies from western Europe (Leira and Santos, 2002; Bjune et al., 2005;) and North America (Shuman et al., 2001; Zhao et al., 2010), which have inferred a cooler and drier climate probably related to weakened ocean conveyor circulation as the rapid, global increase in temperature provoked large input of freshwater from the Laurentide sheet into the North Atlantic, weakening Labrador Sea deep convection (Kaplan and Wolfe, 2006; Renssen et al., 2009, 2012).

Superimposed on the long-term insolation-driven climate trend, the BSM sequence shows significant short-term (submillennial) shifts in pollen percentages and sedimentological features during the Early Holocene. Such shifts occurred at 9.7, 9.3, 8.8 and 8.3 cal ka BP and are mainly characterized by short-term expansion of pine, accompanied by large reductions in all deciduous taxa but most particularly in *Betula*, implying a substantial reduction in humidity. The highest MS values of the whole sequence are also recorded during these events, indicating that these periods are characterised by particularly intense run-off and sediment delivery from the catchment (fig. 2.17). Cold and relatively humid winters with large amount of snow accumulation, and the subsequent snowpack melt and runoff could be responsible for increased erosion in the catchment. This interpretation is supported by the sharp and discontinuous presence of rheophilous and non-strictly lacustrine chironomid taxa during these short-events. Low percentages of TOC and low TOC/N ratio also point to reduced vegetation in the catchment (fig. 2.17). Phases of reduced forest may be due to a downward displacement of the treeline, supporting the occurrence of cooler temperatures. These events were as short-lived periods of drier and cooler conditions. Sedimentary phases with particularly high sedimentation rates associated with arid conditions have been recognised in the Central Ebro Basin complex during this period (Sancho et al., 2008; Gómez-Paccard et al., 2013). The strong response of the vegetation and hydrology at BSM indicates that climate instability was characteristic of the Early Holocene. Similar evidences for Early Holocene climatic oscillations have been widely recognised throughout the North Atlantic region (O´Brien et al., 1995; Alley et al., 1997; Mayewski et al., 2004; Bond et al 1997, 2001; Frigola et al., 2007).

The first Early Holocene cold event is recorded just at the beginning of the BSM sequence at 9.8-9.7 cal ka BP. Since the BSM record starts at 9.8 cal yr BP, we suggest that this may be coincident with the short-lived 9.95 ka cold anomaly detected in the NGRIP record (Rasmussen et al., 2007). The impact of this anomaly has been previously noted in the western Mediterranean as a phase of forest decline (Fletcher et al., 2010b), as in BSM sequence. A global event centred in 9.3 ka cal BP has been widely recorded in many sequences from the North Atlantic and Europe (Haas et al., 1998; Rasmussen et al., 2007; Fletcher et al., 2013b). In the BSM sequence, this interval coincides with an expansion of pine forest and decline in mesophyte taxa but there is no sedimentological change. The next cold and arid event occurs at 8.8 ka cal BP. In BSM sequence, this event is resulted in major shifts in vegetation and sediment deposition and the apparent disappearance of chironomids. This phase coincides with the only occurrence of Facies 3 and the high TOC/TN ratios characteristic of this unit suggest a well-vegetated watershed, dominated by *Pinus*. The 8.8 ka cal BP cool event is reported in the Artic by Ebbesen et al., (2007) but has not previously been reported in southern Europe.

The next event is recorded at 8.3 ka cal BP. This is the most remarkable vegetation shift in the BSM record, with *Pinus* reaching its highest values and *Betula* dropping to its minimum. Taking into account the age-depth model uncertainties for this period (8300 ± 100 cal yr BP), this event could be synchronous with the 8.2 ka cool event (Alley and Agustsdottir, 2005; Rasmussen et al., 2007), triggered by a large freshwater discharge from former glacial Lake Agassiz into the North Atlantic Ocean, causing a reduction of the Atlantic Meridional Overturning Circulation (AMOC) (Hoffman et al. 2012). The high-resolution study carried out in BSM sequence for this period indicates a minimum timing of 150 years and maximum of 200 years for the 8.2 ka event. This timing agrees with the precise characterization of the 8.2 ka event obtained from trapped air in a Greenland ice core (GISP2) (Kobashi et al. 2007). The abrupt increase in pine in BSM matches the spread of *Pinus* recorded in the Alps (Blarquez et al., 2009), Switzerland (Tinner and Lotter, 2001) and northern Spain (Muñoz Sobrino et al., 2007), suggesting a widespread impact in mountain/alpine regions. The 8.2 event is widely recorded in the north-eastern of the Iberian Peninsula, where human settlements located in a particular harsh region of the Central Ebro basin moved towards more humid areas during this interval (González-Sampériz et al., 2009).

The rapid response of the vegetation to these short climate shifts, related to changes in the North Atlantic, seems to be amplified in the BSM sequence because of its ecotonal location for some species. The highly responsive nature of the vegetation record highlights the climate sensitivity of high altitude transitional areas to environmental changes, as previously demonstrated for the central Pyrenees during the Lateglacial period in El Portalet sequence (González-Sampériz et al., 2006).

### 2.5.2. The Mid-Holocene (8100-5700 cal yr BP): the Climatic Optimum

The Mid-Holocene is the period with the greatest forest development in Europe, when treeline moved upward and reached its maximum elevation in most mountain regions (David 1993; Ali et al.2003; Ortu et al., 2008; Carnelli et al., 2004; Favilli et al., 2010; Talon et al., 2010; Cunil et al., 2011; Magyari et al., 2012). In northern Europe, forest expansion is related to higher summer temperature (Davis et al., 2003; Bjune et al., 2005; Nesje et al., 2006), while in southern Europe this is an interval of increased humidity (Carrión et al., 2010; Colonese et al., 2010; Spötl et al., 2010; Stoll et al., 2013).

There is a marked shift in the vegetation composition after ca 8.2 ka BP in the BSM sequence, (fig. 2.17). *Betula*, *Corylus* and deciduous *Quercus* became the dominant AP elements, *Tilia* and other mesophytes were present, and conifers declined to their minimum values, with pine oscillating between 20-30 % and juniper between 2-3% (fig. 2.17). This assemblage is very different from that of a dense conifer community near the lake (Court-Picon et al., 2005). The high values of *Betula* (up to 26%) in the BSM sequence compare fairly well with similar high values recorded in the Pyrenean sequence of El Portalet peatbog (González-Sampériz et al., 2006), located at 1802 m a.s.l, Lake Burg (Pèlachs et al., 2007), located at 1821 m a.s.l. or Tramacastilla lake, at 1682 m a.s.l., where birch accounted for 40% of the total pollen (Montserrat-Martí, 1992). The similarity between these sequences indicates that *Betula* grew at higher altitude, in the upper part of the montane belt and probably reaching the subalpine belt. The rise of birch and the consequent drop of pine at BSM could result from either an increase in annual precipitation or reduced evaporation, as a consequence of decreased continentality, favouring water-demanding taxa. High charcoal values indicate increased regional fire activity (Lasheras et al., 2013). An increase in moisture does not necessarily imply reduced fire activity; the expansion of mesophytes, which are more flammable than most mountain pines (Blarquez and Carcaillet, 2010), provides high amounts of fuel at an altitudinal zone normally devoid of large forest to be burnt. Only minimal changes in summer climate or lightning would be required to promote large and virulent fires, leaving a sizeable imprint in the charcoal record. In addition *Betula* is a pioneer taxum that spreads well after fire disturbances (Blanco, 1997; Morales-Molino et al., 2012; Gil-Romera et al., accepted). This pattern has been also found in El Portalet sequence and in many other Holocene records from the European mountains (Tinner et al., 1999; Colombaroli et al., 2008; Vannière et al., 2008) as well as in current patterns of fire occurrence (Pausas and Paula, 2012).

The interval from 8100-5700 cal yr BP was characterized by stable environmental conditions in the BSM catchment, as inferred from the stable vegetation composition and the lack of marked decreases in any tree taxon despite the high fire activity. Sedimentological and geochemical indicators point out a stable, relatively deep lacustrine environment. The laminated nature of Facies 2 is consistent with high lake level and the activity of several inflow streams. The finer grain size of Facies 2, in comparison to laminated Facies 1 and 3, indicates even higher lake levels. Low values of TIC and Ca suggest dilute water, and the lack of a significant correlation between Ca and MS indicates that delivery of carbonates from the catchment through run-off was negligible. Moreover, the decrease in MS and TOC/N along with the increase in TOC suggests a more vegetated environment that would limit the erosive effect of precipitation. High and constant *Myriophyllum* values and the chironomid association also reflect a well-established, deeper lacustrine environment; as genus *Procladius* presents its highest abundances along the sequence and *Tanytarsus* gr. *lugens* is also important in the chironomid assemblage. Moreover, the increase of littoral and macrophyte-related taxa such as *Corynoneura* or *Pentaneurini* tribe (e.g. Brodersen et al., 2001) during this period, reflects the greater development of aquatic vegetation in the lake favored by milder climate conditions.

The Mid-Holocene warmer conditions occurred when the flux of meltwater from the Laurentide ice sheet stopped and deep convection in the Labrador Sea led to enhanced transport heat over the Atlantic-influenced area (Renssen et al., 2009, 2012). Increased meridional circulation in the North Atlantic as the Laurentide sheet waned could bring warmer conditions to the Iberian Peninsula. Changes in the SST and shifts in insolation triggered reorganization of the atmosphere circulation and strengthened meridional atmosphere circulation. A northward shift of the monsoon system and its associated rainfall belt gave rise to particularly humid conditions in the Sahara and Sahel (deMenocal et al., 2000; Hély et al., 2009). Enhanced westerlies could bring increased summer humidity over the Iberian Peninsula, as inferred from the spread of broad-leaf taxa in this region (Pantaleón-Cano et al., 2003; Carrión et al., 2001, Carrión, 2002).

Although this interval (8.2-5.7 cal ka BP) is the most humid period recorded at BSM, high MS and a slight expansion of *Pinus* indicates a short-lived arid event around 7.5 cal ka BP. However, mesophytes only decrease slightly suggesting this interval was less pronounced than in previous arid intervals. This event is broadly coincident with the arid 7.4 event detected in southern Spain (Jalut et al., 2000) that has been related to the emergence of the Neolithic in southern Iberia (Cortés Sánchez et al., 2012), and also correlates with a phase of forest decline detected in the western Mediterranean (Fletcher et al., 2010a). In the central southern Pyrenees, this phase does not represent a dramatic change in moisture supply and vegetation recovers rapidly.

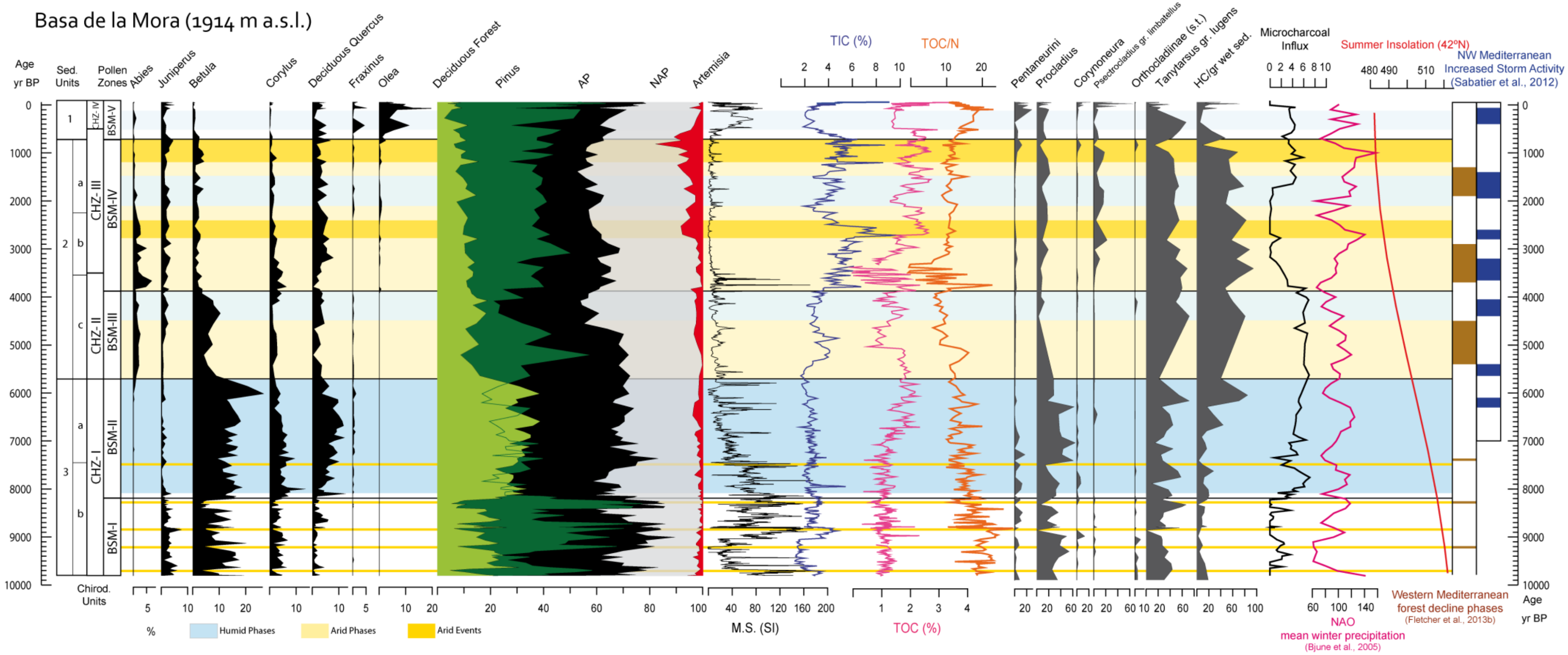


**Figure 2.17**. Diagram plotted in age, including selected pollen taxa, geochemical parameters, chironomid taxa and microcharcoal influx curves of Basa de la Mora sequence compared to NAO summer insolation curve for latitude 24ºN, regional phases of deforestation (Fletcher et al., 2013b) and phases of increased storm activity (Sabatier et al., 2012) in the Western Mediterranean. Note: Orthocladiinae (s.t.) means sum of rheophilous (see page taxa). Blue horizontal bars represent humid phases whereas yellow and orange bands represent arid phases and further arid events respectively.

### 2.5.3. The end of the Middle Holocene (5700-3900 cal yr BP): transition phase

The evolution of the landscape in southern Europe from 6 ka (or even earlier) onwards has been widely assumed to be influenced by both climate and human forcings (Oldfield and Dearing, 2003; Vannière et al., 2008; Roberts et al., 2011, Sadori et al., 2011). Many palynological studies show a clear increase of anthropogenic indicators from the Middle Holocene, pointing to an intensification of human activities and a subsequent change in the vegetation composition related to forest clearance for pastures and agriculture fields (Jalut et al., 2009). However, some of these taxa are naturally found in xeric Mediterranean ecosystems (De Beaulieu et al., 2005) and this makes it difficult to discriminate between climate and anthropogenic forcings. The spread of xeric vegetation across the Mediterranean region during Middle-Holocene does not necessarily imply anthropogenic degradation of the landscape (Collins et al., 2012). In addition, fire activity in Mediterranean areas increased significantly at this time and its impact on vegetation composition has to be taken into consideration (Colombaroli et al., 2007, 2008, 2009; Vannière et al., 2008, 2011). Increased fire activity can result from anthropogenic activities but also reflects the climatic shift towards arid conditions (Carrión et al., 2001a, 2010; Fernández et al., 2007; Fletcher and Sánchez-Goñi 2007; González-Sampériz et al., 2008; Morellón et al., 2008; Jalut et al., 2009; Corella et al., 2010; Anderson et al., 2011). The expansion of heliophytes (like *Artemisia,* Chenopodiaceae, Asteraceae, *Rumex, Plantago,* and Poaceae Mediterranean species similar to *Cerealia* type) observed during this period is favoured by increased fire, increased aridity, and anthropogenic activity. Overall, the complex changes found in Mediterranean areas at the end of the Mid-Holocene are not necessarily related to intense human pressure, but could equally well be explained by the trend towards drier conditions.

There is a sharp change in the vegetation cover and sedimentological features in the BSM sequences at 5.7 cal yr BP. The pollen record in BSM-IV (fig. 2.17) is characterized by a pronounced increase in pine and decrease in mesophytes, mainly *Betula*, in combination with a rise in *Juniperus*, deciduous and evergreen *Quercus* and heliophytes (*Artemisia* and Chenopodiaceae). The replacement of mesophytes by conifers suggests a change from humid to drier conditions or, at least, a significant shift in the seasonal distribution of the precipitation since reduced summer rainfall is unfavourable to the broad-leaf taxa. The sedimentary shift is defined by an increase in carbonates, indicating lower lake levels (Sub-unit 2c). Lower values of MS suggested reduced sediment transport as consequence of lower run-off and inflow streams, which in turn indicates reduced precipitation or meltwater inputs. The decrease in allochthonous sediments is reflected in lowered sedimentation rates and deposition of carbonate Facies 6, which reflects high carbonate productivity in a littoral setting with low and fluctuating water level. The decline in *Myriophyllum* is consistent with a reduction in water level (figs. 2.16 and 2.17). Moreover, the sharp decrease in *Procladius* and the near disappearance of non-lacustrine *Orthocladiinae* taxa also indicates reduced runoff and stream inflow during this period. The increase in chironomid abundances, mainly *Tanytarsus*, could indicate increased decomposition rates in the sediments.

Both biological and sedimentological indicators are consistent with a trend to increased aridity and a persistent arid phase between 5.6 to 4.6 cal ka PB (fig. 2.15). Similar vegetation changes have been recognised in other Pyrenean sequences (Pelachs et al., 2007), in southern Spain (Jiménez-Moreno and Anderson, 2012) and in Mediterranean records (Carrión et al., 2010). Fletcher et al., (2013b) have identified a major phase of deforestation in the Western Mediterranean during this period. The coincidence between lowered lake levels and forest decline supports the idea of climate as the main forcing. A major climate shift has been recognised in many other regions at this time, including the end of wet conditions in the Sahara between 6 and 5.5 cal ka BP (deMenocal et al., 2000; Kröpelin et al., 2008), and lake-level and vegetation changes indicating drier conditions in eastern North America (Shuman et al., 2001; Zhao et al., 2012; Menking et al., 2012). The similarities in climate changes between such different geographic areas during the Mid-Holocene suggest broad-scale changes in the coupled ocean-atmosphere circulation. This large-scale and synchronous climate shift may be related to changes in global atmospheric circulation. The weakened summer insolation in North Hemisphere led to a southward shift in the Inter Tropical Convergence Zone (ITCZ) and thus, the summer Asian monsoon also weakened considerably (Wanner and Brönnimann, 2012). Readjustment of these two main climatic system drivers led to the establishment of similar conditions to present atmospheric tele-connections (ENSO) since ca 5.5 ka (Wanner et al., 2008; Carré et al., 2012; Fletcher and Moreno 2012). Southward movement of the ITCZ favoured southward shift of the sub-tropical North Atlantic high pressure and led to increased summer aridity in the Iberian Peninsula (González-Sampériz et al., 2008; Morellón et al., 2009; Corella et al., 2010; Valero-Garcés et al., 2011; Carrión et al., 2010; Valero-Garcés and Moreno, 2011). As the North Atlantic high-low pressure system moved away, westerlies became weaker and lost their capacity to penetrate inland.

A change towards wetter conditions is observed in the BSM sequence between 4.5 and 3.9 cal ka BP, marked by increased abundance of mesophytes, and the recovery of *Betula* and deciduous *Quercus* values (fig. 2.17). This humid period corresponds well with a phase of increased storm activity recorded in the Gulf of Lion (Sabatier et al., 2012), suggesting stronger and southward migration of the westerlies. However, the total AP decreases during this phase. This reduction of the arboreal pollen in the BSM sequence occurs at the same time as the first deforestation phase recognised in the Pyrenean sequence of Tramacastilla at ca. 4000 BP (Montserrat-Martí, 1992). However, no other indicator of anthropogenic pressure was found during this period in the BSM sequence suggesting that the vegetation shift was mainly climate driven. The high regional fire activity detected during this period is the culmination of a previous trend. Although there was an initial dry phase when fire occurrence was linked to the presence of pine forest, higher charcoal influx values during this subsequent humid phase are linked with the spread of mesophyte forest. The fact that fire is high during both humid and arid spells, reflects on the one hand more permanent drying conditions than any time before in the Holocene leading to frequent fire-conducive conditions coupled with relatively high fuel availability from mesophyte vegetation, and on the other hand, the strengthening of fire activity during any interval of mesophyte forest expansion when fire-conducive conditions occur (Lasheras et al., 2013).

#### 2.5.4. The Late Holocene (3700-700 cal yr BP): aridity crises

Complex societies developed across the Mediterranean during the Late Holocene and human pressure on the landscape intensified and expanded (Carrión et al., 2007, Bal et al., 2011; Finné et al., 2011; Magyari et al., 2012). High altitude palaeoenvironmental records, where anthropogenic activities would have been limited due to both severe weather and difficult access, provide an opportunity to isolate the climate signal influencing vegetation evolution in recent times (Pérez-Sanz et al., 2011).

The BSM sequence reveals a well forested landscape during most of the late Holocene (AP abundance around 70%, BSM-IV), indicating negligible anthropogenic pressure until ca 1150 cal yr BP, when the first evidence of forest management is found. The trend towards increased aridity that started during the Mid-Holocene transition intensified considerably at 3700 cal yr BP. The pollen record (BSM-V) is characterized by a sharp fall of *Betula* and the disappearance of birch from this area (fig. 2.15). The expansion of conifers (*Pinus* and *Juniperus*, which reaches its maximum proportions of the whole record), indicates either reduction in annual mean precipitation or a significant change in the seasonal distribution of precipitation (Franco-Mugica et al., 2000). The *Pinus* expansion in BSM is coeval with an expansion in other high altitude Pyrenean sites (Pèlachs et al., 2011), which suggests it is more likely to be controlled by changed climate than by human action. At ca. 2900 cal yr BP, *Artemisia* starts to spread rapidly and *Myriophyllum* decreases strongly (BSM-V). Traditionally, the *Artemisia* expansion has been explained by an increase in pastoral activity during the Late Holocene. However, as we have indicated before, in reference to current pollen rain data in BSM area, modern values of *Artemisia* rarely reach 2% even though there is moderate pastoral activity in the BSM area (figs. 2.15). Given that there is no evidence for major deforestation at the time of the *Artemisia* expansion, it seems unlikely that this represents an interval of more intense anthropogenic activity than today. This suggests that the *Artemisia* expansion at the Basa de la Mora site indicates a climatically-induced expansion of dry steppe. There is evidences for a period of intensified aridity across the Mediterranean at around 2900-2400 cal yr BP (Jalut et al., 2000).

The deposition of carbonate-rich massive Facies 5, characterized by the presence of authigenic calcite crystals, gastropods, pennate diatoms (fig. 2.13) and mottling textures, indicative of bioturbation, provides evidence for lowered lake levels and the development of a larger palustrine area at the time of the expansion of dry steppe. Facies 5 characterises most of littoral core BSM-2A-1U, supporting our interpretation of the depositional environment. The presence of partially dissolved authigenic crystals of calcite and gypsum in Facies 5 suggests the lake was ephemeral and may have desiccated at times. The strong negative correlation between MS and TIC (table 2.3) indicates that decreased runoff, and thus reduced external water supply into the lake, led to increased concentration of the lake water and authigenic carbonate precipitation. Furthermore, the negative correlation between MS and drought-resistant taxa such us *Pinus* and evergreen *Quercu*s and the positive correlation between MS and *Betula* strengthen the link between lack of run-off and precipiation deficit (table 2.4). Intercalation of organic Facies 4 supports the development of a palustrine area with high accumulation of organic matter. In addition, the high percentages of TOC and low TOC/N ratio indicate increased lacustrine productivity, consistent with shallower conditions. This expansion of littoral areas is consistent with the very high abundance of Cyperaceae while *Myriophyllum* values remain relatively unchanged (Fig. XX). The higher percentages (up to 20%) of *Psectrocladius* gr. *Limbatellus* (Fig. XX) than in previous zones also indicates an increase lacustrine productivity, as this genus is associated with productive environments and/or littoral areas with abundance of biofilm primary production on stones or macrophytes (Rieradevall et al., 1999; Brodersen et al., 2001).

There is no charcoal in the BSM between 3.2-1.5 cal ka BP (Lasheras et al., 2013). An interval of two millennia without fire is highly unusual as fire activity is registered in most southern European sequences during this time (Colombaroli et al., 2010; Tinner et al., 2005: Vescovi et al., 2007; Vannière et al., 2008). Arid pulses could prevent forest development at high altitudes and, therefore, limiting charcoal production through fires but, considering the absence of any other clear biotic or abiotic indicators, it seems more likely that the lack of microcharcoal is linked to taphonomical issues affecting charcoal preservation during oxic periods and/or short sub-aerial exposure events (Facies 5). Failure in laboratory procedures linked to the use of Thoulet solution differential flotation processes may have played a role in the absence of microcharcoal in these samples . Currently, new analyses are in progress in order to establish the presence of charcoal in this interval.

There is a common pattern to the evolution of vegetation across the Western Mediterranean (including southern Iberia, northern Africa and Italy) during this interval. A general phase of forest decline has been recorded in marine record MD95-2043 from the Alborán Sea between 3.7 and 2.9 cal ka BP (Fletcher et al., 2013b). In Zoñar sequence, low values of AP (< 10%) and an expansion of steppe taxa occurred between 4 – 2.9 cal ka BP (Martín-Puertas et al., 2008). At Sierra de Gádor (Carrión et al., 2003), *Pinus* and evergreen oak expand at the expense of deciduous *Quercus* after 3940 cal yr BP. In Sierra de Baza, there was a replacement of mesophytic by more xeric taxa around 3800 cal yr BP (Carrión et al., 2007), while in El Cañizar de Villarquemado, mesophytes and deciduous *Quercus* decreased and steppe herbs increased between 4000-3800 cal yr BP (Aranbarri et al., 2014). A similar pattern has been recorded in Italian sequences, with an expansion of sclerophyllous taxa between 3.9-3.4 ka (Sadori et al., 2010). These changes can all be attributed to both drier climate conditions and human activities, especially considering that several civilizations collapsed at ca. 4000 cal yr BP (i.e., Akkadians: Cullen et al., 2000).

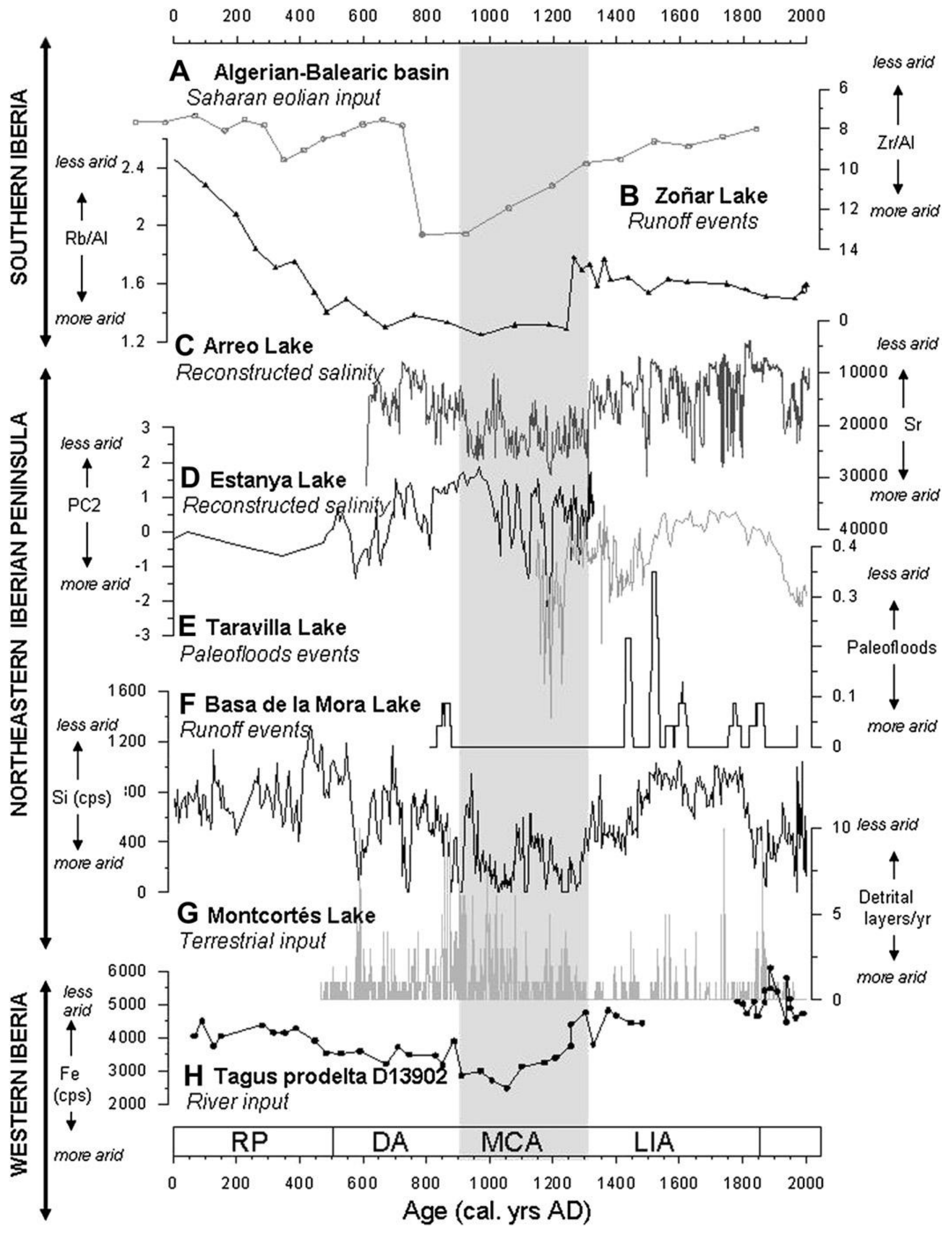


**Figure 2.18**. Selected records from Central and Mediterranean Iberia covering last 2000 years that indicate variations in aridity. From top to bottom: A) Zr/Al ratio from AlgerianeBalearic basin core; B) Rb/Al ratio from Zoñar Lake; C) Sr (cps) from Arreo Lake; D) the aridity reconstruction of Estanya Lake (axis 2 from the Principal Component Analyses applied to the XRF dataset in two cores); E) the number of paleoflood events in Taravilla Lake; F) Si (cps) from Basa de la Mora Lake; G) the number of detrital layers per year from Montcortès Lake and H) Fe (cps) from the Tagus prodelta. Note that all records are plotted to indicate arid conditions towards the bottom. RP: Roman Period; DA: Dark Ages; MCA: Medieval Climate Anomaly; LIA: Little Ice Age. From Moreno et al., 2012.

Peaks in *Artemisia* and high TIC percentages in BSM record (fig. 2.17) mark two periods of increased aridity at 2.9-2.4, and at 1.2-0.7 cal ka BP (800-1300 AD). Both episodes are characterized by high TIC and TOC percentages and low TOC/TN ratios suggesting high precipitation of carbonates and high bioproductivity and content of autochthonous organic matter. These episodes are separated by a relative humid period between 2.1 and 1.5 cal ka BP (fig. 2.17). The arid phase between 2.9-2.4 ka cal BP is synchronous with a dry episode recorded in both western (Ferrio et al., 2006; Aguilera et al., 2012) and eastern Iberia, that led to a prominent decline in deciduous *Quercus* pollen in the Amposta sequence (Pérez-Obiol et al., 2011). Increased water level can be inferred from the significant reduction of TIC percentages between 2.1 and 1.5 cal ka BP. An episode of more humid conditions has been recognized in Iberia (Corella et al., 2010; Martín-Puertas et al., 2008, 2009; Currás et al., 2012), coinciding with the Iberian civilization and the Roman occupation and thus is called the Iberian-Roman Humid Period (IRHP). The NW Mediterranean region also registers an intensification of rainfall reflected by higher storm activity in the Gulf of Lion (Sabatier et al., 2012). However Fletcher et al., (2013b) report another phase of forest decline in Western Mediterranean at this time (fig. 2.17). Since wetter conditions should have positively affected forest development in the Mediterranean, where water is the greatest limiting factor, it is possible that depletion in tree mass could be related in some areas of Iberia to higher land use by the Romans (García-Bellido, 1985). However, we do not observe great exploitation of the subalpine belt at BSM suggesting that the vegetation composition, which runs in parallel with sedimentological features, is still primarily controlled by climate in this area.

The second arid period recorded in BSM sequence matches the well-known Medieval Climate Anomaly (MCA: 900-1300 AD), a period of aridity recognized in most of south-western Europe (Seager et al., 2007; Mann et al., 2009) which led to notable agro-economic crisis in medieval societies. In Spain, it resulted in a major water deficit leading to lower lake levels and expansion of thermophytes and steppe taxa (Moreno et al., 2012b) (fig. 2.18). In the BSM sequence, this phase coincides with the first signal of deforestation, indicated by abrupt decreases in pine percentages (fig. 2.17). Charcoal influx increased ca. 1700 cal BP, most likely because of either warmer conditions or strengthened regional fire activity in the lowlands (Lasheras et al., 2013).

Both episodes of depleted water availability correspond with maxima in reconstructed North Atlantic Oscillation (NAO) indexes (fig. 2.17). This indicates that there is a fast response of palaeoenvironmental changes in the BSM record to changes in the North Atlantic. The persistence of a positive NAO index during 2.9-2.4, and at 1.2-0.7 cal ka BP, led to maximum winter precipitation in Scandinavia and to minimum winter precipitation in the Iberian Peninsula (Trouet et al., 2009).

### 2.5.5. The last centuries (700 cal yr BP-present): anthropogenic impact

In contrast to most Pyrenean studies that indicate intensified human disturbance during at least the last two millennia (Riera et al., 2004; Pèlach et al., 2011; Guiter et al., 2005), the effects of anthropogenic pressure are only detected in the BSM sequence during the last 700 cal yr BP (Pérez-Sanz et al., 2011) (fig, 2.19, BSM-V-A). As seen in figures 2.16, 2.17 and 2.19, the increase in *Olea* marks an expansion of agricultural practises in the lowlands (Cañellas-Boltà et al., 2009) whereas large, short-term reductions in *Pine* indicate phases of deforestation and expansion of grazing lands at higher altitudes (fig. 2.19, BSM-V-B). Parallel to *Olea*, *Fraxinus* also spreads. *Fraxinus* has traditionally been used in the region for hedgerows (Gómez and Fillat, 1981). Its parallel expansion to *Olea* marks the regional establishment of modern and intense agro-pastoral activities. The drop in *Artemisia* synchronous with clear evidence of increasing anthropogenic pressure in the highlands supports the idea that *Artemisia* is not an indicator of human activities in the BSM sequence.

The expansion of *Olea* and *Fraxinus* ceased, and deforestation temporarily stopped, between 1600 and 1850 AD (fig. 2.19; BSM-V-C) coinciding with the second half of the Little Ice Age. This interval is characterized by the coldest conditions in the southern Pyrenees (González-Trueba et al., 2008; Morellón et al., 2012) (fig. 2.20). In BSM sequence a sharp decrease in evergreen *Quercus* coincides with these colder conditions. The rapid recovery of pine after intervals of deforestation emphasizes the fact that human disturbance at high altitudes was not strong and climatic conditions were the main determinant of vegetation changes.

High values of MS and strong negative correlation with TIC during this period (fig. 2.19; BSM-V-C) indicate increased sediment delivery to the lake and decreased carbonate productivity, both indicative of higher lake levels and increased runoff. The abundance of allocthonous organic matter, shown by low TOC and high TOC/N ratios, also supports the inference of high sediment delivery from the catchment. Fire activity was high for most of this period, confirming the occurrence of either regional fires linked to husbandry or local fires correlated with the occasional pine deforestation (Lasheras-Álvarez et al., 2013). Although it is difficult to distinguish between human and climate-induced fires in this period, all other records indicate an intensification of anthropogenic activities after 700 yrs BP. A general decrease in temperature coinciding with the Little Ice Age (LIA i.e. 1300-1850 AD) has been recorded throughout Europe. Higher storm activity occurred in the NW Mediterranean, (Sabatier el al., 2012) (fig. 2.17) while stronger climatic variability has been recognised in Iberia, although generally cold and humid conditions dominated (Benito et al., 2003; Valero-Garcés et al., 2008; Morellón et al., 2012; Moreno et al, 2008, 2012b) (fig. 2.20).

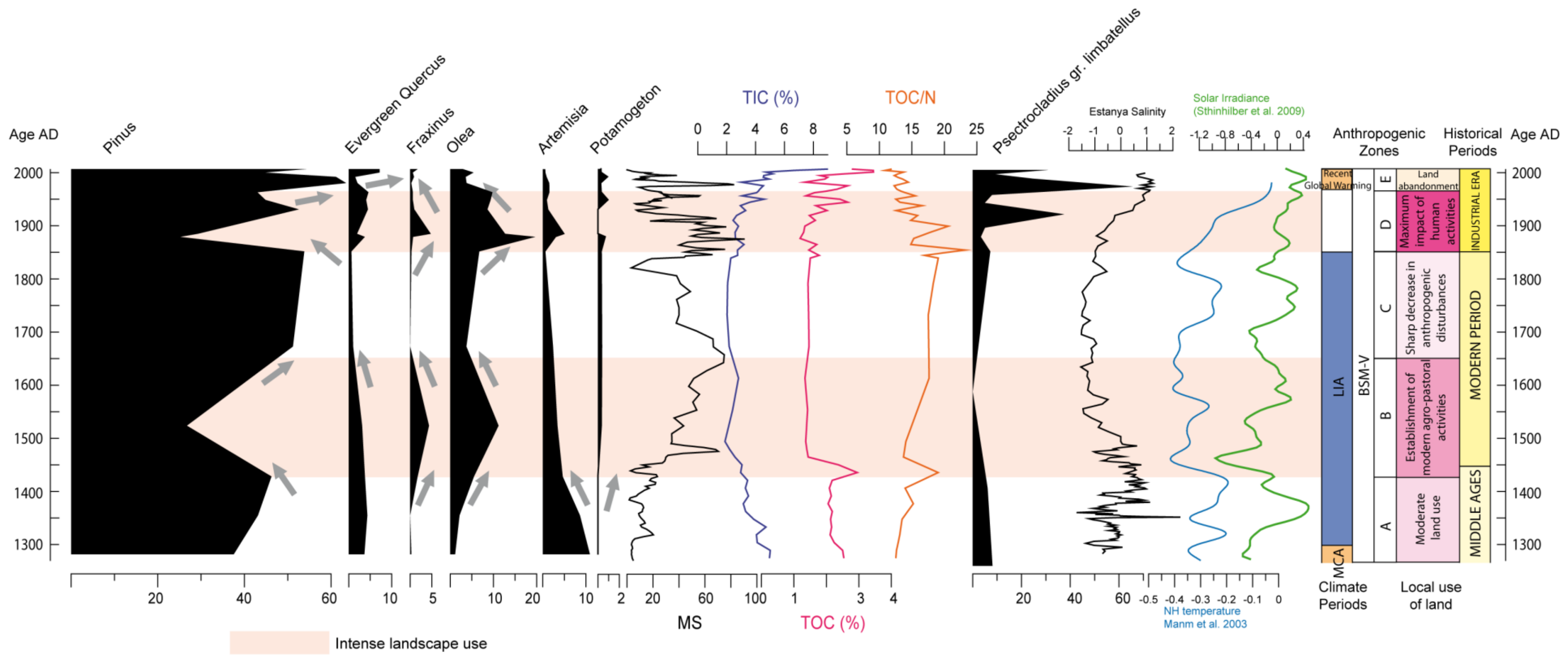


**Figure 2.19**. Comparison of selected curves (pollen –*Pinus*, Evergreen *Quercus, Fraxinus, Olea, Artemisia, Potamogeton*-, geochemical proxies-MS, TIC, TOC, TOC/N- and chironomids –*Psectrocladius* gr. *limbatellus*-) from Basa de la Mora sequence with global and regional records (Estanya salinity (Morellón et al., 2011); NH temperature reconstruction (Mann et al., 2003) and Solar Irradiance (Sthinhiber et al., 2009) for the last 750 years, indicating the main climate and historical periods and the interpretation of local land use. Bands in rose mark the intense periods of anthropogenic activities.

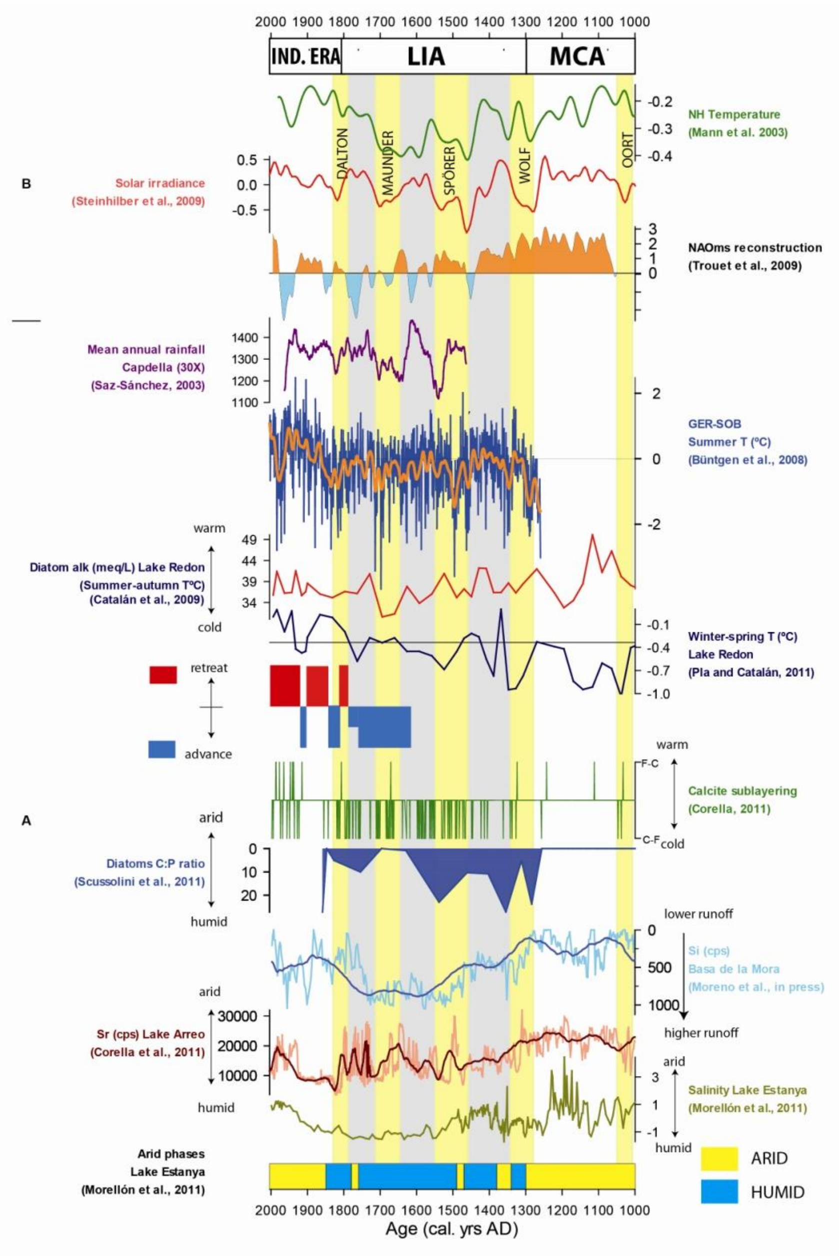


**Figure 2.20**. Selected records from the Southern Pyrenees reviewed in this paper, from top to bottom: Capdella tree-ring based mean annual rainfall (30× moving average) (Saz Sánchez, 2003), GER-SOB summer temperature tree-ring based reconstruction (original data and 20× moving average) (Büntgen et al., 2008), diatom alkalinity-based summer–autumn temperature and chrysophyte-based winter–spring temperatures reconstruction in Lake Redon (Pla and Catalán, 2005; Catalan et al., 2009), phases of advance and retreat of the Pyrenean glaciers (González Trueba et al., 2008), calcite sublayering (Fine–Coarse (F–C) or Coarse–Fine (C–F)) (Corella, 2011) and diatom C:P ratio (Scussolini et al., 2011) in Lake Montcortés, Si (cps) content in Lake Basa de la Mora (original data and 30× moving average) (Moreno et al., 2012), Sr (cps) content in Lake Arreo sequence (original data and 30× moving average) (Corella, 2011) and XRF-based salinity reconstruction and humid/arid phases in Lake Estanya (Morellónn et al., 2011). (B) Supplementary regional and global records, from top to bottom: NH temperature reconstruction (Mann and Jones, 2003), solar irradiance (Steinhilber et al., 2009), and NAOms reconstruction (Trouet et al., 2009). Vertical yellow bars represent the chronology of the grand sunspot minima and temporal divisions Medieval Climate Anomaly (MCA), Little Ice Age (LIA) and Industrial Era (IND. ERA) are also indicated at the uppermost part of the figure. From Morellón et al. 2012.

A significant expansion of *Olea* associated with a marked phase of deforestation of the pine forest occurred right after the LIA (1880 AD) (fig. 2.19, BSM-V-D). The Industrial Revolution in the 17th century brought major advances in agricultural techniques that resulted in increased efficiency and production and led to increased supply of food and raw materials. As result of the improvement of the agricultural sector the population rose and demographic pressure in the southern Pyrenees increased up to its maximum at the end of 19th and the early 20th century (García-Ruiz and Valero-Garcés, 1998).

After 1960 AD pine forest recovered, AP increased up to 65% and there was a reduction in trees (*Olea, Fraxinus*) related to anthropogenic activities (fig. 2.19, BSM-V-E). During the mid-20th century, social and economic changes in Spain forced population to migrate from villages into cities as the industrial sector developed. In Spain, and more specifically in the southern Pyrenees, mass migration took place in the last third of the 20th century, resulting in abandonment of the rural lands and gradual recovery of forests (Lasanta-Martínez et al., 2005). We observe a steep drop in fire activity during this phase, most likely as consequence of rural abandonment (fig.2.19, BSM-V-E). Geochemical proxies suggest a decrease of average lake level during the last 50 years. TIC percentages reach the highest values of the entire sequence, exceeding the values recorded during the MCA. Particularly high bioproductivity is shown by high TOC values, along with TOC/TN ratios and an increase of macrophyte-related taxa, such as *Corynoneura* and *Pentaneurini*, and especially *Psectrocladius* gr. *Limbatellus* (Tarrats et al., 2014). Increases in bioproductivity in the recent period may be linked to the presence of cow stockbreeding near the lake. However, stockbreeding has taken place in this area at least since the last century (Lucio, 1982) but the increase in bioproductivity only occurs during the last 30 years. One possible explanation is that enhanced bioproductivity during the last decades reflects increased water temperatures. A global warming trend has been widely recognised over recent decades (IPCC, 2007) and an increase in temperature is also evident in the Mediterranean area (Brunetti et al., 2004; Vargas-Yáñez et al., 2008; Camuffo et al., 2010) and in north-eastern Spain (El Kenawy et al., 2012). Climate change in the Mediterranean area involves not only increased temperature but often decreased precipitation. A decrease in snowpack depth, snow cover and direct precipitation has been detected in the southern Pyrenees during the most recent period (López-Moreno 2005; López-Moreno and Stähli, 2008). The recent drop in level at Basa de la Mora could be linked to the reduction in water availability in the southern Pyrenees, while the increase in bioproductivity could be related to the occurrence of warmer waters. The impact of the recent climate conditions on the lake sediments confirms the high sensitivity and rapid response of Basa de la Mora record to short-term climate shifts.

## 2.6. CONCLUSIONS

i. The multi-proxy sequence of Basa de la Mora (BSM) has recorded significant climate variability during the last ca. 10 cal ka BP. Consistent shifts in vegetation, fire activity, depositional environments and aquatic communities throughout the sequence can be correlated with other regional and global reconstructions.

ii. Higher seasonality between 10 and 8.2 cal ka BP caused high snow accumulation in winter and subsequent melt during warmer summers resulted in high lake levels. As a consequence of this high seasonal contrast, *Pinus* spread while mesophytes were restricted to watercourses.

iii. High climate instability during this period is illustrated by the occurrence of four short arid intervals at 9.7, 9.3, 8.8 and 8.3 cal ka BP, each characterized by a decrease in mesophytes and increased runoff. The most intense event occurred at 8.3 ± 0.1 cal ka BP, when vegetation diversity and abundance dropped to a minimum.

iv. The most humid period in BSM sequence occurred between 8.2 and 5.7 cal ka BP. During this period, mesophytes expanded, conifers retreated and the highest lake level was recorded. As a consequence of increasing biomass, fire activity also intensified.

v. The end of the Mid-Holocene marks the transition from a significant Atlantic influence (before ca. 5.7 cal ka BP) into a typical Mediterranean climate with summer drought.

vi. A long-term trend towards increasing aridity, with decreasing lake levels and decreasing abundance of mesophytes started at 5.7 cal ka BP and intensified after ca. 3.9 cal ka BP.

vii. During this period and until 700 cal yr BP human exploitation of the subalpine belt was minor and the vegetation composition was primarily controlled by climate.

viii. The BSM record shows that the Central Pyrenees are particularly sensitive to climate changes due to its geographical position between the Mediterranean and the Atlantic climate regimes.

## References

Aguilera, M., Ferrio, J.P., Pérez, G., Araus, J.L., Voltas, J., 2012. Holocene changes in precipitation seasonality in the western Mediterranean Basin: a multi-species approach using δ13C of archaeobotanical remains. Journal of Quaternary Science 27, 192–202.

Ali, A.A., Carcaillet, C., Guendon, J., Quinif, Y., Roiron, P., Terral, J., 2003. The Early Holocene treeline in the southern French Alps: new evidence from travertine formations. Global Ecology and Biogeography 12, 411–419.

Alley, R., Agustsdottir, A., 2005. The 8k event: cause and consequences of a major Holocene abrupt climate change. Quaternary Science Reviews 24, 1123–1149.

Alley, R.B., Mayewski, P.A., Sowers, T., Stuiver, M., Taylor, K.C., Clark, P.U., 1997. Holocene climatic instability: A prominent, widespread event 8200 yr ago. Geology 25, 483-486.

Anderson, R.S., Jiménez-Moreno, G., Carrión, J.S., Pérez-Martínez, C., 2011. Postglacial history of alpine vegetation, fire, and climate from Laguna de Río Seco, Sierra Nevada, southern Spain. Quaternary Science Reviews 30, 1615–1629.

Appley P.G., 2001. Chronostratigraphic techniques in recent sediments. In: Last WM, Smol JP (eds) Tracking environmental change using lake sediments volume 1: basin analysis, coring, and chronological techniques. Kluwer, Dordrecht, pp 171–203

Bal, M.-C., Pelachs, A., Perez-Obiol, R., Julia, R., Cunill, R., 2011. Fire history and human activities during the last 3300cal yr BP in Spain's Central Pyrenees: The case of the Estany de Burg. Palaeogeography, Palaeoclimatology, Palaeoecology 300, 179–190.

Belmonte, A., 2004. La extensión máxima del glaciarismo en el Macizo de Cotiella (Pirineo Oscense). Boletín Glaciológico Aragonés 4, 69–90.

Belmonte, A., in prep. Geomorfología del macizo de Cotiella (Pirineo oscense): cartografía, evolución paleoambiental y dinámica actual. Universidad de Zaragoza, Zaragoza.

Benito, G., Sopeña, A., Sánchez-Moya, Y., Machado, M.J., Pérez-González, A., 2003. Palaeoflood record of the Tagus River (Central Spain) during the Late Pleistocene and Holocene. Quaternary Science Reviews 22, 1737–1756.

Bennett, K.D., 2009. Documentation for psimpoll 4.27 and pscomb 1.03. C programs for plotting and analyzing pollen data. The 14Chrono Centre, Archaeology and Palaeoecology, Queen's University of Belfast, Belfast, UK.

Bjune, A.E., Bakke, J., Nesje, A., Birks, H.J.B., 2005. Holocene mean July temperature and winter precipitation in western Norway inferred from palynological and glaciological lake-sediment proxies. The Holocene 15, 177–189.

Blarquez, O., Carcaillet, C., 2010. Fire, Fuel Composition and Resilience Threshold in Subalpine Ecosystem. PLoS ONE 5, e12480.

Blarquez, O., Carcaillet, C., Bremond, L., Mourier, B., Radakovitch, O., 2009. Trees in the subalpine belt since 11 700 cal. BP: origin, expansion and alteration of the modern forest. The Holocene 20, 139–146.

Bond, G., 1997. A Pervasive Millennial-Scale Cycle in North Atlantic Holocene and Glacial Climates. Science 278, 1257–1266.

Bond, G., Kromer, B., Beer, J., Muscheler, R., Evans, M.N., Showers, W., Hoffmann, S., Lotti-Bond, R., Hajdas, I., Bonani, G., 2001. Persistent Solar Influence on North Atlantic Climate During the Holocene. Science 294, 2130 –2136.

Bordon, A., Peyron, O., Lézine, A.-M., Brewer, S., Fouache, E., 2009. Pollen-inferred Late-Glacial and Holocene climate in southern Balkans (Lake Maliq). Quaternary International 200, 19–30.

Brodersen, K.P., Odgaard, B.V., Vestergaard, O., Anderson, N.J., 2001. Chironomid stratigraphy in the shallow and eutrophic Lake Sobygaard, Denmark: chironomid-macrophyte co-occurrence. Freshwater Biology 46, 253–267.

Brooks, S.J., Birks, H.J.., 2001. Chironomid-inferred air temperatures from Lateglacial and Holocene sites in north-west Europe: progress and problems. Quaternary Science Reviews 20, 1723–1741.

Brooks, S.J., Langdon, P.G., Heiri, O., Quaternary Research Association (Great Britain), 2007. The identification and use of Palaearctic Chironomidae larvae in palaeoecology. DRA Technical Guide No 10, Quaternary Research Association, London.

Brunetti, M., Buffoni, L., Mangianti, F., Maugeri, M., Nanni, T., 2004. Temperature, precipitation and extreme events during the last century in Italy. Global and Planetary Change 40, 141–149.

Büntgen, U., Frank, D., Grudd, H., Esper, J., 2008. Long-term summer temperature variations in the Pyrenees. Clim. Dyn. 31, 615–631.

Cacho, I., Grimalt, J.O., Canals, M., Sbaffi, L., Shackleton, N.J., Schönfeld, J., Zahn, R., 2001. Variability of the western Mediterranean Sea surface temperature during the last 25,000 years and its connection with the Northern Hemisphere climatic changes. Paleoceanography 16, 40-52.

Camuffo, D., Bertolin, C., Barriendos, M., Dominguez-Castro, F., Cocheo, C., Enzi, S., Sghedoni, M., Valle, A., Garnier, E., Alcoforado, M.-J., Xoplaki, E., Luterbacher, J., Diodato, N., Maugeri, M., Nunes, M.F., Rodriguez, R., 2010. 500-year temperature reconstruction in the Mediterranean Basin by means of documentary data and instrumental observations. Climatic Change 101, 169–199.

Cañellas-Boltà, N., Rull, V., Vigo, J., Mercadé, A., 2009. Modern pollen-vegetation relationships along an altitudinal transect in the central Pyrenees (southwestern Europe). The Holocene 19, 1185–1200.

Carnelli, A.L., Theurillat, J.-P., Thinon, M., Vadi, G., Talon, B., 2004. Past uppermost tree limit in the Central European Alps (Switzerland) based on soil and soil charcoal. The Holocene 14, 393–405.

Carré, M., Azzoug, M., Bentaleb, I., Chase, B.M., Fontugne, M., Jackson, D., Ledru, M.-P., Maldonado, A., Sachs, J.P., Schauer, A.J., 2012. Mid-Holocene mean climate in the south eastern Pacific and its influence on South America. Quaternary International 253, 55–66.

Carrión, J.S., 2002. Patterns and processes of Late Quaternary environmental change in a montane region of southwestern Europe. Quaternary Science Reviews 21, 2047–2066.

Carrión, J.S., Andrade, A., Bennett, K.D., Navarro, C., Munuera, M., 2001a. Crossing forest thresholds: inertia and collapse in a Holocene sequence from south-central Spain. The Holocene 11, 635–653.

Carrión, J.S., Fernández, S., González-Sampériz, P., Gil-Romera, G., Badal, E., Carrión-Marco, Y., López-Merino, L., López-Sáez, J.A., Fierro, E., Burjachs, F., 2010. Expected trends and surprises in the Lateglacial and Holocene vegetation history of the Iberian Peninsula and Balearic Islands. Rev. Palaeobot. Palynol. 162, 458–475.

Carrión, J.S., Fernández, S., Jiménez-Moreno, G., Fauquette, S., Gil-Romera, G., González-Sampériz, P., Finlayson, C., 2010. The historical origins of aridity and vegetation degradation in southeastern Spain. Journal of Arid Environments 74, 731–736.

Carrión, J.S., Fuentes, N., González-Sampériz, P., Sánchez Quirante, L., Finlayson, J.C., Fernández, S., Andrade, A., 2007. Holocene environmental change in a montane region of southern Europe with a long history of human settlement. Quaternary Science Reviews 26, 1455–1475.

Carrión, J.S., Munuera, M., Dupre, M., Andrade, A., 2001b. Abrupt vegetation changes in the Segura Mountains of southern Spain throughout the Holocene. Journal of Ecology 89, 783–797.

Carrión, J.S., Sánchez-Gómez, P., Mota, J.F., Yll, R., Chaín, C., 2003. Holocene vegetation dynamics, fire and grazing in the Sierra de Gádor, southern Spain. The Holocene 13, 839–849.

Catalán, J., Pèlachs, A., Gassiot, E., Antolín, F., Ballestero, A., Batalla, M., Burjachs, F., Buchaca, T., Camarero, L., Clemente, I., Clop, X., García, D., Giralt, S., Lluch, L., Madella, M., Mazzuco, N., Mur, E., Ninyerola, M., Obea, L., Oltra, J., Pérez-Obiol, R., Piqué, R., Pla-Rabés, S., Rondón, C.R., Rodríguez, J.M., Rodrígue, D., Sáez, A., Soriano, J.M., 2013. Interacción entre clima y ocupación humana en la configuración del paisaje vegetal del Parque Nacional de Aigüestores i Estany de Sant Maurici a lo largo de los últimos 15.000 años, in: Proyectos de investigación en parques nacionales: 2009-2012. Organismo Autónomo Parques Nacionales, Madrid.

Catalán, J., Pla, S., García-Serrano, J., Camarero, L., 2009. Climate and CO2 saturation in an alpine lake throughout the Holocene. Limnol. Oceanogr. 56, 2542–2552.

Chung, F.H., 1974. Quantitative interpretation of X-ray diffraction patterns of mixtures. II. Adiabatic principle of X-ray diffraction analysis of mixtures. Journal of Applied Crystallography 7, 526–531.

Clark, J.S., 1988. Particle motion and the theory of charcoal analysis: source area, transport, deposition and sampling. Quaternary Research 30, 67–80.

Collins, P.M., Davis, B.A.S., Kaplan, J.O., 2012. The mid-Holocene vegetation of the Mediterranean region and southern Europe, and comparison with the present day. Journal of Biogeography 39, 1848–1861.

Colombaroli, D., Henne, P.D., Kaltenrieder, P., Gobet, E., Tinner, W., 2010. Species responses to fire, climate and human impact at tree line in the Alps as evidenced by palaeo-environmental records and a dynamic simulation model. Journal of Ecology 98, 1346–1357.

Colombaroli, D., Vanniere, B., Emmanuel, C., Magny, M., Tinner, W., 2008. Fire--vegetation interactions during the Mesolithic--Neolithic transition at Lago dell'Accesa, Tuscany, Italy. The Holocene 18, 679–692.

Colonese, A.C., Zanchetta, G., Fallick, A.E., Martini, F., Manganelli, G., Drysdale, R.N., 2010. Stable isotope composition of Helix ligata (Müller, 1774) from Late Pleistocene–Holocene archaeological record from Grotta della Serratura (Southern Italy): Palaeoclimatic implications. Global and Planetary Change 71, 249–257.

Corella Aznar, J.P., 2011. Climate and human impact in Northern Spain since Mid-Holocene: the High Resolution records of lakes Arreo and Moncortès. Universidad de Zaragoza, Instituto Pirenaico de Ecología, Zaragoza.

Corella, J.P., Moreno, A., Morellón, M., Rull, V., Giralt, S., Rico, M.T., Pérez-Sanz, A., Valero-Garcés, B.L., 2010. Climate and human impact on a meromictic lake during the last 6,000 years (Montcortès Lake, Central Pyrenees, Spain). Journal of Paleolimnology 46, 351–367.

Cortés Sánchez, M., Jiménez Espejo, F.J., Simón Vallejo, M.D., Gibaja Bao, J.F., Carvalho, A.F., Martinez-Ruiz, F., Gamiz, M.R., Flores, J.-A., Paytan, A., López Sáez, J.A., Peña-Chocarro, L., Carrión, J.S., Morales Muñiz, A., Roselló Izquierdo, E., Riquelme Cantal, J.A., Dean, R.M., Salgueiro, E., Martínez Sánchez, R.M., De la Rubia de Gracia, J.J., Lozano Francisco, M.C., Vera Peláez, J.L., Rodríguez, L.L., Bicho, N.F., 2012. The Mesolithic–Neolithic transition in southern Iberia. Quaternary Research 77, 221–234.

Court-Picon, M., Buttler, A., Debeaulieu, J., 2005. Modern pollen–vegetation relationships in the Champsaur valley (French Alps) and their potential in the interpretation of fossil pollen records of past cultural landscapes. Review of Palaeobotany and Palynology 135, 13–39.

Cullen, H.M., deMenocal, P.B., Hemming, S., Brown, F.H., Guilderson, T., Sirocko, F., 2000. Climate change and the collapse of the Akkadian empire: Evidence from the deep sea. Geology 28, 379–382.

Cunill, R., Soriano, J.-M., Bal, M.-C., Pèlachs, A., Pérez-Obiol, R., 2011. Holocene treeline changes on the south slope of the Pyrenees: a pedoanthracological analysis. Vegetation History and Archaeobotany 21, 373-384.

Currás, A., Zamora, L., Reed, J.M., García-Soto, E., Ferrero, S., Armengol, X., Mezquita-Joanes, F., Marqués, M.A., Riera, S., Julià, R., 2012. Climate change and human impact in central Spain during Roman times: High-resolution multi-proxy analysis of a tufa lake record (Somolinos, 1280m asl). Catena 89, 31–53.

David, F., 1993. Evolutions de la limite spérieure des arbres dans les Alpes francaise du nord depuis la fin des temps glaciaires. Université d'Aix-Marseille III, 94p.

Davis, B.A.S., Brewer, S., Stevenson, A.C., Guiot, J., 2003. The temperature of Europe during the Holocene reconstructed from pollen data. Quaternary Science Reviews 22, 1701–1716.

Davis, P.T., Menounos, B., Osborn, G., 2009. Holocene and latest Pleistocene alpine glacier fluctuations: a global perspective. Quaternary Science Reviews 28, 2021–2033.

De Beaulieu, J.-L., Miras, Y., Andrieu-Ponel, V., Guiter, F., 2005. Vegetation dynamics in north-western Mediterranean regions: Instability of the Mediterranean bioclimate. Plant Biosystems - An International Journal Dealing with all Aspects of Plant Biology 139, 114–126.

deMenocal, P., Ortiz, J., Guilderson, T., Adkins, J., Sarnthein, M., Baker, L., Yarusinsky, M., 2000. Abrupt onset and termination of the African Humid Period: Quaternary Science Reviews 19, 347–361.

Domínguez-Villar, D., Wang, X., Cheng, H., Martín-Chivelet, J., Edwards, R.L., 2008. A high-resolution late Holocene speleothem record from Kaite Cave, northern Spain: δ18O variability and possible causes. Quaternary International 187, 40–51.

Dupré, M., 1988. Palinología y paleoambiente. Nuevos datos españoles. Referencias. Serie de trabajos varios, S.I.P.,84.

Ebbesen, H., Hald, M., Eplet, T.H., 2007. Lateglacial and early Holocene climatic oscillations on the western Svalbard margin, European Arctic. Quaternary Science Reviews 26, 1999–2011.

El Kenawy, A., López-Moreno, J.I., Vicente-Serrano, S.M., 2012. Trend and variability of surface air temperature in northeastern Spain (1920–2006): Linkage to atmospheric circulation. Atmospheric Research 106, 159–180.

Favilli, F., Cherubini, P., Collenberg, M., Egli, M., Sartori, G., Schoch, W., Haeberli, W., 2009. Charcoal fragments of Alpine soils as an indicator of landscape evolution during the Holocene in Val di Sole (Trentino, Italy). The Holocene 20, 67–79.

Fernández, S., Fuentes, N., Carrión, J.S., González-Sampériz, P., Montoya, E., Gil, G., Vega-Toscano, G., Riquelme, J.A., 2007. The Holocene and Upper Pleistocene pollen sequence of Carihuela Cave, southern Spain. Geobios 40, 75–90.

Ferrio, J.P., Alonso, N., Lopez, J.B., Araus, J.L., Voltas, J., 2006. Carbon isotope composition of fossil charcoal reveals aridity changes in the NW Mediterranean Basin. Global Change Biology 12, 1253–1266.

Finné, M., Holmgren, K., Sundqvist, H.S., Weiberg, E., Lindblom, M., 2011. Climate in the eastern Mediterranean, and adjacent regions, during the past 6000 years – A review. Journal of Archaeological Science 38, 3153–3173.

Fleitmann, D., Burns, S.J., Mangini, A., Mudelsee, M., Kramers, J., Villa, I., Neff, U., Al-Subbary, A.A., Buettner, A., Hippler, D., Matter, A., 2007. Holocene ITCZ and Indian monsoon dynamics recorded in stalagmites from Oman and Yemen (Socotra). Quaternary Science Reviews 26, 170–188.

Fletcher, M.S., Moreno, P., 2012. Have the Southern Westerlies changed in a zonally symmetric manner over the last 14,000 years? A hemisphere-wide take on a controversial problem. Quaternary International 253, 32–46.

Fletcher, W.J., Debret, M., Sanchez Goni, M.F., 2013b. Mid-Holocene emergence of a low-frequency millennial oscillation in western Mediterranean climate: Implications for past dynamics of the North Atlantic atmospheric westerlies. The Holocene 23, 153-166.

Fletcher, W.J., Goñi, M.F.S., 2007. Orbital- and sub-orbital-scale climate impacts on vegetation of the western Mediterranean basin over the last 48,000 yr. Quaternary Research 70, 451–464.

Fletcher, W.J., Sánchez Goñi, M.F., Allen, J.R.M., Cheddadi, R., Combourieu-Nebout, N., Huntley, B., Lawson, I., Londeix, L., Magri, D., Margari, V., Müller, U.C., Naughton, F., Novenko, E., Roucoux, K., Tzedakis, P.C., 2010a. Millennial-scale variability during the last glacial in vegetation records from Europe. Quaternary Science Reviews 29, 2839–2864.

Fletcher, W.J., Sanchez Goñi, M.F., Peyron, O., Dormoy, I., 2010b. Abrupt climate changes of the last deglaciation detected in a Western Mediterranean forest record. Climate of the Past 6, 245–264.

Fletcher, W.J., Zielhofer, C., 2013a. Fragility of Western Mediterranean landscapes during Holocene Rapid Climate Changes. Catena 103, 16-29.

Franco Múgica, F., García Antón, M., Maldonado Ruiz, J., Morla Juaristi, C., Sainz Ollero, H., 2001. The Holocene history of Pinus forests in the Spanish Northern Meseta. The Holocene 11, 343–358.

Franco-Mugica, F., Gómez-Manza, F., Maldonado, J., Morla, C., Postigo, J.M., 2000. El papel de los pinares en la vegetación holocnena de la Península Ibérica. Ecología 14, 61–67.

Frigola, J., Moreno, A., Cacho, I., Canals, M., Sierro, F.J., Flores, J.A., Grimalt, J.O., Hodell, D.A., Curtis, J.H., 2007. Holocene climate variability in the western Mediterranean region from a deepwater sediment record. Paleoceanography 22. PA2209, doi:10.1029/2006PA001307

García-Bellido, A., 1985. La Península Ibérica en los comienzos de su historia. Colegio universitario Ediciones Istmo, Madrid.

García-Ruiz, J.M., Beguería, S., López-Moreno, J.I., Lorente, A., Seeger, M., 2001. Los recursos hídricos superficiales del Pirineo aragonés y su evolución reciente. (Surface wáter resources in the Aragonese Pyrenees and their recent evolution. Geoforma, Logroño, 191p.

García-Ruiz, J.M., Puigdefábregas, J., Creus, J., 1985. Los recursos hídricos superficiales del Alto Aragón. Instituto de Estudios Altoaragoneses.

García-Ruiz, J.M., Valero-Garcés, B.L., 1998. Historical geomorphic processes and human activites in the Central Spanis Pyrenees. Mountain Research and Development 18, 3009–320.

Gil-Romera, G., González-Sampériz, P., Lasheras-Álvarez, L., Sevilla-Callejo, M., Moreno, A., Valero-Garcés, B., López-Merino, L., Pérez-Sanz, A., Aranbarri, J., García-Prieto Fronce, E., Accepted. Long-term biomass-modulated fire dynamics at the Southern Pyrenees. Palaeogeography, Palaeoclimatology, Palaeoecology

Gómez, D., Fillat, F., 1981. La cultura ganadera del fresno. Pastos 11, 295–302

Gómez-Paccard, M., Larrasoaña, J.C., Sancho, C., Muñoz, A., McDonald, E., Rhodes, E.J., Osácar, M.C., Costa, E., Beamud, E., 2013. Environmental response of a fragile, semiarid landscape (Bardenas Reales Natural Park, NE Spain) to Early Holocene climate variability: A paleo- and environmental-magnetic approach. Catena. 103, 30-43.

González-Sampériz, P., Utrilla, P., Mazo, C., Valero-Garcés, B., Sopena, M., Morellón, M., Sebastián, M., Moreno, A., Martínez-Bea, M., 2009. Patterns of human occupation during the early Holocene in the Central Ebro Basin (NE Spain) in response to the 8.2 ka climatic event. Quaternary Research 71, 121–132.

González-Sampériz, P., Valero-Garcés, B.L., Moreno, A., Jalut, G., García-Ruiz, J.M., Martí-Bono, C., Delgado-Huertas, A., Navas, A., Otto, T., Dedoubat, J.J., 2006. Climate variability in the Spanish Pyrenees during the last 30,000 yr revealed by the El Portalet sequence. Quaternary Research 66, 38–52.

González-Sampériz, P., Valero-Garcés, B.L., Moreno, A., Morellón, M., Navas, A., Machín, J., Delgado-Huertas, A., 2008. Vegetation changes and hydrological fluctuations in the Central Ebro Basin (NE Spain) since the Late Glacial period: Saline lake records. Palaeogeography, Palaeoclimatology, Palaeoecology 259, 157–181.

González-Trueba, J.J., Moreno, R.M., Martinez de Pison, E., Serrano, E., 2008. `Little Ice Age' glaciation and current glaciers in the Iberian Peninsula. The Holocene 18, 551–568.

Gottfried, M., Pauli, H., Futschik, A., Akhalkatsi, M., Barančok, P., Benito Alonso, J.L., Coldea, G., Dick, J., Erschbamer, B., Fernández Calzado, M.R., Kazakis, G., Krajči, J., Larsson, P., Mallaun, M., Michelsen, O., Moiseev, D., Moiseev, P., Molau, U., Merzouki, A., Nagy, L., Nakhutsrishvili, G., Pedersen, B., Pelino, G., Puscas, M., Rossi, G., Stanisci, A., Theurillat, J.-P., Tomaselli, M., Villar, L., Vittoz, P., Vogiatzakis, I., Grabherr, G., 2012. Continent-wide response of mountain vegetation to climate change. Nature Climate Change 2, 111–115.

Greatbatch, R. J., 2000. The North Atlantic Oscillation. Stochastic Environmental Research and Risk Assessment 14, 213-242.

Guiter, F., Andrieu-Ponel, V., Digerfeldt, G., Reille, M., Beaulieu, J.-L., Ponel, P., 2005. Vegetation history and lake-level changes from the Younger Dryas to the present in Eastern Pyrenees (France): pollen, plant macrofossils and lithostratigraphy from Lake Racou (2000 m a.s.l.). Vegetation History and Archaeobotany 14, 99–118.

Haas, J.N., Richoz, I., Tinner, W., Wick, L., 1998. Synchronous Holocene climatic oscillations recorded on the Swiss Plateau and at timberline in the Alps. The Holocene 8, 301–309.

Heiri, O., Wick, L., Van Leeuwen, J.F.., Van der Knaap, W.O., Lotter, A.F., 2003. Holocene tree immigration and the chironomid fauna of a small Swiss subalpine lake (Hinterburgsee, 1515 m asl). Palaeogeography, Palaeoclimatology, Palaeoecology 189, 35–53.

Hély, C., Braconnot, P., Watrin, J., Zheng, W., 2009. Climate and vegetation: Simulating the African humid period. Comptes Rendus Geoscience 341, 671–688.

Hofmann, W., 1986. Chironomid analysis, in: Handbook of Holocene Paleoecology and Paleohydrology. Wiley and Sons, Chichester, pp. 715–727.

Hoffman, J.S, Carlson, E., Winsor, K., Klinkhammer, G.P., LeGrande, A.N., Andrews, J.T., Strasser, J.C., 2012. Linking the 8.2 ka event and its freshwater forcing in the Labrador Sea. Geophysical Research Letters, 39, L18703, doi:10.1029/2012GL053047.

IPCC, 2007. Climate Change 2007: impacts, adaptation and vulnerability., Contribution of working group II to the fourth assessment report of the intergovernmental panel on cliamte change. ed. Cambridge University Press, Reino Unido.

Jalut, G., Dedoubat, J.J., Fontugne, M., Otto, T., 2009. Holocene circum-Mediterranean vegetation changes: Climate forcing and human impact. Quaternary International 200, 4–18.

Jalut, G., Esteban Amat, A., Bonnet, L., Gauquelin, T., Fontugne, M., 2000. Holocene climatic changes in the Western Mediterranean, from south-east France to south-east Spain. Palaeogeography, Palaeoclimatology, Palaeoecology 160, 255–290.

Jiménez-Moreno, G., Anderson, R. S., 2012. Holocene vegetation and climate change recorded in alpine bog sediments from the Borreguilles de la Virgen, Sierra Nevada, southern Spain. Quaternary Research 77, 44–53.

Kaplan, M.R., Wolfe, A.P., 2006. Spatial and temporal variability of Holocene temperature in the North Atlantic region. Quaternary Research 65, 223–231.

Kobashi, T., Severinghaus, J.P., Brook, E.J., Barnola, J.M., Grachev, A.M., 2007. Precise timing and characterization of abrupt climate change 8200 years ago from air trapped in polar ice. Quaternary Science Reviews 26, 1212–1222.

Kröpelin, S., Verschuren, D., Lézine, A.-M., Eggermont, H., Cocquyt, C., Francus, P., Cazet, J.-P., Fagot, M., Rumes, B., Russell, J.M., Darius, F., Conley, D.J., Schuster, M., Von Suchodoletz, H., Engstrom, D.R., 2008. Climate-Driven Ecosystem Succession in the Sahara: The Past 6000 Years. Science 320, 765 –768.

Lasanta-Martínez, T., Vicente-Serrano, S.M., Cuadrat-Prats, J.M., 2005. Mountain Mediterranean landscape evolution caused by the abandonment of traditional primary activities: a study of the Spanish Central Pyrenees. Applied Geography 25, 47–65.

Lasheras-Álvarez, L., Pérez-Sanz, A., Gil-Romera, G., González-Sampériz, P., Sevilla-Callejo, M., Valero-Garcés, B.L., in press. Historia del fuego y la vegetación en una secuenica holocena del Pirineo Central: La Basa de la Mora. Cuad. Investig. Geográfica 39, 77–95.

Leira, M., Santos, L., 2002. An early Holocene short climatic event in the northwest Iberian Peninsula inferred from pollen and diatoms. Quaternary International 93-94, 3–12.

Lionello, P., Malanotte-Rizzoli, P., Boscolo, R., Alpert, P., Artale, V., Li, L., Luterbacher, J., May, W., Trigo, R., Tsimplis, M., Ulbrich, U., Xoplaki, E., 2006. The Mediterranean climate: An overview of the main characteristics and issues, in: Developments in Earth and Environmental Sciences. Elsevier, pp. 1–26.

López-Merino, L., Cortizas, A.M., López-Sáez, J.A., 2010. Early agriculture and palaeoenvironmental history in the North of the Iberian Peninsula: a multi-proxy analysis of the Monte Areo mire (Asturias, Spain). Journal of Archaeological Science 37, 1978–1988.

López-Merino, L., Moreno, A., Leira, M., Sigró, J., González-Sampériz, P., Valero-Garcés, B.L., López-Sáez, J.A., Brunet, M., Aguilar, E., 2011. Two hundred years of environmental change in Picos de Europa National Park inferred from sediments of Lago Enol, northern Iberia. J. Paleolimnol. 46, 453–467.

López-Moreno, J.I., 2005. Recent variations of snowpack depth in the Central Spanish Pyrenees. Artic, Antartic, and Alpine Research 37, 253–260.

López-Moreno, J.I., Stähli, M., 2008. Statistical analysis of the snow cover variability in a subalpine watershed: Assessing the role of topography and forest interactions. Journal of Hydrology 348, 379–394.

Lucio, J.V., 1982. Estudio del Medio Físico del Sobrarbe. Aprovechamiento de los pastos estivales en el Valle de Gistain. Explotación actual y capacidad potencial. ICONA, Huesca.

Magny, M., De Beaulieu, J.-L., Drescher-Schneider, R., Vannière, B., Walter-Simonnet, A.-V., Miras, Y., Millet, L., Bossuet, G., Peyron, O., Brugiapaglia, E., Leroux, A., 2007. Holocene climate changes in the central Mediterranean as recorded by lake-level fluctuations at Lake Accesa (Tuscany, Italy). Quaternary Science Reviews 26, 1736–1758.

Magny, M., Vannière, B., Calo, C., Millet, L., Leroux, A., Peyron, O., Zanchetta, G., La Mantia, T., Tinner, W., 2011. Holocene hydrological changes in south-western Mediterranean as recorded by lake-level fluctuations at Lago Preola, a coastal lake in southern Sicily, Italy. Quaternary Science Reviews 30, 2459–2475.

Magyari, E.K., Chapman, J., Fairbairn, A.S., Francis, M., Guzman, M., 2012. Neolithic human impact on the landscapes of North-East Hungary inferred from pollen and settlement records. Vegetation History and Archaeobotany 21, 279–302.

Mann, M.E., Zhang, Z., Rutherford, S., Bradley, R.S., Hughes, M.K., Shindell, D., Ammann, C., Faluvegi, G., Ni, F., 2009. Global Signatures and Dynamical Origins of the Little Ice Age and Medieval Climate Anomaly. Science 326, 1256–1260.

Marshall, J., Kushnir, Y., Battisti, D., Chang, P., Czaja, A., Dickons, R., Hurrell, J., McCartney, M., Saravanan, R., Visbeck, M., 2002. North Atlantic climate variability: phenomena, impacts and mechanisms. International Journal of Climatology 21, 1863–1898.

Martín-Puertas, C., Valero-Garcés, B.L., Brauer, A., Mata, M.P., Delgado-Huertas, A., Dulski, P., 2009. The Iberian–Roman Humid Period (2600–1600 cal yr BP) in the Zoñar Lake varve record (Andalucía, southern Spain). Quaternary Research 71, 108–120.

Martín-Puertas, C., Valero-Garces, B.L., Pilar Mata, M., Gonzalez-Samperiz, P., Bao, R., Moreno, A., Stefanova, V., 2008. Arid and humid phases in southern Spain during the last 4000 years: the Zonar Lake record, Cordoba. The Holocene 18, 907–921.

Mayewski, P.A., 2004. Holocene climate variability. Quaternary Research 62, 243–255.

Menking, K.M., Peteet, D.M., Anderson, R.Y., 2012. Late-glacial and Holocene vegetation and climate variability, including major droughts, in the Sky Lakes region of southeastern New York State. Palaeogeography, Palaeoclimatology, Palaeoecology 353-355, 45–59.

Meyers, P.A., 2003. Applications of organic geochemistry to paleolimnological reconstructions: a summary of examples from the Laurentian Great Lakes. Organic Geochemistry 34, 261–289.

Millán, M.M., Estrela, M.J., Miró, J., 2005. Rainfall Components: Variability and Spatial Distribution in a Mediterranean Area (Valencia Region). Journal of Climate 18, 2682–2705.

Miras, Y., Ejarque, A., Riera, S., Palet, J.M., Orengo, H., Eubab, I., 2007. Dynamique holocène de la végétation et occupation des Pyrénées andorranes depuis le Néolithique ancien, d'après l'analyse pollinique de la tourbière de Bosc dels Estanyons (2180 m, Vall del Madriu, Andorre). Comptes Rendus Palevol 6, 291–300.

Montserrat-Martí, J., 1992. Evolución glaciar y postglaciar del clima y la vegetación en la vertiente sur del Pirineo: estudio palinológico., Monografías del Instituto Pirenaico de Ecología-CSIC. Zaragoza.

Moore, P.D., Webb, J.A., 1978. An illustrated guide to pollen analysis. Hodder and Stoughton, London.

Moore, P.D., Webb, J.A., Collinson, M.E., 1991. Pollen Analysis, Second. ed. Blackwell Scientifc Publications. Oxford.

Morales-Molino, C., 2013. Dinámica vegetal desde el Tadiglaciar en la cuenca del Duero: interacciones con el clima, fuego e impacto humano. Universidad Politécnica de Madrid, Madrid.

Morales-Molino, C., Postigo-Mijarra, J.M., Morla, C., Garcia-Antón, M., 2012. Long-term persistence of Mediterranean pine forests in the Duero Basin (central Spain) during the Holocene: The case of Pinus pinaster Aiton. The Holocene 22, 561–570.

Morellón, M., Pérez-Sanz, A., Corella, J.P., Büntgen, U., Catalán, J., González-Sampériz, P., González-Trueba, J.J., López-Sáez, J.A., Moreno, A., Pla-Rabes, S., Saz-Sánchez, M. á., Scussolini, P., Serrano, E., Steinhilber, F., Stefanova, V., Vegas-Vilarrúbia, T., Valero-Garcés, B., 2012. A multi-proxy perspective on millennium-long climate variability in the Southern Pyrenees. Climate of the Past 8, 683–700.

Morellón, M., Valero-Garcés, B., Moreno, A., González-Sampériz, P., Mata, P., Romero, O., Melchor Maestro, Navas, A., 2008. Holocene palaeohydrology and climate variability in northeastern Spain: The sedimentary record of Lake Estanya (Pre-Pyrenean range). Quaternary International 181, 15–31.

Morellón, M., Valero-Garcés, B., Vegas-Vilarrúbia, T., González-Sampériz, P., Romero, Ó., Delgado-Huertas, A., Mata, P., Moreno, A., Rico, M., Corella, J.P., 2009. Lateglacial and Holocene palaeohydrology in the western Mediterranean region: The Lake Estanya record (NE Spain). Quaternary Science Reviews 28, 2582–2599.

Moreno, A., López-Merino, L., Leira, M., Marco-Barba, J., González-Sampériz, P., Valero-Garcés, B.L., López-Sáez, J.A., Santos, L., Mata, P., Ito, E., 2011. Revealing the last 13,500 years of environmental history from the multiproxy record of a mountain lake (Lago Enol, northern Iberian Peninsula). Journal of Paleolimnology 46, 327–349.

Moreno, A., González-Sampériz, P., Morellón, M., Valero-Garcés, B.L., Fletcher, W.J., 2012. Northern Iberian abrupt climate change dynamics during the last glacial cycle: A view from lacustrine sediments. Quaternary Science Reviews 36, 139–153.

Moreno, A., Pérez, A., Frigola, J., Nieto-Moreno, V., Rodrigo-Gámiz, M., Martrat, B., González-Sampériz, P., Morellón, M., Martín-Puertas, C., Corella, J.P., Belmonte, Á., Sancho, C., Cacho, I., Herrera, G., Canals, M., Grimalt, J.O., Jiménez-Espejo, F., Martínez-Ruiz, F., Vegas-Vilarrúbia, T., Valero-Garcés, B.L., 2012b. The Medieval Climate Anomaly in the Iberian Peninsula reconstructed from marine and lake records. Quaternary Science Reviews 43, 16–32.

Moreno, A., Valero-Garcés, B.L., González-Sampériz, P., Rico, M., 2008. Flood response to rainfall variability during the last 2000 years inferred from the Taravilla Lake record (Central Iberian Range, Spain). Journal of Paleolimnology 40, 943–961.

Muñoz Sobrino, C., Ramil-Rego, P., Gómez-Orellana, L., 2007. Late Würm and early Holocene in the mountains of northwest Iberia: biostratigraphy, chronology and tree colonization. Vegetation History and Archaeobotany 16, 223–240.

Muñoz Sobrino, C., Ramil-rego, P., Gómez-Orellana, L., Varela, R.A.D., 2005. Palynological data on major Holocene climatic events in NW Iberia. Boreas 34, 381–400.

Nesje, A., Bjune, A.E., Bakke, J., Dahl, S.O., Lie, Ø., Birks, H.J.B., 2006. Holocene palaeoclimate reconstructions at Vanndalsvatnet, western Norway, with particular reference to the 8200 cal. yr BP event. The Holocene 16, 717–729.

O'Brien, S.R., Mayewski, P.A., Meeker, L.D., Meese, D.A., Twickler, M.S., Whitlow, S.I., 1995. Complexity of Holocene Climate as Reconstructed from a Greenland Ice Core. Science 270, 1962–1964.

Oldfield, F., Dearing, J.A., 2003. The role of human activities in past environmental change, in: Paleoclimate, Global Change and the Future, IGBP. Berlin, pp. 143–162.

Ortu, E., Peyron, O., Bordon, A., De Beaulieu, J.L., Siniscalco, C., Caramiello, R., 2008. Lateglacial and Holocene climate oscillations in the South-western Alps: An attempt at quantitative reconstruction. Quaternary International 190, 71–88.

Pantaleón-Cano, J., Yll, E.-I., Pérez-Obiol, R., Roure, J.M., 2003. Palynological evidence for vegetational history in semi-arid areas of the western Mediterranean (Almería, Spain). The Holocene 13, 109–119.

Pausas, J.G., Paula, S., 2012. Fuel shapes the fire-climate relationship: evidence from Mediterranean ecosystems. Global Ecology and Biogeography 21, 1074–1082.

Pèlachs, A., Julià, R., Pérez-Obiol, R., Soriano, J.M., Bal, M.-C., Cunill, R., Catalan, J., 2011. Potential influence of Bond events on mid-Holocene climate and vegetation in southern Pyrenees as assessed from Burg lake LOI and pollen records. The Holocene 21, 95 –104.

Pèlachs, A., Soriano, J.M., Nadal, J., Esteban, A., 2007. Holocene environmental history and human impact in the Pyrenees. Contributions to Science 3, 421–429.

Pérez-Obiol, R., Bal, M.-C., Pèlachs, A., Cunill, R., Soriano, J.M., 2012. Vegetation dynamics and anthropogenically forced changes in the Estanilles peat bog (southern Pyrenees) during the last seven millennia. Vegetation History and Archaeobotany 21, 385–396.

Pérez-Obiol, R., Jalut, G., Julia, R., Pelachs, A., Iriarte, M.J., Otto, T., Hernandez-Beloqui, B., 2011. Mid-Holocene vegetation and climatic history of the Iberian Peninsula. The Holocene 21, 75–93.

Pérez-Sanz, A., González-Sampériz, P., Valero-Garcés, B., Moreno, A., Morellón, M., Sancho, C., Belmonte, A., Gil-Romera, G., Sevilla, M., Navas, A., 2011. Clima y actividades humanas en la dinámica de la vegetación durante los últimos 2000 años en el Pirineo central: el registro palinológico de la Basa de la Mora (Macizo de Cotiella). Zubía 23, 17–38.

Pla, S., Catalán, J., 2005. Chrysophyte cysts from lake sediments reveal the submillennial winter/spring climate variability in the northwestern Mediterranean region throughout the Holocene. Climate dynamics 24, 263–278.

Prat, N., Real, M., Rieradevall, M., 1992. Benthos of Spanish lakes and reservoirs. Limnetica 8, 221–229.

Rasmussen, S.O., Vinther, B.M., Clausen, H.B., Andersen, K.K., 2007. Early Holocene climate oscillations recorded in three Greenland ice cores. Quaternary Science Reviews 26, 1907–1914.

Reille, M., Lowe, J.L., 1995. Atlas. Pollen et spores d'Europe et d'Afrique du nord. Éditions du Laboratorie de botanique historique et palynologie, Marselle. 530p.

Reimer, P.J., Baillie, M.G.L., Bard, E., Bayliss, A., Beck, J.W., Blackwell, P.G., Bronk Ramsey, C., Buck, C.E., Burr, G.S., Edwards, R.L., Friedrich, M., Grootes, P.M., Guilderson, T.P., Hajdas, I., Heaton, T.J., Hogg, A.G., Hughen, K.A., Kaiser, K.F., Kromer, B., McCormac, F.G., Manning, S.V., Reimer, R.W., Richards, D.A., Southon, J.R., Talamo, S., Turney, C.S.M., Van der Plicht, J., Weyhenmeyer, C.E., 2009. INTCAL09 and MARINE09 radiocarbon age calibration curves, 0-50,000 years cal. BP. Radiocarbon 51, 1111–1150.

Renssen, H., Goosse, H., Fichefet, T., 2007. Simulation of Holocene cooling events in a coupled climate model. Quaternary Science Reviews 26, 2019–2029.

Renssen, H., Seppä, H., Crosta, X., Goosse, H., Roche, D.M., 2012. Global characterization of the Holocene Thermal Maximum. Quaternary Science Reviews 48, 7–19.

Renssen, H., Seppä, H., Heiri, O., Roche, D.M., Goosse, H., Fichefet, T., 2009. The spatial and temporal complexity of the Holocene thermal maximum. Nature Geoscience 2, 411–414.

Riera, S., Wansard, G., Julià, R., 2004. 2000-year environmental history of a karstic lake in the Mediterranean Pre-Pyrenees: the Estanya lakes (Spain). Catena 55, 293–324.

Rieradevall, M., Bonada, N., Prat, N., 1999. Community structure and water quality in the Mediterranean streams of a natural park (St. Llorenc del Munt, NE Spain). Limnetica 17, 45–56.

Rieradevall, M., Brooks, S.J., 2001. An identification guide to subfossil Tanypodinae larvae (Insecta: Diptera: Chironomidae) based on cephalic setation. Journal of Paleolimnology 25, 81–99.

Roberts, N., Eastwood, W.J., Kuzucuoglu, C., Fiorentino, G., Caracuta, V., 2011. Climatic, vegetation and cultural change in the eastern Mediterranean during the mid-Holocene environmental transition. The Holocene 21, 147–162.

Rubiales, J.M., García-Amorena, I., Hernández, L., Génova, M., Martínez, F., Manzaneque, F.G., Morla, C., 2010. Late Quaternary dynamics of pinewoods in the Iberian Mountains. Review of Palaeobotany and Palynology 162, 476–491.

Sabatier, P., Dezileau, L., Colin, C., Briqueu, L., Bouchette, F., Martinez, P., Siani, G., Raynal, O., Von Grafenstein, U., 2012. 7000years of paleostorm activity in the NW Mediterranean Sea in response to Holocene climate events. Quaternary Research 77, 1–11.

Sadori, L., Jahns, S., Peyron, O., 2011. Mid-Holocene vegetation history of the central Mediterranean. The Holocene 21, 117–129.

Sadori, L., Mercuri, A.M., Mariotti Lippi, M., 2010. Reconstructing past cultural landscape and human impact using pollen and plant macroremains. Plant Biosystems - An International Journal Dealing with all Aspects of Plant Biology 144, 940–951.

Saether, O.A., 1979. Chironomid communities as water quality indicators. Holartic Ecology 2, 65–74.

Sancho, C., Peña, J.L., Muñoz, A., Benito, G., McDonald, E., Rhodes, E.J., Longares, L.A., 2008. Holocene alluvial morphopedosedimentary record and environmental changes in the Bardenas Reales Natural Park (NE Spain). Catena 73, 225–238.

Santos, L., Romani, J.R.V., Jalut, G., 2000. History of vegetation during the Holocene in the Courel and Queixa Sierras, Galicia, northwest Iberian Peninsula. J. Quat. Sci. 15, 621–632.

Saz Sánchez, M.A., Consejo de Protección de la Naturaleza de Aragón, 2003. Temperaturas y precipitaciones en la mitad norte de España desde el siglo XV. Estudio dendrocimático. Consejo de Protección de la Naturaleza de Aragón, [Zaragoza].

Schnurrenberger, D., Russell, J., Kelts, K., 2003. Classification of lacustrine sediments based on sedimentary components. Journal of Paleolimnology 29, 141–154.

Scussolini, P., Vegas-Vilarrúbia, T., Rull, V., Corella, J.P., Valero-Garcés, B., Gomà, J., 2011. Middle and late Holocene climate change and human impact inferred from diatoms, algae and aquatic macrophyte pollen in sediments from Lake Montcortès (NE Iberian Peninsula). J. Paleolimnol. 46, 369–385.

Seager, R., Graham, N., Herweijer, C., Gordon, A.L., Kushnir, Y., Cook, E., 2007. Blueprints for Medieval hydroclimate. Quaternary Science Reviews 26, 2322–2336.

Seguret, M., 1972. Etude tectonique des nappes et seris décollées de la partie centrale du versant sud des Pyrénees. Caractère synsédimentaire, rôle de la compression et de lagravité, Publications USTELA. Série Géologie Structurale nº 2, Montpellier, 155 p.

Shuman, B., Bravo, J., Kaye, J., Lynch, J.A., Newby, P., Webb, T., 2001. Late Quaternary Water-Level Variations and Vegetation History at Crooked Pond, Southeastern Massachusetts. Quaternary Research 56, 401–410.

Spötl, C., Nicolussi, K., Patzelt, G., Boch, R., 2010. Humid climate during deposition of sapropel 1 in the Mediterranean Sea: Assessing the influence on the Alps. Global and Planetary Change 71, 242–248.

Steinhilber, F., Beer, J., Fröhlich, C., 2009. Total solar irradiance during the Holocene. Geophys. Res. Lett. 36.

Stockmarr, J., 1971. Tablets with spores used in absolute pollen analysis. Pollen Spores 13, 614–621.

Stoll, H.M., Moreno, A., Mendez-Vicente, A., Gonzalez-Lemos, S., Jimenez-Sanchez, M., Dominguez-Cuesta, M.J., Edwards, R.L., Cheng, H., Wang, X., submitted. Growth rates of speleothems in NW Iberian Peninsula over the last two glacial cycles and relationship with climate. Quaternary Research

Talon, B., 2010. Reconstruction of Holocene high-altitude vegetation cover in the French southern Alps: evidence from soil charcoal. The Holocene 20, 35–44.

Tarrats, P., 2011. Paleoenvironmental reconstruction of Basa de la Mora Lake (Central Pyrenees) during the Holocene using chironomid record (insecta: diptera). Universidad de Barcelona, Barcelona.

Tarrats, P., Rieradevall, M., González-Sampériz, P., Pérez-Sanz, A., Valero-Garcés, B., Moreno, A., 2014. Relating actual with subfossil chironomid assemblages. Holocene habitat changes and paleoenvironmental reconstruction of Basa de la Mora Lake (Central Pyrenees). Presented at the Erupean Geoscience Union, Vienna.

Tinner, W., Conedera, M., Ammann, B., Lotter, A.F., 2005. Fire ecology north and south of the Alps since the last ice age. The Holocene 15, 1214–1226.

Tinner, W., Hu, F.S., 2003. Size parameters, size-class distribution and area-number relationship of microscopic charcoal: relevance for fire reconstruction. The Holocene 13, 499–505.

Tinner, W., Hubschmid, P., Wehrli, M., Ammann, B., Conedera, M., 1999. Long-term forest fire ecology and dynamics in southern Switzerland. Journal of Ecology 87, 273–289.

Tinner, W., Lotter, A., 2001. Central European vegetation response to abrupt climate change at 8.2 ka. Geology 29, 551–554.

Trigo, R., Osborn, T., Corte-Real, J., 2002. The North Atlantic Oscillation influence on Europe: climate impacts and associated physical mechanisms. Climate Research 20, 9–17.

Trouet, V., Esper, J., Graham, N.E., Baker, A., Scourse, J.D., Frank, D.C., 2009. Persistent Positive North Atlantic Oscillation Mode Dominated the Medieval Climate Anomaly. Science 324, 78–80.

Valero-Garcés, B.L., González-Sampériz, P., Delgado-Huertas, A., Navas, A., Machín, J., Kelts, K., 2000. Lateglacial and Late Holocene environmental and vegetational change in Salada Mediana, central Ebro Basin, Spain. Quaternary International 73/74, 29–46.

Valero-Garcés, B.L., Moreno, A., 2011. Iberian lacustrine sediment records: responses to past and recent global changes in the Mediterranean region. Journal of Paleolimnology 46, 319–325.

Valero-Garcés, B.L., Moreno, A., Navas, A., Mata, P., Machín, J., Delgado Huertas, A., González Sampériz, P., Schwalb, A., Morellón, M., Cheng, H., Edwards, R.L., 2008. The Taravilla lake and tufa deposits (Central Iberian Range, Spain) as palaeohydrological and palaeoclimatic indicators. Palaeogeography, Palaeoclimatology, Palaeoecology 259, 136–156.

Vannière, B., Colombaroli, D., Chapron, E., Leroux, A., Tinner, W., Magny, M., 2008. Climate versus human-driven fire regimes in Mediterranean landscapes: the Holocene record of Lago dell'Accesa (Tuscany, Italy). Quaternary Science Reviews 27, 1181–1196.

Vargas-Yáñez, M., Jesús García, M., Salat, J., García-Martínez, M.C., Pascual, J., Moya, F., 2008. Warming trends and decadal variability in the Western Mediterranean shelf. Global and Planetary Change 63, 177–184.

Venables, W.N., Smith, D.M., R Development Core Team, 2008. An introduction to R notes on R, a programming environment for data analysis and graphics. Dept. of Statistics and Mathematics, Wirtschaftsuniversität Wien, Wien, Austria.

Vescovi, E., Ravazzi, C., Arpenti, E., Finsinger, W., Pini, R., Valsecchi, V., Wick, L., Ammann, B., Tinner, W., 2007. Interactions between climate and vegetation during the Lateglacial period as recorded by lake and mire sediment archives in Northern Italy and Southern Switzerland. Quaternary Science Reviews 26, 1650–1669.

Wanner, H., Beer, J., Bütikofer, J., Crowley, T.J., Cubasch, U., Flückiger, J., Goosse, H., Grosjean, M., Joos, F., Kaplan, J.O., Küttel, M., Müller, S.A., Prentice, I.C., Solomina, O., Stocker, T.F., Tarasov, P., Wagner, M., Widmann, M., 2008. Mid- to Late Holocene climate change: an overview. Quaternary Science Reviews 27, 1791–1828.

Wanner, H., Brönnimann, S., 2012. Is there a global Holocene climate mode? PAGES news 20, 44-45.

Wanner, H., Solomina, O., Grosjean, M., Ritz, S.P., Jetel, M., 2011. Structure and origin of Holocene cold events. Quaternary Science Reviews 30, 3109–3123.

Wiederholm, T., 1983. Chironomidae of the Holarctic region. Keys and diagnoses. Part I. Larvae, Wiederholm. ed. Museum of Zoology and Entomology, Lund University.

Zhao, C., Yu, Z., Ito, E., Zhao, Y., 2010. Holocene climate trend, variability, and shift documented by lacustrine stable-isotope record in the northeastern United States. Quaternary Science Reviews 29, 1831–1843.

## APPENDIX

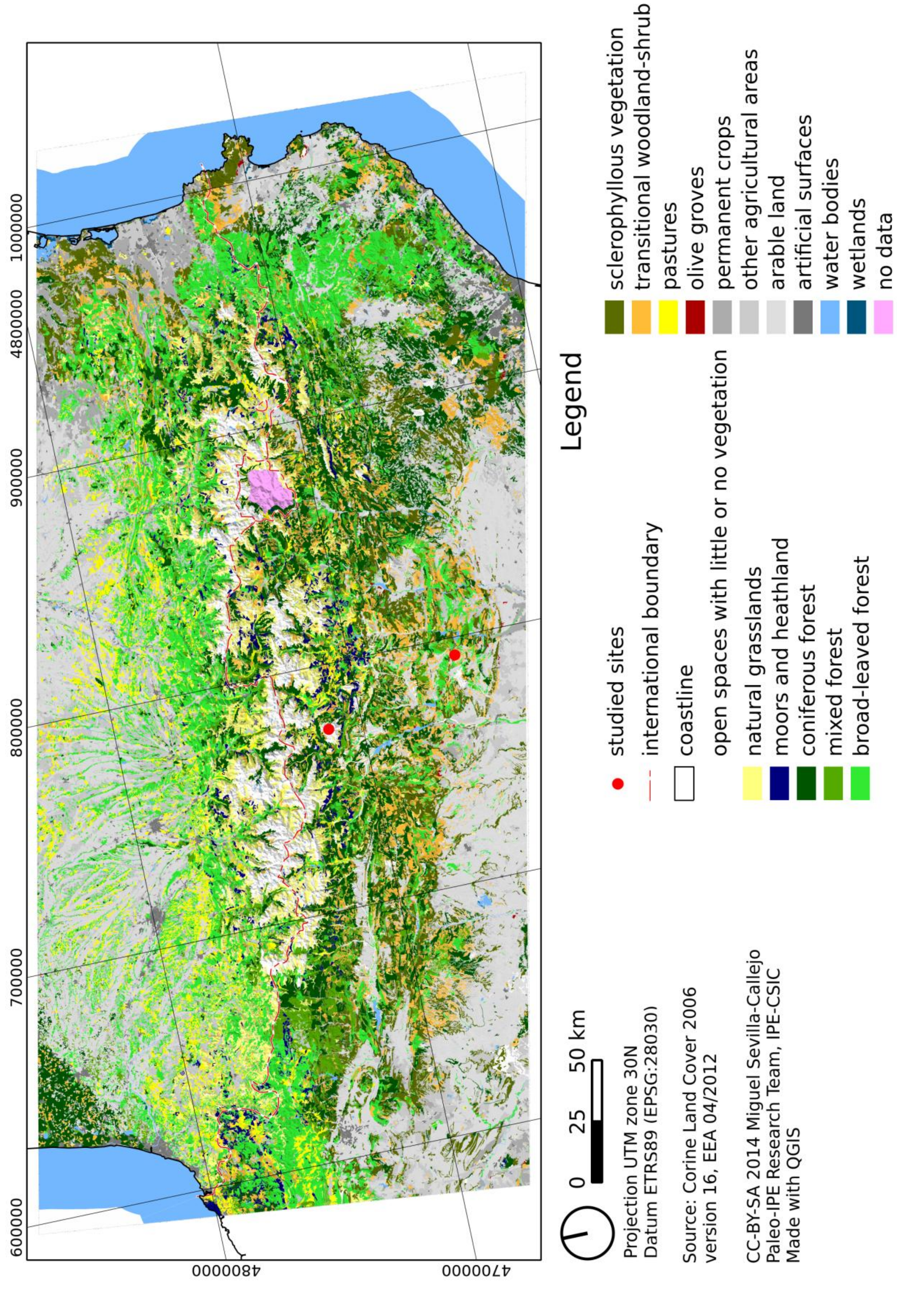


**Figure A2.1**. Vegetation map of hte Pyrenees. Map plotted by Miguel Sevilla Callejo.

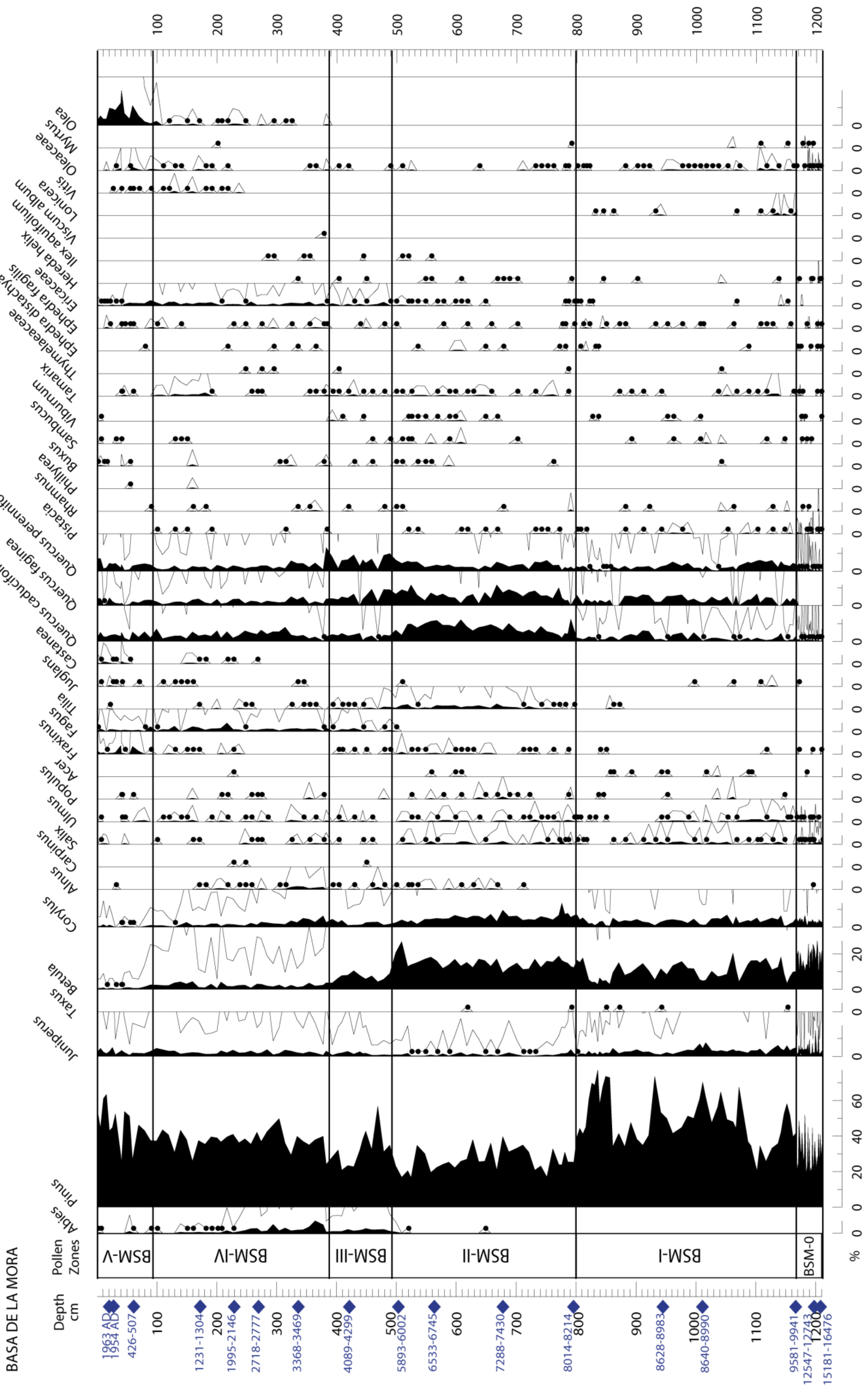


**Figure A2.2**. Arboreal pollen from Basa de la Mora sequence.

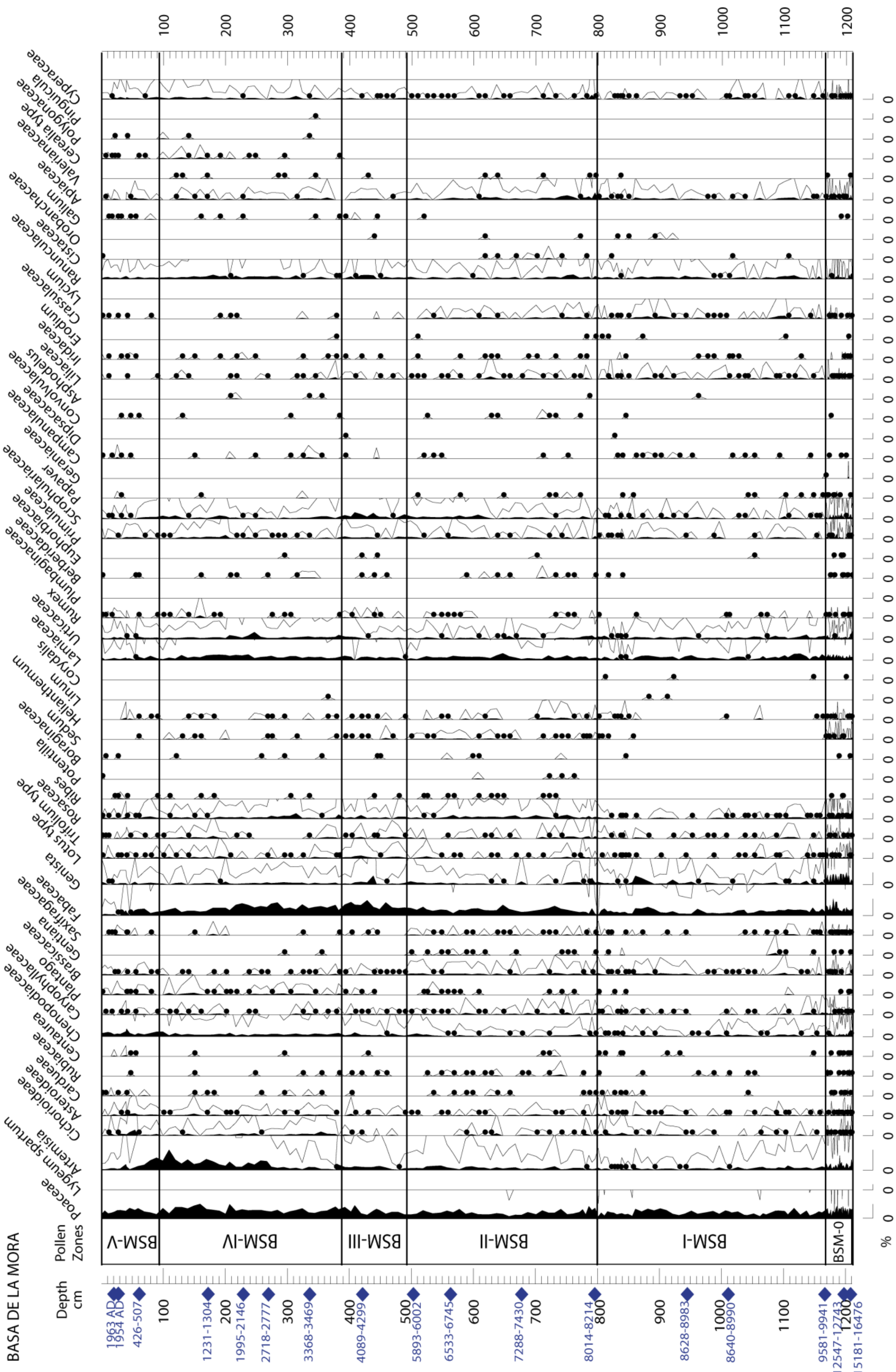


**Figure A2.3**. Non-Arboreal pollen from Basa de la Mora sequence.

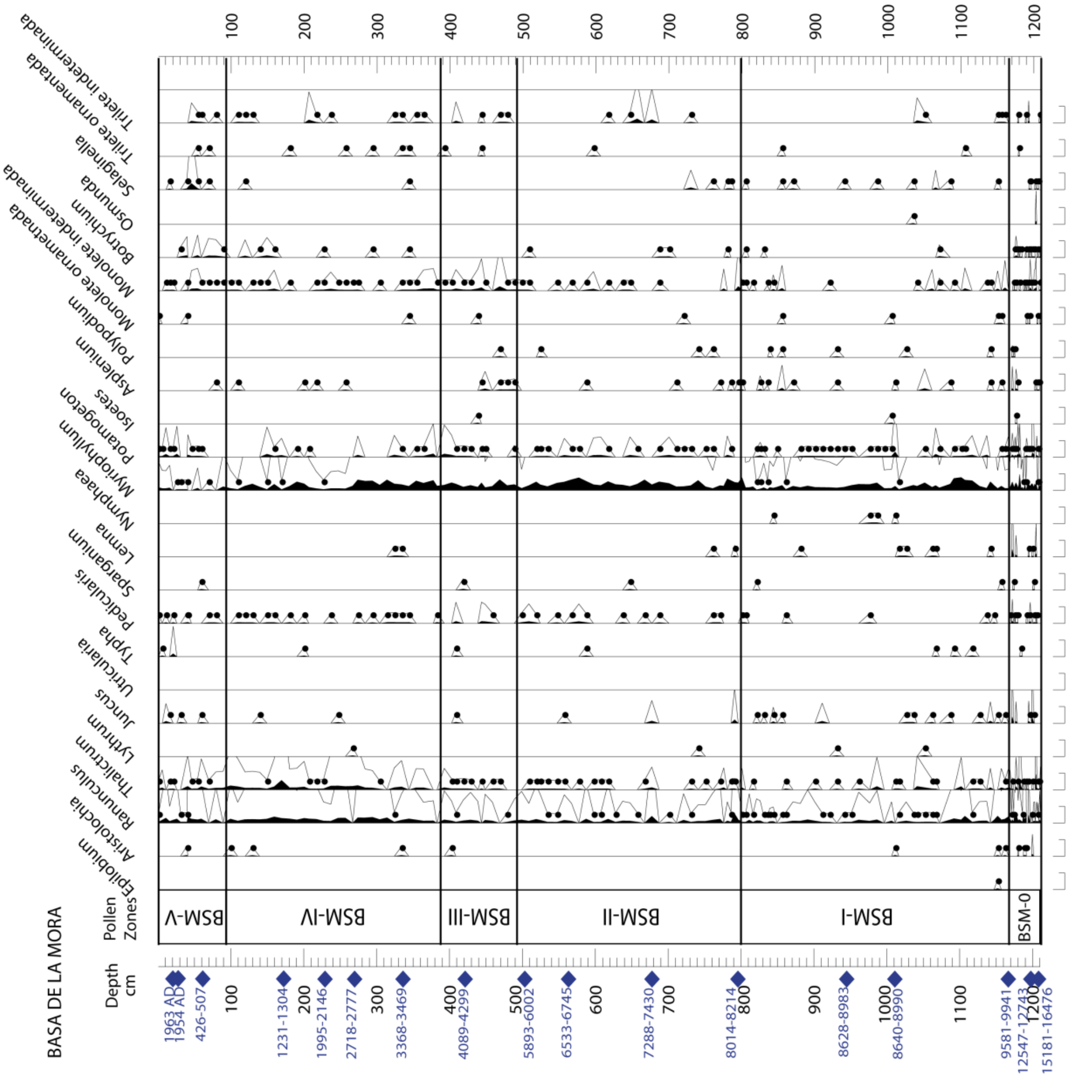


**Figure A23**. Aquatic pollen from Basa de la Mora sequence.

# 3

# The Estanya sequence. Climate at low altitudes

## Outline

The palynological record from Lake Estanya constitutes the first Holocene vegetation reconstruction from the basal belt of the southern Pyrenees. Comparison with other Pyrenean pollen sequences located at higher altitudes reveals the dynamics of the altitudinal shift of the Pyrenean vegetation belts during the Holocene, and provides a climate framework at a regional scale.

## 1.1. INTRODUCTION

The impact of the current climate change in the Mediterranean basin is high, as the frequency of drought events has increased during recent times (Hoerling et al., 2012) and it is expected to continue and possibly to intensify in the near future (Meehl et al., 2007; Giorgi and Lionello, 2008; Nikulin et al., 2011). *The expected changes in the hydrological cycle in the Mediterranean region have drawn the attention of the international research community,* as future precipitation projections and climate scenarios for this region are requested by government agencies and the public (MedCORDEX initiative, ref). However, the simulation of the Mediterranean hydrological cycle is not easy because the precipitation displays a complex pattern due to the influence of a number of climate sub-systems (Xoplaki et al., 2003; Luterbacher et al., 2006; Rodwell and Hoskins, 2001; Raicich et al., 2003; Gaetani et al., 2011; Lionello, 2012). In order to better simulate the Mediterranean hydrological cycle, attention must be paid to the reconstruction of the hydrological cycle in the past through the analysis of paleodata.

During the Holocene, ecosystems in the Mediterranean region underwent marked shifts as a result of long-term climate variations triggered mainly by changes in the atmosphere-ocean circulation and changes in the solar insolation (Mayewski et al., 2004). Palaeo-environmental archives provide the needed information to understand past climate changes and their subsequent variation in the hydrological cycle resulting from shifts in the climate components (Roberts et al., 2004).

The Pyrenees, as a mid-latitude high-mountain range, presents a great altitude gradient and consequently the temperature and humidity range in the northern and southern slopes is high. Furthermore, as we have described before in the Introduction of this Thesis (Chapter 1), this region displays numerous ecosystems related to the different temperature and precipitation regimens (Domínguez-Llovería and Puente-Cabeza, 2003) providing a unique opportunity to investigate the evolution of Mediterranean climate evolution. The vegetation is particularly versatile at low and middle altitudes, where small changes in precipitation prompt changes in the flora composition, while the uppermost forest, close to the treeline, is mainly limited by the low temperatures (Ninot et al., 2007). In addition, the southern slope of the central Pyrenees (NE Spain) is in contact with the northernmost semi-arid region of southern Europe, the central Ebro Basin, adding the presence of xerophytic vegetation communities (Domínguez-Llovería and Puente-Cabeza, 2003). The proximity of such a number of different ecosystems in a relatively small area turns the Pyrenees into an extraordinary sensitive place to climate changes, as it has been proven by a recent work that highlights an ongoing vegetation shift as a response to the current global warming (Gottfried et al., 2012). This sensitivity to both temperature and precipitation fluctuations provides an exceptional chance to study and understand abrupt past climate changes, as those occurred during the Holocene.

### 1.1.1. Objectives

This chapter aims to investigate the altitudinal vegetation shifts in the southern Central Pyrenees in order to evaluate the role of temperature and humidity as main drivers of the vegetation dynamics during the Holocene. In order to achieve this goal, we present the first Holocene pollen sequence from the lowermost vegetation belt of the southern Pyrenees: the Lake Estanya sequence (670 m a.s.l.) (fig 3.1). The Estanya results are compared with the available regional palaeoenvironmental data from high mountain areas in the region (Montserrat-Martí, 1992; Pla and Catalan, 2005; González-Sampériz et al., 2006; Miras et al., 2007; Pèlachs et al., 2007; Ejarque et al., 2009; Rull et al., 2011; Pérez-Obiol et al., 2012; Pérez-Sanz et al., 2013) (fig 3.1) in order to reveal the altitudinal vegetation shifts in the central southern Pyrenees during the Holocene and the possible mechanisms beyond those changes.

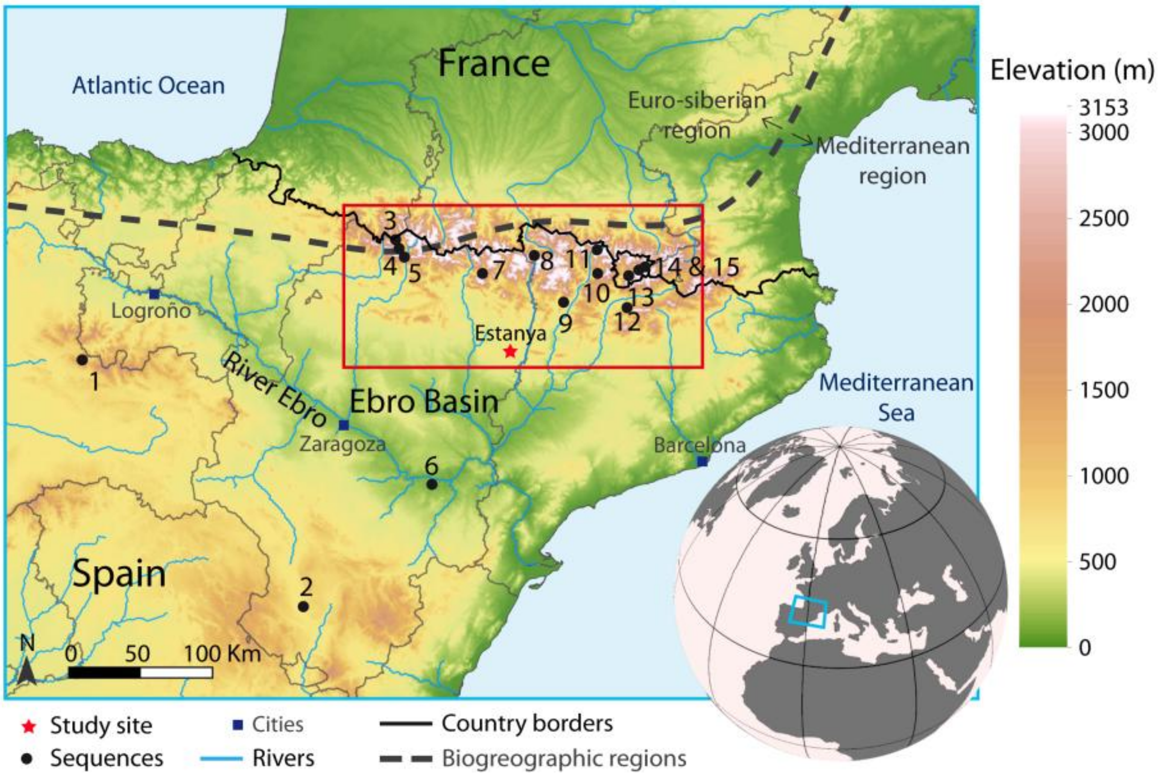


**Figure 3.1.** Geographical position of Lake Estanya and the rest of sequences from northern Spain named in the text. The red square marks the area represented in figure 2. Sequences from west to east are: 1: Las Pardillas (Sánchez-Goñi and Hannon, 1999); 2: Villarquemado (Aranbarri et al., 2014); 3: Portalet (González-Sampériz et al., 2006); 4: Tramacastilla (Montserrat-Martí, 1992); 5 : Paul de Bubal (Montserrat-Martí, 1992); 6: Chiprana (Valero-Garcés et al., 2000); 7: Basa de la Mora-BSM (Pérez-Sanz et al., 2013); 8: Redo (Pla and Catalan, 2005); 9: Montcortés (Rull et al., 2011); 10: Burg (Pèlachs et al., 2007); 11: Estanilles (Pérez-Obiol et al., 2012); 12: Pradell (Ejarque et al., 2009); 13: Planels de Perafita-PDP(Miras et al., 2010) 14: Bosc dels Estanyons-BDE (Miras et al., 2007); 15: Riu dels Orris (Ejarque et al., 2010). Map plotted by Saul Fontaneda.

## 1.2. SETTINGS

Lake Estanya is a low altitude karstic lake (fig. 3.2) placed in the Southern Pre-Pyrenees (42°02'N, 0°32'E, 670 m a.s.l.), in the Mediterranean bioclimatic regime (fig. 3.1). Mean temperature variation ranges from 4°C in the coldest month (January) to 24° C in the warmest (July). The scarce mean annual precipitation (470 mm/year) is seasonally distributed with a long dry season during the summer. Additionally, Lake Estanya is located in a transition zone between the nearby semi-desert area of the Ebro River Basin, (350 m a.s.l.) and the high peaks of the Pyrenees (up to 3400 m a.s.l.). As a result of this sharp altitudinal gradient both temperature and precipitation varies greatly in a relative small area, from 14°C and less than 350mm/yr at the Ebro Basin, to around 5°C and more than 2000mm/yr at 2000 m asl.

**Figure 3.2**. Lake Estanya panoramic view.

The Lake Estanya surrounding vegetation is formed by Mediterranean communities, represented by *Quercus rotundifolia, Buxus sempervirens* and *Juniperus oxycedrus,* and by submediterranean associations, dominated by *Quercus faginea* and *Quercus cerrioides*. These communities are mixed with patches of cereal crops. The lake is bordered by a hygrophyte band formed by *Phragmites australis, Typha angustifolia, Juncus* spp., and *Scirpus* spp.

Given its position in the lowermost altitudinal zone of the Pyrenees, Estanya sequence provides vegetation information from both the basal (up to 700 m a.s.l.) and part of the submontane belt (700-1100 m a.s.l.) (fig.3.3 a, b).

a)

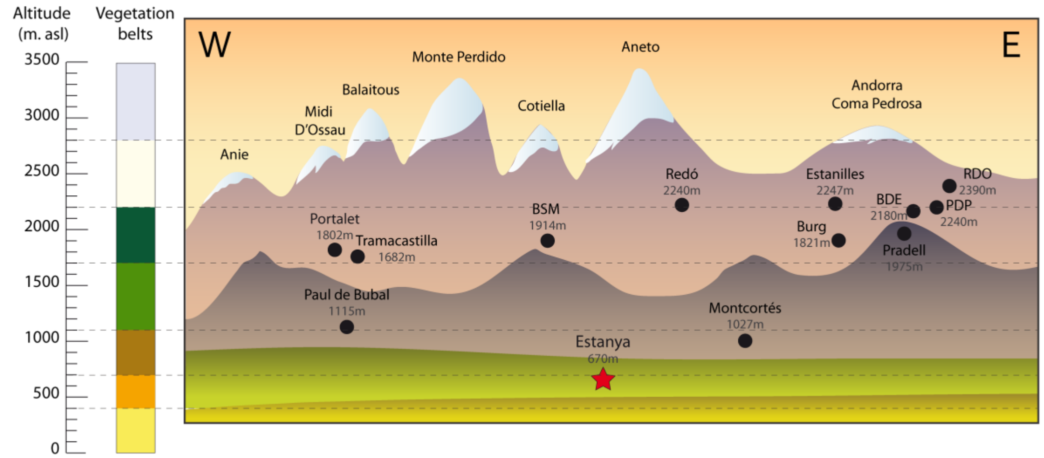


b)

| Belt Name | Altitude (m) | Trees | Shrubs/Bushes | Herbs |
|---|---|---|---|---|
| Nival | 2800-upwards | Absence of vegetation | | |
| Alpine | 2200-2800 | | | *Festuca gautieri, Elyna myosuroides, Festuca eskia, Nardus stricta, Dryas octopetala* |
| Sub-Alpine | 1700-2200 | ***Pinus uncinata**, Abies alba, Betula pendula* | *Juniperus communis* subsp. *alpina, Rhododendron ferrugineum, Vaccinium myrtillus, Sorbus aucuparia, S. chamaemespilus* | *Festuca scoparia, Helicotrichon sedenense, Thymelaeae nivalis* |
| Montane | 1100-1700 | ***Pinus sylvestris**, Abies alba, Fagus sylvatica, Corylus avellana, Betula pendula, Fraxinus excelsior, Tilia platyphyllos* | *Buxus sempervirens, Rhamnus alpina, Echinospartum horridum, Veronica officinalis, Arctostaphylos uva-ursi* | *Primula veris, Aquilegia vulgaris, Ranunculus tuberosus, Lilium pyrenaicum* |
| Sub-Montane | 700-1100 | ***Quercus faginea, Q. rotundifolia**, Q. pubescens, Q. humilis, Pinus sylvestris, P. nigra,* | *Buxus sempervirens, Juniperus communis, J. oxycedrus, J. phoenicea, Genista scorpius, Phillyrea angustifolia, Lonicera etrusca* | *Carex hallerana, Coronilla emerus, Rubia peregrina* |
| Basal | 400-700 | ***Quercus rotundifolia**, Pinus halepensis* | *Quercus coccifera, Juniperus phoenicea, J. oxycedrus, Pistzacia lentiscus, Rhamnus alaternus, Arbutus unedo, Genista scorpius* | *Salvia officinalis, Stipa pennata, S. offneri, Convolvulus lanuginosus* |
| Semi-Arid | up to 400 | *Pinus halepensis* | ***Juniperus thurifera, J. phoenicea**, J. communis, J. oxycedrus, Retama sphaerocarpa, Ephedra sp.* | *Lygeum spartum, Brachypodium retusum, Artemisia herba-alba* |
| Riparian forest | | *Populus nigra, Corylus avellana, Betula pendula, Salix alba, Populus tremula, Fraxinus excelsior, F. angustifolia* | *Clematis vitalba, C. recta, Frangula alnus* | *Saponaria officinalis, Polygonum persicaria, P. lapathifolium,* |

**Figure 3.3**. a) Schematic representation of the vegetation zones of the Southern Pyrenees including the location and altitude of all the paleoenvironmental sequences available in the area.From west to east: Portalet: González-Sampériz et al., 2006; Paul de Bubal: Montserrat-Martí, 1992; Tramacastilla: Montserrat-Martí, 1992; BSM (Basa de la Mora): Pérez-Sanz et al., 2013; Estanya: present study; Morellón et al., 2009a,b; Redo: Pla and Catalan, 2005; Montcortés: Corella et al., 2010; Rull et al., 2011; Burg: Pèlachs et al., 2007; Estanilles: Pérez-Obiol et al., 2012; Pradell: Ejarque et al., 2009; BDE (Bosc dels Estanyons): Miras et al., 2007; PDP (Planells de Perafita): Miras et al., 2010; RDO (Rius del Orris): Ejarque et al., 2010. b) Vegetation description of the different vegetation belt of the Pyrenees. The definition of the vegetation belts are based on Villar (1997), Domínguez-Lovería and Puente-Cabeza (2003) and Ninot et al., (2007). The description includes the main trees, shrubs and herbs that for each belt, sorted out by order of abundance. Main species are highlighted in bold.

## 1.3. MATERIAL AND METHODS

The fieldwork (coring and sampling), sedimentological and geochemical analyses and age-depth model for Lake Estanya sequence have been previously published in Morellón et al., 2009a. In the present Thesis radiocarbon dates for the Holocene have been calibrated with the INTCAL09 curve (Reimer et al., 2009) (table 3.1). Sedimentological and paleo-hydrological evolution of Lake Estanya for the last 22 cal ka BP has been published elsewhere (Morellón et al., 2009b) (fig. 3.4). The pollen sequence of the last 800 years was included in Morellón et al., 2011. The Lateglacial diatom-vegetation relationships have been considered in a recent work (Vegas-Vilarrúbia et al., 2013) (fig. 3.5). Here we present the palynological data concerning the whole Holocene period from the same set of cores used by Morellón et al (2009, 20119. Previous sedimentological, geochemical, biological and pollen studies in short cores from Estanya cover the last 2000 years (Riera et al., 2004)

| Lab Code | Depth (cm) | Sample type | $^{14}C$ age (yr BP) | Calibrated age, 2σ (yr cal BP) |
|---|---|---|---|---|
| 137Cs | 14 | | | -13 |
| Poz-24749 | 28.5 | Phragmites stem | 155 ±30 | 198 ± 32 |
| Poz-12245 | 54.5 | Terrestrial macrorrest | 405 ±30 | 472 ± 43 |
| Poz-12246 | 170 | Terrestrial macrorrest | 895 ±35 | 823 ± 88 |
| Poz-15972 | 189.5 | Bulk organic matter | 2120 ± 30 | 1175 ± 242 |
| Poz-12247 | 233 | Salix leave | 3315 ±3 | 3572 ± 324 |
| Poz-12248 | 330 | Gramineae seed | 5310 ± 60 | 6097 ±116 |
| Poz-15973 | 349 | Bulk organic matter | 6230 ± 40 | 6195 ± 289 |
| Poz-15974 | 393 | Bulk organic matter | 8550 ± 50 | 8647 ± 345 |
| Poz-9891 | 432 | Wood fragment | 8510 ± 50 | 9497 ± 49 |
| Poz-17190 | 493 | Plant macroremain | 8830 ± 50 | 9834 ± 136 |
| Poz-17191 | 564 | Bulk organic matter | 10 680 ± 60 | 11443 ± 384 |

**Table 3.1**. AMS radiocarbon dates from Lake Estanya core. Dates have been updated from Morellón et al., 2009b with the INTCAL09 curve.

The palynological analyses of the whole sequence were carried out every 10 cm, and laboratory procedures followed the classic chemical method (Moore et al., 1991), modified according Dupré (1992), including use of HCl, KOH, HF digestion and gravitational separation with Thoulet solution (2.0 gr/cm$^3$ density). *Lycopodium clavatum* tablets were added to calculate pollen concentrations (Stockmarr, 1971). Pollen sum was always higher than 300 terrestrial grains and taxa number not less than 20. Aquatic plants, ferns and algal remains were excluded of percentages calculation. Pollen diagrams included in this paper only concern the Holocene sequence and have been drawn using GRAPHER 4® and graphic design software ADOBE ILLUTRATOR CS4®.

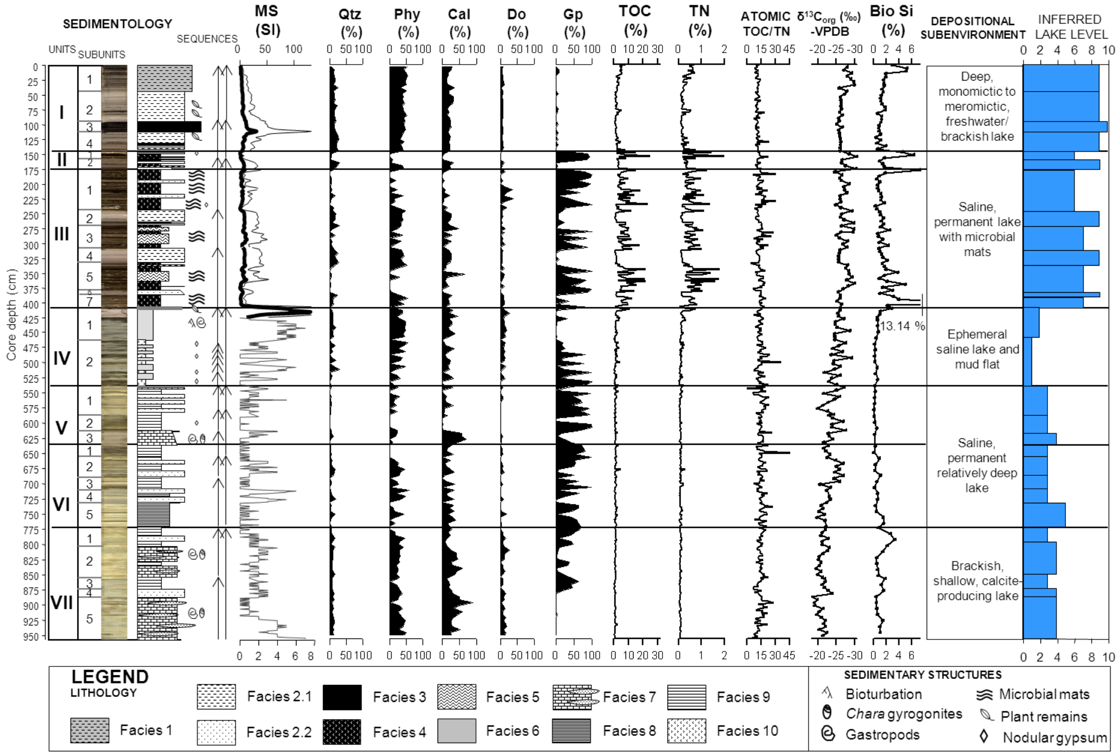


**Figure 3.4**. Sedimentological, compositional and mineralogical profiles; depositional environments and lake level fluctuation of the Lake Estanya sequence for the last 22 cal ka BP. From Morellón et al. 2009b.

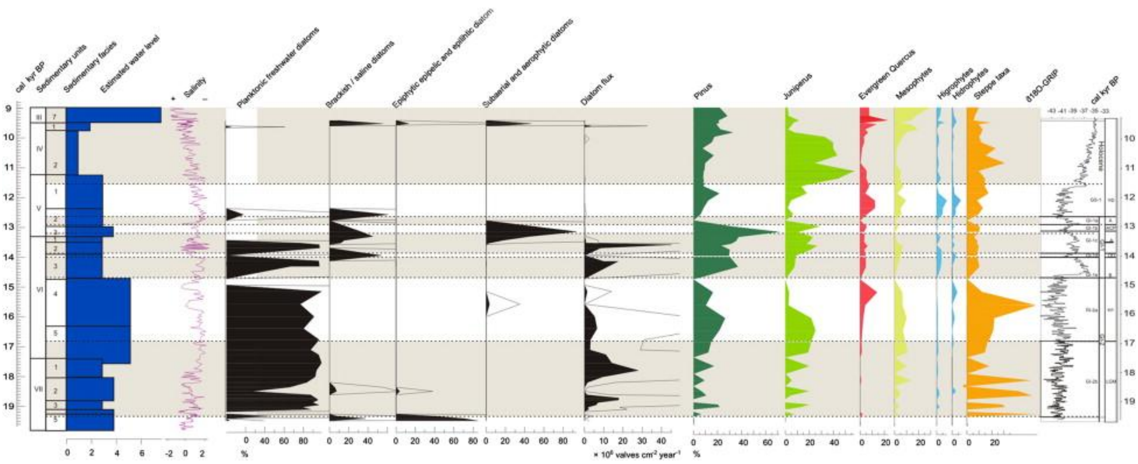


**Figure 3.5**. Diatoms-vegetation relationship fin Lake Estanya during the Late Glacial. From Vegas-Vilarúbia et al. 2013.

## 1.4. RESULTS

The Holocene Estanya pollen record shows great variety of arboreal, herbaceous and aquatic taxa. *Pinus*, semi-deciduous *Quercus*, *Corylus*, evergreen *Quercus*, and *Juniperus* are the main components of the arboreal pollen (AP) (fig. 3.6). The herbaceous taxa (NAP) are widely represented by Poaceae, *Artemisia*, Chenopodiaceae and increasing Ruderals in recent times (see fig. 3.6 for taxa included in the vegetation groups). The aquatic component, including hydrophytes and hygrophytes, keeps relatively low values; *Potamogeton* is rather remarkable at some levels, and Cyperaceae and *Ranunculus* rise at the top of the sequence reaching up to 20%. Based on major changes on tree taxa, six main pollen zones have been described (fig. 3.6). Correlation with the sedimentological units defined by Morellón et al., (2009a) is also shown in figure 3.6. Appendix II (figs A.3.1, A3.2 and A3.3), located at the end of the thesis, shows all taxa found for the BSM sequence

EST-I (570–490 cm; 11.700-9800 cal yr BP cal BP)

This zone is dominated by *Juniperus* (up to 55%). Other significant taxa within the AP are *Pinus*, semi-deciduous and evergreen *Quercus* and *Betula*. The most noticeable taxa on the herbaceous component are *Poaceae*, *Artemisia* and Chenopodiaceae (fig. 3.6). Both the hygrophytes and the hydrophytes display the minimum values of the Holocene.

EST-II (490–385 cm; 9800-8200 cal yr BP )

The onset of this zone is characterized by a sharp decline of *Juniperus* while *Corylus* and *Pinus* spread. Semi-deciduous *Quercus*, evergreen *Quercus*, Other Mesophytes and Mediterranean Shrubs also increase at this moment while *Tilia* and *Fagus* appear for the first time. In the NAP, Poaceae expands and reaches its maximum along the sequence (up to 20%) while *Artemisia* compared to the previous zone. The aquatic components increase their presence, particularly *Cyperaceae* and *Potamogeton* (fig. 3.6).

EST-III (385–320 cm; 8200-6000 cal yr BP)

The decline of *Corylus* and increase of semi-deciduous *Quercus*, evergreen *Quercus* and *Pinus* define this period. The herbaceous component is reduced and experiences some significant changes (fig. 3.6). Poaceae decreases to less than 10% and *Artemisia* and Chenopodiaceae contents strongly vary, reaching both their maxima and minima within this zone. The aquatic component reflects the drop of *Potamogeton*, which even disappears in some intervals.

EST-IV (320-260 cm; 6000-4800 cal yr BP)

This zone is defined on the basis of the expansion of semi-deciduous and evergreen *Quercus*, and *Abies,* while a decrease in *Pinus* and a further reduction in *Corylus* and Other Mesophytes are also recorded. In the herbaceous component Poaceae and *Artemisia* are reduced while in the aquatic component the hydro and hygrophytes curves barely change (fig. 3.6).

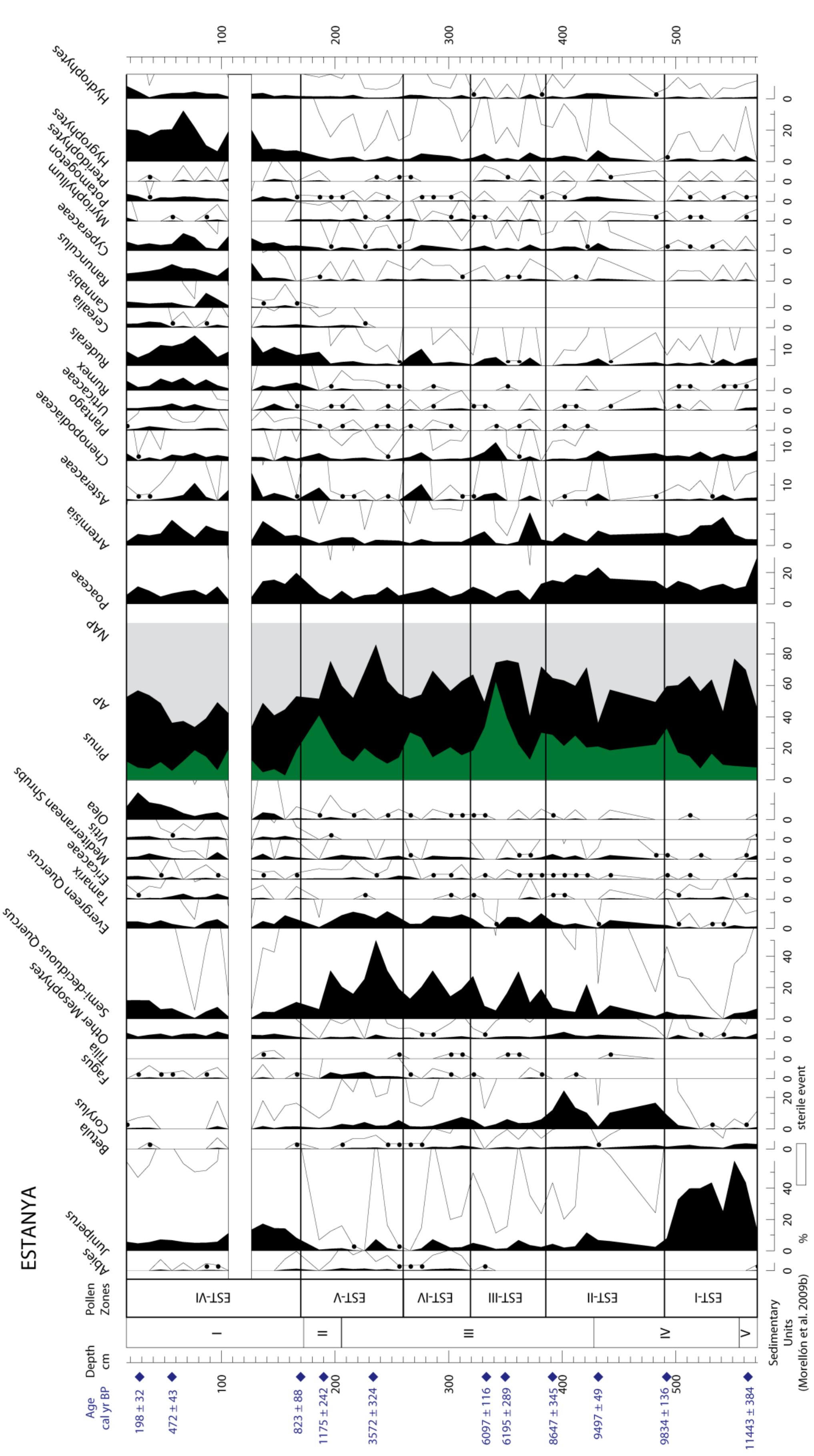


**Figure 3.6**. Selected curves from Estanya pollen diagram represented in depth. Other Mesophytes include: *Alnus*, *Carpinus*, *Salix*, *Ulmus*, *Populus*, *Acer Fraxinus* and *Juglans*. Mediterranean Shrubs include: *Pistacia*, *Rhamnus*, *Phyllyrea*, *Buxus* and *Sambucus*. Ruderals include: Cichorioideae, Carduae, Asteroideae, *Centaurea*, *Plantago*, *Rumex*, Brassicaceae, Urticaceae, Geraniaceae, Malvaceae. Hygrophytes include: *Epilobium*, *Aristolochia*, *Ranunculus*, *Thalictrum*, *Lythrum*, *Juncus*, *Utricularia*, *Cyperaceae*, *Typha Pedicularis* and *Sparganium*. Hydrophytes include: *Lemna*, *Nymphaea*, *Myriophyllum*, *Potamogeton* and *Ruppia*.

<u>EST-V (260-170 cm; 4800-800 cal yr BP)</u>

Thermophilous taxa such as semi-deciduous *Quercus* and evergreen *Quercus* reach the maximum expansion of the Holocene in this zone. Conversely, mesophytes such as *Betula* and *Corylus* keep decreasing and *Tilia* disappears (fig. 3.6). Nevertheless *Fagus* peaks at this time. The herbaceous component is characterized by the sequence's minima of Poaceae and *Artemisia*, and, more interesting, the first appearance of *Juglans*, *Cerealia* and *Vitis* and the continuous presence of *Rumex*. The Hydrophytes keep low values and the Hygrophytes decrease towards the middle of the zone and increase upwards.

<u>EST-VI (170-0 cm; 800-0 cal yr BP, 1150-1950 AD)</u>

This zone is characterized by a decrease in the AP values and the large expansion of the anthropic component such as *Olea*, *Vitis*, *Juglans*, *Cerealia* and *Cannabis* related to agricultural practises and *Rumex*, Urticaceaea and *Plantago* related to pastoral practises. All of them reach the maximum values in the 100-top cm. On the aquatic component is remarkable the expansion of *Ranunculus,* Cyperaceae and *Potamogeton*. A charcoal–rich layer found at 110 cm depth -and previously identified by Morellón et al., (2009a) - has resulted sterile - white band in figures 6 and 7- likely due to differential pollen conservation (Morellón et al., 2011) (fig. 3.7).

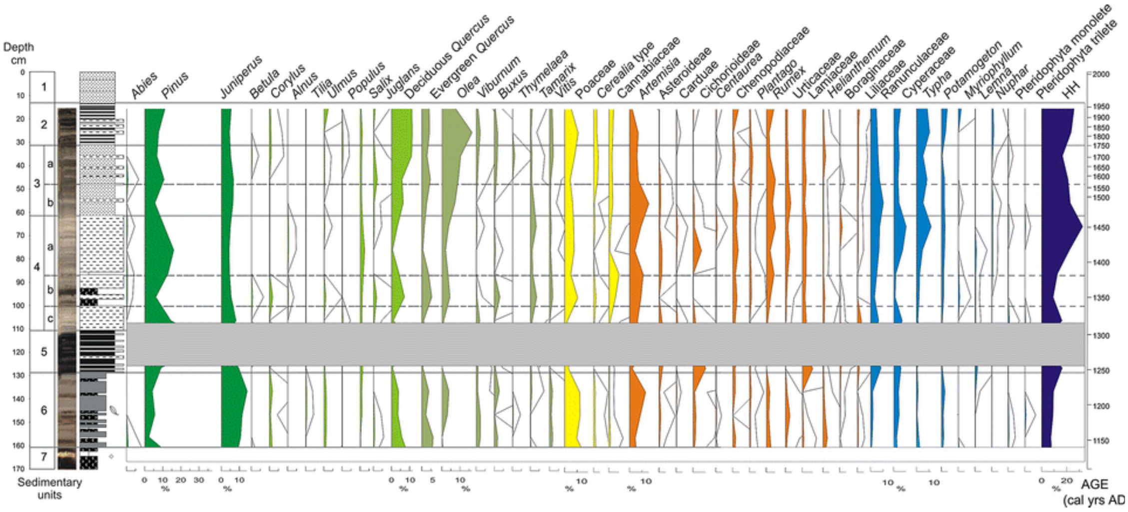


**Figure 3.7**. Selected pollen taxa from Lake Estanya sequence of the last 800 years. From Morellón et al. 2011.

## 1.5. DISCUSSION

The comparison between the vegetation changes in the Lake Estanya sequence and the vegetation changes recorded in other Pyrenean sequences placed at higher altitudes illustrates the vertical vegetation shifts in the southern Pyrenees and allow us to infer the regional climate evolution during the Holocene.

### 1.5.1. The onset of the Holocene (11.700-9800 cal yr BP): high continentality

Extremely high values of *Juniperus* and *Artemisia* and scarcity of temperate trees such as semi-deciduous and evergreen *Quercus* characterize the beginning of the Holocene in Lake Estanya (fig. 3.8). The absence or low presence of temperate trees is also observed both in inner continental Iberian sequences like Villarquemado (Aranbarri et al., 2014), Ayoó de Vidriales (Morales-Molino and García-Antón, 2013), Fuentillejo, (Vegas et al., 2010), or Espinosa del Cerrato (Franco-Múgica et al., 2001) among others, and higher altitude sequences located in the eastern part of the Pyrenees like Estanilles (Pérez-Obiol et al., 2012) or La Pouretère (Aubert et al., 2004), which are characterized by the dominance of conifers (mainly *Pinus* but also *Juniperus*).

The large proportion of junipers in Estanya and the limited expansion of the temperate forest at higher altitudes, in contrast to more Atlantic-influenced sequences from northern Spain like El Portalet (González-Sampériz et al., 2006), Enol lake (Moreno et al., 2011) or Monte Areo (López-Merino et al., 2010) among others, point to severe climate conditions in the region at the beginning of the Holocene. Current *Juniperus thurifera* communities in Iberia, including those from the nearby area of the central Ebro Basin, are found under harsh environmental conditions characterized by extreme temperatures, low precipitation and poor soil development (Blanco-Castro, 2005). The environmental conditions recorded at the onset of the Holocene in Estanya and other inner continental sequences (Carrión et al., 2010 and references therein) show some similarities to the current juniper community niche. Firstly, the onset of the Holocene was characterized by a maximum in summer and a minimum in winter insolation in the Northern Hemisphere (Kutzbach and Webb, 1993), resulting in extremely high continentality with maximum contrast between summer and winter temperatures. Secondly, linked to the high summer temperature, high evaporation-rates were likely to occur resulting in strong summer water deficits. Thirdly, the long-lasting glacial period produced gelifraction processes causing a lack of well-developed soil horizons at the Holocene onset. Analogue vegetation composition with dominance of *Juniperus* and *Artemisia* has been also recognised in other sequences from the semi-arid Central Ebro Basin (González-Sampériz et al., 2008; Davis and Stevenson, 2007) highlighting the widespread severe climate conditions in extensive areas of North-Eastern Iberia.

Particularly cold winter temperatures affecting the Pyrenees at this time are supported firstly, by the absence of temperate trees both in Estanya and at higher altitude sequences (i.e. La Paul de Bubal by Montserrat, 1992: fig. 3.3 (find references therein)), and secondly by the downwards shift of the treeline as observed in the Estanilles sequence (2250 m a.s.l.) (Pérez-Obiol et al., 2012) (fig. 3.3), where pine proportions reached the lowest values at the beginning of the Holocene. Further evidence of limited forest expansion in altitude in the Pyrenees is also provided by the absence of pine stomes in the Bosc del Estanyons sequence (BDE hereafter) (2200 m a.s.l.) (Miras et al., 2007) (fig. 3.3) and by the absence of wood charcoals until ca 10.5 cal ka BP in Plaus de Boldís-Montarenyo area (2000-2200 m a.s.l.) (Cunill et al., 2012). These cold conditions still recorded in the Pyrenees are in agreement with the Alborán SST reconstruction curve from Cacho et al., 2001 (fig. 3.8c), supporting the role of low temperatures in both ocean and atmosphere to avoid forest development across inner Iberia during the first millennia of the Holocene.

In addition, the dense juniper landscape at lowlands indicates a year-round water shortage accompanying the high seasonal contrast. Nevertheless, rainfall reconstructions during the first stages of the Holocene show a large variability: while Lake Estanya displays the lowest lake levels of the Holocene (Morellón et al., 2009b), the river discharge into the western Mediterranean seems to have reached very high values at this time, according to the highest values of the K/Al recorded in the marine sequence MD99-2343 (fig. 3.8b) by Frigola et al., 2007. Particularly dry conditions have been also recognised across the northern Mediterranean coast during the first millennium of the Holocene (Magny et al., 2013). This water shortage was responsible for a long delay on the establishment of well-developed forests across the region. The increased runoff into the Mediterranean (Frigola et al., 2007) may be a result of the scarce vegetation in the watersheds as well as of melting processes in the Late Glacial-inherited Pyrenean glaciers, rather than a direct increase in the precipitation.

Hence, the absence of a forested landscape in Estanya may be a result of a combination of factors such as high continentality, low effective humidity and absence of well-developed soil, as well as in many areas of Mediterranean Iberia (Carrión et al., 2010).

### 1.5.2. The Early Holocene (9800-8200 cal yr BP): increasing humidity

The expansion of the forest in Estanya took place at ca. 9.8 cal ka BP and was characterized by a marked increase in broad-leaf taxa (mainly *Corylus*) and a slight increase in *Quercus* species and Mediterranean shrubs (fig. 3.6). The marked shift from a continental steppe landscape, dominated by *Juniperus* and *Artemisia,* toward a wooded landscape, dominated by *Corylus,* suggests both more humid conditions and an increase in winter temperatures. The presence of deciduous taxa in higher altitude sequences in the Pyrenees like i.e., Paul de Bubal, El Portalet, Lake Burg, BSM, Lake Racou, BDE or Estanilles (figs. 3.1 and 3.3: references therein) is also relevant during this period, indicating the upwards treeline shift due to the occurrence of milder temperatures. In addition, both the chrysophyte cysts-based temperature anomaly curve from the Pyrenean Lake Redo (figs. 3.1, 3.3 and 3.8d) and the SST reconstruction from the Alboran Sea (fig. 3.8c), reflect the fast increase in mean annual temperatures at the western Mediterranean area, likely as a result of meaningful warmer winters.

The large spread of deciduous taxa in Estanya sequence and the palaeohydrological reconstruction carried out by Morellón et al., (2009a) showing a water level rise at this moment (fig. 3.8h), indicate that the precipitation would have increased significantly. In agreement with increased water availability, in altitude, the palaeohydrological reconstruction from Lake Basa de la Mora (BSM) (fig. 3.2) highlights the occurrence of high lake levels at this moment too (Pérez-Sanz et al., 2013). Accordingly, more humid conditions have been recognised across the Mediterranean area during this period (Magny et al., 2013). Nevertheless, the distribution of the precipitation throughout the year and whether there was summer drought or not is a subject of much debate. According to Magny et al., 2013, until ca. 4.5 ka, there was contrasting precipitation seasonality in the central Mediterranean with humid winters and dry summers north of 40°N and humid winters and humid summers south of ca 40°N. In our study site, placed at ca 42°N in the western Mediterranean, the signals are also opposite. The vegetation composition at highlands, i.e. BSM, Estanilles or Redo sequences (fig. 3.3), with dominance of conifers and low values of mesophytes (fig. 3.8f) supports the occurrence of an unevenly-distributed precipitation throughout the year, in agreement with the seasonal pattern for north of 40°N in the Central Mediterranean (Magny et al., 2013). However, the large presence of *Corylus* in Estanya suggests the absence of summer drought and would indicate a contrasting pattern with the BSM precipitation seasonality. Nevertheless, due to the location of our study site in the basal level of a great mountain range such as the Pyrenees, the spread of deciduous taxa in the lowlands (like in Estanya area) could be related to riparian formations (fig. 3.3b) that could have been favoured by increased river flows resulting from high rates of snow melting. In fact, the highest values of the magnetic susceptibility curve (fig. 3.8e) and the chironomid assemblage obtained from the BSM record, point out intense runoff processes and indicate that water inputs into the lake were dominated by snowpack melting (Pérez-Sanz et al., 2013). Therefore, summer water supplies into the lowlands could have been higher than during the previous stage and responsible for large deciduous formations associated to riparian environments. Nevertheless, the seasonal precipitation pattern in Lake Estanya and indeed in the whole Pyrenean region and North-eastern Iberia cannot be unequivocally inferred.

### 1.5.3. The Mid Holocene (8200-6000 cal yr BP): the Climatic Optimum

A relevant shift in the vegetation landscape composition took place in Estanya after 8.2 cal ka BP. The semi-deciduous and evergreen *Quercus* replaced the broad-leaf taxa (mainly *Corylus*) (fig. 3.6) suggesting a relevant increase in winter temperatures, as *Quercus* taxa in the Iberian Peninsula are better adapted than mesophytes to warmer winters. The vegetation shifts recorded at higher altitudes in the Pyrenees also support warmer winters. Deciduous forests replaced pinewoods in Tramacastilla (1682 m asl) (fig. 3.3) and BSM (1914 m asl) (fig. 3.8f) indicating that broad-leaf taxa could occupy the middle altitudes and even reach the subalpine belt in some parts of the Pyrenees. Although with lower proportions, higher altitude sequences such as BDE (2180 m a.s.l.), Redo (2240 m a.s.l.) or Estanilles (2247 m a.s.l.) (fig. 3.3) also record a peak in broad-leaf taxa at this moment, proving the upward expansion of the deciduous forest, probably reaching the treeline. The spread of deciduous trees at high altitudes as a result of warmer winters is in agreement with the winter temperature anomaly reconstruction carried out in the Pyrenean Lake Redo (fig. 3.8d). In general, this period witnessed an overall warming trend clearly reflected in the high SST recorded in the Western Mediterranean during more than 2000 years within this period (fig. 3.8c).

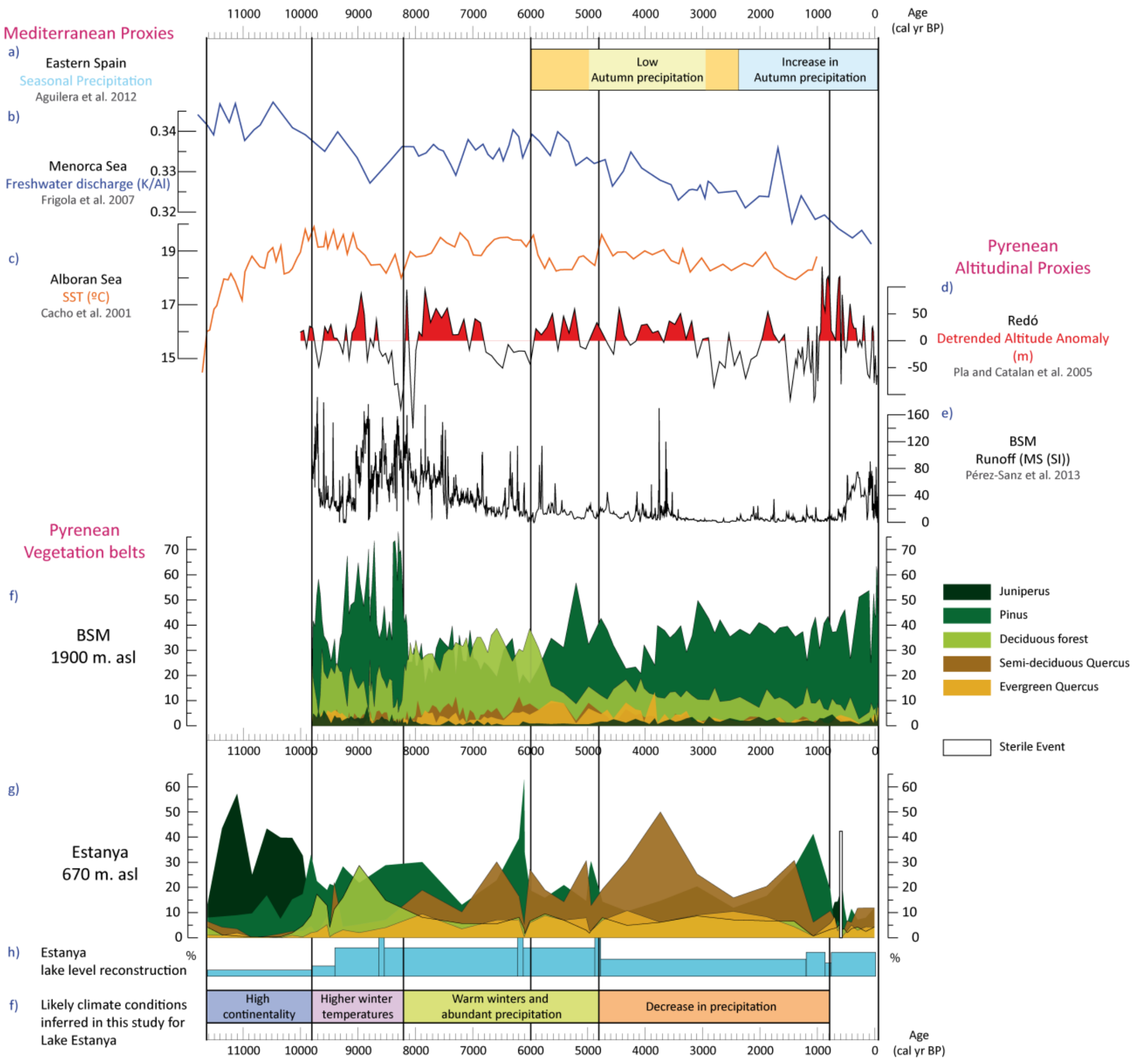


**Figure 3.8**. Comparison between the Estanya pollen-record and others Holocene climate indicators from the Pyrenees and the Mediterranean area. a) Seasonal precipitation in Valencia region, western Mediterranean (Aguilera et al., 2012). b) Freshwater discharge into the Menorca Sea, Western Mediterranean, from Iberian rivers (Frigola et al., 2007). c) Sea Surface Temperature from the Alboran Sea, south-western Mediterranean (Cacho et al., 2001). d) Altitude anomaly in winter temperatures from Pyrenean Lake Redo (Pla and Catalan, 2005). e) Runoff activity in the Pyrenean Lake Basa de la Mora-BSM (Pérez-Sanz et al., 2013). f) Pollen evolution from the BSM lake (Pérez-Sanz et al., 2013). g) Vegetation evolution from Lake Estanya (present study). h) Lake level changes from Lake Estanya (Morellón et al., 2009a). f) Likely climate conditions inferred in this study for Lake Estanya during the Holocene. Note that chronological framework is plotted from past on the left to present on the right.

A well-developed deciduous forest at high altitude requires, not only rise in temperature but also, a change in the precipitation regime with a more evenly distributed rainfall. In this regard, both Estanya and BSM lakes record one of their highest lake levels during the Mid-Holocene (fig. 3.8h). Giving the fast response to inter-annual changes in precipitation in both BSM and Estanya lakes (Morellón et al., 2009b, Tarrats et al., 2014), permanent high lake levels at this time could only be supported by increasing precipitation and the absence of a long-lasting dry season (fig. 3.9). In addition, lower MS values in BSM sequence (fig. 3.8e) indicate reduced activity of the streams and more diffuse run-off. This could reflect a higher contribution of rainfall *versus* snowmelt in the hydrological cycle, hence, an evenly distributed rainfall throughout the year. Highest Holocene lake levels have also been recorded during this time in Lake Racou, at the Eastern Pyrenees (Guiter et al., 2005). According to these data, water would not be a limiting factor to deciduous trees to survive in Estanya and therefore the replacement of broad-leaf taxa by semi-deciduous and evergreen *Quercus* in this area support the rise in winter temperatures as the main reason for this altitudinal vegetation shift. More humid conditions in the Pyrenees with increased lake levels agree with the long-lasting period of high river discharges into the Menorca Sea recognised by Frigola et al., 2007 (fig. 3.8b) and are in agreement with high lake level reconstruction across de Mediterranean region (Harrison and Digerfeldt, 1993; Magny et al., 2002) and with recurrent flood events in the River Tagus watershed in the central part of the Iberian Peninsula (Benito et al., 2003). Nevertheless, these results for the Pyrenees, placed at ca 42°N, contrast with the precipitation pattern recorded in Italy during this period with the occurrence of dry summers in areas placed north of 40°N (Magny et al., 2013) pointing out the complex precipitation pattern of the Mediterranean region during the Mid-Holocene.

**Figure 3.9**. Comparison between humid (top) and dry (bottom) seasons in Lakes Estanya (left) and Basa de la Mora (right).

### 1.5.4. The end of the Mid-Holocene (6000-4800 cal yr BP): transition phase

The vegetation record from Estanya barely experienced any important change at this period, apart from a slight decrease in *Pinus*. In contrast, at higher altitudes, the BSM sequence (fig. 3.8f) underwent a sharp change, characterized by a marked replacement of mesophytes by *Pinus* which in turn became the most relevant tree. A decrease in mesophytes is also recorded in other high-altitude sequences in the Pyrenees such as Estanilles, Redo or Lake Burg (fig. 3.3). This situation suggests a shift in the water budget with a decrease in annual precipitation or at least a significant change in the seasonal distribution of rainfall with the establishment of a dry season. Regarding the latter possibility, in a study based on carbon isotope composition ($\delta^{13}C$) of archaeobotanical remains, Aguilera et al., (2012) found that a phase of particular sharp decrease in the autumn precipitation took place between 6 and 5 cal ka BP (fig. 3.8a). The onset of a sustained dry season could have been responsible of deep changes in the vegetation altitudinal zones, especially where water-demanding taxa were widespread such as in BSM (Pérez-Sanz et al., 2013). In contrast, conifer communities are relatively more drought-tolerant, thus, changes in the treeline altitude, mainly formed by pines, were more unnoticed (Miras et al., 2007, 2010; Ejarque et al., 2010; Pérez-Obiol et al., 2012). The establishment of a longer dry season would have given place to an important spread of drought-resistant taxa across Iberia (Pérez-Obiol and Juliá, 1994; Jalut et al., 2000; Carrión, 2002; de Bealieau et al., 2005; Fernández et al., 2007; Anderson et al., 2011; Carrión et al., 2010; Pérez-Obiol et al., 2011; Aranbarri et al., 2014). Nevertheless, high lake level in Estanya and relative high input of river discharge into the Menorca Sea (fig. 3.8b), at least until ca 5.5 cal ka BP, suggest that the total amount of annual rainfall could be still significant. This situation is in agreement with humid conditions recorded in the central Mediterranean for this period (Magny et al., 2013) and supports that the vegetation changes recognised at high altitudes in the Pyrenees –decrease in deciduous trees- may be linked to shifts in the precipitation seasonality rather than to a sharp decrease in year-round rainfall. This change in the distribution of the precipitation would not affect the pine and semi-deciduous oak formations at lowlands, as i.e. in the Estanya sequence, well adapted to a dry season.

Finally, this period is also characterized by the onset of a worldwide long-term cooling trend, starting at ca 5.5 cal ka BP (Marcott et al., 2013). In agreement with this global temperature trend, the regional SST in the western Mediterranean records a marked drop just at 5.5 cal ka BP (fig. 3.8c). However, winter temperatures in the Pyrenees seem to hardly have changed in comparison with the previous period (fig. 3.8d) supporting that the mentioned shifts recorded in the Pyrenean vegetation belts may be mainly explained by changes in the precipitation regimen with the installation of a long-lasting dry season.

### 1.5.5. The Late Holocene (4800-800 cal yr BP): aridity trend and onset of the anthropogenic activities

The Late Holocene in Estanya was characterized by a marked spread of semi-deciduous *Quercus*, a slight increase in evergreen *Quercus* and a reduction in *Pinus*, while mesophytes kept low values similarly to previous periods. At higher altitudes, broad-leaf taxa continued to withdraw in those sequences that recorded this contraction beforehand (BSM, Estanilles, Redo or Lake Burg) (fig. 3.3) and started to drop in the rest of eastern sequences (RDO, BDE and PDP) (fig. 3.3). Taking into account that in the previous stage (6-4.8 cal ka BP) took place the establishment of the occurrence of a dry season in the hydrological cycle, the expansion of drought-resistant taxa at lower altitudes along with the reduced presence of broad-leaf taxa in middle altitudes at this moment, indicates a likely yearly reduction in precipitation. Decreased in annual rainfall is supported by rapid changes in water levels recorded in Lake Estanya (Morellón et al., 2009a, 2009b), Lake Montcortés (fig. 3.3: Corella et al., 2010) or BSM lake (Pérez-Sanz et al., 2013) at this time. Indeed, the BSM Lake registers the lowest MS values (fig. 3.8a) and precipitation of endogenig crystals of calcite and gypsum, and periods of total desiccation (Pérez-Sanz et al., 2013). The K/Al record for the Menorca Sea shows a marked decreasing trend in river discharge into the western Mediterranean (fig. 3.8b) supporting the decline in runoff because of a sharp decrease in total precipitation. This drought trend recognised in Iberia agrees with the pronounced hydrological change toward much drier condition registered in Italy at ca 4.5 ka (Magny et al., 2013).

Along with decreased moisture availability, pollen indicators also suggest a general decrease in temperature. A decreasing trend in the pine pollen content at this time in Estanilles (fig. 3.3) indicates a downward movement of the treeline. Furthermore, an expansion trend of *Juniperus* is recorded in BSM too (fig. 3.8f), as well as in Estanya, suggesting the increasing presence of a juniper understory as a consequence of a likely forest opening at different altitudes. Both the treeline movement to lower altitudes and reduction of forest density are in agreement with the cooling trend in winter temperatures recorded in Lake Redo, particularly after ca 3 cal ka BP (fig. 3.8d). General drop in mean annual temperatures are also supported by the lowest SST in the Alborán Sea (fig. 3.8c).

### 1.5.6. Anthropogenic activity

Additionally, during this period the Estanya sequence witnessed the first evidence of agricultural and deforestation practises (at 3.1 cal ka BP, 1150 BC) with the appearance of *Cerealia* type (fig. 3.5 and fig. 3.10) and the occurrence of a slight drop in AP values. During the Iberian-Roman and Visigoth Times (200 BC - 750 AD) a slight intensification of the agricultural activities as pointed by the appearance of *Vitis* and an increase in *Olea* percentages, occur in Estanya, although nitrophilous plants are not relevant at this moment (fig. 3.10).

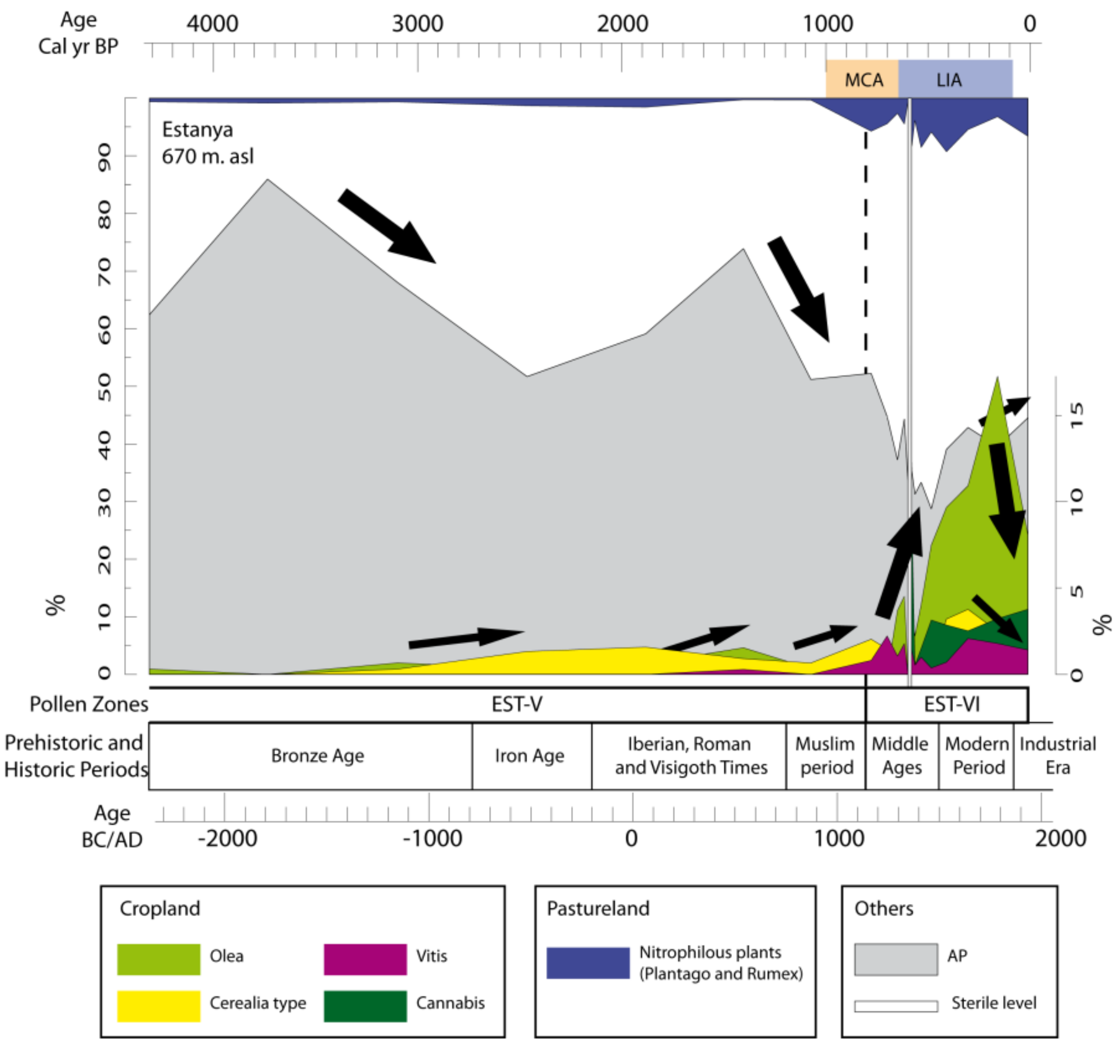


**Figure 3.10**. Evolution of the different anthropogenic indicators in the Estanya sequence during the last 4000 years. The selected taxa to represent the agricultural activities are *Olea*, *Vitis*, *Cerealia* and *Cannabis*. On the other hand, the nitrophilous plants representing the pastoral activities include *Rumex* and *Plantago*. The scale for the AP is located at the left side of the plot. The scale for the selected taxa is placed in the right side and multiplied by three in order to amplify their evolution.

During the Medieval Climate Anomaly (MCA: 900-1300 AD), signals of human activities steadily increased, coinciding with the establishment of the Muslims in the region. Cultivated taxa, namely *Vitis*, *Olea* and *Cerealia* type rose significantly as well as it began a marked expansion of the nitrophilous plants while the AP proportions underwent a marked drop (fig. 3.10), suggesting human activities as main forcing of vegetation landscape composition as already documented by (Riera et al., 2004) in a study of short cores. However, an increase in the presence of *Juniperus* and heliophytes such as *Artemisia* and a decrease in the presence of deciduous trees (fig. 3.10), could indicate that the vegetation in Lake Estanya was also influenced by the drier conditions reconstructed for the MCA in northeaster Iberia (Moreno et al., 2012) (fig. 3.11). In agreement with these drier conditions, lower lake levels and higher water salinity were recorded in Estanya at this time (Morellón et al., 2011), as well as in other regional sequences (Morellón et al., 2012).

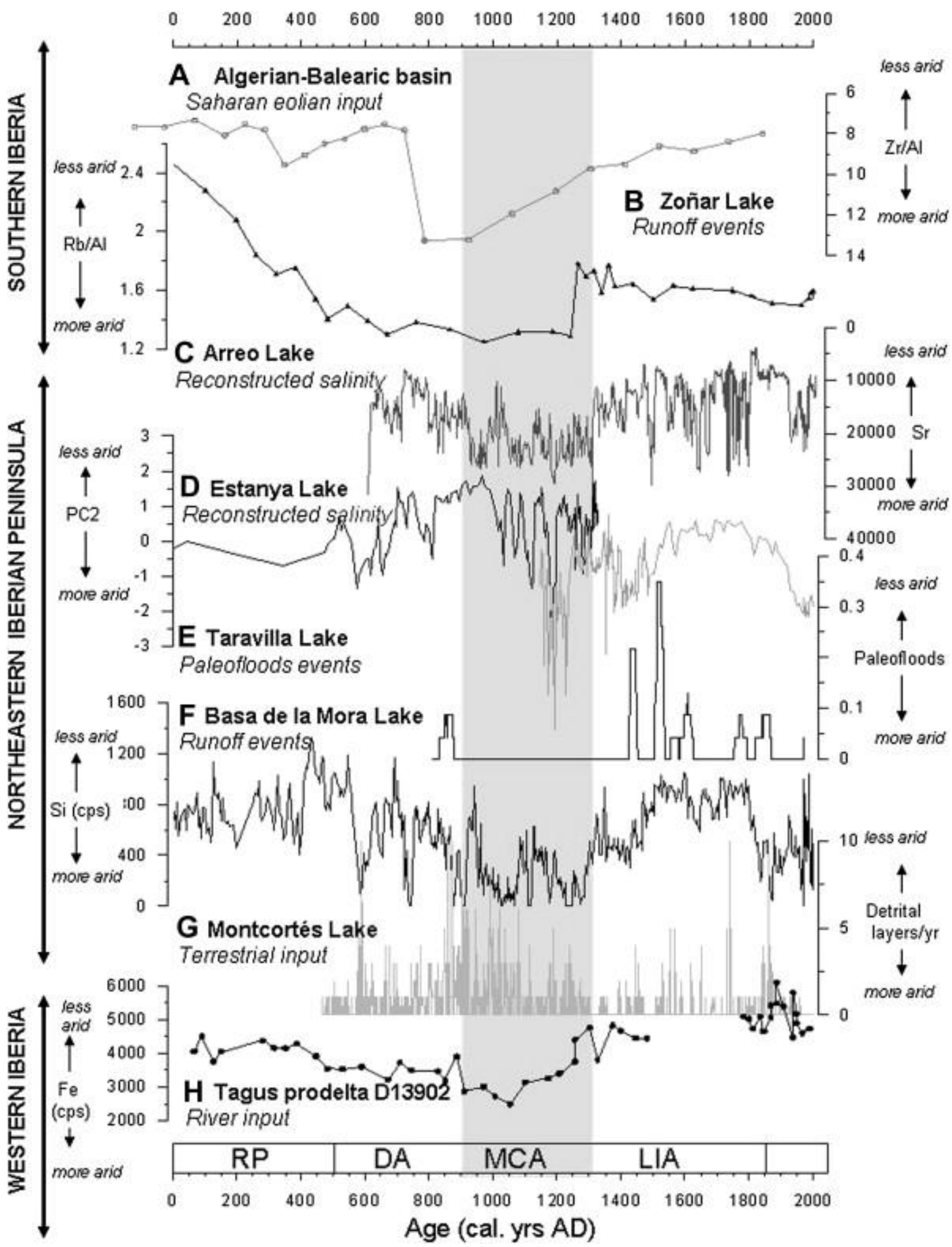


**Figure 3.11**. Reconstructed dry conditions for the MCA from Iberian records. A) Zr/Al ratio from Algerian–Balearic basin core; B) Rb/Al ratio from Zoñar Lake; C) Sr (cps) from Arreo Lake; D) the aridity reconstruction of Estanya Lake (axis 2 from the Principal Component Analyses applied to the XRF dataset in two cores); E) the number of paleoflood events in Taravilla Lake; F) Si (cps) from Basa de la Mora Lake; G) the number of detrital layers per year from Montcortès Lake and H) Fe (cps) from the Tagus prodelta. From Moreno et al. 2012.

Nevertheless, apart from the last stage of this period when the landscape underwent some human-related changes, in general, the vegetation changes recorded in Estanya sequence between 4800 and 800 cal yr BP are in agreement, firstly, with the palaeohydrological reconstruction carried out in the same lake by Morellón et al., (2009b), and secondly, with changes observed in other environmental reconstructions from higher altitudes in the Pyrenees (Pérez-Sanz et al., 2011), indicating that, despite some human influence, vegetation shifts were primarily climate-driven during this period.

### 1.5.7. The last centuries (800-0 cal yr BP / 1150-1950 AD): crossing a threshold in landscape management

Increasing landscape management in Estanya took place at 0.8 cal ka BP through the spread of grazing and farming practices (Riera et al., 2004; Morellón et al., 2011). The sharp increase in *Olea* and in ruderal and nitrophilous plants such as *Rumex*, along with the appearance of *Cannabis* and a sharp decline in the AP values (fig. 3.10, EST-VI), marks a threshold in the agro-pastoral activities at this moment, coinciding with the origin of the Crown of Aragon and the beginning of the Middle Ages (Carreras-Ares, 1996). This marked human-induced vegetation change has been documented in other Pyrenean sequences (Pèlachs et al., 2007; Miras et al., 2010; Ejarque et al., 2010), indicating a massive use of the forest at all levels in order to open the landscape for extensive agro-pastoral systems.

However, despite the mentioned increase of human activities, some vegetation sequences also show imprints of the colder and more humid conditions that characterized the latter half of the Little Ice Age (LIA: 1500-1850 AD) in the Pyrenees (Morellón et al., 2012) (fig. 3.10). Firstly, in the lowlands, though the Estanya sequence records the highest expansion of *Vitis* and *Cerealia* type and the intensification of *Cannabis* and *Olea* cultivation at this point, it also shows an increase in mesophytes and in the aquatic component, in contrast to the drop in these taxa and the increase in *Juniperus* recorded during the MCA (fig. 3.6 and 3.10). This increase in water-demanded taxa coincides with a more positive water balance in the lake (Morellón et al., 2011; Morellón et al., 2012) in agreement with more humid conditions. On the other hand, pollen sequences placed at higher altitudes show a partial recovery of the forest and a decrease in cultivated taxa (Pérez-Obiol et al., 2012; Pérez-Sanz et al., 2011, 2013) indicating a decline in human pressure on the highlands. During the LIA, the Pyrenees recorded a remarkable development of glacial systems pointing out a drop in temperatures and an increase in moisture (González-Trueba et al., 2008; Chueca-Cía et al., 2005). These cold conditions could be responsible for a temporal abandonment of human activities in the highlands (Pérez-Sanz et al., 2011), which indeed intensified in the lowlands, likely further favoured by an increase in water availability. These facts prove that both humans and climate forcings have been always implied in the vegetation shifts occurred in the Pyrenees, even during the last centuries.

Since the onset of the 20$^{th}$ century and especially during the second half of that century, it took place an important change in the social organization in Spain that led to a major migration from the villages into the cities (Lasanta-Martínez et al., 2005). The Estanya pollen sequence only records de first half of the 20th century but it shows evidence of this major socio-economical shift. Agricultural-related taxa such as *Olea*, *Cerealia* type and *Vitis* decreased considerably since their maximum values recorded between the 17th and 19th centuries (fig. 3.10). Additionally, the AP values increased slightly in agreement with less agricultural pressure in the region. However, both nitrophilous plants and *Cannabis* increase (fig. 3.10) pointing out yet some important anthropogenic activity in the area. At a more regional scale, higher altitude sequences of the southern Pyrenees show a progressive increase in forest recovery (Ejarque et al., 2009; Cunill et al., 2012; Pérez-Obiol et al., 2012; Pérez-Sanz et al., 2013) indicating the spread of pine formations in the subalpine belt in agreement with reduced anthropogenic pressure also in the highlands. Nevertheless, recent works have demonstrated that the upwards migration of the treeline and the increase in tree density, that the subalpine forest of the Pyrenees have been experiencing lately, is also a result of the current Global Change and the recent rise in temperatures (Camarero and Gutiérrez, 2004; Batllori and Gutiérrez, 2008). This fact proves the fast response of the Pyrenean forests to climate changes, particularly under low-degree anthropogenic pressure, supporting the climate-driven vegetation shifts reconstructed in this chapter for the regional Holocene evolution.

## 1.6. CONCLUSIONS

i. The synchrony and consistency of the altitudinal vegetation shifts indicates that the vegetation dynamic in the Pyrenees has been climate-driven during most part of the Holocene until approximately 0.8 cal Ka BP (1150 AD), when the anthropogenic activities caused high-degree degradation on the landscape.

ii. Severe climate conditions characterized by extremely seasonal contrast and water deficit determined the presence of steppe communities in the lowlands and limited the forest development at high altitudes from the onset of the Holocene until 9.8 cal ka BP.

iii. After 9.8 cal ka BP, the mesophyte communities spread in the lowlands. This expansion during a period of wet and cold winters but relative dry summers could have been favoured by high water inputs as snowmelt from the Pyrenees

iv. Between 8200 and 6000 cal yr BP, an increase in winter temperatures along with a change in the regimen precipitation with a more evenly distribution of the rainfall favoured the vegetation belts to rise in altitude, leading to the establishment of a well-developed Mediterranean forest in the lowlands and a deciduous forest in the subalpine belt.

v. A change in the precipitation pattern with a development of a dry season was responsible for the substitution of the deciduous forest of the subalpine belt by pine-dominant formations at ca. 6 cal Ka BP. The Mediterranean forest located in the lowlands was hardly affected until 4.8 cal ka BP, when a trend toward drier conditions along with a moderate decrease in winter temperatures resulted in semi-deciduous *Quercus* in Estanya and the opening of the pine forest at higher altitudes.

vi. The first signs of anthropogenic activities are recognised at ca. 3.1 cal ka BP with the appearance of *Cerealia* type and a likely deforestation phase. The large spread of agro-pastoral activities are recorded at ca 0.8 cal ka BP, when the expansion of grazing and farming-related taxa and a sharp decrease in the forest cover indicate a threshold in sustainable land management.

vii. Climate has secondarily controlled altitudinal vegetation shifts during the periods of most intense anthropogenic pressure, as it has also determine the location and intensity of human activities in the lowlands and highlands.

## References


Aguilera, M., Ferrio, J.P., Pérez, G., Araus, J.L., Voltas, J., 2012. Holocene changes in precipitation seasonality in the western Mediterranean Basin: a multi-species approach using δ13C of archaeobotanical remains. J. Quat. Sci. 27, 192–202.

Anderson, R.S., Jiménez-Moreno, G., Carrión, J.S., Pérez-Martínez, C., 2011. Postglacial history of alpine vegetation, fire, and climate from Laguna de Río Seco, Sierra Nevada, southern Spain. Quat. Sci. Rev. 30, 1615–1629.

Aranbarri, J., González-Sampériz, P., Valero-Garcés, B., Moreno, A., Gil-Romera, G., Sevilla-Callejo, M., García-Prieto, E., Di Rita, F., Mata, M.P., Morellón, M., Magri, D., Rodríguez-Lázaro, J., Carrión, J.S., 2014. Rapid climatic changes and resilient vegetation during the Lateglacial and Holocene in a continental region of south-western Europe. Glob. Planet. Change 114, 50–65.

Aubert, S., Belet, J.-M., Bouchette, A., Otto, T., Dedoubat, J.-J., Fontugne, M., Jalut, G., 2004. Dynamique tardiglaciaire et holocène de la végétation à l'étage montagnard dans les Pyrénées centrales. C. R. Biol. 327, 381–388.

Batllori, E., Gutiérrez, E., 2008. Regional tree line dynamics in response to global change in the Pyrenees. J. Ecol. 96, 1275–1288.

Benito, G., Sopeña, A., Sánchez-Moya, Y., Machado, M.J., Pérez-González, A., 2003. Palaeoflood record of the Tagus River (Central Spain) during the Late Pleistocene and Holocene. Quat. Sci. Rev. 22, 1737–1756.

Blanco Castro, E., 2005. Los Bosques ibéricos: una interpretación geobotánica. Planeta, Barcelona.

Cacho, I., Grimalt, J.O., Canals, M., Sbaffi, L., Shackleton, N.J., Schönfeld, J., Zahn, R., 2001. Variability of the western Mediterranean Sea surface temperature during the last 25,000 years and its connection with the Northern Hemisphere climatic changes. Paleoceanography 16, 40–52.

Camarero, J.J., Gutiérrez, E., 2004. Pace and Pattern of Recent Treeline Dynamics: Response of Ecotones to Climatic Variability in the Spanish Pyrenees. Clim. Change 63, 181–200.

Carreras-Ares, J.J., 1996. Historia de Aragón II.: economía y sociedad: resumen de las lecciones impartidas en los cursos 1987-88 y 1988-89. Institución Fernando el Católico, Zaragoza.

Carrión, J.S., 2002. Patterns and processes of Late Quaternary environmental change in a montane region of southwestern Europe. Quat. Sci. Rev. 21, 2047–2066.

Carrión, J.S., Fernández, S., González-Sampériz, P., Gil-Romera, G., Badal, E., Carrión-Marco, Y., López-Merino, L., López-Sáez, J.A., Fierro, E., Burjachs, F., 2010. Expected trends and surprises in the Lateglacial and Holocene vegetation history of the Iberian Peninsula and Balearic Islands. Rev. Palaeobot. Palynol. 162, 458–475.

Chueca-Cía, J., Julián-Andrés, A., Saz-Sánchez, M.A., Creus-Novau, J., López-Moreno, J.I., 2005. Responses to climatic changes since the Little Ice Age on Maladeta Glacier (Central Pyrenees). Geomorphology 68, 167–182.

Corella, J.P., Moreno, A., Morellón, M., Rull, V., Giralt, S., Rico, M.T., Pérez-Sanz, A., Valero-Garcés, B.L., 2010. Climate and human impact on a meromictic lake during the last 6,000 years (Montcortès Lake, Central Pyrenees, Spain). J. Paleolimnol. 46, 351–367.

Cunill, R., Soriano, J.-M., Bal, M.-C., Pèlachs, A., Pérez-Obiol, R., 2012. Holocene treeline changes on the south slope of the Pyrenees: a pedoanthracological analysis. Veg. Hist. Archaeobotany 21, 373–384.

Davis, B.A.S., Stevenson, A.C., 2007. The 8.2 ka event and Early–Mid Holocene forests, fires and flooding in the Central Ebro Desert, NE Spain. Quat. Sci. Rev. 26, 1695–1712.

De Beaulieu, J.L., Miras, Y., Andrieu-Ponel, V., Guiter, F., 2005. Vegetation dynamics in north-western Mediterranean regions: Instability of the Mediterranean bioclimate. Plant Biosyst. - Int. J. Deal. Asp. Plant Biol. 139, 114–126.

Domínguez-Llovería, J.A., Puente-Cabeza,, J., 2003. La vegetación de la cuenca del Ebro. Heraldo de Aragón, Zaragoza.

Dupré, M., 1992. Palinología. Sociedad Española de Geomorfología.

Ejarque, A., Julià, R., Riera, S., Palet, J.M., Orengo, H.A., Miras, Y., Gascón, C., 2009. Tracing the history of highland human management in the eastern Pre-Pyrenees: an interdisciplinary palaeoenvironmental study at the Pradell fen, Spain. The Holocene 19, 1241 –1255.

Ejarque, A., Miras, Y., Riera, S., Palet, J.M., Orengo, H.A., 2010. Testing micro-regional variability in the Holocene shaping of high mountain cultural landscapes: a palaeoenvironmental case-study in the eastern Pyrenees. J. Archaeol. Sci. 37, 1468–1479.

Fernández, S., Fuentes, N., Carrión, J.S., González-Sampériz, P., Montoya, E., Gil, G., Vega-Toscano, G., Riquelme, J.A., 2007. The Holocene and Upper Pleistocene pollen sequence of Carihuela Cave, southern Spain. Geobios 40, 75–90.

Franco Múgica, F., García Antón, M., Maldonado Ruiz, J., Morla Juaristi, C., Sainz Ollero, H., 2001. The Holocene history of Pinus forests in the Spanish Northern Meseta. The Holocene 11, 343–358.

Frigola, J., Moreno, A., Cacho, I., Canals, M., Sierro, F.J., Flores, J.A., Grimalt, J.O., Hodell, D.A., Curtis, J.H., 2007. Holocene climate variability in the western Mediterranean region from a deepwater sediment record. Paleoceanography 22.

Gaetani, M., Pohl, B., Douville, H., Fontaine, B., 2011. West African Monsoon influence on the summer Euro-Atlantic circulation. Geophys. Res. Lett., L09705 38, n/a–n/a.

Giorgi, F., Lionello, P., 2008. Climate change projections for the Mediterranean region. Glob. Planet. Change 63, 90–104.

González-Sampériz, P., Valero-Garcés, B.L., Moreno, A., Jalut, G., García-Ruiz, J.M., Martí-Bono, C., Delgado-Huertas, A., Navas, A., Otto, T., Dedoubat, J.J., 2006. Climate variability in the Spanish Pyrenees during the last 30,000 yr revealed by the El Portalet sequence. Quat. Res. 66, 38–52.

González-Sampériz, P., Valero-Garcés, B.L., Moreno, A., Morellón, M., Navas, A., Machín, J., Delgado-Huertas, A., 2008. Vegetation changes and hydrological fluctuations in the Central Ebro Basin (NE Spain) since the Late Glacial period: Saline lake records. Palaeogeogr. Palaeoclimatol. Palaeoecol. 259, 157–181.

González-Trueba, J.J., Moreno, R.M., Martinez de Pison, E., Serrano, E., 2008. `Little Ice Age' glaciation and current glaciers in the Iberian Peninsula. The Holocene 18, 551–568.

Gottfried, M., Pauli, H., Futschik, A., Akhalkatsi, M., Barančok, P., Benito Alonso, J.L., Coldea, G., Dick, J., Erschbamer, B., Fernández Calzado, M.R., Kazakis, G., Krajči, J., Larsson, P., Mallaun, M., Michelsen, O., Moiseev, D., Moiseev, P., Molau, U., Merzouki, A., Nagy, L., Nakhutsrishvili, G., Pedersen, B., Pelino, G., Puscas, M., Rossi, G., Stanisci, A., Theurillat, J.-P., Tomaselli, M., Villar, L., Vittoz, P., Vogiatzakis, I., Grabherr, G., 2012. Continent-wide response of mountain vegetation to climate change. Nat. Clim. Change 2, 111–115.

Guiter, F., Andrieu-Ponel, V., Digerfeldt, G., Reille, M., Beaulieu, J.-L., Ponel, P., 2005. Vegetation history and lake-level changes from the Younger Dryas to the present in Eastern Pyrenees

(France): pollen, plant macrofossils and lithostratigraphy from Lake Racou (2000 m a.s.l.). Veg. Hist. Archaeobotany 14, 99–118.

Harrison, S.P., Digerfeldt, G., 1993. European lakes as palaeohydrological and palaeoclimatic indicators. Quat. Sci. Rev. 12, 233–248.

Hoerling, M., Eischeid, J., Perlwitz, J., Quan, X., Zhang, T., Pegion, P., 2012. On the Increased Frequency of Mediterranean Drought. J. Clim. 25, 2146–2161.

Jalut, G., Esteban Amat, A., Bonnet, L., Gauquelin, T., Fontugne, M., 2000. Holocene climatic changes in the Western Mediterranean, from south-east France to south-east Spain. Palaeogeogr. Palaeoclimatol. Palaeoecol. 160, 255–290.

Kutzbach, J.., Webb, T., 1993. Conceptual basis for understanding late-Quaternay climatess, in: Global Climates since the Last Glacial Maximum. University of Minnesota Press.

Lionello, P., 2012. The climate of the Mediterranean Region from the past to the future. Elsevier Science, Burlington.

López-Merino, L., Cortizas, A.M., López-Sáez, J.A., 2010. Early agriculture and palaeoenvironmental history in the North of the Iberian Peninsula: a multi-proxy analysis of the Monte Areo mire (Asturias, Spain). J. Archaeol. Sci. 37, 1978–1988.

Luterbacher, J., Xoplaki, E., Casty, C., Wanner, H., Pauling, A., Kuttel, M., Rutishauser, T., Bronnimann, S., Fischer, E., Fleitmann, D., 2006. Chapter 1 Mediterranean climate variability over the last centuries: A review, in: Developments in Earth and Environmental Sciences. Elsevier, pp. 27–148.

Magny, M., Combourieu-Nebout, N., de Beaulieu, J.L., Bout-Roumazeilles, V., Colombaroli, D., Desprat, S., Francke, A., Joannin, S., Ortu, E., Peyron, O., Revel, M., Sadori, L., Siani, G., Sicre, M.A., Samartin, S., Simonneau, A., Tinner, W., Vannière, B., Wagner, B., Zanchetta, G., Anselmetti, F., Brugiapaglia, E., Chapron, E., Debret, M., Desmet, M., Didier, J., Essallami, L., Galop, D., Gilli, A., Haas, J.N., Kallel, N., Millet, L., Stock, A., Turon, J.L., Wirth, S., 2013. North-south palaeohydrological contrasts in the central Mediterranean during the Holocene: tentative synthesis and working hypotheses. Clim. Past 9, 2043–2071.

Magny, M., Miramont, C., Sivan, O., 2002. Assessment of the impact of climate and anthropogenic factors on Holocene Mediterranean vegetation in Europe on the basis of palaeohydrological records. Palaeogeogr. Palaeoclimatol. Palaeoecol. 186, 47–59.

Marcott, S.A., Shakun, J.D., Clark, P.U., Mix, A.C., 2013. A Reconstruction of Regional and Global Temperature for the Past 11,300 Years. Science 339, 1198–1201.

Mayewski, P.A., 2004. Holocene climate variability. Quat. Res. 62, 243–255.

Meehl, G.A., Stocker, T.F., Collins, W.D., Friedlingstein, P., Gaye, A.T., Gregory, J.M., Kitoh, A., Knutti, R., Murphy, J.M., Nodas, A., Raper, S.C.B., Watterson, I.G., Weaver, A.J., Zhao, Z.C., 2007. Global Climate Projections, in: Solomon, S., Quin, D., Manning, M., Chen, Z., Marquis, M., Averyt, K.B., Tignor, M., Miller, H.L. (Eds.), Climate Change 2007: The Physical Science Basis. Contribution of Working Group I to the Fourth Assessment Report of the Intergovernmental Panel on Climate Change. Cambridge University Press, Cambridge, UK and New York, USA.

Miras, Y., Ejarque, A., Orengo, H., Mora, S.R., Palet, J.M., Poiraud, A., 2010. Prehistoric impact on landscape and vegetation at high altitudes: An integrated palaeoecological and archaeological approach in the eastern Pyrenees (Perafita valley, Andorra). Plant Biosyst. - Int. J. Deal. Asp. Plant Biol. 144, 924–939.

Miras, Y., Ejarque, A., Riera, S., Palet, J.M., Orengo, H., Eubab, I., 2007. Dynamique holocène de la végétation et occupation des Pyrénées andorranes depuis le Néolithique ancien, d'après l'analyse pollinique de la tourbière de Bosc dels Estanyons (2180 m, Vall del Madriu, Andorre). Comptes Rendus Palevol 6, 291–300.

Montserrat-Martí, J., 1992. Evolución glaciar y postglaciar del clima y la vegetación en la vertiente sur del Pirineo: estudio palinológico., Monografías del Instituto Pirenaico de Ecología-CSIC. Zaragoza.

Moore, P.D., Webb, J.A., Collinson, M.E., 1991. Pollen Analysis, Second. ed. Blackwell Scientifc Publications.

Morales-Molino, C., García-Antón, M., 2013. Vegetation and fire history since the last glacial maximum in an inland area of the western Mediterranean Basin (Northern Iberian Plateau, NW Spain). Quat. Res.

Morellón, M., Pérez-Sanz, A., Corella, J.P., Büntgen, U., Catalán, J., González-Sampériz, P., González-Trueba, J.J., López-Sáez, J.A., Moreno, A., Pla-Rabes, S., Saz-Sánchez, M. á., Scussolini, P., Serrano, E., Steinhilber, F., Stefanova, V., Vegas-Vilarrúbia, T., Valero-Garcés, B., 2012. A multi-proxy perspective on millennium-long climate variability in the Southern Pyrenees. Clim. Past 8, 683–700.

Morellón, M., Valero-Garcés, B., Anselmetti, F., Ariztegui, D., Schnellmann, M., Moreno, A., Mata, P., Rico, M., Corella, J.P., 2009a. Late Quaternary deposition and facies model for karstic Lake Estanya (North-eastern Spain). Sedimentology 56, 1505–1534.

Morellón, M., Valero-Garcés, B., González-Sampériz, P., Vegas-Vilarrúbia, T., Rubio, E., Rieradevall, M., Delgado-Huertas, A., Mata, P., Romero, Ó., Engstrom, D.R., López-Vicente, M., Navas, A., Soto, J., 2011. Climate changes and human activities recorded in the sediments of Lake Estanya (NE Spain) during the Medieval Warm Period and Little Ice Age. J. Paleolimnol. 46, 423–452.

Morellón, M., Valero-Garcés, B., Vegas-Vilarrúbia, T., González-Sampériz, P., Romero, Ó., Delgado-Huertas, A., Mata, P., Moreno, A., Rico, M., Corella, J.P., 2009b. Lateglacial and Holocene palaeohydrology in the western Mediterranean region: The Lake Estanya record (NE Spain). Quat. Sci. Rev. 28, 2582–2599.

Moreno, A., López-Merino, L., Leira, M., Marco-Barba, J., González-Sampériz, P., Valero-Garcés, B.L., López-Sáez, J.A., Santos, L., Mata, P., Ito, E., 2011. Revealing the last 13,500 years of environmental history from the multiproxy record of a mountain lake (Lago Enol, northern Iberian Peninsula). J. Paleolimnol. 46, 327–349.

Moreno, A., Pérez, A., Frigola, J., Nieto-Moreno, V., Rodrigo-Gámiz, M., Martrat, B., González-Sampériz, P., Morellón, M., Martín-Puertas, C., Corella, J.P., Belmonte, Á., Sancho, C., Cacho, I., Herrera, G., Canals, M., Grimalt, J.O., Jiménez-Espejo, F., Martínez-Ruiz, F., Vegas-Vilarrúbia, T., Valero-Garcés, B.L., 2012. The Medieval Climate Anomaly in the Iberian Peninsula reconstructed from marine and lake records. Quat. Sci. Rev. 43, 16–32.

Nikulin, G., KjellströM, E., Hansson, U., Strandberg, G., Ullerstig, A., 2011. Evaluation and future projections of temperature, precipitation and wind extremes over Europe in an ensemble of regional climate simulations. Tellus A 63, 41–55.

Ninot, J.M., Carrillo, E., Font, X., Carreras, J., Ferré, A., Masalles, R.M., Soriano, I., Vigo, J., 2007. Altitude zonation in the Pyrenees. A geobotanic interpretation. Phytocoenologia 37, 371–398.

Pèlachs, A., Soriano, J.M., Nadal, J., Esteban, A., 2007. Holocene environmental history and human impact in the Pyrenees. Contrib. Sci. 3, 421–429.

Pérez-Obiol, R., Bal, M.-C., Pèlachs, A., Cunill, R., Soriano, J.M., 2012. Vegetation dynamics and anthropogenically forced changes in the Estanilles peat bog (southern Pyrenees) during the last seven millennia. Veg. Hist. Archaeobotany 21, 385–396.

Pérez-Obiol, R., Jalut, G., Julia, R., Pelachs, A., Iriarte, M.J., Otto, T., Hernandez-Beloqui, B., 2011. Mid-Holocene vegetation and climatic history of the Iberian Peninsula. The Holocene 21, 75–93.

Pérez-Obiol, R., Juliá, R., 1994. Climatic Change on the Iberian Peninsula Recorded in a 30,000-Yr Pollen Record from Lake Banyoles. Quat. Res. 41, 91–98.

Pérez-Sanz, A., González-Sampériz, P., Moreno, A., Valero-Garcés, B., Gil-Romera, G., Rieradevall, M., Tarrats, P., Lasheras-Álvarez, L., Morellón, M., Belmonte, A., Sancho, C., Sevilla-Callejo, M., Navas, A., 2013. Holocene climate variability, vegetation dynamics and fire regime in the central Pyrenees: the Basa de la Mora sequence (NE Spain). Quat. Sci. Rev. 73, 149–169.

Pla, S., Catalan, J., 2005. Chrysophyte cysts from lake sediments reveal the submillennial winter/spring climate variability in the northwestern Mediterranean region throughout the Holocene. Clim. Dyn. 24, 263–278.

Raicich, F., Pinardi, N., Navarra, A., 2003. Teleconnections between Indian monsoon and Sahel rainfall and the Mediterranean. Int. J. Climatol. 23, 173–186.

Reimer, P.J., Baillie, M.G.L., Bard, E., Bayliss, A., Beck, J.W., Blackwell, P.G., Bronk Ramsey, C., Buck, C.E., Burr, G.S., Edwards, R.L., Friedrich, M., Grootes, P.M., Guilderson, T.P., Hajdas, I., Heaton, T.J., Hogg, A.G., Hughen, K.A., Kaiser, K.F., Kromer, B., McCormac, F.G., Manning, S.V., Reimer, R.W., Richards, D.A., Southon, J.R., Talamo, S., Turney, C.S.M., van der Plicht, J., Weyhenmeyer, C.E., 2009. INTCAL09 and MARINE09 radiocarbon age calibration curves, 0-50,000 years cal. BP. Radiocarbon 51, 1111–1150.

Riera, S., Wansard, G., Julià, R., 2004. 2000-year environmental history of a karstic lake in the Mediterranean Pre-Pyrenees: the Estanya lakes (Spain). CATENA 55, 293–324.

Rodwell, M.J., Hoskins, B.J., 2001. Subtropical Anticyclones and Summer Monsoons. J. Clim. 14, 3192–3211.

Rull, V., González-Sampériz, P., Corella, J.P., Morellón, M., Giralt, S., 2011. Vegetation changes in the southern Pyrenean flank during the last millennium in relation to climate and human activities: the Montcortès lacustrine record. J. Paleolimnol. 46, 387–404.

Sánchez Goñi, M.F., Hannon, G.E., 1999. High-altitude vegetational pattern on the Iberian Mountain Chain (north-central Spain) during the Holocene. The Holocene 9, 39–57.

Stockmarr, J., 1971. Tablets with spores used in absolute pollen analysis. Pollen Spores 13, 614–621.

Tarrats, P., Rieradevall, M., González-Sampériz, P., Pérez-Sanz, A., Valero-Garcés, B., Moreno, A., 2014. Relating actual with subfossil chironomid assemblages. Holocene habitat changes and paleoenvironmental reconstruction of Basa de la Mora Lake (Central Pyrenees). Presented at the Erupean Geoscience Union, Vienna.

Valero-Garcés, B.L., Navas, A., Machin, J., Stevenson, T., Davis, B., 2000. Responses of a Saline Lake Ecosystem in a Semiarid Region to Irrigation and Climate Variability. The History of Salada Chiprana, Central Ebro Basin, Spain. Ambio 29, 344–350.

Vegas, J., Ruiz-Zapata, B., Ortiz, J.E., Galán, L., Torres, T., García-Cortés, Á., Gil-García, M.J., Pérez-González, A., Gallardo-Millán, J.L., 2010. Identification of arid phases during the last 50 cal. ka BP from the Fuentillejo maar-lacustrine record (Campo de Calatrava Volcanic Field, Spain). J. Quat. Sci. 25, 1051–1062.

Vegas-Vilarrúbia, T., González-Sampériz, P., Morellón, M., Gil-Romera, G., Pérez-Sanz, A., Valero-Garcés, B., 2013. Diatom and vegetation responses to Late Glacial and Early Holocene climate changes at Lake Estanya (Southern Pyrenees, NE Spain). Palaeogeogr. Palaeoclimatol. Palaeoecol. 392, 335–349.

Villar, L., Sesé Franco, J.A., Ferrández, J.V., 1997. Atlas de la flora del Pirineo aragonés. Consejo de Protección de la Naturaleza de Aragón, Instituto de Estudios Altoaragoneses, [Spain].

Xoplaki, E., González-Rouco, F., Luter, J., Wanner, H., 2003. Mediterranean summer air temperature variability and its connection to the large-scale atmospheric circulation and SSTs. Clim. Dyn. 20, 723–739.

## APPENDIX

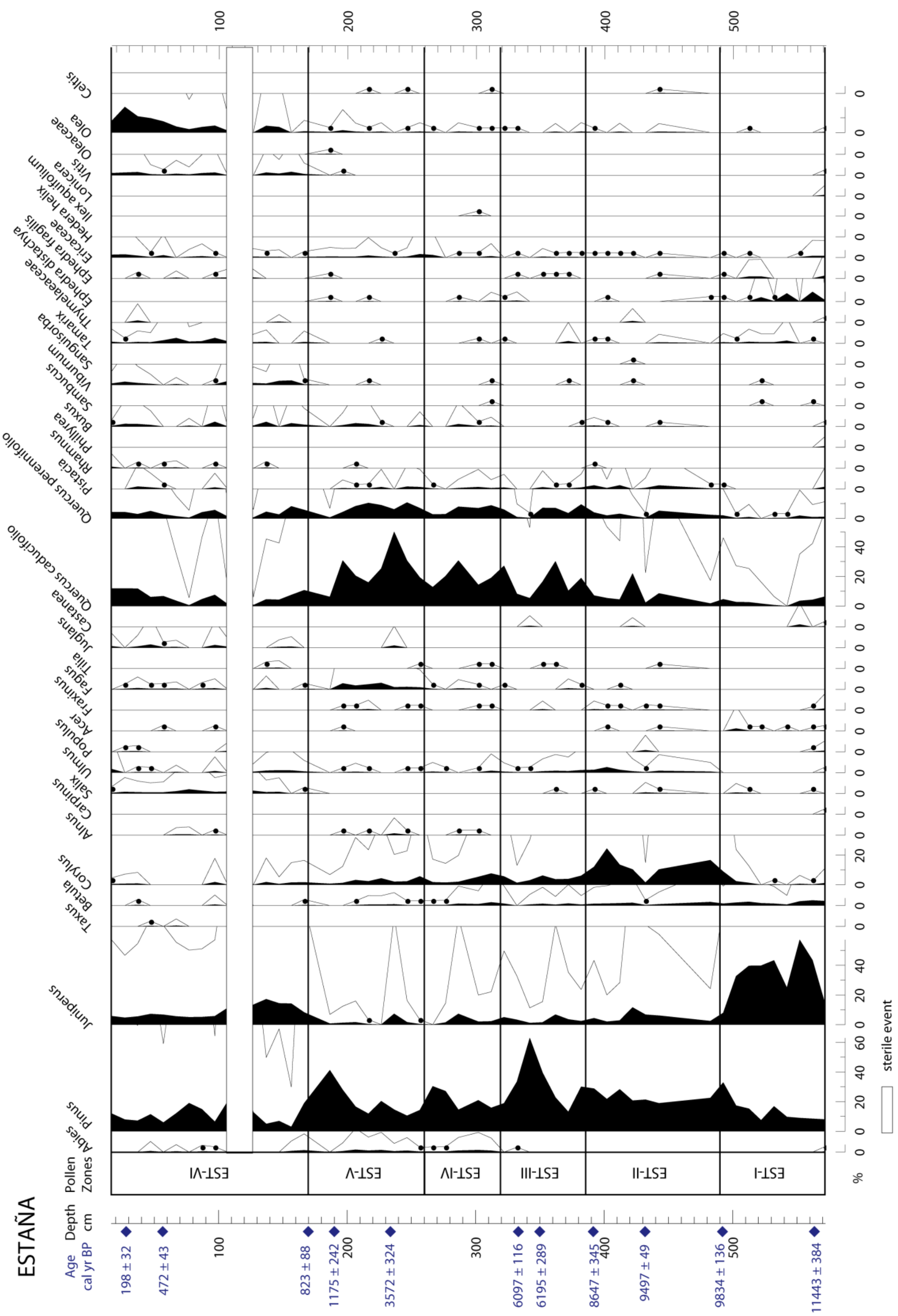


**Figure A3.1**. Arboreal pollen from Lake Estaña sequence.

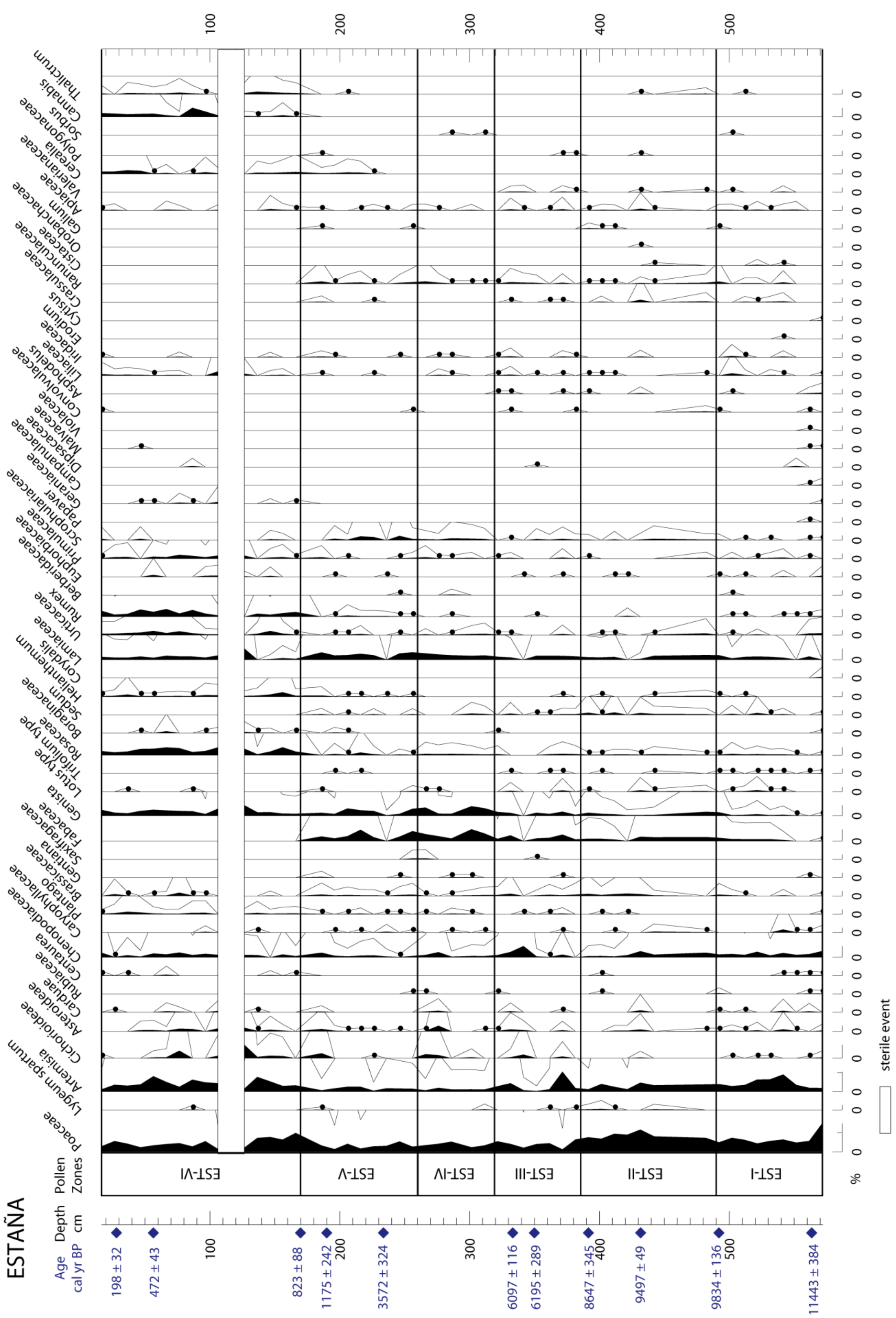


**Figure A3.2**. Non-Arboreal pollen from Lake Estaña sequence.

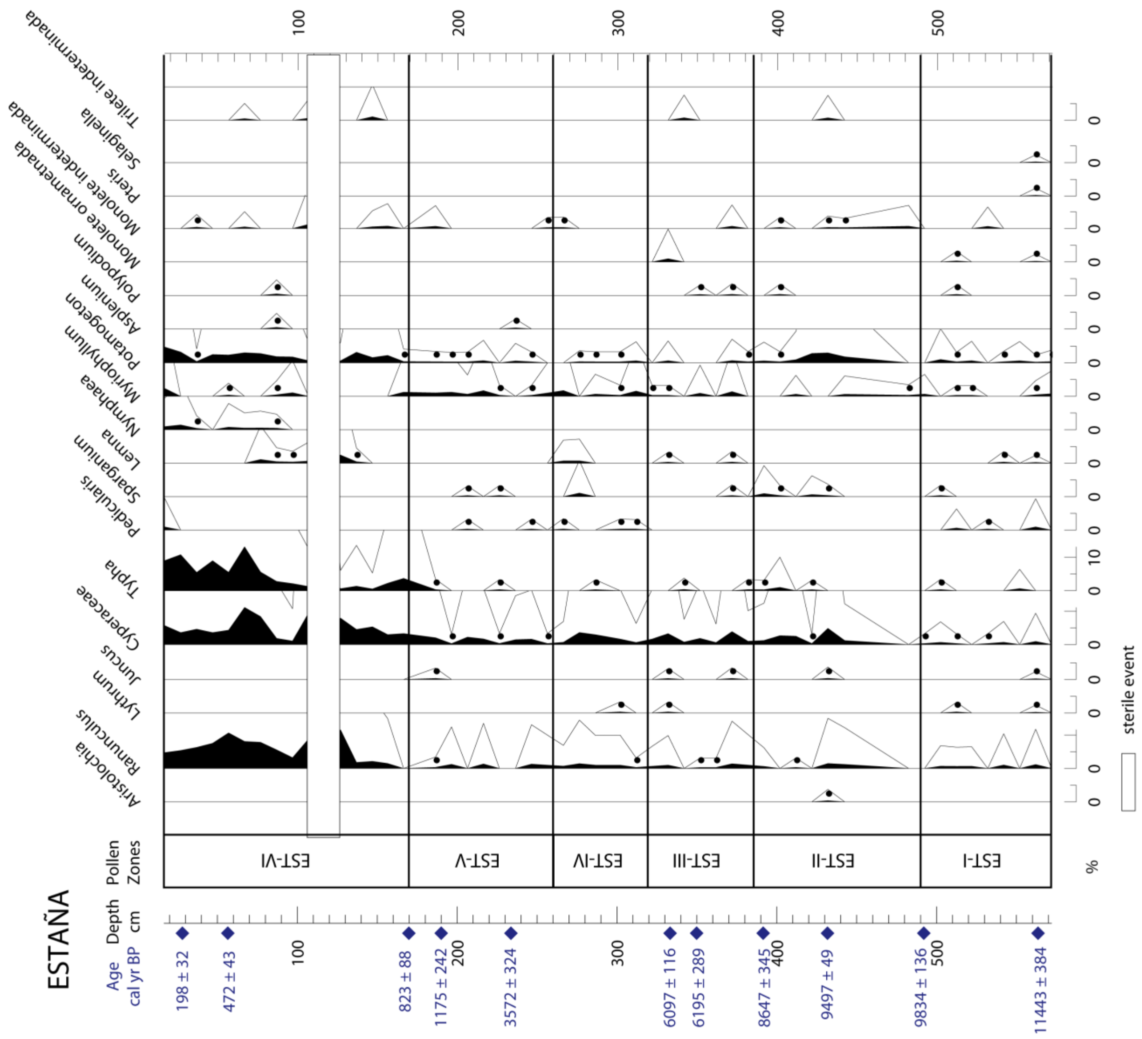


**Figure A3.3**. Aquatic pollen from Lake Estaña sequence.

# 4

# Climate models. Mid-Holocene and modern precipitation simulations over the Mediterranean.

## Outline

Climate models are outstanding tools to inform us about the potential future climate changes. Confidence in models is based on their performance to simulate modern and past climates. Thus, palaeoclimate research is essential not only to know the evolution of the climate but also to provide the ground truth, i.e. the climate reconstructions to compare with the climate model outputs so we can assess their ability to simulate different climate scenarios. The Mid-Holocene was characterized by much more humid conditions than present as it has been recognized in BSM and EST sequences (previous chapters) and across the whole Mediterranean region. Mid-Holocene climate simulations and paleo-data provide an opportunity to understand the climate mechanisms driven such deep changes in the precipitation regimen in the Mediterranean and to check the reliability of different simulations to reproduce past climates. Comparison of CMIP5 model precipitation outputs against actual and Mid Holocene observations in the Mediterranean region underlines that current state-of-the-art General Circulation Models still fail to simulate both past and present climates in an accurate way at a regional level.

## 4.1. INTRODUCTION

Currently, the Mediterranean area, including southern Europe and northern Africa, is characterized by a highly seasonal climate with summer drought and a wet season between October and March (Mehta and Yang, 2008). The generally low precipitation and marked seasonality gives rise to drought-adapted, sclerophyllous vegetation that is highly susceptible to wildfire during the dry season (Moreira et al., 2011). The Mediterranean region has experienced warming and increased drought in recent years (Camuffo et al. 2010; Hoerling et al. 2012; European Environment Agency, 2012) and has been identified as highly vulnerable to future climate changes (Giorgi, 2006). Model projections indicate large increases in temperatures and a reduction in mean annual precipitation (e.g. Meehl et al., 2007; Giorgi and Lionello, 2008; Nikulin et al., 2011), both of which would lead to large changes in vegetation cover and exacerbate wildfires (Amatulli et al., 2013). Given the high socio-economic costs of such changes, it is important to assess the reliability of model projections. Measures of how well the models simulate modern climate do not provide a measure of whether the simulation of climate changes is realistic. However, the evaluation of model performance in the past does provide a way of making such an assessment (Braconnot et al., 2012; Schmidt et al., 2013).

Not every period of past climate change is adequate to compare with model outputs. The Mid-Holocene constitutes a key period to determine the ability of models to reproduce climate states that are different from those of today and to increase our understanding of climate changes (Braconnot et al., 2007). This is because the climate was different from today´s, particularly in the Mediterranean area, but the atmospheric composition was analogous to the pre-Industrial times and the land-ocean-ice configuration was similar to present conditions (i.e., the extent of the ice caps had reduced significantly since the Late Glacial reaching present values). As a result, changes in the climate during the Mid-Holocene are mainly related to shifts in the seasonal and latitudinal distribution of incoming solar radiation (insolation) caused by changes in orbital parameters. Since the values of the seasonal insolation are well-known, the Mid-Holocene climate simulations allow us evaluate the ability of climate models to transfer properly those changes in the external forcing into the atmospheric and ocean circulations that are responsible for the Earth's climate at a large-scale.

Palaeoenvironmental evidence demonstrates that, 6000 years ago, during the Mid-Holocene, the climate was much different. Lake levels across the Mediterranean region were higher than present (Kohfeld and Harrison, 2000; Magny et al., 2002; Roberts et al., 2008), indicating a more positive balance between precipitation and evaporation. Speleothem records also indicate increased precipitation compared to present (Roberts et al., 2011). The observed expansion of deciduous trees across the region (Prentice et al., 1996; Roberts et al., 2004; Carrión et al., 2010) indicates that there was a change in rainfall seasonality with increased summer rainfall (Prentice et al., 1996). The observed decrease of fires in lowland areas in the northern Pyrenees and an increase at higher elevations, has been explained as a reflection of generally more humid conditions that would suppress fires in the already forested lowlands but allow them to increase as forests expanded into higher elevation areas (Vannière et al., 2011). The changes in climate were spatially complex (Roberts et al., 2011), but pollen-based climate reconstructions (e.g. Cheddadi et al., 1997; Davis et al., 2003; Bartlein et al., 2011) show that most of the Mediterranean region was characterized by an increase in plant-available moisture.

These regional palaeo-climate data from the Mediterranean area during the Mid-Holocene are in agreement, as we have described before, with the results obtained in the present PhD dissertation from the BSM and EST sequences (chapters 2 and 3 respectively). According to the palaeo-environmental reconstructions accomplished in the previous chapters, the Mid-Holocene in the Pyrenees was a period of particularly mild climate conditions characterized by warm winters and humid conditions that lead to the establishment of a Mediterranean-forest type dominated by semi-deciduous *Quercus* in the lowlands (EST sequence, chapter 3), and a well-developed deciduous forest dominated by *Betula*, *Corylus* and deciduous *Quercus* in the highlands (BSM sequence, chapter 2), reaching up to the treeline (fig.4.1).

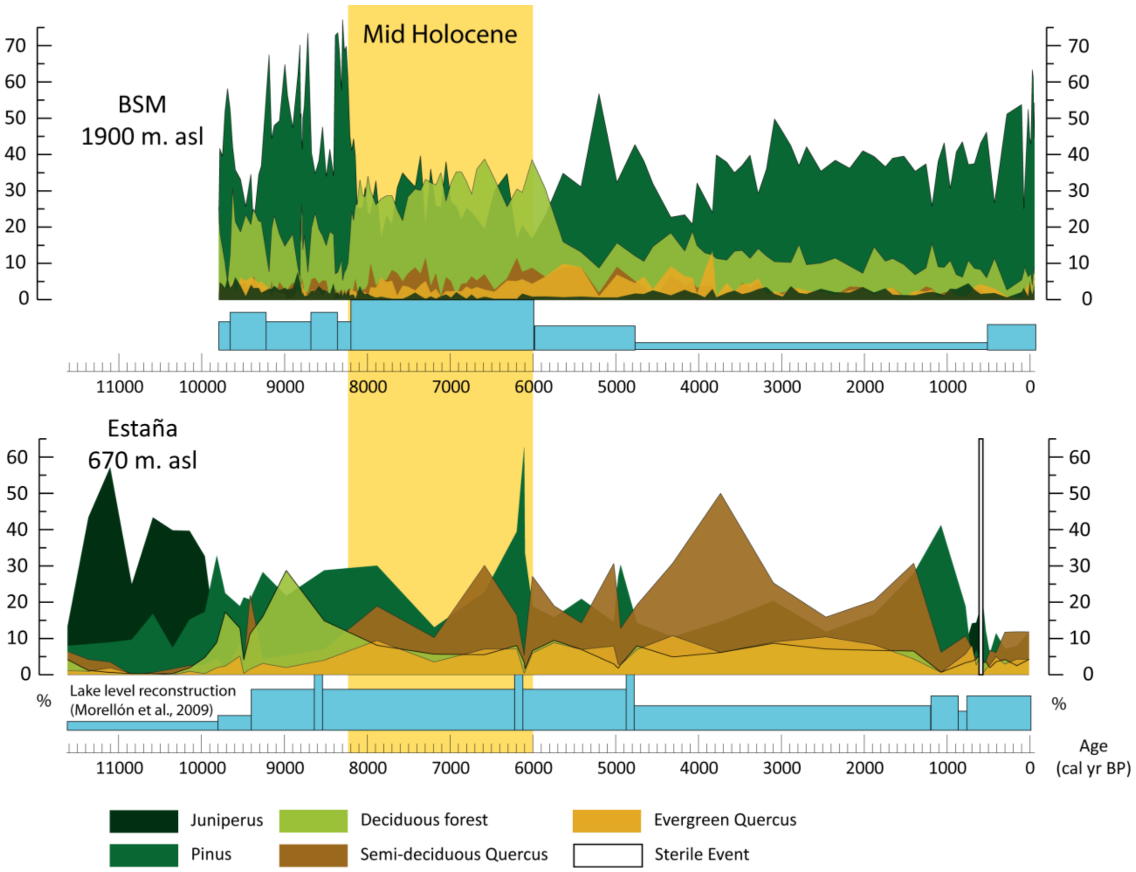


**Figure 4.1**. Vegetation and lake level reconstructions for lakes Estanya and Basa de la Mora. The Mid Holocene is highlighted in yellow. The lake level reconstruction for Lake Estaña has been published by Morellón et al. (2009).

Such changes in precipitation and temperature compared to today require large-scale shifts in atmospheric and oceanic patterns. Nevertheless, though palaeo-climate data allow us to know the evolution of the climate in the past, the mechanisms beyond those changes cannot be easily deduced. To this purpose, climate models attempt to simulate past climates mechanisms based on prescribed Earth's physico-chemical parameters such as solar insolation, orbital configuration, atmosphere composition, ocean temperature or ice-sea extent among others. Considering climate features in the Mediterranean region during the Mid-Holocene are relatively well-know at a regional scale, this period provides an opportunity to examine climate-model performance.

Systematic comparisons with observations have shown that global climate models are unable to reproduce the observed MH patterns of rainfall changes in the Mediterranean. In particular, they do not show a sufficiently large increase in summer rainfall to explain the shift towards deciduous vegetation. This was identified as a problem in atmosphere-only simulations of the mid-Holocene made during the first phase of the Palaeoclimate Modelling Intercomparison Project (PMIP1: see e.g. Masson et al., 1999; Guiot et al., 1999; Bonfils et al., 2004). Coupled ocean-atmosphere simulations made during PMIP2 were able to simulate the types of climate changes seen in the Mediterranean, but the geographic placement of these climate types, the spatial extent and the magnitude of the changes were not well captured (Brewer et al., 2007). In particular, the simulated changes in precipitation are small and insufficient to explain the observed expansion of deciduous forests in the region.

The Mediterranean climate involves a complex interaction between different processes acting at several different spatio-temporal scales (Xoplaki et al., 2003; Luterbacher et al., 2006; CLIVAR, 2010; Lionello, 2012). However, interannual variability in Mediterranean summer precipitation is linked to variability in the strength of the Afro-Asian monsoon system (Rodwell and Hoskins, 2001; Raicich et al. 2003; Gaetani et al 2011). Analyses of climate model simulations of the present day suggest that Mediterranean summer precipitation is suppressed during years when the Afro-Asian monsoon system is strong. This results from intensification of the Hadley cell and enhanced subsidence in the subtropics (i.e. strengthening of the Azores High), leading to high pressure over the eastern Mediterranean which results in decreased rainfall (Gaetani et al., 2011). However, when monsoon intensification is accompanied by northward movement of the intertropical convergence zone, as model simulations indicate occurred in the mid-Holocene (Braconnot et al., 2007a; Marzin and Braconnot, 2009), the Azores high is also displaced northeastward and weakened (e.g. Harrison et al., 1992). This has been shown to have a significant impact on precipitation in the eastern North America (Forman et al., 1995; van Soelen et al., 2012) and could potentially lead to increased summer rainfall in the Mediterranean region.

The PMIP2 simulations show a significant enhancement and northward expansion of the African monsoon during the Mid-Holocene in response to changes in insolation forcing (Braconnot et al. 2007a). However, comparisons with pollen-based estimates of the change in mean annual precipitation (Joussaume et al., 1999; Bartlein et al., 2011) show that the models underestimate the increase in precipitation by between 20 and 50% (Braconnot et al. 2007a; Braconnot et al., 2012). Most models fail to produce a sufficient northward expansion of the monsoon. This underestimation of monsoon expansion is also present in the CMIP5 MH simulations (see e.g. Harrison et al., 2013). It is possible that this bias in the simulation of the African monsoon is linked to the failure to simulate the MH Mediterranean climate accurately, since larger shifts in the position of the monsoon are produced by models incorporating land-surface feedbacks and/or with higher spatial resolution (Levis et al., 2004; Wohlfahrt et al., 2004; Bosmans et al., 2012).

MH model simulations, made with the same models that are used for future projections, have been made as part of the fifth phase of the Coupled Model Intercomparison Project (CMIP5: Taylor et al., 2012) and are being analysed as part of the third phase of the Palaeoclimate Modelling Intercomparison Project (PMIP3: Bracconnot et al., 2012).

Kelley et al. (2012) have shown that the simulation of the seasonal cycle of precipitation in the Mediterranean region under modern conditions is reasonable, although as in earlier versions of the models the amplitude of the cycle is more muted than observed with too little rain in winter and too much rain in summer (Brands et al., 2013). However, evaluation of CMIP5 model performance against modern observations suggests that some aspects of the simulation of the Afro-Asian monsoons (see e.g. Monerie et al., 2012; Roehrig et al., 2013; Sperber et al., 2012) are improved compared to earlier versions of the models, although preliminary assessments of the CMIP5 model indicate that improvements in the modern simulations do not translate into improvements in the simulation of the MH monsoon climate (Harrison et al., 2013), and thus, given the dynamic links between the monsoon and Mediterranean precipitation, in MH Mediterranean climate changes.

### 4.1.1. Objectives

In this chapter, we examine the performance of the CMIP5 models for modern and MH climates, and compare the simulated climates with modern and palaeo-observations from Bartlein et al., (2011) data base. This allows us to assess whether biases in the control simulations influence the MH simulations and to investigate whether regional biases in the simulation of MH monsoon changes influence model performance in the Mediterranean.

## 4.2. METHODS

We present analyses of the pre-Industrial (*piControl*) and MH (*midHolocene*) made by 12 coupled ocean-atmosphere models from the fifth phase of the Coupled Climate Modelling Intercomparison Project (CMIP5). In order to investigate whether biases in the control simulation influence the realism of the *midHolocene* climates, we first evaluate the *piControl* simulation. We use modern observations from the CRU TS3.1 data set, in the absence of climate reconstructions from northern African for the *piControl* interval. The *piControl* simulation is driven by boundary conditions appropriate for 1850 AD, but comparisons with a subset of transient historical simulations show that the spatial patterns and magnitudes of seasonal climates are very similar. In order to evaluate whether models capture the spatial expression of specific seasonal patterns, we define a number of climate types using the modern observations and apply these definitions to delimit these climate types in the *piControl* and *midHolocene* simulations. We evaluate the *midHolocene* simulations using quantitative climate reconstructions derived from a global data base of pollen records which still not include the BSM and EST data presented in this Thesis.

Although there are many kinds of palaeorecord that indicate that northern Africa and the circum-Mediterranean region were wetter during the mid-Holocene, including e.g. lake-level and archaeological records, these other sources of information do not provide quantitative estimates of the change in precipitation. Comparisons of simulated and observed climates are based on the simulated precipitation both within climate zones and within geographic zones.

### 4.2.1. Data sources: CMIP5 simulations

We examine precipitation changes between a MH (*midHolocene*, 6000 yr B.P) equilibrium simulation and a control simulation representing pre-industrial conditions (*piControl*) using 12 models from the fifth phase of the Coupled Modelling Intercomparison Project (CMIP5). Both the *midHolocene* and *piControl* are equilibrium simulations. We use the *midHolocene* and *piControl* simulations in the CMIP5 (http://cmip-pcmdi.llnl.gov/cmip5/data_portal.html) archive as of 15$^{th}$ August 2012 (table 4.1). Seven of these simulations are made with ocean-atmosphere (OA) models, and the other 5 models include an interactive carbon cycle (OAC). The *piControl* simulation has boundary conditions (insolation, greenhouse gas concentrations) appropriate for 1850 CE. The *midHolocene* experiment shows the response to changes in the seasonal and latitudinal distribution in insolation 6000 years ago; greenhouse gas concentrations are set at *piControl* levels (for details of the experimental protocol see Taylor et al., 2012; Braconnot et al., 2012). To assess whether the *piControl* state differs from recent observed climates, we used outputs from a historical simulation (*historical*: 1850 to 2005 CE) available for 6 of the models. The *historical* simulation is forced by time-varying changes in solar, volcanic, and greenhouse gases (Taylor et al., 2012; Braconnot et al., 2012).

The output from each model was interpolated to a common grid (0.5°) using bilinear interpolation to facilitate comparisons and the calculation of zonal averages. Long-term mean monthly, seasonal, and annual precipitation values were obtained by averaging the last 100 years of the *piControl* and *midHolocene* simulations, except in the case of HADGEM2-CC where only 35 years of *midHolocene* simulated outputs are available. Long-term means of the six *historical* simulations were obtained by averaging the last 30 years of each simulation. All averages were areally-weighted (by the area of the model grid cells).

| **Model name** | **Type** | **Resolution (number of gridcells: latitude, longitude)** | | | **Year length** | **Simulations** | | |
|---|---|---|---|---|---|---|---|---|
| | | **Atmosph** | **Ocean** | **Sea Ice** | | ***Mid Holocene*** | ***PI Control*** | ***hist*** |
| **BCC-CSM1-1** | OAC | 64, 128 | 232, 360 | 232, 360 | 365 | X | X | |
| **CCSM4** | OA | 192, 288 | 320384 | 320384 | 365 | X | X | X |
| **CNRM-CM5** | OA | 128, 256 | 292, 362 | 292, 362 | 365-366 | X | X | |
| **CSIRO-Mk3-6-0** | OA | 96, 192 | 189, 192 | 96, 192 | 365 | X | X | |
| **CSIRO-Mk3L-1-2** | OA | 56, 64 | 128, 225 | 56, 64 | 365 | X | X | |
| **GISS-E2-R** | OA | 90, 144 | 90, 144 | 90, 144 | 365 | X | X | X |
| **HadGEM2-CC** | OAC | 145, 192 | 216, 360 | 216, 360 | 360 | X | X | |
| **HadGEM2-ES** | OAC | 145, 192 | 216, 360 | 216, 360 | 360 | X | X | |
| **IPSL-CM5A-LR** | OAC | 96, 96 | 149, 182 | 149, 182 | 365 | X | X | X |
| **MIROC-ESM** | OAC | 64, 128 | 192, 256 | 192, 256 | 365 | X | X | X |
| **MPI-ESM-P** | OA | 96, 192 | 220, 256 | 220, 256 | 365-366 | X | X | X |
| **MRI-CGCM3** | OA | 160, 320 | 360, 368 | 360, 368 | 365 | X | X | X |

Table 4.1. Characteristics of the CMIP5 models used in these analyses.

### 4.2.2. Data sources: Modern and mid-Holocene climate data

Observations of the modern climate are taken from the CRU TS3.1 data set (Harris et al., 2013), which provides monthly precipitation values on a 0.5º grid for the interval 1850 to 2006. We have created a monthly precipitation climatology using data from January 1961 through to December 1990. Zonal averages are constructed by areally-weighting the gridded values.

Bartlein et al. (2011) provide quantitative reconstructions of mean annual precipitation (MAP), expressed as anomalies from the present, from a global data base of pollen and plant macrofossil records. The original site-based reconstructions were averaged to provide gridded values on a 2x2º grid, and differences between the site reconstructions within each grid were used to provide an estimate of reconstruction uncertainty (as a pooled estimate of the standard error). The data set provides mid-Holocene estimates of MAP anomalies for 62 cells (out of a possible 397 cells) within the area of interest (latitude: 0ºN-45ºN, longitude: 20ºW-30ºE).

### 4.2.3. Definition of climate regions

Precipitation regimes can be characterized by a combination of the form of the seasonal cycle, seasonal concentration, and magnitude. We determined these characteristics of modern precipitation (using the CRU TS3.1 data set) for zonally averaged 5º latitude bands between 0 and 45ºN. The seasonal cycle of precipitation in each 5º latitude band was characterized according to the number of distinct rainfall peaks present in the 12-month precipitation climatology, using the R package "pastecs" to determine whether there was a significant 'pit' or 'peak' in any month. A pit or peak is considered significant if the probability of turning points occurring in a random series is <0.05, given by:

$$(\mathrm{P(t)} = 2/n(t-1)!\,(n-1)!)$$

where n is the number of observations at time t (Ibanez, 1982).

We calculated the total precipitation in each season (spring: March, April, May; summer: June, July, August; autumn: September, October, November; winter: December, January, February) and for the whole year. A measure of seasonal concentration was calculated following Kelley et al. (2013), where the magnitude of precipitation in each month is represented by the length of a vector in the complex plane and the direction of the vector represents the timing (with January set to 0º). The length of the mean vector divided by the annual precipitation provides an index of seasonal concentration (C), where C is 1 when the precipitation is concentrated in a single month and 0 when it is evenly distributed throughout the year.

We applied these definitions to determine the position of different precipitation regimes in the *piControl* and *midHolocene* simulations. Comparison of the observed limits and those identified in the *piControl* allows us to examine (a) whether the models produce these distinctive precipitation regimes and (b) how well they simulate their placement independently of whether they simulate the correct magnitude of precipitation. Comparison of the *piControl* and *midHolocene* limits allows us to characterize shifts in precipitation regimes, again independent of changes in precipitation magnitude.

### 4.2.4. Analyses of the Model Simulations

We evaluate model performance for *piControl* simulation in two steps. First we examine whether the models reproduce the spatial extent of different precipitation regimes, and then we examine whether they reproduce the magnitude of total annual and of seasonal precipitation. Long-term means for the period 1961-1990 from the CRU TS3.1 data set (Harris et al., 2013) are compared with long-term averages for the last 100 years of the *piControl*. The standard deviation (SD) of the observations provides a measure of the significance of the difference between observations and simulations. We examine the differences between simulated and observed climate for the latitude band corresponding to a given precipitation regime in the observations. We also compare the differences in the amount of precipitation for the geographic region identified as falling within a specific precipitation regime in each model, which may be less/more extensive than the region identified in the observations.

We also examine the change in precipitation in the mid-Holocene in two steps. First we identify the spatial extent of each precipitation regime in the *midHolocene* simulations and compare this with the spatial extent shown in the *piControl* simulation of the same model. This allows us to identify whether there have been shifts in the precipitation regimes. We then examine the magnitude of the precipitation change in the latitude band characterized by a specific regime in both the *piControl* and the *midHolocene* simulations for each model. This allows us to identify whether there has been a change in precipitation *in situ*. We use the standard deviation of the *piControl* simulation for each model to determine whether the change between *midHolocene* and *piControl* is significant.

We examine whether the biases in simulated precipitation (both the bias in spatial extent of a given precipitation regime and the bias in the magnitude of the simulated precipitation) influence the simulated change in precipitation between *piControl* and *midHolocene*. The bias and anomaly values have been obtained firstly for discrete geographical zones (the zones characterized by different rainfall regimes today, as defined from the CRU data set) and secondly for the model-defined regions of these different rainfall regimes (e.g. the region where the simulated rainfall is of the monsoon type). We use linear regression to examine the relationship between precipitation biases and anomalies for all models, and for the OA and OAC classes of models.

The realism of the simulated change in precipitation (*midHolocene-piControl*) is assessed by comparing with reconstructions of mean annual precipitation (MAP) from the Bartlein et al. (2011) data set. Comparisons are made by averaging the simulated precipitation for the grid cells where there are observations within each 5º latitude band. There are sufficient data in most of the 5º latitude bands to make robust comparisons.

## 4.3. RESULTS

### 4.3.1. Modern observed climate

The modern climate of the region can be divided into four distinct latitudinal zones, differentiated by marked differences in the seasonal distribution and amount of rainfall (fig. 4.2). In the south, the equatorial band is characterized by high rainfall (~1800 mm) throughout the year (fig. 4.3) but with peaks in precipitation in spring (~ 460 mm) and autumn (~600 mm) and less rainfall in summer. This pattern reflects the seasonal migration north and south of the inter-tropical convergence zone. The “double-peak” rainfall pattern (hereafter DP) occurs between 0 to 5ºN. The region further north (5-20 ºN) is characterized by summer monsoonal rainfall and dry winters. The amount of rainfall declines progressively from ca 650 mm in summer (June, July, August) in the south to less than 100 mm in the north. The desert area (20-30ºN) is characterized by low rainfall (<100 mm/yr). There is no pronounced seasonal differentiation in rainfall in the desert, although southern regions tend to have slightly more rain in summer than winter and northern regions slightly more rainfall in winter than summer. The Mediterranean zone (30-45ºN) is characterized by higher rainfall, increasing from 200 mm/year in the south band to 780 mm/year in the north. The rainfall is concentrated in the winter half-year, with a pronounced summer drought.

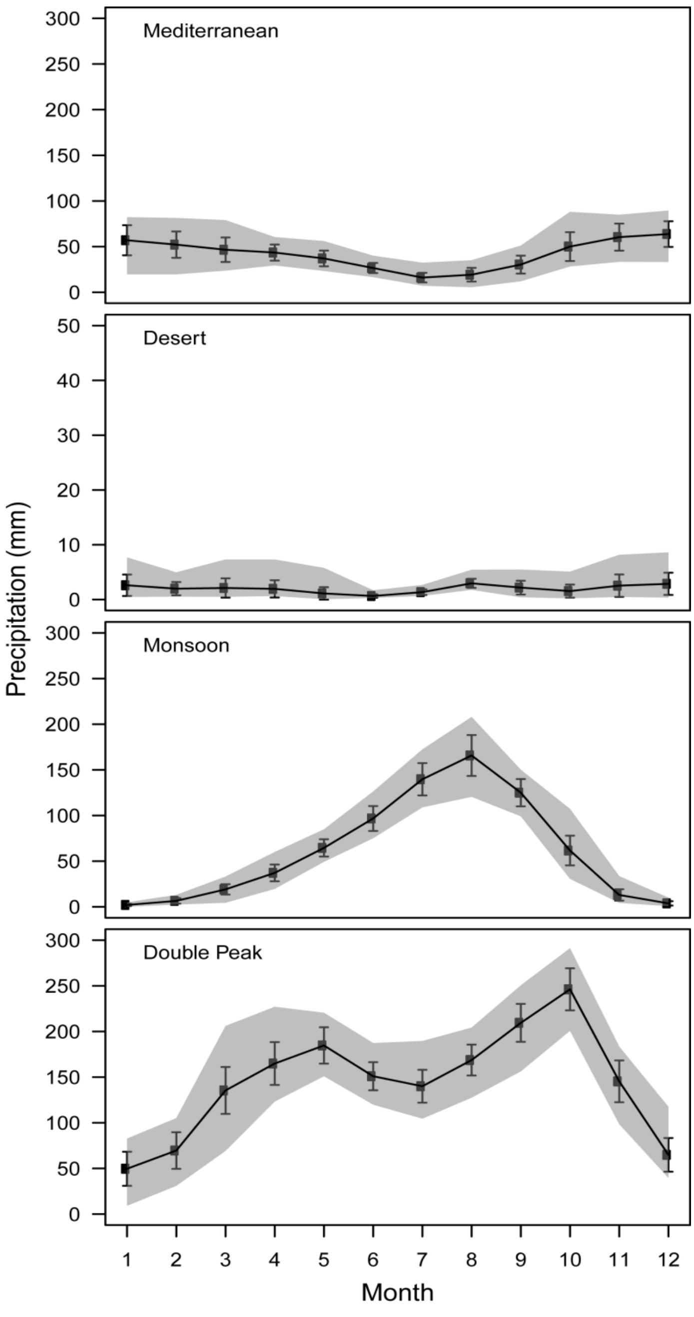


**Figure 4.2**: Observed seasonal cycle of precipitation in each of the defined climate zones, using the CRU T3.1 data set (Harris et al., 2013). The mean precipitation each month (mm) is shown by the black line, with the standard deviation shown by the bars. The grey shading shows the maximum and minimum rainfall experienced within the observation period (1961 to 1990). Note that the scale for the desert region differs from that used for the other regions. Months are numbered consecutively from January (1) through to December (12).

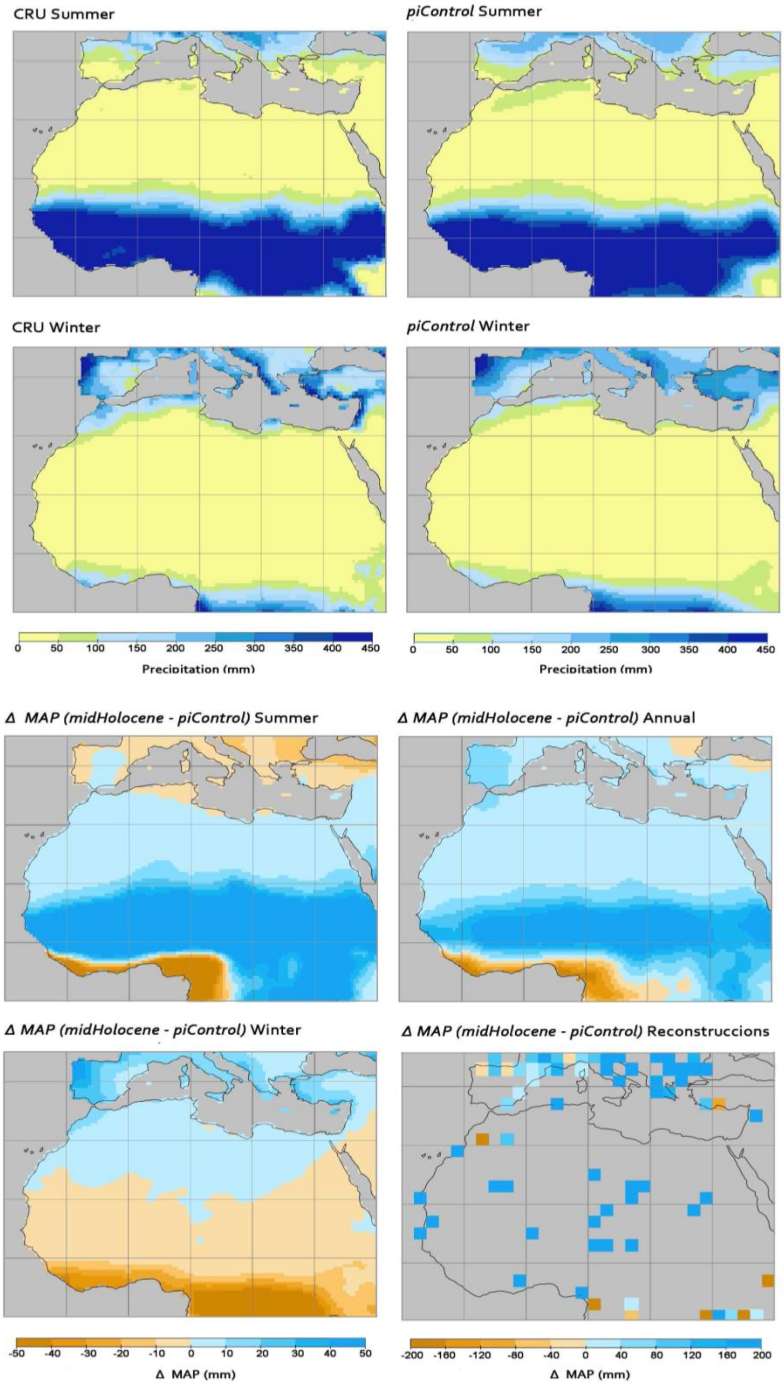


**Figure 4.3**: Observed and simulated modern and palaeo-precipitation patterns. The total summer (June, July, August) and winter (December, January, February) precipitation from the CRU T3.1 data set (Harris et al., 2013) are compared to ensemble averages of the *piControl* outputs of the 12 CMIP5 models. The simulated change in precipitation between the Mid-Holocene and *piControl* simulations (*midHolocene-piControl*) is shown based on the ensemble average of the *midHolocene* outputs of the 12 CMIP5 models. The observed anomalies in mean annual precipitation (MAP) between the mid-Holocene and the present day are average values for 2x2º grids from the Bartlein et al. (2011) data set.

### 4.3.2. PiControl simulations

These four rainfall regimes can generally be identified in the *piControl* simulations, although two of the models (CNRM-CM5, MRI-CGCM3) fail to reproduce the DP pattern in the equatorial zone. However, several models represent the spatial extent of the regimes poorly. Thus 5 out of the 12 models show monsoon penetration further north than observed (fig. 4.4a). Most models place the northern limit of the desert correctly, but two models (CSIRO-

Mk3L-1-2, IPSL-CM5A-LR) show the area of low rainfall and low rainfall seasonality extending further north than observed.

| | Season Anomaly | BCC-CSM1.1 | CCSM4 | CNRM-CM5 | CSIRO-Mk3-6-0 | CSIRO-Mk3L-1-2 | GISS-E2-R |
|---|---|---|---|---|---|---|---|
| **Mediterranean** | annual | 15.0 | 24.4 | 32.6 | -21.2 | 8.4 | **75.7** |
| | spring | 13.9 | 3.7 | 16.1 | 13.0 | 4.2 | **28.4** |
| | summer | -4.3 | 2.7 | 4.7 | -10.7 | -2.4 | 20.5 |
| | autumn | -0.4 | 10.5 | 14.0 | -21.6 | 6.6 | 20.3 |
| | winter | 5.8 | 7.4 | -2.3 | -1.9 | 0.0 | 6.5 |
| **Desert** | annual | 7.7 | **29.5** | **32.7** | -18.5 | 4.6 | **22.8** |
| | spring | 0.1 | 0.6 | 3.6 | 0.8 | 1.3 | 10.6 |
| | summer | 0.8 | **14.3** | **9.6** | -7.4 | **3.2** | 7.7 |
| | autumn | 2.8 | **13.9** | **18.5** | -11.5 | 0.9 | 3.9 |
| | winter | 4.1 | 0.6 | 1.0 | -0.5 | -0.8 | 0.7 |
| **Monsoon** | annual | **47.4** | **148.6** | **155.8** | -53.5 | **47.2** | **116.1** |
| | spring | -11.2 | -2.6 | -7.4 | -2.6 | -2.7 | -7.5 |
| | summer | **33.6** | **80.4** | **97.2** | -20.3 | **21.5** | **91.6** |
| | autumn | **29.8** | **76.6** | **78.7** | -28.3 | **32.9** | **41.4** |
| | winter | -4.7 | -5.9 | **-12.6** | -2.3 | **-4.5** | **-9.4** |
| **DP** | annual | -76.7 | -13.3 | - | **-208.8** | -36.4 | 2.8 |
| | spring | -41.3 | 0.5 | - | -12.7 | -0.6 | **-56.2** |
| | summer | 1.1 | 43.8 | - | **-68.1** | 33.9 | **87.1** |
| | autumn | 29.1 | 53.1 | - | **-106.8** | **63.2** | **71.0** |
| | winter | **-65.5** | **-110.7** | - | -21.1 | **-132.9** | **-99.1** |

| | Season Anomaly | HadGEM2-CC | HadGEM2-ES | IPSL-CM5A-LR | MIROC-ESM | MPI-ESM-P | MRI-CGCM3 |
|---|---|---|---|---|---|---|---|
| **Mediterranean** | annual | 30.9 | 9.2 | 40.1 | 30.8 | 14.3 | 15.4 |
| | spring | 14.5 | 13.0 | 22.2 | 11.6 | 17.6 | 10.4 |
| | summer | **40.6** | -8.8 | 14.0 | 0.8 | 3.5 | -2.8 |
| | autumn | **-40.9** | 2.9 | 8.0 | 6.0 | -3.9 | -5.9 |
| | winter | 16.7 | 2.1 | -4.1 | 12.4 | -2.9 | 13.8 |
| **Desert** | annual | 4.5 | 4.4 | **6.8** | **26.1** | **14.3** | 7.7 |
| | spring | 0.6 | 2.1 | **1.8** | 4.2 | 2.1 | 0.1 |
| | summer | **3.4** | **4.2** | **2.8** | **12.3** | **6.7** | 0.8 |
| | autumn | 2.1 | -1.3 | **2.3** | **10.1** | **5.1** | 2.8 |
| | winter | -1.7 | -0.5 | -0.1 | -0.4 | 0.4 | 4.1 |
| **Monsoon** | annual | **207.6** | **210.4** | **202.4** | **182.1** | **219.9** | **88.5** |
| | spring | **-39.1** | **19.3** | 6.0 | -19.7 | **17.5** | -1.9 |
| | summer | 15.4 | **122.8** | **110.0** | **142.4** | **132.8** | **68.3** |
| | autumn | **233.6** | **72.5** | **89.6** | **72.2** | **70.2** | **23.7** |
| | winter | -2.2 | -4.3 | **-3.2** | **-12.7** | -0.7 | -1.5 |
| **DP** | annual | **123.0** | **142.0** | - | **-244.4** | 14.3 | - |
| | spring | **-100.9** | -1.7 | - | **-87.2** | -32.0 | - |
| | summer | -1.8 | 8.6 | - | 29.3 | 38.7 | - |
| | autumn | **154.9** | **168.9** | - | -9.6 | **55.6** | - |
| | winter | **70.7** | **-33.9** | - | **-176.9** | **-48.1** | - |

**Table 4.2**. Summary of area-averaged climate anomalies (*midHolocene* minus *piControl*) for individual models for individual seasons and for mean annual precipitation. Bold font indicates values that are significantly different from the interannual variability of the modern observations. The seasons are spring: March, April, May; summer: June, July, August; autumn: September, October, November; winter: December, January, February.

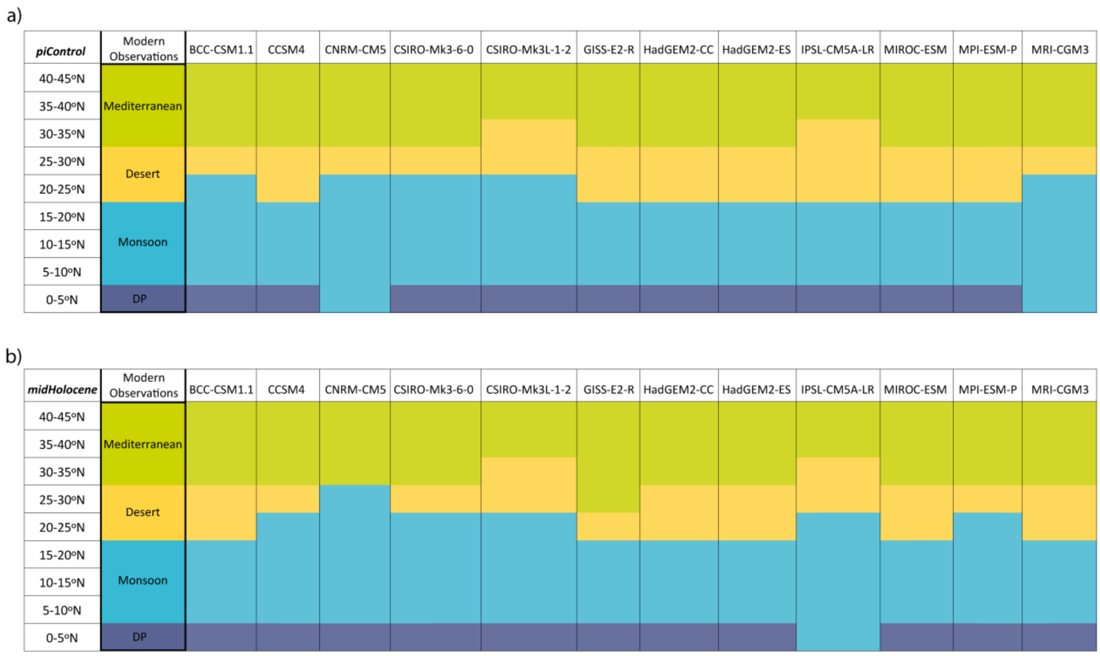


**Figure 4.4**. a) The location of the four precipitation zones in the CMIP5 pre-industrial (*piControl*) simulations compared to the limits defined using the CRU TS3.1 data set (Harris et al., 2013). The precipitation regime was characterised using zonally-averaged long-term means for 5º latitiude bands. b) The location of the four precipitation zones in the CMIP5 mid-Holocene (*midHolocene*) simulations compared to the limits defined using the CRU TS3.1 data set (Harris et al., 2013). The precipitation regime was characterised using zonally-averaged long-term means for 5º latitude bands.

Since there are no reconstructions of pre-industrial climate, we evaluate how well the models reproduce the magnitude of seasonal precipitation within each precipitation regime by comparing to observations for the period 1961-1990. Comparison of the *piControl* and *historical* simulations (fig. 4.5), for the six models where both runs are available, shows that differences in the simulated patterns and amount of precipitation between the two simulations are small. Differences between the two simulations are generally much smaller than the difference between the simulated and observed climate.

Comparison of the *piControl* with modern observations shows that most models fail to reproduce the magnitude of the precipitation (fig. 4.6). Only two models (CSIRO-Mk3L-1-2, MPI-ESM-P) correctly reproduce the amount of rainfall in the DP band, while 6 models overestimate the rainfall by between 350 and 790 mm/yr. Although some models overestimate the amount of precipitation in every season, the positive biases are largest in spring (75-290 mm), autumn (90-325 mm) and winter (50-290 mm). Only two models (GISS-E2-R, CNRM-CM5) simulate the correct magnitude of mean annual precipitation in the monsoon zone. Seven models underestimate, and three models overestimate, the mean annual rainfall in the monsoon zone. The bias ranges from 280 mm less than observed to 270 mm more than observed. Models that underestimate the total amount of rainfall in the monsoon zone (e.g. BBC-CSM1.1, CSIRO-Mk3L-1-2, HadGEM2-CC, HadGEM2-ES, IPSL-

CM5A-LR, MPI-ESM-P and MRI-CGCM3) do so because of simulating too little precipitation in summer and autumn, i.e. because the simulation of the monsoon is too weak. However, models that overestimate the total precipitation in this zone (e.g. CCSM4, CNRM-CM5, CSIRO-Mk3-6 and MIROC-ESM), generally overestimate the rainfall in all seasons of the year. Seven models simulate too much precipitation in the desert zone (10-55 mm/yr), with too much rainfall in spring, summer and autumn. Given that the desert zone is by definition confined to regions with <100 mm precipitation, the overestimation of rainfall in this zone is large. Four models underestimate the Mediterranean precipitation (by between 35 to 90 mm/yr), because of underestimation of the autumn and winter rainfall, although they overestimate the summer rainfall. However, the IPSL-CM5A-LR and GISS-E2-R models overestimate total precipitation in this region: GISS produces too much rainfall in spring (45 mm), summer (100 mm) and autumn (60 mm), while IPSL-CM5A-LR simulates too much rainfall (130 mm) in summer only. Comparison of results from models that correctly simulate the location of each regime (compared to the observations) and those in which the area characterized by a given regime is too extensive or too small, show that the biases in simulated precipitation are not related to whether models reproduce the spatial location of each regime correctly.

### 4.3.3. Mid-Holocene simulations

The location of the DP regime does not change between the *piControl* and *midHolocene* simulations of most (9) of the models (fig. 4.4b). The two models (CNRM-CM5, MRI-CGCM3) that failed to simulate a DP pattern in the equatorial zone in the *piControl*, nevertheless simulate this pattern in the *midHolocene* experiment. However, in the IPSL-CM5A-LR *midHolocene* simulation, the precipitation in the equatorial zone is more monsoon-like than in the model's *piControl* simulation. Most of the models (6) show no change in the northern limit of the monsoon; four models (CCSM4, IPSL-CM5A-LR, MRI-CGCM3, CNRM-CM5) show a northward displacement of the northern limit of the monsoon, while two models (BCC-CSM1.1, MRI-CGCM3) show a southward displacement of the northern limit of the monsoon as a result of southward expansion of the desert regime. Only two models (BBC-CSM1.1, MRI-CGCM3) show a northward displacement of the northern limit of the desert zone. Thus, in most of the *midHolocene* simulations, the desert regime occupies either a similar (5 models) or a slightly contracted area (4 models) compared to the *piControl*. Only one model (GISS-E2-R) shows a southward expansion of the Mediterranean precipitation regime; otherwise, this zone occupies the same position as in the *piControl* simulations.

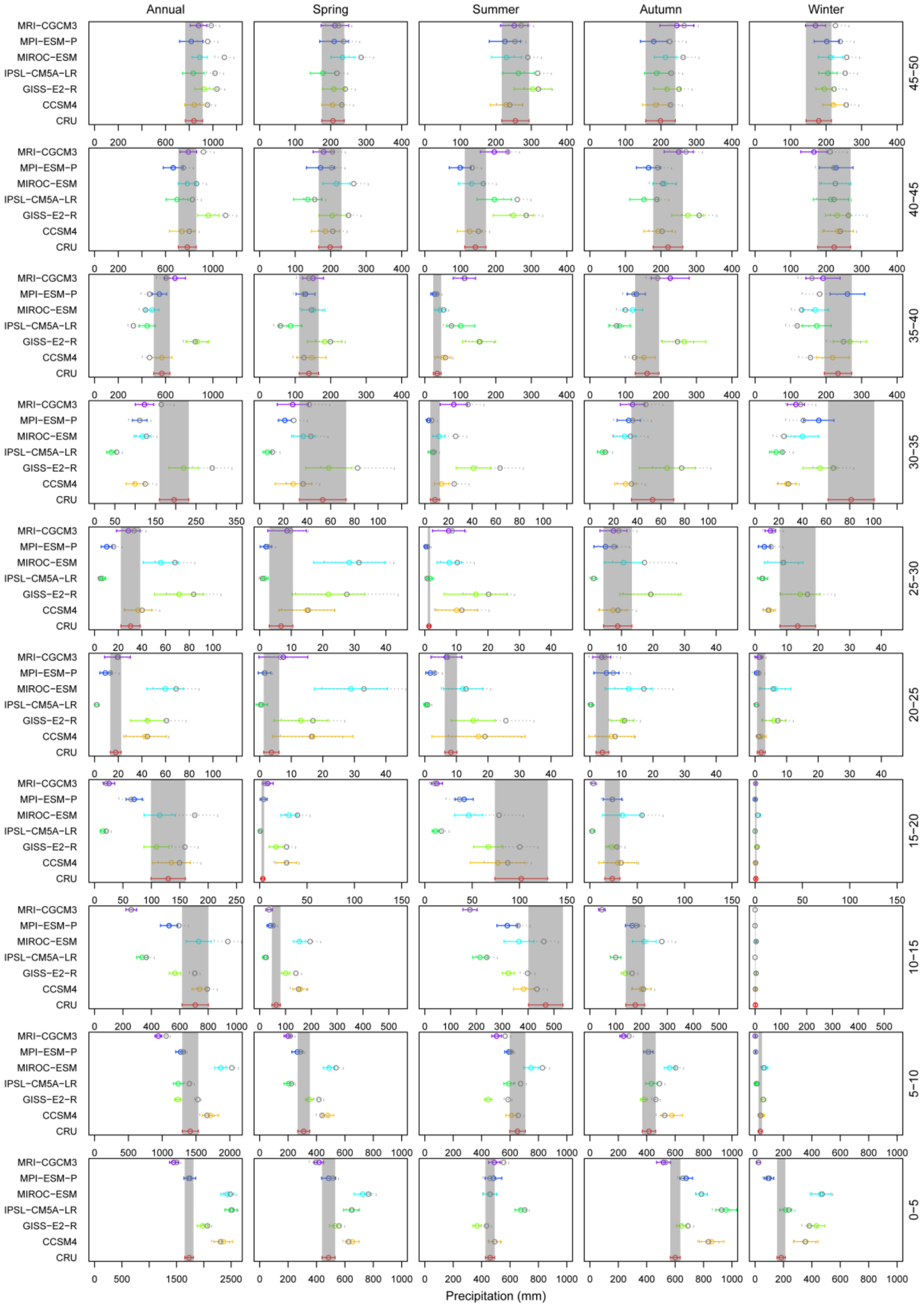


**Figure 4.5**. Comparison of the mean annual and mean seasonal precipitation (mm) between the CRU data and *historical* simulations for each 5 latitude band. Because there is a very small amount of precipitation is some latitude band, the axis scale starts at 0 but differs in the maximum value depending on the total rainfall values. Only six models have *historical* simulations. For these models we also present the *piControl* simulations. The historical simulations are shown in color while the *piControl* simulations for each model are shown by a dash line. The grey bars represent one standard deviation of the mean annual and mean seasonal precipitation from observations. The seasons are defined as spring (March, April, May), summer (June, July, August), autumn (September, October, November) and winter (December. January, February).

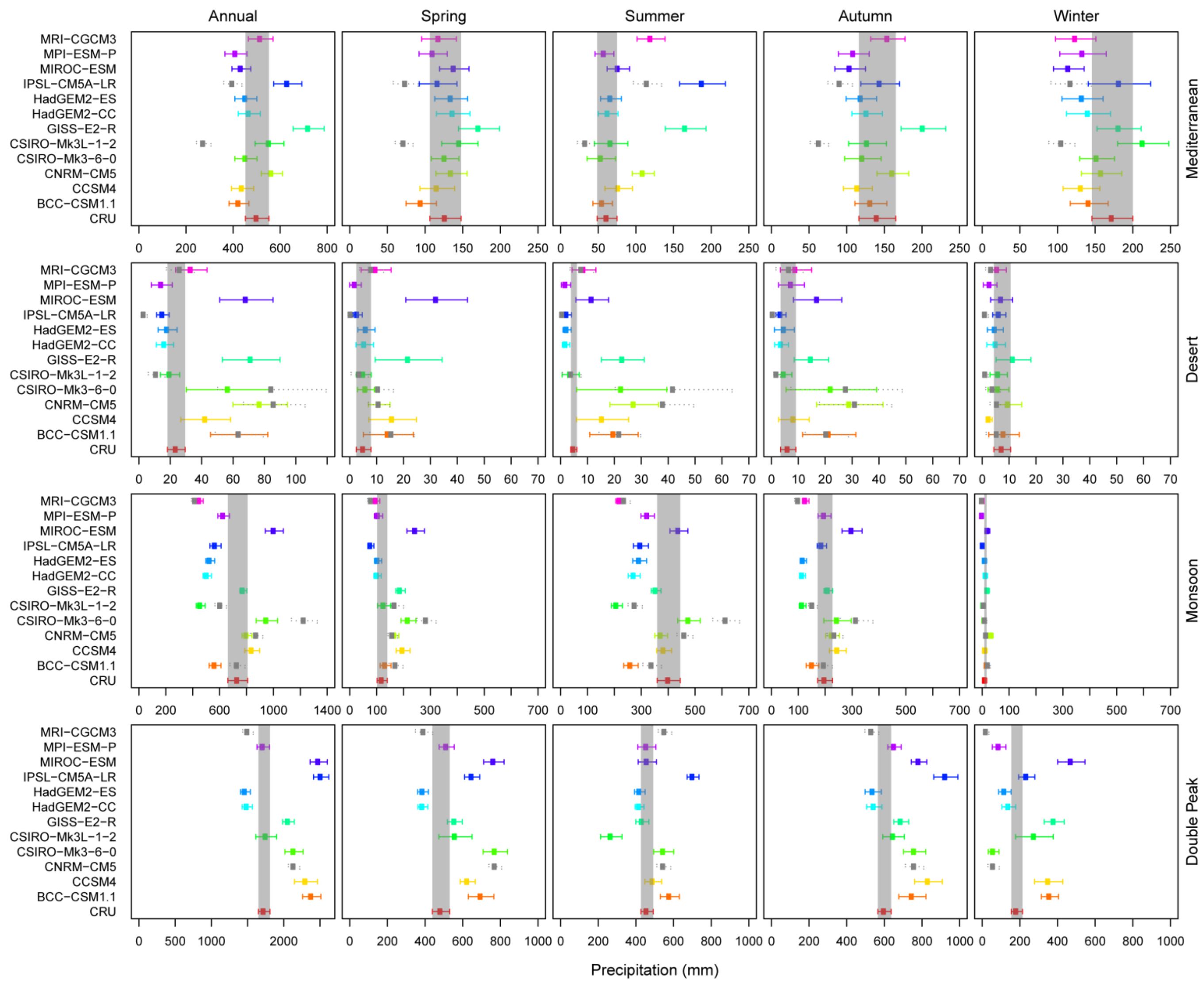


**Figure 4.6**: Comparison of simulated and observed mean annual and mean seasonal precipitation (mm) for each of the defined precipitation regimes (Mediterranean, desert, monsoon, double peak). The simulated precipitation (mean and standard deviation) is shown for both the climate zone as defined by the observations (solid line) and as defined in the *piControl* simulation itself (dotted line). The difference between these two lines for each model provides a measure of the degree to which incorrect placement of a given climate affects the zonal means. The grey bars represent one standard deviation of the mean annual and mean seasonal precipitation from observations. The seasons are defined as spring (March, April, May), summer (June, July, August), autumn (September, October, November) and winter (December. January, February).

We necessarily confine our comparisons of the magnitude of changes within each precipitation regime to those models that simulate a given regime in both the *piControl* and *midHolocene* simulations.

The changes in the DP regime are not consistent and in general do not exceed the variability shown by the *piControl*. Only two models (CSIRO-Mk3-6-0, MIROC-ESM) show a significant reduction in precipitation (of 200 and 250 mm respectively) in the *midHolocene* compared to the *piControl* (fig. 4.7; table 4.2). In the case of the CSIRO-Mk3-6-0 model, this is the result of a large decrease in autumn precipitation but in the case of the MIROC-ESM the decrease is concentrated in the spring.

The monsoon zone is characterized by a significant increase in precipitation, except in the case of the CSIRO-Mk3-6-0 model.  The anomalies range from +50 to +200 mm/year, reflecting large increases in summer (15-140 mm) and autumn (20 to 250 mm) rainfall. Changes in winter and spring precipitation in winter and spring are not significant.

Most models show an increase in mean annual precipitation in the desert regime (5 to 35 mm) as a result of increased summer and autumn rainfall, but the change only exceeds *piControl* variability in three cases (CCSM4, GISS-E2-R and MIROC-ESM).

Most of the models (11) show an increase in mean annual precipitation (10 to 75 mm) in the Mediterranean regime, although this increase only exceeds the *piControl* variability in the case of the GISS-E2-R model. The simulated increase in mean annual precipitation in the GISS-E2-R model results from an increase in spring, summer and autumn and a negligible change in winter. All of the models show an increase in spring precipitation, and two models (IPSL-CM5A-LR, HADGEM2-CC) show an increase in summer rainfall accompanied by either a small increase or no change in winter.

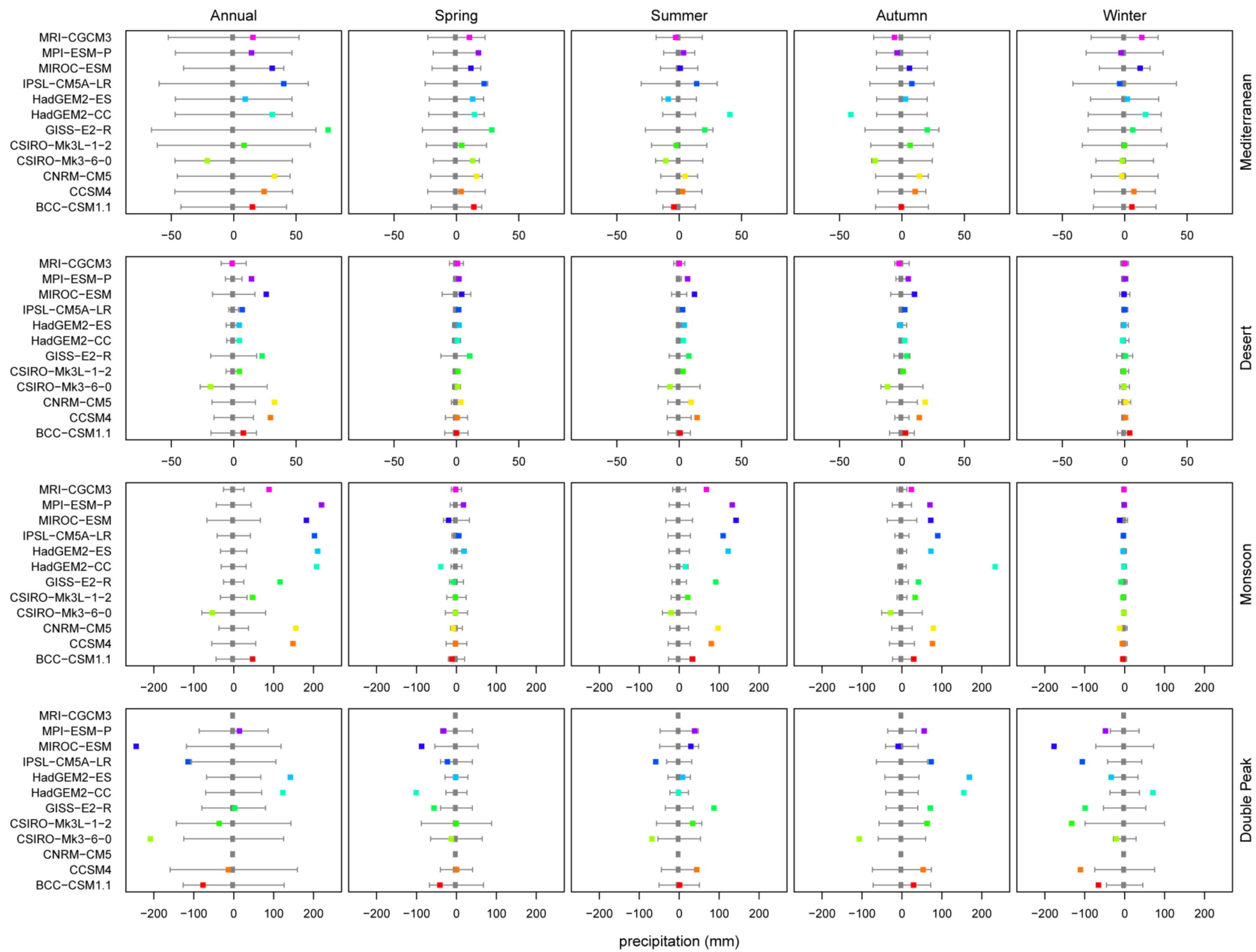


**Figure 4.7**: Simulated changes in total and seasonal precipitation in the mid-Holocene (*midHolocene*) compared to the pre-industrial control (*piControl*) for each of the four precipitation regimes (Mediterranean, desert, monsoon, double peak) for the region that is common between the two sets of simulations. The standard deviation of precipitation in the *piControl* control simulation of each model is shown (grey bars) to provide a visual measure of the significance of the simulated change in precipitation. The seasons are defined as spring (March, April, May), summer (June, July, August), autumn (September, October, November) and winter (December. January, February).

### 4.3.4. Comparison of mid-Holocene simulation mid-Holocene observations

Reconstructions of the change in mean annual precipitation in the mid-Holocene (fig. 4.7) show somewhat drier conditions (ca 40 mm/year) in the equatorial zone (0-5º N), an increase in precipitation of between 300-400 mm/year between 10-30º N, and an increase of between 100-150 mm/year in the Mediterranean (35-45º N). The simulated changes lie within the observed range between 0-5º N, with only 3 of the models lying outside the 25-75% range. Several models simulate changes within the range of the observed increase in precipitation between 10-15 º N (e.g. MRI-CGCM3, HADGEM2-CC, HADGEM2-ES, MIROC-ESM, IPSL-CM5a_LR, CCSM4). However, none of the models simulates the observed increase in precipitation (mean of ca 390 mm/year) between 15-30 º N or indeed simulate changes within the range of the observations (fig. 4.8). This is true even in the southernmost zone (15-20º N), although in this zone some of the models (e.g. MIROC-ESM) simulate a change of ca 50% of the observed mean change in precipitation. Models underestimate the reconstructed change in precipitation in the Mediterranean zone (35-45º N), although most models lie within the extremes of the observational range. The highest simulated change in precipitation is ca 50 mm/year (GISS-E2-R) compared to the reconstructed mean change of between 100-150 mm/year.

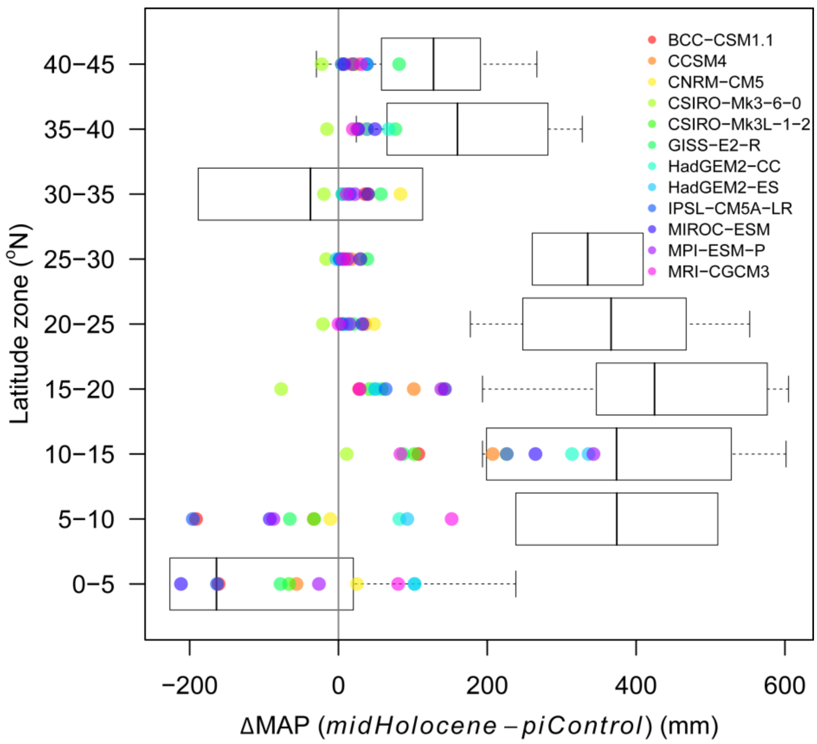


**Figure 4.8**: Comparison of simulated and reconstructed changes in mean annual precipitation in the mid-Holocene for 5º latitude bands between 0 and 45º N. The reconstructions are from the Bartlein et al. (2011) data set. The mean, 25-75% range and full range of the reconstructions are shown (for those latitude bands with sufficient data points). The model results are averages for the grid cells with observations.

### 4.3.5. Comparison between bias and anomaly

Comparison of the *piControl* bias and *midHolocene* anomaly suggests that model performance in the control simulations directly affects model performance in the *midHolocene* simulations in the DP, desert and Mediterranean regions (fig. 4.9). In the DP region, there is a significant negative significant correlation (fig. 4.9), all models, black line: slope=-0.23, $R^2$=0.74, p=0.0) between the bias and the anomaly: models that overestimate precipitation in the *piControl* show the largest reductions in precipitation in the *midHolocene* simulations (e.g. BCC-CSM1.1, CSIRO-Mk3-6-0 and MIROC-ESM). The overall relationship is driven by the OAC simulations (red line: $R^2$=0.88, p=0.02); the slope for the OA models is not significant (blue line; $R^2$=0.37, p=0.2). Indeed, as examination of these relationships in model-defined DP regions shows, the negative relationship shown by the OA models in the 0-5º N is driven by the two models that simulate monsoon-like regimes in this zone in the *piControl*.

There is no relationship between the *piControl* bias and the *midHolocene* anomaly in the monsoon zone (fig. 4.9), whether this is defined geographically (slope=0.00, $R^2$=0.0, p=0.98) or using the model-based regimes (slope=0.08, $R^2$=0.05, p=0.49). Thus, the ability to simulate the correct magnitude of modern precipitation appears to have no influence on the magnitude of the response of the monsoon to changed forcing. However, the OA and OAC models appear to show opposite tendencies: the OA models show a weakly positive relationship between the bias and the anomaly (models that simulate less rainfall than observed in the *piControl* produce smaller MH anomalies) whereas the OAC models show a (very) weakly negative relationship.

There is a significant positive correlation between the *piControl* bias and *midHolocene* anomaly in the desert region (fig. 4.9). This is true whether the region is defined geographically (slope=0.32, $R^2$=0.58, p=0.01) or using the model-defined desert regimes (slope=0.32, $R^2$=0.48, p=0.02). Models that produce a reasonable simulation of modern rainfall in this region fail to produce a significant enhancement in the *midHolocene* simulation (CSIRO-Mk3L-1-2, HadGEM2-CC, IPSL-CM5A-LR) whereas models that are too wet in the *piControl* produce large changes in the *midHolocene* (CCSM4, GISS-E2-R and MIROC-ESM). However, these relationships are driven by the OA simulations; the OAC simulations do not show any significant relationship between the *piControl* bias and the *midHolocene* anomaly.

There is also a significant positive correlation between bias and anomaly in the Mediterranean region (fig. 4.9), whether the region is defined geographically (slope=0.14, $R^2$=0.58, p=0.01) or using the model-defined regimes (slope=0.15, $R^2$=0.48, p=0.02). Models that underestimate precipitation in this zone in the *piControl* show only small increases in the *midHolocene* (BCC-CSM1.1, CCSM4 and MPI-ESM) while models with positive bias (GISS-E2-R and IPSL-CM5A-LR) produce larger changes in precipitation. However, the relationship for the OAC simulations is again non-significant.

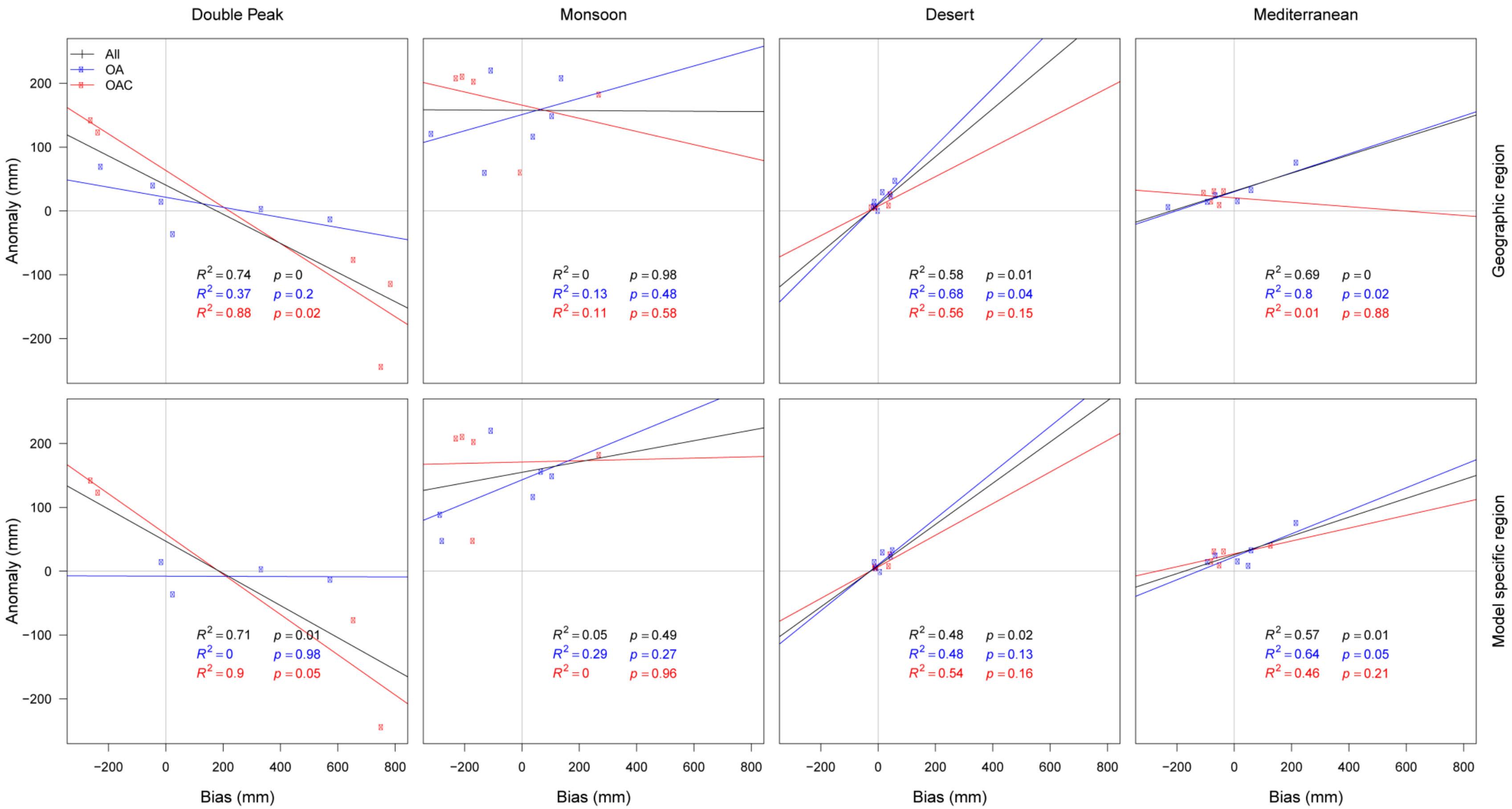


**Figure 4.9**: Relationship between biases in the *piControl* simulation of mean annual precipitation (mm) and mid-Holocene precipitation anomalies (*midHolocene-piControl*) as simulated by each of the CMIP5 models for each of the precipitation regimes (Double Peak, Monsoon, Desert, Mediterranean). The upper panels show biases and anomalies calculated for specific latitudinal bands as defined from the modern observed spatial extent of each regime (geographic region). The lower panels show biases and anomalies calculated for the region identified as characterized by a given regime in each model and simulation (model specific region). The regressions are calculated for all models (all: black), for the coupled ocean-atmosphere models (OA: blue) and for the carbon-cycle models (OAC: red).

Even in those regions where there are significant relationships between *piControl* bias and the *midHolocene* anomaly, the $R^2$ value ranges from 0.48 to 0.75 Thus, the bias in the *piControl* is not the only factor that determines whether the simulated magnitude of the MH climate change is correct. Furthermore, biases in the *piControl* appear to have less (or no) influence on the simulated *midHolocene* anomaly in the OAC simulations, except in the DP zone.

## 4.4. DISCUSSION

Our analyses suggest that the CMIP5 models fail to reproduce key aspects of both the modern and MH climate of the northern Africa and Mediterranean region.

Although the models generally reproduce the four characteristic seasonal patterns of precipitation, they do not always simulate these patterns in the correct place. They also tend to underestimate the magnitude of seasonal changes in precipitation. For example, they underestimate the amount of winter rainfall and overestimate the summer rainfall in the Mediterranean region. This is consistent with previous analyses of Mediterranean climates in both the CMIP3 (Giorgi and Lionello, 2008) and CMIP5 (Kelley et al., 2012) simulations. The models overestimate the precipitation in the DP zone, again a feature identified from previous analyses (Roehrig et al. 2013). Previous analyses of the CMIP5 models (e.g. Roehrig et al. 2013; Brands et al., 2013) have suggested that there is a tendency for models to underestimate precipitation in the Sahel zone. While our analyses confirm this, with 8 out of 12 models showing less summer precipitation than observed, some of the models (e.g. CSIRO−Mk3L−1−2, BCC−CSM1.1) show a distinct improvement when the comparison is made between regions defined by precipitation regimes rather than geographically (fig. 4.6).

Furthermore, the temporal interval used for comparison also plays a role: MIROC-ESM, for example, simulates summer precipitation correctly but annual rainfall is too large because the simulated monsoon season is too long. Our evaluations are based on the assumption that the difference in climate between the *piControl* (1850 AD) and the 1961-1990 modern climatology is small. Comparisons of the *piControl* and *historical* simulations (fig. 4.5) for a sub-set of the models appear to support this assumption: the differences between the simulations are smaller than the difference between the simulated and observed climates. There is no synthesis of data for the pre-industrial era from northern Africa, but a data-base from the Mediterranean region, despite it is incomplete, does not suggest substantial differences (e.g. Davis et al., 2003).

The models produce a northward shift and amplification of monsoon precipitation in the MH in response to insolation forcing. While the broad-scale patterns of change are consistent with the observations, the magnitude of these changes is significantly underestimated (fig. 4.8). The failure to simulate a sufficiently large expansion of the African monsoon has been a major criticism of previous generations of climate models (Joussaume et al., 1999; Coe and Harrison, 2002; Braconnot et al., 2007a; Brayshaw et al. 2011; Zhao and Harrison, 2011; Braconnot et al., 2012). Comparisons between CMIP5 and PMIP2 models (fig. 4.10) show that the two ensembles are indistinguishable in terms of simulated changes over this study region. Global comparisons of these two sets of simulations (e.g. Harrison et al., 2013) appear to confirm that the CMIP5 models are no better at simulating climate changes than previous generations of models. It was originally suggested that the underestimation of monsoon expansion reflected the failure to include feedbacks associated with climate-induced changes in land-surface characteristics, including wetter and more organic soils, the replacement of desert by grassland and shrubland, and the expansion of lakes and wetlands. Indeed, simulations in which the impacts of changes in land-surface characteristics were prescribed through changing albedo produced much larger monsoons (Street-Perrott et al., 1990; Kutzbach et al., 1996; Coe and Bonan, 1997; Broström et al., 1998).

However, this effect is not as pronounced in asynchronously-coupled climate-vegetation simulations (Claussen and Gaylor, 1996; Texier et al., 1997; Braconnot et al., 1999), models with dynamic vegetation from PMIP2 (Braconnot et al., 2012), or indeed coupled carbon-climate models in CMIP 5 (Harrison et al., 2013). In general, these models produce a strengthening of the monsoon *in situ* and only a minor northward expansion of the zone of monsoon rainfall. If we assume that the coupled models are behaving reasonably, this shows that the changes to the energy budget produced by the prescribed changes in albedo are compensated by changes in the partitioning between latent and sensible heating through increased evapotranspiration. This implies that some other mechanism, for example associated with changes in circulation, is required to produce the observed expansion of rainfall in the Sahara.

Our MH model evaluation is based on pollen-based global data base reconstructions of mean annual precipitation. Although the increase in monsoon precipitation is large (300-400 mm between 5 and 30º N) and spatially coherent, there are some zonal bands where the number of reconstructions is limited (see fig. 4.8). However, other sources of palaeoenvironmental data, including vegetation (Hoelzmann et al., 1998; Prentice et al., 2000; Watrin et al., 2009; Niedermeyer et al., 2010), lake-level reconstructions (Kohfeld and Harrison, 2000; Tierney et al., 2011), and archaeological evidence (Kuper and Kröpelin, 2006; Dunne et al., 2012), show that the magnitude of the reconstructed precipitation changes in these zones is plausible. Furthermore, the reconstructions of climate conditions in the Mediterranean region are based on a much larger number of individual data points (Bartlein et al., 2011), despite Iberian records, for example, are not specially abundant. Nevertheless, the discrepancies between the model simulations and the observations are not simply a result of lack of regional information.

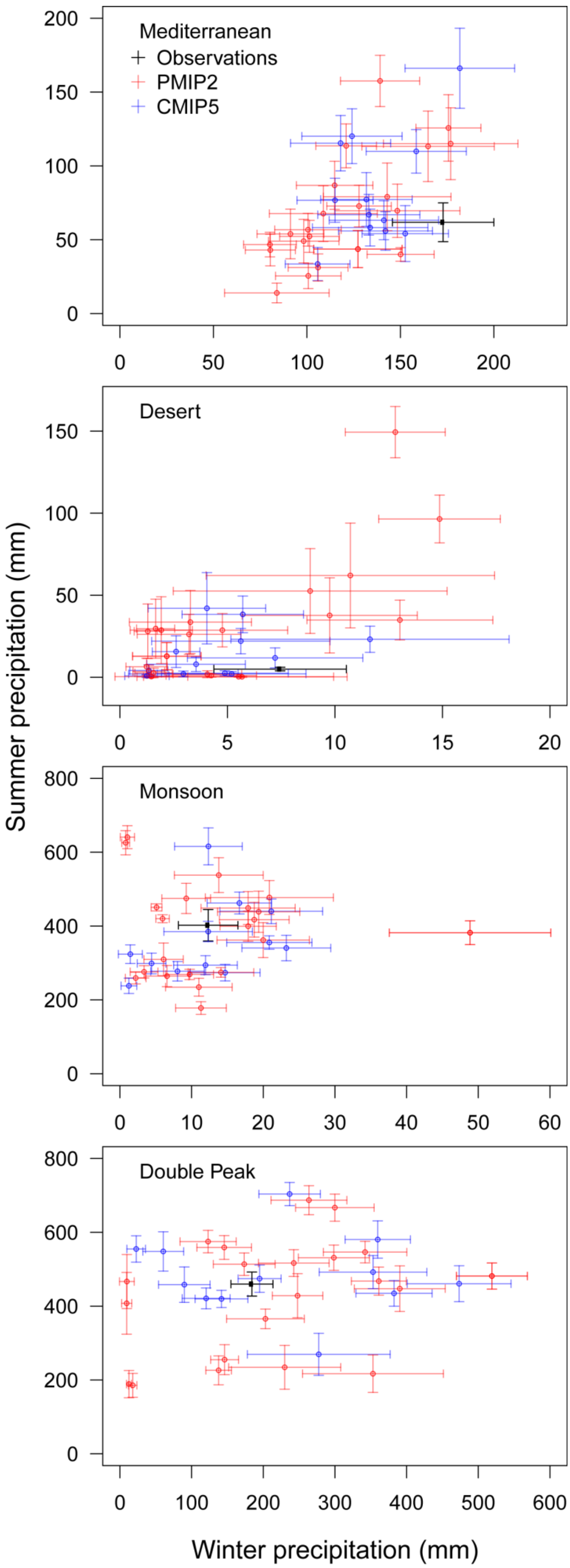


**Figure 4.10**. Comparison of simulated and observed summer and winter precipitation in each of the four precipitation regimes (Mediterranean, Desert, Monsoon, Double Peak). The observations (black) are the average for the period 1961-1990 from the CRU T3.1 data set (Harris et al., 2013). The simulated mean and standard deviation of precipitation from the CMIP5 models (blue) is based on the last 100 years of the *piControl.* These simulations can be compared with results from coupled ocean-atmosphere simulations made during the second phase of the Palaeoclimate Modelling Intercomparison Project (PMIP2: Braconnot et al., 2012; shown in red). The PMIP2 results are the mean and standard deviation based on the last 100 years of a *piControl*, except in three cases where only 50 years of data were available. Model results are calculated for each precipitation regime based on the observed geographic extent characterized by these regimes, as defined using the CRU TS3.1 data set. Summer is defined as June, July, and August; winter is December, January, February.

It would be possible to use the qualitative information about changes in water balance provided by lake-level records and isotope data to constrain pollen-based climate reconstructions (see e.g. Cheddadi et al., 1997). In this regard, the study carried out in the BSM sequence (chapter 2) and the comparison with the EST sequence (chapter 3) confirms the great opportunity to reconstruct seasonal precipitation patterns through multi-proxy and multi-dimensional studies. These multidisciplinary studies provide information of past climates parameters and help to understand our knowledge of likely climate mechanisms required to trigger such climate conditions. This could provide more robust reconstructions of the observed change in precipitation. However, for northern Africa the number of observations would still necessarily be limited to sites where both pollen and lake-level records are available, which is not abundant. Model inversion provides an alternative approach to use lake-level data for climate reconstruction (see e.g. Vassiljev et al., 1998), and one that has already been successfully used with pollen data (Wu et al., 2007). However, changes in lake water-balance can be brought about by changes in multiple climate parameters (temperature, precipitation, seasonality of precipitation, cloudiness, vapour pressure, wind speed) and the magnitude of the lake-level changes that occur in response to changes in catchment water-balance are influenced by morphometric factors (lake depth and shape, lake size relative to catchment size) (Harrison et al., 2002), and the methodology for taking account of all these factors has not yet been developed.

The simulated increase in mean annual precipitation in the Mediterranean region is small and, in comparison with the variability already present in the *piControl*, is not significant. However, although just half of the models show an increase in summer, all of them show an increase in precipitation in spring and some of them also show an increase in autumn. Thus, some of the models produce an increase in growing season moisture that, although too small, is consistent with the expansion of deciduous forest in this region during the mid-Holocene. Temperate deciduous forests occur in mid-latitude regions with > 700 mm of annual precipitation, spread throughout the year (see Harrison et al., 2010). Temperate deciduous forest occurs, for example, around Lake Banyoles in eastern Spain, where mean annual precipitation is ca 800 mm and nearly half of this falls in spring and summer (Soler et al., 2007). According to the mid-Holocene simulations for the Mediterranean area, the largest increase in growing-season precipitation is ca 30 mm in spring and 40 mm in summer (GISS-E2-R and HadGEM2-CC respectively), and the overall change in mean annual precipitation is <75 mm (GISS-E2-R). This is less than the increase required for deciduous trees to grow. Nevertheless, these simulations point to mechanism that could help to explain the observed vegetation changes in the Mediterranean. Furthermore, if the absence of a significant increase in summer rainfall in the Mediterranean is linked to underestimation of the northward migration of the African monsoon, then improvements in the simulation of monsoonal changes should also lead to a more realistic simulation of Mediterranean climate.

We have shown that there is a significant relationship between the bias in the control simulation and the magnitude of the simulated MH changes in precipitation for the DP, desert and Mediterranean zones, although no such relationship is present in the monsoon zone. However, the relationship in the desert and Mediterranean zones is only apparent in the OA models; the *piControl* bias does not seem to affect the *midHolocene* anomaly in the OAC models. The OA models also show a weakly positive (though non-significant) relationship between *piControl* bias and *midHolocene* anomaly in the monsoon region. Thus, the apparently significant relationships between bias and anomaly found when considering all the models are not a consistent feature of these simulations. Even in the DP, desert and Mediterranean zones, the bias in the OA *piControl* simulations only explains part of the variability in simulated climate changes. Previous studies have also had difficulties in finding consistent relationships between control biases and MH changes in precipitation. Comparison of control and MH atmosphere-only simulations made in the first phase of the

Palaeoclimate Modelling Intercomparison Project (PMIP1) showed that inter-model differences in the position of the intertropical convergence zone in the control simulation was reflected in the inter-model differences of its position in the MH simulation (Joussaume et al., 1999). However, there was no clear relationship between the amount of precipitation in the control and the increase in precipitation in the MH (Braconnot et al., 2002). Braconnot et al. (2007b), analysing OA simulations from PMIP2, showed that the relationship between the simulated precipitation in the control to the ratio of the change in precipitation between MH and control was negative: models that simulated very little rainfall tended to produce larger changes at the MH. However, this relationship was clearly driven by only three models, and the remaining models show no trend between the precipitation in the control simulation and the ratio of change in the MH. Thus, this seems to be consistent with our analyses. It is hard to escape the conclusion that improvements to the simulation of modern climate (see e.g. Haerter et al. 2011) will not guarantee that climate changes will be correctly simulated.

In this chapter, we have analysed the realism of simulated climates both in terms of climate regimes and by comparing specific geographic bands. The use of climate regimes places less stringent requirements on model performance, allowing an assessment for example of whether a model can simulate changes in seasonality independent of location. One reason for adopting this approach is the concern that model resolution, particularly in regions of complex topography, could affect geographic patterning (see e.g. Brewer et al., 2007). However, it can be difficult to find objective criteria for the definition of these climate regimes. Although we have been able to distinguish DP from monsoon, and monsoon from desert, climates solely on the basis of precipitation seasonality, it is not possible to use this type of criterion to distinguish desert and Mediterranean climates. Brewer et al. (2007) used k-means clustering to define climate regimes in Europe. Although this is an approach that needs to be further explored, it involves some arbitrary decisions about the climate variables used for clustering as well as the number of clusters considered.

Many of the large-scale features characteristic of projected climate changes are a feature of past climate changes, and comparison with palaeo-observations shows that current models reproduce these features in a realistic way (e.g. Braconnot et al., 2012; Izumi et al., 2013; Schmidt et al., 2013; Li et al., 2013). Models, as we confirm here for northern Africa and the Mediterranean region, are also able to simulate precipitation regimes and shifts in these regimes in a realistic way (Joussaume et al., 1999; Braconnot et al., 2007a; Brewer et al., 2007). However, there are still important discrepancies between the simulated and observed magnitude of changes in precipitation, despite the increasing complexity and resolution of the CMIP5 models compared to earlier generations of models. Given that the ability to simulate the magnitude of MH changes in seasonal climates does not appear to be systematically related to biases in the control simulations, focusing on improving the simulation of modern climate will not ensure that future projections or retrodictions of the climate of the Mediterranean and northern Africa will be more reliable. This is of concern given the environmental problems associated with recent climate changes in the Mediterranean and the importance of monsoonal rainfall for agriculture in northern Africa.

## 4.5. CONCLUSIONS

i. A detailed knowledge of modern and past climates is required to check the ability of climate models to reproduce the earth's climate system. While present conditions are sufficiently monitored, increasing number of well-constrained past climate reconstructions is still needed. This is particularly important in the Mediterranean area, when the seasonality of the precipitation is essential to understand the environmental changes and to investigate the likely climate mechanisms beyond them.

ii. The CMIP5 models fail to reproduce key aspects of both the modern and MH climate of the northern Africa and Mediterranean region, including the correct geographical location of zonal precipitation regimes in the pre-industrial simulation and the magnitude of MH changes in these regimes.

iii. Although biases in the OA simulations explain part of the variability in simulated climate changes, a similar relationship is not found for the OAC simulations. Thus overall, biases in the control simulations cannot explain the failure to reproduce MH changes in precipitation.

iv. As in previous generations of model simulations, the CMIP5 simulations underestimate the northward shift and the magnitude of observed changes in the northern African monsoon.

v. In the Mediterranean region, the simulations show a tendency for increased growing-season precipitation. Such a shift is required to explain observed vegetation changes in this region in the MH, but the simulated shift is much too small. We speculate that this is linked to the underestimation of changes in the northern African monsoon, suggesting that improved simulation of Mediterranean climates is linked to improvements in simulating the climate of northern Africa.

vi. The failure to simulate observed mid-Holocene changes in the northern Africa monsoon and the potentially linked failure to simulate the observed shift in rainfall seasonality in the Mediterranean raises concerns about the reliability of model projections of future climates in these regions.

## References


Amatulli, G., Camia, A. and San-Miguel-Ayanz, J.: Estimating future burned areas under changing climate in the EU-Mediterranean countries, Sci. Total Environ., 450-451, 209–222, 2013.

Bartlein, P. J., Harrison, S. P., Brewer, S., Connor, S., Davis, B. A. S., Gajewski, K., Guiot, J., Harrison-Prentice, T. I., Henderson, A., Peyron, O., Prentice, I. C., Scholze, M., Seppä, H., Shuman, B., Sugita, S., Thompson, R. S., Viau, A. E., Williams, J. and Wu, H.: Pollen-based continental climate reconstructions at 6 and 21 ka: a global synthesis, Clim. Dynam., 37, 775–802, 2011.

Bonfils, C., de Noblet-Ducoudré, N., Guiot, J. and Bartlein, P.: Some mechanisms of mid-Holocene climate change in Europe, inferred from comparing PMIP models to data, Clim. Dynam., 23, 79-98, 2004.

Bosmans, J. H. C., Drijfhout, S. S., Tuenter, E., Lourens, L. J., Hilgen, F. J. and Weber, S. L.: Monsoonal response to mid-holocene orbital forcing in a high resolution GCM, Clim. Past., 8, 723–740, 2012.

Braconnot, P., S. Joussaume, O. Marti, and N. de Noblet: Synergistic feedbacks from ocean and vegetation on the African monsoon response to mid-Holocene insolation. Geophys. Res. Lett., 26, 2481-2484, 1999.

Braconnot, P., Harrison, S. P., Kageyama, M., Bartlein, P. J., Masson-Delmotte, V., Abe-Ouchi, A., Otto-Bliesner, B. and Zhao, Y.: Evaluation of climate models using palaeoclimatic data, Nature Clim. Change, 2, 417–424, 2012.

Braconnot, P., Loutre, M., Dong, B., Joussaume, S. and Valdes, P.: How the simulated change in monsoon at 6 ka BP is related to the simulation of the modern climate: results from the Paleoclimate Modeling Intercomparison Project, Clim. Dynam., 19, 107–121, 2002.

Braconnot, P., Otto-Bliesner, B., Harrison, S., Joussaume, S., Peterchmitt, J.-Y., Abe-Ouchi, A., Crucifix, M., Driesschaert, E., Fichefet, T., Hewitt, C. D., Kageyama, M., Kitoh, A., Laîné, A., Loutre, M.-F., Marti, O., Merkel, U., Ramstein, G., Valdes, P., Weber, S. L., Yu, Y. and Zhao, Y.: Results of PMIP2 coupled simulations of the Mid-Holocene and Last Glacial Maximum – Part 1: experiments and large-scale features, Clim. Past., 3, 261–277, 2007a.

Braconnot, P., Otto-Bliesner, B., Harrison, S., Joussaume, S., Peterchmitt, J.-Y., Abe-Ouchi, A., Crucifix, M., Driesschaert, E., Fichefet, T., Hewitt, C. D., Kageyama, M., Kitoh, A., Loutre, M.-F., Marti, O., Merkel, U., Ramstein, G., Valdes, P., Weber, L., Yu, Y. and Zhao, Y.: Results of PMIP2 coupled simulations of the Mid-Holocene and Last Glacial Maximum – Part 2: feedbacks with emphasis on the location of the ITCZ and mid- and high latitudes heat budget, Clim. Past., 3, 279–296, 2007b.

Brands, S., Herrera, S., Fernández, J. and Gutiérrez, J. M.: How well do CMIP5 Earth System Models simulate present climate conditions in Europe and Africa?: A performance comparison for the downscaling community, Clim. Dynam., 41, 803–817, 2013.

Brayshaw, D. J., Rambeau, C. M. C. and Smith, S. J.: Changes in Mediterranean climate during the Holocene: Insights from global and regional climate modelling, Holocene, 21, 15–31, 2011.

Brewer, S., Guiot, J. and Torre, F.: Mid-Holocene climate change in Europe: a data-model comparison, Clim. Past., 3, 499–512, 2007.

Broström, A., Coe, M., Harrison, S.P., Gallimore, R., Kutzbach, J.E., Foley, J., Prentice, I.C. and Behling, P.: Land surface feedbacks and palaeomonsoons in northern Africa. Geophys. Res. Lett., 25: 3615-3618, 1998.

Camuffo, D., Bertolin, C., Barriendos, M., Dominguez-Castro, F., Cocheo, C., Enzi, S., Sghedoni, M., Valle, A., Garnier, E., Alcoforado, M.J., Xoplaki, E., Luterbacher, J., Diodato, N., Maugeri, M. Nunes, M.F. and Rodriguez, R.: 500-years temperatura reconstruction in the Mediterranean Basin by means of documentary data and instrumental observations, Climatic Change, 101, 169-199, 2010.

Carrión, J. S., Fernández, S., González-Sampériz, P., Gil-Romera, G., Badal, E., Carrión-Marco, Y., López-Merino, L., López-Sáez, J. A., Fierro, E. and Burjachs, F.: Expected trends and surprises in the Lateglacial and Holocene vegetation history of the Iberian Peninsula and Balearic Islands, Rev. Palaeobot. Palyno., 162, 458–475, 2010.

Cheddadi, R., Yu, G., Guiot, J., Harrison, S. P. and Prentice, I. C.: The climate of Europe 6000 years ago, Clim. Dynam., 13, 1–9, 1997.

Claussen, M. and Gaylor, V.: The greening of the Sahara during the mid-Holocene: results of an interactive atmosphere-biosphere model. Global Ecol. Biogeogr., 6: 369-377, 1997.

CLIVAR. Climate in Spain: Past, Present and Future. Regional climate change assessment report. Editors: Fiz F. Pérez and Roberta Boscolo. Ministerio de Ciencia e Innovación, Madrid, 83 pp, 2010.

Coe, M.T. and Bonan, G.: Feedbacks between climate and surface water in northern Africa during the middle Holocene. J. Geophys. Res., 102(D10), 11087–11101, 1997.

Coe, M. T. and Harrison, S. P.: The water balance of northern Africa during the mid-Holocene: an evaluation of the 6 ka BP PMIP simulations, Clim. Dynam., 19, 155–166, 2002.

Collins, W., Bellouin, N., Doutriaux-Boucher, M., Gedney, N., Halloran, P., Hinton, T., Hughes, J., Jones, C., Joshi, M., and Liddicoat, S.: Development and evaluation of an Earth-system model–HadGEM2, Geosci. Model Dev. Discuss., 4, 997-1062, 2011.

Davis, B. A. S., Brewer, S., Stevenson, A. C. and Guiot, J.: The temperature of Europe during the Holocene reconstructed from pollen data, Quaternary Sci. Rev., 22, 1701–1716, 2003.

Dufresne, J.-L., Foujols, M.-A., Denvil, S., Caubel, A., Marti, O., Aumont, O., Balkanski, Y., Bekki, S., Bellenger, H., and Benshila, R.: Climate change projections using the IPSL-CM5 Earth System Model: from CMIP3 to CMIP5, Clim. Dynam., 9-10: 2123-2165, 2013.

Dunne, J., Evershed, R. P., Salque, M., Cramp, L., Bruni, S., Ryan, K., Biagetti, S. and di Lernia, S.: First dairying in green Saharan Africa in the fifth millennium bc, Nature, 486(7403), 390–394, 2012.

European Environment Agency: Climate change, impacts and vulnerability in Europe 2012: an indicator-based report., European Environment Agency, Copenhagen., 2012.

Forman, S. L., Oglesby, R., Markgraf, V. and Stafford, T.: Paleoclimatic significance of Late Quaternary eolian deposition on the Piedmont and High Plains, Central United States, Global Planet. Change, 11(1-2), 35–55, 1995.

Gaetani, M., Pohl, B., Douville, H. and Fontaine, B.: West African Monsoon influence on the summer Euro-Atlantic circulation, Geophys. Res. Lett., 38, L09705, 2011.

Gent, P. R., Danabasoglu, G., Donner, L. J., Holland, M. M., Hunke, E. C., Jayne, S. R., Lawrence, D. M., Neale, R. B., Rasch, P. J., and Vertenstein, M.: The community climate system model version 4. J. Climate, 24, 4973–4991, 2011.

Giorgi, F.: Climate change hot-spots, Geophys. Res. Lett., 33(8), L08707, 2006.

Giorgi, F. and Lionello, P.: Climate change projections for the Mediterranean region, Global Planet. Change, 63(2-3), 90–104, 2008.

Guiot, J., Boreux, J. J., Braconnot, P. and Torre, F.: Data-model comparison using fuzzy logic in paleoclimatology, Clim. Dynam., 15(8), 569–581, 1999.

Haerter, J. O., Hagemann, S., Moseley, C. and Piani, C.: Climate model bias correction and the role of timescales, Hydrol. Earth Syst. Sc., 15(3), 1065–1079, 2011.

Harris, I., Jones, P. D., Osborn, T. J. and Lister, D. H.: Updated high-resolution grids of monthly climatic observations - the CRU TS3.10 Dataset, Int. J. Climatol., 2013.

Harrison, S.P., Yu, G. and Vassiljev, J.: Climate changes during the Holocene recorded by lakes from Europe. In: Wefer, G., Berger, W., Behre, K.-E. and Jansen, E. (Eds) Climate Development and History of the North Atlantic Realm. Springer-Verlag, Berlin/Heidelberg, pp. 191-204 2002.

Harrison, S. P., Prentice, I. C. and Bartlein, P. J.: Influence of insolation and glaciation on atmospheric circulation in the North Atlantic sector: Implications of general circulation model experiments for the Late Quaternary climatology of Europe, Quaternary Sci. Rev., 11(3), 283–299, 1992.

Harrison, S.P., Bartlein, P.J., Brewer, S., Prentice, I.C., Boyd, M., Hessler, I., Holmgren, K., Izumi, K., and Willis, K.: Model benchmarking with glacial and mid-Holocene climates. Clim. Dynam., 2013.

Hoelzmann, P., Jolly, D., Harrison, S. P., Laarif, F., Bonnefille, R. and Pachur, H.-J.: Mid-Holocene land-surface conditions in northern Africa and the Arabian Peninsula: A data set for the analysis of biogeophysical feedbacks in the climate system, Glob. Biogeochem. Cy, 12(1), 35–51, 1998.

Hoerling, M., Eischeid, J., Perlwitz, J., Quan, X., Zhang, T. and Pegion, P.: On the increased frequency of Mediterranean drought. J. Climate, 25(6), 2146-2161, 2012.

Ibanez, F.: Sur une nouvelle application de la théorie de 1'information à la description des séries chronologiques planctoniques, J. Plankton Res., 4(3), 619–632, 1982.

Izumi, K., Bartlein, P. J. and Harrison, S. P.: Consistent large-scale temperature responses in warm and cold climates, Geophys. Res. Lett., 40(9), 1817–1823, 2013.

Joussaume, S., Taylor, K. E., Braconnot, P., Mitchell, J. F. B., Kutzbach, J. E., Harrison, S. P., Prentice, I. C., Broccoli, A. J., Abe-Ouchi, A., Bartlein, P. J., Bonfils, C., Dong, B., Guiot, J., Herterich, K., Hewitt, C. D., Jolly, D., Kim, J. W., Kislov, A., Kitoh, A., Loutre, M. F., Masson, V., McAvaney, B., McFarlane, N., de Noblet, N., Peltier, W. R., Peterschmitt, J. Y., Pollard, D., Rind, D., Royer, J. F., Schlesinger, M. E., Syktus, J., Thompson, S., Valdes, P., Vettoretti, G., Webb, R. S. and Wyputta, U.: Monsoon changes for 6000 years ago: Results of 18 simulations from the Paleoclimate Modeling Intercomparison Project (PMIP), Geophys. Res. Lett., 26(7), 859–862, 1999.

Kelley, C., Ting, M., Seager, R. and Kushnir, Y.: Mediterranean precipitation climatology, seasonal cycle, and trend as simulated by CMIP5, Geophys. Res. Lett., 39(21), L21703, doi:10.1029/2012GL053416, 2012.

Kelley, D. I., Colin Prentice, I., Harrison, S. P., Wang, H., Simard, M., Fisher, J. B. and Willis, K. O.: A comprehensive benchmarking system for evaluating global vegetation models, Biogeosciences Discuss., 9(11), 15723–15785, 2012.

Kohfeld, K. E. and Harrison, S. P.: How well can we simulate past climates? Evaluating the models using global palaeoenvironmental datasets, Quaternary Sci. Rev., 19(1-5), 321–346, 2000.

Kuper, R. and Kröpelin, S.: Climate-Controlled Holocene Occupation in the Sahara: Motor of Africa's Evolution, Science, 313(5788), 803–807, 2006.

Kutzbach, J.E., Bonan, G.B., Foley, J.A. and Harrison, S.P.: Vegetation and soils feedbacks on the response of the African monsoon response to orbital forcing in early to middle Holocene. Nature 384: 623-626, 1996.

Levis, S., Bonan, G. B. and Bonfils, C.: Soil feedback drives the mid-Holocene North African monsoon northward in fully coupled CCSM2 simulations with a dynamic vegetation model, Clim. Dynam., 23(7-8), 791–802, 2004.

Li, G., Harrison, S. P., Bartlein, P. J., Izumi, K. and Colin Prentice, I.: Precipitation scaling with temperature in warm and cold climates: An analysis of CMIP5 simulations, Geophys. Res. Lett., 40, 4018–4024, , 2013

Lionello, P.: The climate of the Mediterranean Region from the past to the future, Elsevier Science, Burlington, 2012.

Luterbacher, J., Xoplaki, E., Casty, C., Wanner, H., Pauling, A., Kuttel, M., Rutishauser, T., Bronnimann, S., Fischer, E. and Fleitmann, D.: Chapter 1 Mediterranean climate variability over the last centuries: A review, in Developments in Earth and Environmental Sciences, vol. 4, pp. 27–148, Elsevier, 2006.

Magny, M., Miramont, C. and Sivan, O.: Assessment of the impact of climate and anthropogenic factors on Holocene Mediterranean vegetation in Europe on the basis of palaeohydrological records, Palaeogeogr. Palaeocl., 186(1–2), 47–59, 2002.

Marzin, C. and Braconnot, P.: Variations of Indian and African monsoons induced by insolation changes at 6 and 9.5 kyr BP, Clim. Dynam., 33(2-3), 215–231, 2009.

Masson, V., Cheddadi, R., Braconnot, P., Joussaume, S. and Texier, D.: Mid-Holocene climate in Europe: what can we infer from PMIP model-data comparisons?, Clim. Dynam., 15(3), 163–182, 1999.

Meehl, G. A., Stocker, T. F., Collins, W. D., Friedlingstein, P., Gaye, A. T., Gregory, J. M., Kitoh, A., Knutti, R., Murphy, J. M., Nodas, A., Raper, S. C. B., Watterson, I. G., Weaver, A. J. and Zhao, Z. C.: Global Climate Projections, in Climate Change 2007: The Physical Science Basis. Contribution of Working Group I to the Fourth Assessment Report of the Intergovernmental Panel on Climate Change, edited by S. Solomon, D. Quin, M. Manning, Z. Chen, Marquis, K. B. Averyt, M. Tignor, and H. L. Miller, Cambridge University Press, Cambridge, UK and New York, USA., 2007.

Mehta, A. V. and Yang, S.: Precipitation climatology over Mediterranean Basin from ten years of TRMM measurements, Adv. Geosci., 17, 87–91, 2008.

Monerie, P.-A., Fontaine, B. and Roucou, P.: Expected future changes in the African monsoon between 2030 and 2070 using some CMIP3 and CMIP5 models under a medium-low RCP scenario, J. Geophys. Res., 117(D16), 2012.

Moreira, F., Viedma, O., Arianoutsou, M., Curt, T., Koutsias, N., Rigolot, E., Barbati, A., Corona, P., Vaz, P., Xanthopoulos, G., Mouillot, F. and Bilgili, E.: Landscape – wildfire interactions in southern Europe: Implications for landscape management, J. Environ. Manage., 92(10), 2389–2402, 2011.

Morellón, M., Valero-Garcés, B., Vegas-Vilarrúbia, T., González-Sampériz, P., Romero, Ó., Delgado-Huertas, A., Mata, P., Moreno, A., Rico, M., Corella, J.P. Lateglacial and Holocene palaeohydrology in the western Mediterranean region: The Lake Estanya record (NE Spain). Quat. Sci. Rev. 28, 2582–2599, 2009.

Niedermeyer, E. M., Schefuß, E., Sessions, A. L., Mulitza, S., Mollenhauer, G., Schulz, M. and Wefer, G.: Orbital- and millennial-scale changes in the hydrologic cycle and vegetation in the western African Sahel: insights from individual plant wax δD and δ13C, Quaternary Sci. Rev., 29(23-24), 2996–3005, 2010.

Nikulin, G., KjellströM, E., Hansson, U., Strandberg, G. and Ullerstig, A.: Evaluation and future projections of temperature, precipitation and wind extremes over Europe in an ensemble of regional climate simulations, Tellus, 63(1), 41–55, 2011.

Phipps, S., Rotstayn, L., Gordon, H., Roberts, J., Hirst, A., and Budd, W.: The CSIRO Mk3L climate system model version 1.0–Part 1: Description and evaluation, Geosci. Model Dev., 4, 483-509, 2011.

Prentice, C., Guiot, J., Huntley, B., Jolly, D. and Cheddadi, R.: Reconstructing biomes from palaeoecological data: a general method and its application to European pollen data at 0 and 6 ka, Clim. Dynam., 12(3), 185–194, 1996.

Prentice, I. C. and Jolly, D.: Mid-Holocene and glacial-maximum vegetation geography of the northern continents and Africa, J. Biogeogr., 27(3), 507–519, 2000.

Raddatz, T., Reick, C., Knorr, W., Kattge, J., Roeckner, E., Schnur, R., Schnitzler, K.-G., Wetzel, P., and Jungclaus, J.: Will the tropical land biosphere dominate the climate–carbon cycle feedback during the twenty-first century?, Clim. Dynam., 29, 565-574, 2007.

Raicich, F., Pinardi, N. and Navarra, A.: Teleconnections between Indian monsoon and Sahel rainfall and the Mediterranean, Int. J. Climatol., 23(2), 173–186, 2003.

Roberts, N., Eastwood, W. J., Kuzucuoglu, C., Fiorentino, G. and Caracuta, V.: Climatic, vegetation and cultural change in the eastern Mediterranean during the mid-Holocene environmental transition, Holocene, 21, 147–162, 2011.

Roberts, N., Jones, M. D., Benkaddour, A., Eastwood, W. J., Filippi, M. L., Frogley, M. R., Lamb, H. F., Leng, M. J., Reed, J. M., Stein, M., Stevens, L., Valero-Garcés, B. and Zanchetta, G.: Stable isotope records of Late Quaternary climate and hydrology from Mediterranean lakes: the ISOMED synthesis, Quaternary Sci. Rev., 27(25-26), 2426–2441, 2008.

Roberts, N., Stevenson, T., Davis, B., Cheddadi, R., Brewster, S. and Rosen, A.: Holocene climate, environment and cultural change in the circum-Mediterranean region, in Past Climate Variability through Europe and Africa, vol. 6, edited by R. W. Battarbee, F. Gasse, and C. E. Stickley, pp. 343–362, Springer Netherlands, Dordrecht, 2004.

Rodwell, M. J. and Hoskins, B. J.: Subtropical Anticyclones and Summer Monsoons, J. Climate, 14(15), 3192–3211, 2001.

Roehrig, R., Bouniol, D., Guichard, F., Hourdin, F. and Redelsperger, J.-L.: The present and future of the West African monsoon: a process-oriented assessment of CMIP5 simulations along the AMMA transect., J. Climate., 130314153438000, 2013.

Schmidt, G. A., Annan, J. D., Bartlein, P. J., Cook, B. I., Guilyardi, E., Hargreaves, J. C., Harrison, S. P., Kageyama, M., LeGrande, A. N., Konecky, B., Lovejoy, S., Mann, M. E., Masson-Delmotte, V., Risi, C., Thompson, D., Timmermann, A., Tremblay, L.-B. and Yiou, P.: Using paleo-climate comparisons to constrain future projections in CMIP5, Clim. Past Discuss., 9(1), 775–835, 2013.

Schmidt, G.A., M. Kelley, L. Nazarenko, R. Ruedy, G.L. Russell, I. Aleinov, M. Bauer, S.E. Bauer, M.K. Bhat, R. Bleck, V. Canuto, Y.-H. Chen, Y. Cheng, T.L. Clune, A. Del Genio, R. de Fainchtein, G. Faluvegi, J.E. Hansen, R.J. Healy, N.Y. Kiang, D. Koch, A.A. Lacis, A.N. LeGrande, J. Lerner, K.K. Lo, E.E. Matthews, S. Menon, R.L. Miller, V. Oinas, A.O. Oloso, J.P. Perlwitz, M.J. Puma, W.M. Putman, D. Rind, A. Romanou, Mki. Sato, D.T. Shindell, S. Sun, R.A. Syed, N. Tausnev, K. Tsigaridis, N. Unger, A. Voulgarakis, M.-S. Yao, and J. Zhang: Configuration and assessment of the GISS ModelE2 contributions to the CMIP5 archive. J. Adv. Model. Earth Syst., 2014.

Soler, M., Serra, T., Colomer, J. and Romero, R.: Anomalous rainfall and associated atmospheric circulation in the northeast Spanish Mediterranean area and its relationship to sediment fluidization events in a lake, Water Resour. Res., 43(1), 2007.

Sperber, K. R., Annamalai, H., Kang, I.-S., Kitoh, A., Moise, A., Turner, A., Wang, B. and Zhou, T.: The Asian summer monsoon: an intercomparison of CMIP5 vs. CMIP3 simulations of the late 20th century, Clim. Dynam., 2012.

Street-Perrot, F. A., Mitchell, J. F. B., Marchand, D. S. & Brunner, J. S.: Milankovitch and albedo forcing of the tropical monsoon: a comparison of geological evidence and numerical simulations for 9000 y BP. Trans. R. Soc. Edinb.:Earth Sciences 81, 407−427, 1990.

Texier, D. de Noblet, N., Harrison, S.P., Haxeltine, A., Joussaume, S., Jolly, D., Laarif, F., Prentice, I.C. and Tarasov, P.E.: Quantifying the role of biosphere-atmosphere feedbacks in climate change: coupled model simulation for 6000 years B.P. and comparison with palaeodata for northern Eurasia and northern Africa. Clim. Dynam., 13, 865-882, 1997.

Taylor, K. E., Stouffer, R. J. and Meehl, G. A.: An Overview of CMIP5 and the Experiment Design, B. Am. Meteorol. Soc., 93(4), 485–498, 2012.

Tierney, J. E., Lewis, S. C., Cook, B. I., LeGrande, A. N. and Schmidt, G. A.: Model, proxy and isotopic perspectives on the East African Humid Period, Earth Planet. Sc. Lett., 307(1-2), 103–112, 2011.

van Soelen, E., Brooks, G., Larson, R., Sinninghe Damste, J. and Reichart, G.: Mid- to late-Holocene coastal environmental changes in southwest Florida, USA, Holocene, 22(8), 929–938, 2012.

Vanniere, B., Power, M. J., Roberts, N., Tinner, W., Carrion, J., Magny, M., Bartlein, P., Colombaroli, D., Daniau, A. L., Finsinger, W., Gil-Romera, G., Kaltenrieder, P., Pini, R., Sadori, L., Turner, R., Valsecchi, V. and Vescovi, E.: Circum-Mediterranean fire activity and climate changes during the mid-Holocene environmental transition (8500-2500 cal. BP), Holocene, 21(1), 53–73, 2011.

Vassiljev, J., Harrison, S.P. and Guiot, J.: Simulating the Holocene lake-level record of Lake Bysjön, southern Sweden. Quat. Res. 49, 62-71, 1998.

Voldoire, A., Sanchez-Gomez, E., y Mélia, D. S., Decharme, B., Cassou, C., Sénési, S., Valcke, S., Beau, I., Alias, A., and Chevallier, M.: The CNRM-CM5. 1 global climate model: description and basic evaluation, Clim. Dynam., 9-10:2091-2121, 2013.

Watrin, J., Lézine, A.-M. and Hély, C.: Plant migration and plant communities at the time of the "green Sahara," C. R. Geosci., 341(8-9), 656–670, 2009.

Wohlfahrt, J., Harrison, S. P. and Braconnot, P.: Synergistic feedbacks between ocean and vegetation on mid- and high-latitude climates during the mid-Holocene, Clim. Dynam., 22(2-3), 223–238, 2004.

Wu, H., Guiot, J., Brewer, S. and Guo, Z.: Climatic changes in Eurasia and Africa at the last glacial maximum and mid-Holocene: reconstruction from pollen data using inverse vegetation modeling. Clim. Dynam., 29, 211–229, 2007.

Wu, T., Li, W., Ji, J., Xin, X., Li, L., Wang, Z., Zhang, Y., Li, J., Zhang, F., and Wei, M.: Global carbon budgets simulated by the Beijing Climate Center Climate System Model for the last century. J. Geophys. Res. Atmos., 118, 4326–4347, 2013.

Xoplaki, E., González-Rouco, F., Luter, J. and Wanner, H.: Mediterranean summer air temperature variability and its connection to the large-scale atmospheric circulation and SSTs, Clim. Dynam., 20(7-8), 723–739, 2003.

Yukimoto, S., Yoshimura, H,. Hosaka, M., Sakami, T., Tsujino, H., Hirabara, M., Tanaka, TY., Deushi, M., Obata, A., Nakano, H., Adachi, Y., Shindo, E., Yabu, S., Ose, T., Kitoh, A.: Meteorological

Research Institute Earth System Model Version 1 (MRI-ESM1): Model Description - Technical reports of the meteorological research institute No.64, pp88, 2011.

Zhao, Y. and Harrison, S. P.: Mid-Holocene monsoons: a multi-model analysis of the inter-hemispheric differences in the responses to orbital forcing and ocean feedbacks, Clim. Dynam., 39(6), 1457–1487, 2011.

# 5

# Concluding remarks

## OUTLINE

The aim of this chapter is to summarize, integrate and point out the implications of the main results described in previous chapters in order to outline how the questions raised in the introduction have been answered.

To focus the discussion it is worth remembering the main objectives of the present PhD dissertation proposed in the Introduction (chapter 1):

- To investigate past precipitation and temperature changes in the Central Pyrenees based on vegetation dynamics and lake level variations through multi-dimensional and multi-proxy analyses, in order to improve our understanding of the long-term climate evolution and the impact of the abrupt climate changes in the Western Mediterranean during the Holocene.
- To check the ability of climate models from the CMIP5 to simulate the recognized more humid conditions in the Mediterranean region during the Mid-Holocene in order to measure their reliability on future climate scenarios.
- To study the timeline of the human activities in the Pyrenees in order to find out patterns of occupation, landscape modifications and effects of climate events on populations.

To accomplish its goal, this chapter consists of three main sections:

- The first section (Holocene environmental changes in the Pyrenees: climate implications and model evaluation) covers the two first objectives of the thesis.
    - Based on the results obtained from the Basa de la Mora (chapter 2) and Estanya (chapter 3) sequences, this section establish relative changes in both precipitation and temperature through the Holocene in the Central Pyrenees, integrating the data with the possible climate mechanisms beyond those changes.
    - Additionally, results from precipitation simulations for the Mediterranean region in the Mid Holocene (chapter 4) are discussed in order to examine the ability of climate models to simulate the precipitation shift required to explain the environmental changes recognised in the Central Pyrenees during the Mid Holocene.
- The second section (Anthropogenic impact in the southern Pyrenees) covers the third objective of the thesis based on the analyses of the anthropogenic indicators found in BSM and EST sequences and comparison with other Pyrenean sites.
- The third section summarises the main results of this PhD thesis, about the evolution during the Holocene of the altitudinal vegetation belts in the Central Pyrenees transect.

## 5.1. HOLOCENE ENVIRONMENTAL CHANGES IN THE PYRENEES: CLIMATE IMPLICATIONS AND MODEL EVALUATION

Given the vulnerability of the Mediterranean region to the current Global Changes, climate projections have largely increased during the last decades in order to investigate and implement mitigation and adaptation strategies. Therefore, confidence in climate simulations is essential to this purpose. Nevertheless, regional projections for the Mediterranean basin are extremely difficult because of the complexity and natural variability of the climate in the region. Paleo-climate research allows us to investigate the climate mechanism operating in the Mediterranean at large scales providing us with a deeper Knowledge and vision of the evolution of the climate in the area as result of changing some key components of the Earth’s climate system.

This thesis contributes to palaeo-climate research in the Mediterranean region with two new and valuable sequences located in the key area of the Pyrenees, providing with a detailed regional Holocene climate reconstruction with particular stress on seasonal changes in precipitation and temperatures.

The multi-proxy study (pollen, sedimentology, geochemistry, chironomids and charcoal) carried out in the Basa de la Mora sequence (BSM) provides us with the most robust Holocene palaeo-environmental and palaeo-climate reconstruction in the Pyrenees up to date. Due to the key position of the BSM Lake in the subalpine belt of the Central Pyrenees (2000 m a.s.l.), its study allows us to evaluate the fluctuating Mediterranean and Atlantic influences in the Pyrenees throughout the Holocene. The basis for this reconstruction comes from the ecotonal shifts between the deciduous forest, which is typical of the Atlantic formations, and the conifers forest, which is more typical of the Mediterranean dry areas. The shifts between both ecosystems in the Central Pyrenees inform about the dominance and/or prevalence of one or another climate regimen across time. Besides, sedimentological changes and lake-level variations interpreted in the BSM sequence further helped to disentangle the patterns of precipitation changes occurred in the Central Pyrenees along the Holocene associated to the vegetation variability.

In addition, the reconstruction of the vegetation evolution carried out in the Estanya sequence (EST), placed at 670 m a.s.l. in the Mediterranean area of the Pre-Pyrenean range, provides us with detailed information about the Holocene forest dynamics in the colline belt of the Pyrenees. Thus, these new palynological data complete the regional available information about Holocene vegetation history. The comparison of both, BSM and EST sequences allow us to detect shifts in the vegetation belts in the southern Pyrenees providing further climatic information related, not only to precipitation shifts due to changes in large –scale climate patterns but also to temperature changes due to altitudinal features.

According to the main environmental changes detected in both sequences, the Holocene climate evolution affecting the Central Pyrenees can be divided in five main periods. This section is structured according to these five stages:

- The onset of the Holocene, from 11.7 to 9.8 ka BP
- The Early Holocene, from 9.8 to 8.2 cal yr BP.
- The Mid Holocene, from 8.2 to 6 ka BP.
- A transition phase from the Mid Holocene to the Late Holocene, from 6 to 4.8 ka BP.
- The Late Holocene, from 4.8 to 0.8 ka BP. This period ends at 0.8 cal ka BP due to the high-degree of human disturbances detected since then, that easily mask the climate signal in both sequences and in most Pyrenean sites.

Having in mind the results obtained in chapters 2 and 3, this section attempt to establish relative changes in both temperature and precipitation in the Central Pyrenees for each of periods defined previously. Additionally, the section that refers to the Mid-Holocene (8.2-6 ka) includes a broad analysis of the climate model simulations carried in chapter 4 for the precipitation regimen in the Mediterranean region during the Mid Holocene.

### 5.1.1. The onset of the Holocene: 11.700- 9800 cal yr BP

In this Thesis, the first two millennia of the Early Holocene are only covered by the Lake Estanya sequence due to the lack of well-dated sediment record in Basa de la Mora until ca 9.8 cal ka BP. Hence, new data about vegetation evolution for this period come exclusively from the lowland sequence, but it can be placed in a regional framework due to previous studies in other sites by other researchers (see chapter 3).

Sequences from continental areas in NE Spain (highlands of the Iberian Range) (i.e., Las Pardillas: Sánchez-Goñi and Hannon, 1999; Montes Universales: Stevenson, 2000; Villarquemado paleolake: Aranbarri et al., 2014) show an onset of the Holocene in Iberia characterized by dry and cold or cool conditions. During the beginning of the Holocene, Lake Estanya displays very high pollen values of *Juniperus* and *Artemisia* and low of temperate trees such as semi-deciduous and evergreen *Quercus* (fig. 5.1). Such vegetation composition of large steppe community and absence of temperate trees, as we have described in detail in chapter 3, points out to harsh climate conditions with high seasonal contrast and likely very cold winter temperatures. However, though high continentally could explain this vegetation composition by itself, shortage of water could be an added environmental factor causing extended steppe communities and hindering tree growth. In fact a phase of extreme low water levels in Estanya even with desiccation events, was identified by sedimentological and geochemical indicators from 11.6 to 9.4 cal ka BP (Morellón et al. 2009) and demonstrates the prevalence of arid conditions during the beginning of the Holocene. These results are in agreement with the dry and cold conditions displayed by the inner Iberian sequences, supporting and highlighting the strong impact of higher seasonality and continentality in the regional vegetation dynamics and the water balance during the beginning of the Holocene.

Due to variations in the orbital parameters, the Northern Hemisphere experienced a maximum difference between winter and summer insolation during the onset of the Holocene, with minimum values for winters and highest for summers. This led to a high seasonal contrast or continentality. The cold winter temperatures would be one of the main causes for the absence of temperate trees while the hot summer temperatures could have favoured high rates of evaporation avoiding the development of water-demanded taxa (Kutzbach and Webb, 1993).

The impact of this water deficit in vegetation during the early Holocene has been documented in the whole Mediterranean region. Relatively dry conditions prevented the deciduous forest expansion in many parts of southern Europe, particularly over the eastern Mediterranean (Lawson et al., 2004) and some zones of the central Mediterranean (Magny et al., 2011; Calò et al., 2012). In the western Mediterranean, and more specifically in the eastern/southeastern part of the Iberian Peninsula, trees could develop although their sclerophyll nature also point to water as limiting factor (Dormoy et al., 2009; Carrión, 2002; Pons and Reille, 1988; Jalut et al., 2009; Carrión et al., 2010). Marine pollen record from Alboran Sea, which reflect wide pollen source area for southern Spain and northern Morocco, reveals restricted expansion of the temperate Mediterranean forest as consequence of limited moisture availability during the known as “Preboreal oscillation” (11.7-10.6 cal ka BP) (Combourieu-Nebout et al., 2009; Fletcher et al., 2010).

### 5.1.2. The Early Holocene: 9800-8200 cal yr BP

Most Mediterranean Iberia sequences show the development of varied forest formations (not only conifers) during the second part of the Early Holocene (Carrión et al., 2010 and references therein). As we have described in this Thesis, the Estanya sequence was characterized by a marked shift from a steppe landscape dominated by *Juniperus* and *Artemisia* toward a more forested scenery, characterised by the sharp development of *Corylus* and a slight increase in *Quercus* species (both evergreen and semi-deciduous types) (fig. 5.1). The spread of the forest along with the appearance of temperate trees indicate ameliorated winter temperatures.

In contrast, the BSM sequence was still characterized by the dominance of conifers over mesophytes and relatively high values of *Juniperus* (fig. 5.1), reflecting a continental Mediterranean-climate influence with a significant summer drought during this period. However, these Mediterranean-like conditions coincide with relatively higher lake levels in BSM as indicated by clastic and laminated sedimentary facies. These apparently opposite climate signals can be explained by the different altitude of both sites. In BSM, large snowpack accumulation during the winter would supply the needed water to maintain high lake levels during the summer drought. This hypothesis of significant seasonal water and sediment delivery to the lake is further supported by the high values of magnetic susceptibility of the sediments and the type of chironomid communities composed mainly of inlet-related taxa such as *Orthocladiinae*. Both sedimentological and biological evidence point to high-energy transport and intense run-off processes in the watershed likely related to permanent and ephemeral creek activity. Lake Estanya also indicates more humid conditions during this period by the abrupt drop of junipers, and maximum percentages of Mesophytes (15-20%) as well as the increase in both hygrophytes and hydrophytes. A rapid lake level increased was recognised by Morellón et al., (2009) at 9.4 cal ka BP.

Although the difference between winter and summer insolation was steadily decreasing during the Early Holocene, the seasonality was still high during the whole Early Holocene. This high seasonality has been largely recognised in others vegetation studies in the Pyrenees. The presence of *Viscum album* - a rather tolerant species to cold winter temperatures and to warm summers according to Iversen (1944) - in Tramacastilla and Bubal sequences was related to high seasonal thermal contrast (Montserrat-Martí, 1992). Furthermore, chrysophyte-based anomaly-temperature reconstruction carried out by Pla and Catalán (2005) in the Lake Redo also points out to great seasonality during this period. To sum up, ecological and sedimentological evidence from available Early Holocene Pyrenean sites underpin the high seasonal contrast with cold and humid winters, conducive to large amount of snow accumulation in the Pyrenean summits that would be providing water to fed lakes and rivers during the hot and dry summers and favouring the expansions of deciduous forests in the lowlands, particularly along the main Pyrenean rivers serving as meltwaters collectors.

#### 5.1.2.1. Abrupt climate changes

Superimposed on the long-term insolation-driven climate trend, sub-millennial climate variability has been recognised for the Early Holocene in both North Atlantic and Mediterranean areas, mainly in marine sequences (O'Brien et al., 1995; Alley et al., 1997; Mayewski et al., 2004; Bond et al., 2001; Frigola et al., 2007; Fletcher et al., 2012). The identification of these abrupt changes in continental records is not always evident due to, i.e., local factors, poor chronological control or low resolution.. In this Thesis, we have identified in the BSM sequence significant short-term shifts in pollen percentages and sedimentological features that point out to the impact of the mentioned high climate instability during this period. Such shifts occurred at 9.7, 9.3, 8.8 and 8.3 cal ka BP and are mainly characterized by short-term expansion of pine, accompanied by large reductions in all deciduous taxa but most particularly in *Betula* (fig. 5.1), implying a substantial reduction in humidity. The most intense event occurred at 8.3 ± 0.1 cal ka BP, when vegetation diversity and abundance dropped to a minimum. This event is likely to correspond with the 8.2 ka event (Alley and Agustsdottir, 2005; Rasmussen et al., 2007). The high-resolution study carried out in BSM sequence for this period indicates a minimum timing of 150 years and maximum of 200 years for the 8.2 ka event. This timing agrees with the precise characterization of the 8.2 ka event obtained from trapped air in a Greenland ice core (GISP2) (Kobashi et al., 2007).

Episodes of forest decline related to drier atmospheric conditions have also reported in the Western Mediterrnean (Fletcher et al. 2012). The shutdown or slowdown of the AMOC as a result of large inputs of freshwater into the North Atlantic may be behind the origin of most of these climate events (Wanner et al., 2008). Although the source of the water is thought to come mainly from disintegration of the Laurentide Ice Sheet as a result of increased temperatures, the 8.2 ka event seems to be a consequence of a particularly large input of freshwater that could come from the drainage of the Lake Agassiz, an especially large proglacial lake formed in North America as a result of the retreat of the Laurentide ice sheet (Hoffman et al., 2012).

A previous study carried out in El Portalet peatbog (González-Sampériz et al., 2006), have already identified a high climate variability during the Lateglacial in the subalpine belt of the Central Pyrenees. The occurrence of abrupt changes in the highlands of the Pyrenees during the Early Holocene (BSM sequence) further suggests a strong link between Pyrenean climate variability at centennial scale and the North Atlantic events. The identification of similar climate variability impacts on vegetation has not been possible in the EST sequence palynological study carried out in this Thesis. Thus, it is still under discussion if the absence of abrupt changes in the lowlands is the result of a relatively low-resolution work (at around 200 years/sample) or the different sensitivity between lowlands and high altitude areas.

### 5.1.3. The Mid-Holocene: 8200-6000 cal yr BP

The mid-Holocene in the Pyrenees witnessed a large change in vegetation dynamics and landscape configuration, greatly illustrated by the spread of deciduous trees (Montserrat-martí, 1992; González-Samperiz et al., 2006). Both Estanya and Basa de la Mora sequences recorded a marked landscape change at 8.2 cal ka BP. In Estanya this rapid shift was characterized by the replacement of mesophytes by temperate trees, such as semi-deciduous *Quercus*, *Pinus* and evergreen *Quercus*. In La Basa de la Mora *Pinus* was replaced by deciduous taxa, mainly *Betula*, deciduous *Quercus* and *Corylus* (fig. 5.1). The spread of Mediterranean-like forest in the lowlands and the deciduous forest in higher altitudes would have been favoured by an increase in winter temperatures. Neither semi-deciduous *Quercus* nor evergreen *Quercus* tolerate well the cold temperatures. In fact, the growth of *Q. ilex* in Padul sequence during the Late Glacial for example, has been attributed to periods of temperature improvement (Pons and Reille, 1988). Thus, we can consider the rapid *Quercus* expansion in Lake Estanya as good indicator of ameliorations of cold winter temperatures. Additionally, the rise of mesophytes to the subalpine belt surely point out to higher winter temperatures.

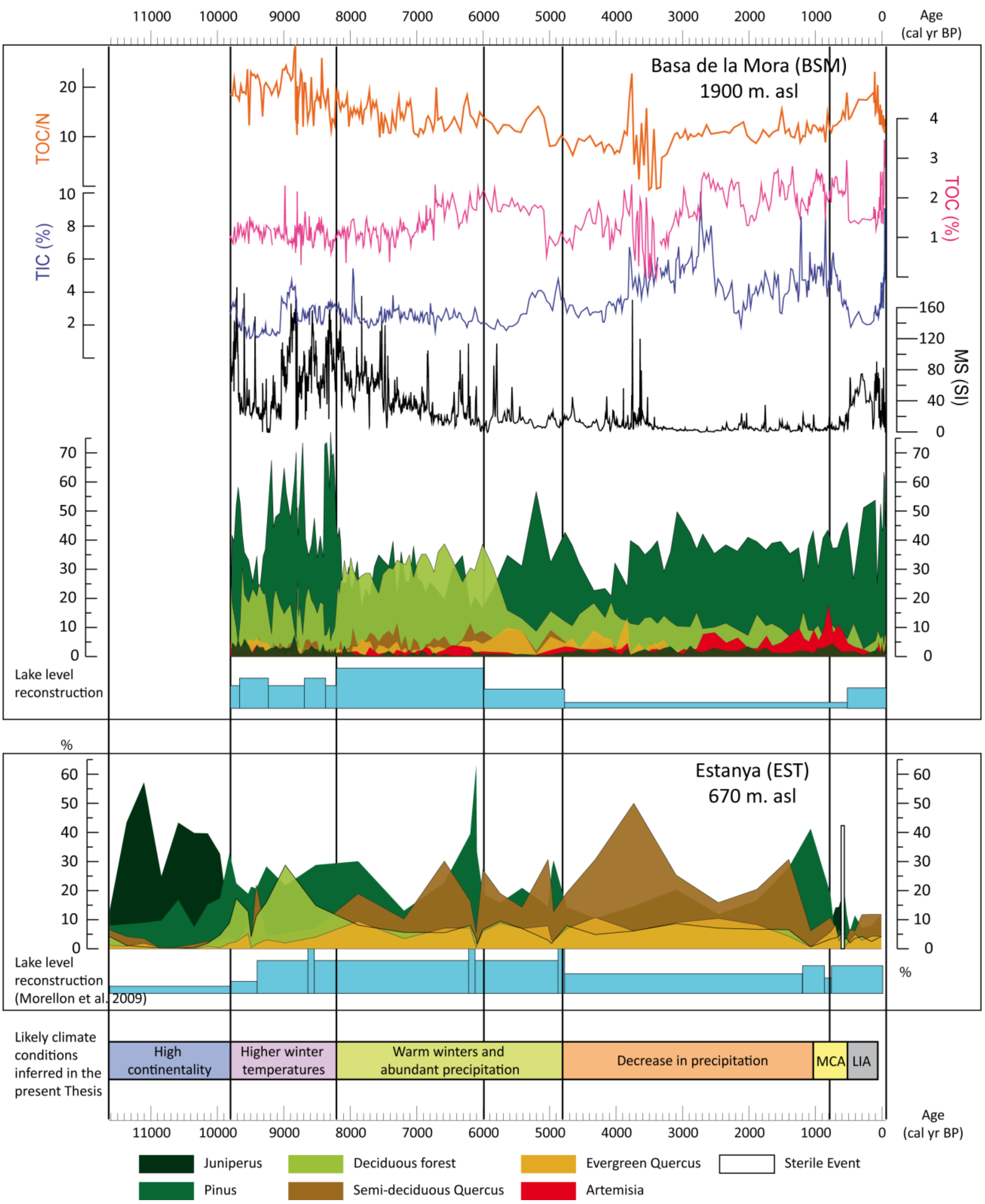


**Figure 5.1**.Comparison of main pollen taxa, and lake level reconstructions for lakes Estaña and Basa de la Mora.

The sharp expansion of the mesophytes, such as *Betula*, *Corylus* and deciduous *Quercus*, in BSM requires not only higher winter temperatures but also a significant increase in the water availability with a change in the precipitation regimen toward more precipitation during the summer leading to a reduction of the dry season. These humid conditions with increase in the year-round precipitation are further supported by the lake level reconstructions for both BSM and EST lakes. The sedimentary facies in BSM suggest that during this period lake levels were even higher than during the Early Holocene, but, conversely, lower values in magnetic susceptibility indicates lower sediment delivery from the watershed suggesting lower stream activity and run-off but more positive water balances in the lake. High lake levels in Estanya also point out to more positive hydrological balance in the lake during this period (Morellón et al., 2009)

More humid conditions in northern Spain during the mid-Holocene are a reflection of global climate changes. More humid conditions in the Central Pyrenees could have been favored by stronger Westerlies that could penetrate further inland and changes in SST. While the reconstruction of sea water temperatures is easier, the reconstruction of the atmospheric patterns results more problematic.  Warmer SST in the Bay of Biscay –Cantabrian Sea- during the Mid-Holocene is well documented by the presence of planktonic foraminifera species related to subtropical gyres -*Globorotalia truncatulinoides*- in marine sediments (Mojtahid et al., 2013). In addition, the presence in caves of the Cantabrian coast of bones of a temperate water monk seal (*Monachus monachus*), currently only in the Mediterranean Sea and southern latitudes of the North Atlantic, indicates that this animal was consumed by the local populations (Marín et al., 2011). Both lines of evidence support the existence of warm water advections in the Bay of Biscay. Warmer SST in the Bay of Biscay would have caused higher water content in the atmosphere as a result of higher rates of evaporation. Under these circumstances, the Westerlies could have brought humid condition farther east in the Pyrenees leading to a stronger Atlantic influence in the Central part of the Pyrenees. In addition, northern Spain would have been benefited from the thermoregulation effect of warmer waters leading to less seasonal contrast with warmer winters and less hot summers.

The atmospheric circulation pattern during the Mid-Holocene was significantly different to today's. The ITCZ was undoubtedly placed further north as the monsoon precipitation penetrated into the Sahara-Sahel desert resulting in the development of vegetation and perennial lakes over North Africa (deMenocal et al., 2000; Gasse, 2000). The northward displacement of the ITCZ along with warmer waters in the North Atlantic would have resulted in significant variations of the North Atlantic atmospheric circulation, which is one of the main responsible of the climate in Western Europe (Marshall et al., 2001). Given the difficulty to reconstruct the atmospheric patterns through palaeo-climate data, climate models attempt to simulate past large-scale features of circulation, temperature, and precipitation patterns through the prescription of some physical parameter well known, such as the solar insolation, the atmospheric composition of the SST (Taylor et al., 2012).

#### 5.1.3.1. Mid-Holocene precipitation simulations for the Mediterranean region

Though the humid conditions recognized in the Central Pyrenees might be primarily explained by the increase in SST in the North Atlantic and the Cantabrian Sea, global, larger-scale mechanisms have to be invoked to explain the development of humid conditions in the whole Mediterranean region during the Mid-Holocene (Roberts et al., 2011). Despite numerous studies for the last decades produced interesting data (Sadori et al., 2011; Pérez-Obiol et al., 2011; Ocakoglu et al., 2013), the final causes of this particular climate conditions in the Mediterranean Basin are not so easily reconstructed. Obviously, if the easternmost part of the Mediterranean Basin also recorded at this time much more humid conditions than today (Kohfeld and Harrison, 2000; Roberts et al., 2011), a large scale forcing mechanisms including atmospheric and oceanic circulations and teleconnections must have been in place (Roberts et al., 2011; Fletcher et al., 2012). Given that summer drought and annual water deficits are characteristic of the Mediterranean climate, the mid-Holocene effective moisture increase has drawn many climate simulations in order to understand the climate mechanisms driving such deep changes in the precipitation regimen during the last 6000 years.

The spread of deciduous trees that took place in the Pyrenees but also across the whole Mediterranean region during the Mid-Holocene (Prentice et al., 1996; Roberts et al., 2004; Carrión et al., 2010) requires a significant increase in precipitation during the growing season, that is, during the spring, and likely also a shorter dry season, that is, wetter summers. However, though the CMIP5 precipitation simulations carried out in the present thesis show a tendency for increased growing-season precipitation, the amount of precipitation simulated is far from enough to have produced the vegetation changes observed in the palaeo-data.

The Mediterranean climate is driven by a combination of several processes (Lionello et al., 2012), including North Atlantic dynamics and tropical variability such as the ITCZ shifts, which determines the area of influence of the Africa and Asian monsoon (Marshall et al., 2001). At a large scale, the ITCZ position is determined by the summer insolation. Due to higher solar insolation, the ITCZ was placed further north and the monsoon was strengthen during the Early and Mid-Holocene, resulting in particularly humid conditions in the Sahara and Sahel during this period (deMenocal et al., 2000; Hély et al., 2009). Could this northward movement be ultimately responsible for the precipitation increase over the Mediterranean? In agreement to changes in the insolation forcing, most CMIP5 models produce the expected northward shift and amplification of monsoon precipitation in the Mid-Holocene but this movement does not go deep enough into the north, indicating that the ITCZ shift was not a direct responsible for the increase in precipitation in the Mediterranean region during the Mid-Holocene, as it was in the Sahara-Sahel region. However, at a larger scale, changes in tropical dynamics could be ultimately responsible via oceanic and atmospheric teleconnections to large humidity changes in the Mediterranean (Lionello et al., 2012).

Why do models fail to reproduce past humidity changes in the Mediterranean? Though CMIP5 models are able to simulate the correct shift in the large-scale mechanisms, such as the ITCZ, they are unable to simulate the total amount of precipitation over the Mediterranean resulting from such changes. So, clearly there must be some other feedbacks and synergies playing a key role in the amount of precipitation. There has been considerable investigation of the possibility that land-surface feedbacks, including vegetation, soil moisture, freshwater lake and marshes, could be responsible for enhanced monsoon and increased precipitation in the Sahel and Mediterranean, but so far, modelling work has not confirmed that this is indeed the case (Kutzbach et al., 1996; Joussaume et al., 1999; Ghienne et al., 2002; Levis et al., 2004; Bracconot et al., 2007; Liu et al., 2007), highlighting that there is still relevant uncertainty regarding the mechanisms beyond the observed changes in the Mid-Holocene.

Changes in the North Atlantic atmospheric circulation patterns could be responsible –or at least play a significant role– for the increase in precipitation recorded across the Mediterranean during the Mid-Holocene since, currently the North Atlantic Oscillation –NAO- exerts a dominant influence on winter precipitation and temperatures over western Europe and to some extent to the Mediterranean (Trigo et al., 2002). Past climate changes in Europe and the Mediterranean, particularly during the Holocene have been related to long-term shifts in the dominant state of the NAO modes (Nesje et al., 2000; Magny et al., 2013a; Simonneau et al., 2013; Vannière et al., 2013; Fletcher et al., 2012). Presently the location of the NAO centers is largely controlled by the North Atlantic Ocean Circulation (AMOC) and its associated pole–equator temperature gradient, and also by the position of the ITCZ among others (Marshall et al., 2001). A stronger AMOC, which would be in agreement with the warmer waters recorded in the Bay of Biscay (Marín et al., 2011; Mojtahid et al., 2013), would have increased the magnitude of the pole–equator temperature gradient over the Atlantic sector, leading to the strengthening of the mid-latitude jet stream, that is, enhancing the penetration of the westerlies into Europe (Renssen et al., 2005).

To sum up, the main reason for the discrepancies between precipitation amounts projected by models and reconstructed by paleodata in the Mediterranean, and particularly the western region, seems to be the inability of models to reproduce the atmospheric patterns expected over the North Atlantic as a result of shifts in the AMOC and in the ITCZ.

#### 5.1.4. Transitional phase: 6000-4800 cal yr BP

Around 6 cal ka BP took place a marked global climate shift as a result of a worldwide reorganization of the ocean and atmosphere circulations. Regarding the atmosphere, the most noticeable change, at least in the Northern Hemisphere, was the southward migration of the ITCZ, which resulted in the end of the African Humid Period (deMenocal et al., 2000). Additionally the ocean circulation also experienced a shift in the Northern Hemisphere with the weakening of the AMOC starting at ca 6.5 cal ka BP (Hoogakker et al., 2011).

These large global changes are differently recorded in the two sections studied in this Thesis. The BSM sequence is characterized by a sharp change in the vegetation at around 6 ka, but the EST sequence does not show any significant shift. In BSM the forests changed from deciduous-dominated to pine-dominated forest in altitude (fig. 5.1), suggesting a change in the distribution of the precipitation with a more marked summer drought. This vegetation change is accompanied by significant palaeohidrological fluctuations in Basa de la Mora record. The lower MS values and the almost disappearance of the non-lacustrine and stream-related *Orthocladiinae* taxa suggest reduced sediment transport as a consequence of lower precipitation or meltwater inputs. The deposition of carbonated facies and a decline in *Myriophyllum*, indicate a reduction in the lake level and suggest that the longer dry season would have contributed to a year-round reduction in the precipitation.

Interestingly, the Lake Estanya does not show any relevant change, neither in the vegetation composition nor in the lake levels (Morellón et al., 2009). If colder winter temperatures have occurred during this period, it would have resulted in reduction of the temperate taxa and maybe a downward movement of the mesophytes belt that would have caused an increased presence of broad-leaf taxa in Estanya. If winter temperatures would have been warmer, they could have favored the expansion of the temperate trees. The absence of any vegetation trends suggests that no significant changes in temperature occurred at the end of the Mid Holocene. In addition, since lake levels maintained during this transitional phase in the lowlands, the reduction in precipitation in the highlands would have been also slight, since the lowlands, which gather incoming water from multiple Pyrenean sources, did not undergo relevant hydrological changes. Annual water budgets would have remained similar, and the main change in the precipitation regimen would have been in the seasonal distribution of the rainfall.

Around 6 cal ka BP took place a marked global climate shift as a result of a worldwide reorganization of the ocean and atmosphere circulations. Regarding the atmosphere, the most noticeable change, at least in the Northern Hemisphere, was the southward migration of the ITCZ, which resulted in the end of the African Humid Period (deMenocal et al., 2000). Additionally the ocean circulation also experienced a shift in the Northern Hemisphere with the weakening of the AMOC starting at ca 6.5 cal ka BP (Hoogakker et al., 2011).

The marked changes in global climate at the end of the mid Holocene are related to the evolution of the orbital parameters (insolation), that led to lowered temperature gradients between the tropical and the north-latitude waters and between the ocean and the land air surface temperatures (deMenocal et al., 2000; Hoogakker et al., 2011). Although the decrease in the insolation was gradual, the regional climate and environmental impact was abrupt in some records (deMenocal et al., 2000) while it was more gradual in others (Kröpelin et al., 2008). The mid-holocene transition shows the complexity of the climate system and the unpredictable consequences of crossing boundary conditions.

The main consequence of the new organization of the climate elements was a global cooling trend (Marcott et al., 2013). The surface water of the Bay of Biscay recorded the onset of the cooling trend around 6.6 cal ka BP (Mojtahid et al., 2013) indicating the weakening of the AMOC and the heat transport in the North Atlantic. The cooling of the surface water in the Bay of Biscay would have resulted in lowered water vapor content in the atmosphere leading to a reduction in the intensity of the humid Atlantic fronts into the Pyrenees and thus resulting in an extended influence of the Mediterranean climate in the Central Pyrenees. At a regional scale, the effects of cooling trend were unnoticed in the Central Pyrenees until 4.8 cal ka BP, as reflected by the stability of the temperate taxa, the most sensible to temperature changes in BSM sequence. Furthermore, a chrysophyte -based temperature anomaly reconstruction does not show any significant change in winter temperature compared to the mid Holocene (Pla and Catalan, 2005). Shifts in the Central Pyrenean vegetation belts may be mainly explained by changes in the precipitation regimen with the installation of a longer summer drought as a result of a reduced influence of the Atlantic fronts, while changes in temperature seems to be less important during this period.

### 5.1.5. The Late Holocene: 4800-800 cal yr BP

An aridity trend has been widely recognized in southern Europe during the late Holocene by the large decrease in mesophytes across the Mediterranean region (Carrión et al., 2003, 2007; Colombaroli et al., 2007; González-Sampériz et al., 2008; di Rita and Magri, 2009; Mercuri et al., 2011; Anderson et al., 2011; Pérez-Obiol et al., 2011; Jiménez-Moreno and Anderson, 2012) and lowered lake levels (Magny et al., 2002; Morellón et al., 2009; Corella et al., 2010).

The onset of the Late Holocene in the Estanya sequence shows the most marked change in the vegetation composition, with a sharp expansion of semi-deciduous oaks, a slight increase in evergreen oaks and the decrease of pines (fig. 5.1), suggesting a drop in water availability year around. This shift in vegetation cover occurred synchronously to a marked decrease in the water level at 4.8 cal ka BP documented by facies and geochemical indicators (Morellón et al., 2009) and with lowered percentages in aquatic taxa. The BSM sequence also favour drier conditions during this period, as *Juniperus* and *Artemisia* increased, deciduous taxa decreased and lake levels dropped with the occurrence of some periods of total desiccation (fig. 5.1). This low lake levels are inferred from the deposition of carbonate-rich massive facies, characterized by the presence of authigenic calcite crystals, gastropods, pennate diatoms and mottling textures, indicative of bioturbation and subaerial exposure.

The establishment of a well-developed Mediterranean forest in Estanya and the decreasing trend in mesophytes in BSM along with a marked drop in the lake levels in both lakes point out an evident decrease in the annual water availability as a result of less precipitation. Neverthelees, this period is also characterized by a cooling trend at a global scale (Marcott et al., 2013). However in the Mediterranean region and more concretely in Spain, this temperature trend is difficult to recognise since there is a large expansion of temperate trees such as semi-deciduous and evergreen *Quercus*, which do not support significant decrease in temperatures. However, the opening of the forest at higher altitudes (BSM) could be also a result of decreased winter temperatures. Nevertheless, in a temperate area such as the Mediterranean region, the expected changes in temperature could have had lower effects than moisture changes and the expansion of temperate tress could be a main consequence of decreased precipitation.

At a global scale, lower seasonal insolation differences, a weakening in the thermohaline circulation (Mojtahid et al., 2013) and changes in the Western Mediterranean Sea (Frigola et al., 2007) could have played a role in the decreased precipitation pattern recognized in the western Mediterranean region during the Late Holocene. Additionally, a pervasive negative NAO-like mode with strong westerlies has been also proposed as responsible for the decline in mesophytes across the Mediterranean (Fletcher et al., 2012).

Two main climate phases have occurred during the last two millennia: the Medieval Climate Anomaly (MCA) and the Little Ice Age (LIA) (Bradley et al., 2003). As summarized in the next sections, both sequences studied in this Thesis document large changes in vegetation dynamics in the high and low lands synchronous to both phases.

#### 5.1.5.1. The Medieval Climate Anomaly: 900-1300 Ad

The higher human impact and the relatively low sample resolution carried out in Lake Estanya, precluded the identification of clear evidence of the Medieval Climate Anomaly (MCA) impact on the vegetation in the lowlands. Nevertheless, a previous work in Lake Estanya found evidence of the impact of the MCA in the lake level, which lowered considerably, as well as in the vegetation composition, wchich experienced a decrease in deciduous taxa (Riera et al., 2004). However, in the BSM sequence, due to its higher altitude with less human impact, and its higher sample resolution, a clearer signal of the impact of this climate anomaly in both lake level and vegetation formations has been observed. The BSM shows particularly arid conditions coinciding with the MCA as indicated by the deposition of carbonate, organic-rich facies during low lake level phases and a wide expansion of the steppe taxa *Artemisia* and the increase in *Juniperus* (fig. 5.1).

Relatively arid conditions during the MCA have widely recognized in other part of the Iberian Peninsula by lowered lake levels (Martín-Puertas et al., 2010; Morellón et al., 2012; Corella et al., 2012), expansion of xerophitic vegetation (Moreno et al., 2012), less flood events in the Tagus River basin (Benito et al., 2003; Moreno et al., 2008) and less river discharge in the Portugal coast (Lebreiro et al., 2009; Alt-Epping et al., 2009). The final causes of the MCA remain under discussion, although a role in north Atlantic atmosphere dynamics with prevailing positive North Atlantic Oscillation indexes (NAO) (Björck et al., 2006; Trouet et al., 2009) and increase in solar irradiance (Mann et al., 2009) have been postulated.

#### 5.1.5.2. The Little Ice Age: 1300-1850 AD

The LIA was characterized by colder and fluctuating moister conditions in the Pyrenees (Morellón et al., 2011). During the LIA, more than 20 different mountain systems developed glacial activity in the Pyrenees (González-Trueba et al., 2008) and some glaciers reached their maximum extent during the late Holocene around the first half of the XIX century (Chueca-Cía et al., 2005), supporting the occurrence of particularly cold and humid conditions in the Pyrenean submits.

Both Estanya and Basa de la Mora sequences show an intensification of the anthropogenic activities in the area during the last 8 centuries. The increase in the land management was particularly severe in the case of Estanya, when it took place a massive deforestation phase in order to expand the agro-pastoral activities (fig. 5.1) (Riera et al., 2004; Morellón et al., 2011) Nevertheless, despite the high anthropogenic pressure, the impact of the Little Ice Age can be recognized in both sequences.

Higher water availability in the EST sequence is supported by an increase in mesophytes and in the aquatic component and a more positive water balance in the lake as deduced from facies deposition and salinity reconstructions (Morellón et al., 2011; Morellón et al., 2012). In agreement with more humid condition, the BSM sequence shows a rise of the lake levels, supported by increased sediment delivery to the lake and decreased carbonate productivity The abundance of allocthonous organic matter, shown by high TOC/TN ratios, supports the increase of sediment delivery from the catchment as a result of more intense snow melting during summers (fig. 5.1).

In addition, the BSM sequence shows evidences of an abandonment of the anthropogenic activities in the watershed with the recovery of the pine forest (fig. 5.1), while the EST sequence displays an increase in the human pressure. This suggests a migration of the populations from the cold highlands into the milder lowlands of the Pyrenees. For a more detailed explanation of the anthropogenic activities in EST and BSM sequences during the last centuries, see section 6.2.5 of this chapter.

## 5.2. CHRONOLOGY OF THE ANTHROPOGENIC IMPACT IN THE SOUTHERN PYRENEES

Human occupation in Northeastern Spain can be traced back to the middle Palaeolithic (i.e., Montes-Ramírez et al., 2006; Carbonell and Rodríguez, 2007; Barandiarán et al., 20012).

However, until the early appearance of agriculture and farming, the human presence was exclusively related to hunter-gathered activities resulting in seasonal exploitation of local resources (González-Sampériz et al., 2009; Allué et al., 2012; Ejarque et al., 2010). Therefore the real impact of these ancient nomadic communities over the landscape can be considered as negligible at regional scales. Here we focus on the last 4000 years, when first important and permanent signs of sedentary agricultural practises are recognised in lowland Pyrenees (Estanya lake sequence). The first clear evidence of anthropogenic impact in high altitudes (Basa de la Mora) is found much later.

The comparison of both records and its contextualization with other Pyrenean lacustrine sequences allow us to assess the evolution of the human impacts in vegetation formations across an altitudinal transect in the southern Pyrenees.

To identify the different land uses we have focused on the presence of:

- agriculture-related taxa **-** cereal, olive tree, vine or cannabis-
- grazing-related taxa - nitrophilous plants, i.e. *Rumex* and *Plantago*- and finally;
- relevant deforestation phases**.**

Although the recent literature focuses on some non-pollen palynomorphs (NPP'S) as excellent indicators of anthropogenic activities (Van Geel, 1978; Ejarque, 2011; López-Merino et al., 2010; Morales-Monilo, 2013), the content of coprophilous fungi was negligible in BSM record. Furthermore, the presence of these fungi was particularly low in the modern pollen rain collected in Basa de la Mora area (see chapter 2, section 2.4.3) despite the occurrence of moderate grazing activity in current times. In addition, the existence of wild ungulates in the mountainous areas of the Pyrenees since ancient times could have caused the presence of some coprophilous fungi not related to human activities. For these reasons the coprophilous fungi content has not be considered as an indicator of anthropogenic activities in this Thesis.

### 5.2.1. 2000-500 BC (4-2.5 cal ka BP): first intensification of human impact in lowlands

Estanya sequence records the first clear evidence of anthropogenic deforestation at 3.7 cal ka BP, prior to the beginning of a continuous *Cerealia* curve at ca. 3.1 cal ka BP. The clearance affected largely the semi-deciduous *Quercus* forest (fig. 5.2)**.** Nevertheless, nitrophilous plants are no recorded at this moment, probably indicating the dominance of agricultural activities in the area. Though the spread of agriculture in the Iberian Peninsula is documented at least from 7 cal ka BP during the Neolithic (Zapata et al., 2004; Stika et al., 2005; Carrión et al., 2010), in Estanya lacustrine sequence it is not clearly recognised until approximately 2 millennia later, during the Bronze Age.

Conversely, crop taxa or nitrophilous plants are absent in Basa de la Mora during this period, pointing out to negligible human activities in the subalpine belt of the Central Pyrenees. Similarly, other high-altitudinal sequences like Estanilles also shows negligible values of agricultural and pastoral-related taxa (Pérez-Obiol et al., 2012) supporting the absence of general, continuous and intense anthropogenic impact in highlands before 2 ka cal BP. Nevertheless, according to other authors, anthropogenic disturbances in some localities of the subalpine belt of the Pyrenees can be traced back to the Early and Mid-Holocene (Miras et al., 2007, 2010; Ejarque et al., 2010) and intensified in the Late Holocene after 3.6 cal ka BP (Miras et al., 2007; Pèlachs et al., 2007; Ejarque et al., 2010; Cunill et al., 2012). Nevertheless, those phases of interpreted increased human activities do not match with stages of significant and persistent forest decline as it happens in Estanya at 3.7 ka cal, indicating that the real impact of these activities on the landscape early in the Holocene was local, intermittent, uneven and slight.

### 5.2.2. 500 BC-750 AD (2.5-1.2 cal ka BP): expansion of agricultural activities in lowlands during the Iberian-Roman and Visigoth Times

The Lake Estanya sequence recorded the intensification of cereal cultivation, the first slight increase of *Olea* and the appearance of *Vitis* ca. 500 BC. Nevertheless, the presence of nitrophilous plants is still irrelevant, suggesting that stockbreeding and grazing were poorly developed in the area. The highest values of *Cerealia* type are found around 2 cal ka BP, coinciding with the Roman period (fig. 5.2). Similarly, a previous study in Lake Estanya carried out by Riera et al., (2004) also found the spread of olive trees and cereals during the Late Roman times supporting the diversification of the agricultural activities during that period. The progressive Romanisation in Iberia brought a complex system of land management that involved several changes in the landscape. During this period, clearance phases for agricultural production have been widely recognised in many sites (Carrión, 2002; Carrión et al., 2007, 2010; Muñoz-Sobrino et al., 2005; González-Sampériz et al., 2008; Martín-Puertas et al., 2008; Corella, 2011; Gil-Romera et al., 2010). The location of most of these places, mainly in middle and lower elevations across all Spain, illustrates the wide land management of the lower montane belts and foothills during this period.

In contrast, a lower-degree of anthropogenic impact is still recorded at highland locations. The Basa de la Mora sequence does not show cultivation, stockbreeding or deforestation signals during this period (fig. 5.2). The same results are found in the nearby sequence of Estanilles (Pérez-Obiol et al., 2012) supporting a low-degree impact of human activities. However, some studies from the eastern Pyrenees point to anthropogenic perturbations in the subalpine zone, suggesting more intense pastoral activities and forest retreat (Miras et al., 2007; Ejarque et al., 2010) followed by phases of forest renewal (Ejarque et al., 2010, Miras et al., 2010). However, none of those sequences show a clear sharp decrease in AP during this period, at least until 500 AD (1450 cal yr BP) suggesting a low local grazing pressure.

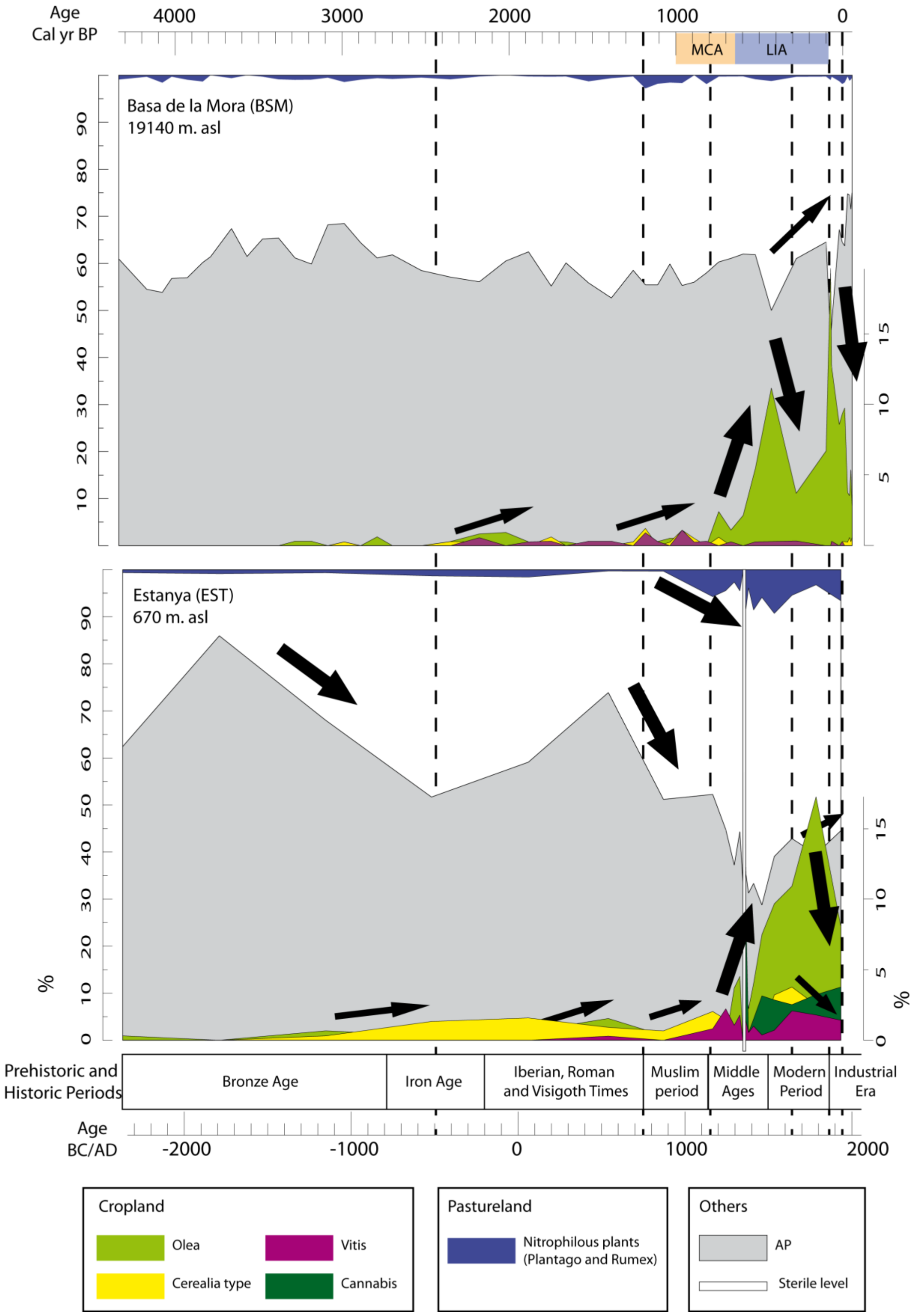


**Figure 5.2**. Comparison of main anthropogenic indicators between the Estaña and Basa de la Mora pollen records.

### 5.2.3. 750-1150 AD (1.2-0.8 cal ka BP): rise of grazing practises in lowlands and increasing impact in highlands during the Muslim period

During this period, the Estanya sequence records the beginning of a marked expansion of the nitrophilous plants and a rise in cultivated taxa, namely *Vitis*, *Olea* and *Cerealia* type, while the AP proportions underwent a marked drop (fig. 5.2). This forest clearance coincides with a maximum in charcoal concentration detected by Riera et al., (2004) in Lake Estanya between the 9 and 11th centuries indicating that the anthropogenic landscape management included increased frequency of burning.  This period corresponds with the Muslim period in the region, characterized by an increase in agricultural and pastoral activities and an intense trade including alimentary products and also textile elements such as fur and wool. In addition, construction, based on wood materials, was another major element of Muslim's economy (Carreras-Ares, 1996 ; Remie-Constable, 1996) resulting in major deforestation processes in the mid-mountain (Muñoz-Sobrino et al., 2005; López-Sáez et al., 2009; Rull et al., 2011).

The growing demand for construction materials and land dedicated to cultivation and livestock also resulted in anthropogenic disturbances at higher altitude in the Pyrenees, though the intensity of the forest decrease was lower than in the lowlands (Ejarque et al., 2010; Cunill et al., 2012; Pérez-Obiol et al., 2012). . The existence of deforestation phases, the expansion of grassland and the increase in nitrophilous and cultivated-related plants recorded across an altitudinal transect in the Pyrenees, and in general northern Spain, can be attributed to the land-use change prompted by the arrival of Muslims that led to an intensification and diversification of agricultural and pastoral activities in the lowlands and increased pressure in the highlands. Nevertheless, though the Basa de la Mora sequence records the aforesaid increase in cultivation and livestock taxa in the lowlands, there was no decrease in AP values during this period (fig. 5.2), suggesting that the deforestation impact in the subalpine belt was uneven across the Pyrenees.

### 5.2.4. 1150-1650 AD (0.8-0.3 cal ka BP): threshold in land management in low and highlands during the Middle Ages

During this period, the Estanya record witnessed the most intense and sharp change in the vegetation cover characterized by a marked clearance phase with AP values lower than 30% (fig. 5.2). Synchronously, the nitrophilous plants reach their maximum values as well as all cultivated taxa increase sharply, including *Cannabis*, which appears for the first time and spread rapidly. In a previous study carried out also in Lake Estanya, Riera et al., (2004) had already documented the spread of cultivated taxa, mainly olive tree and hemp, during this period in Lake Estanya. During the 12th century the region witnessed the wars between the Christian and Muslim Kingdoms and the origin of the Crown of Aragon, and large social changes as a result of the emergence of the Feudalism (Carreras-Ares, 1996). The population rose, the economy grew and it took place major technological advances in methods of production such as the rotation system for crops. All these facts resulted in deep changes with significant consequences in the vegetation landscape (Montserrat-Martí, 1992; Riera et al., 2004; Rull et al., 2011).

In agreement with these profound land-use changes, vegetation at higher altitudes, which were less disturbed until now, started to show evidences of management. Increase in human-related taxa is recognised in Basa de la Mora with the expansion of *Olea* and large, short-term reductions in *Pinus* (fig. 5.2)**.** *Olea* and *Fraxinus* also spread. *Fraxinus* has traditionally been used in the region for hedgerows (Gómez and Fillat, 1981). Its parallel expansion to *Olea* marks the regional establishment of modern and intense agro-pastoral activities. Other Pyrenean high altitude sequences also witness the intensification of the expansion of olive trees during this period (Pèlachs et al., 2007; Miras et al., 2010; Ejarque et al., 2010; Pérez-Obiol et al., 2011)**.** Modern Pyrenean pollen rain data demonstrate that maximum values of *Olea* are found in the subalpine belt, while the olive tree is commonly located under 800 m a.s.l. (Cañellas-Boltá et al., 2009). These data point out that the occurrence of this taxon in the high-altitude sequences of the Pyrenees marks the presence of the tree in the lower vegetation belts.

The expansion of farming and grazing-derived plants along with the reduction of the forests in low and highlands underlines the cross of a threshold in agro-pastoral activities during the middle ages, characterized by a massive use of the forest at all altitudes in the central Pyrenees. The particular increase in livestock-taxa agrees with the great development of the transhumance –Mesta-, an extensive sheep pastoral system that was the base of the economy in Spain during the Middle Ages (Pascua-Echegaray, 2012). It must be also remarked that the 16$^{th}$ century coincides with the maximum expansion of the Spanish Empire and its struggle to dominate overseas that led to further clearance of the forests, i.e., in order to use the wood to build the fleet. This deforestation phase is easily recognised in other Pyrenean sequences like Estanilles (2247 m asl, Pérez-Obiol et al., 2012), Montcortés (1027 m asl, Rull et al. 2011), Valencia d'Aneu (1150 m asl, Ejarque, 2011) or lake Burg (1821 m asl, Pèlachs et al. 2007) (to further geographical setting see figs. 1.3 and 3.1) with different impact but showing, as well as in EST and BSM, an important decrease of the AP proportions. As a result of the deforestation processes in the Pyrenees, soil erosion in the slopes rose sharply, and an important phase of the development of the Ebro River Delta occurred (García-Ruiz et al., 2005).

This marked human-induced vegetation landscape across the Pyrenees also coincide with an increased regional use of fire. The intensification of the fire frequency in order to open or to maintain the open landscapes has been widely recognised in the Pyrenees during the Medieval Ages (Esteban-Amat et al., 2003; Ejarque et al., 2009; Bal et al., 2011; Rius et al., 2012; Pérez-Obiol et al., 2012). . Nevertheless, the impact in the highlands had significant regional differences.  A comparatively more moderate forest clearance in BSM, which coincides with an expansion of *Olea* (regional) but low presence of grazing-related taxa (local), would indicate a lower human use of this valley compared to other in the Pyrenees.

### 5.2.5. 1650-1800 AD (0.3-0.15 cal ka BP): concentration of human activities in lowlands during the second half of the Little Ice Age

The Estanya sequence records the highest expansion of *Vitis* and *Cerealia* type and the intensification of *Cannabis* and *Olea* cultivation (fig. 5.2), pointing to intense agricultural management of the catchment area; the decrease in nitrophilous plants suggests lower pastoral pressure. Riera et al., (2004) documented a peak in hemp cultivation at this moment too. The 17$^{th}$ and first half of 18$^{th}$ centuries were characterized by an important economic decline in Spain as a consequence of overseas and internal succession wars, leading to social disruption and deep transformation of the agro-pastoral system with a reduced role of transhumance. During this period, most of the population was dedicated to agricultural production. Similar agriculture-dedicated land-use with a sharp increase in olive and hemp cultivation is recognised in the nearby sequence of Montcortés (Rull et al., 2011), highlighting a regional change in the production system.

Differently to EST and Montcortés sequences, the Basa de la Mora shows a decrease in *Olea* and *Fraxinus* cultivation and a temporal cease of deforestation (fig. 5.2). Other high altitude sequences also showed a decrease in cultivated taxa and **a** partial recovery of the forest (Pérez-Obiol et al., 2011) during the 17$^{th}$-19$^{th}$ centuries. This period corresponds to the second phase of the Little Ice Age (LIA), which was characterized by particularly cold conditions in the Pyrenees (see section 6.1.5.2. of the present chapter). Colder conditions during the LIA would have hindered human activities in some places at high altitudes, where climate conditions would have been especially adverse, favouring the movement and concentration of populations into the lowlands.

### 5.2.6. 1800-1950 AD (0.15-0 cal ka BP): spread of extensive agriculture practises after the Industrial Revolution

The Estanya sequence recorded outstanding values of *Olea,* reaching almost 20%, along with the expansion of *Cannabi*s and a new decline in AP values, at the onset of the 19$^{th}$ century (fig. 5.2). This period illustrates another intense phase of regional deforestation and olive and hemp cultivation. According to Riera et al., (2004) this period would have witnessed the maximum forest degradation. However, according to our data, though this period records the highest values in some cultivated taxa, the evolution of AP values suggests that the strongest impact in the forest cover would have taken place earlier the 14 and 16$^{th}$ centuries. During the 19$^{th}$ century it took place the most profound reform of the agrarian system in Spain. The agrarian reform limited the Mesta privileges, re-distributed the land and supported and encouraged the internal trade within Spain through economic societies. Additionally, as a result of the technical advantages brought by the Industrial Revolution, there was an outstanding improvement of the cultivation techniques that led to increased food production and a fast demographic expansion. The effects of the boost in the agricultural sector can be also recognised in different regional records like the nearby sequence of Montcortés (Rull et al., 2011).

At higher altitudes (BSM sequence) a significant expansion of *Olea* associated with a marked phase of deforestation of the pine forest occurred (fig. 5.2). Other high altitude sequences in the Pyrenees also record peak values in *Olea* during this period (Ejarque et al., 2009; Miras et al., 2010; Pérez-Obiol et al., 2011) marking the start of olive and crop production at large scale in north-eastern Spain, and growing regional exports of olive oil and crops to northern Europe (Harrison, 1990). The intensification of the agricultural activities in the highlands is further supported by strong phases of forest clearance (Pérez-Obiol et al., 2011). The rise of new and more sophisticated agricultural technologies along with better climate conditions after the end of the LIA favoured people to moved back to the highlands, in order to exploit the resources giving rise to the maximum occupation of the Pyrenees since the end of the 19$^{th}$ and till the mid-20$^{th}$ century (Lasanta, 1988; García-Ruiz and Valero-Garcés et al., 1998).

### 5.2.7. Current times

The studied Estanya sequence lacks the latter half of the XX century. Nevertheless, the BSM sequence presents a good resolution for this period.

The Basa de la Mora sequence shows the recovery of the pine forest as well as a reduction in trees related to anthropogenic activities (*Olea, Fraxinus*) (fig. 5.2). The latter half of the XX century was characterized by a new social and economic change in Spain that led to a major migration from the villages into the cities (Lasanta-Martínez et al., 2005). As a consequence of the abandon of the rural land, the forest definitely recovered at all altitudes of the Pyrenees as seen in different sequences (Ejarque et al., 2009; Cunill et al., 2012; Pérez-Obiol et al., 2012) and in documentary archives (Lasanta-Martínez et al., 2005). This abandonment of the rural lands and gradual recovery of forests is also supported by the increase in AP proportions and a steep drop in fire activity in Basa de la Mora (Lasheras-Álvarez et al., 2013).

In addition, a decrease in the lake level, recognized by the highest TIC percentages of the whole sequence, is recorded in BSM during the last 50 years (fig. 5.2). In addition, high bioproductivity is also recorded during the second half of the 20$^{th}$ century as it can be recognised by high TOC values along with an increase of macrophyte-related taxa. Stockbreeding around the lake has taken place in this area at least since the last century (Lucio, 1982) but the increase in bioproductivity only occurs during the last 30 years suggesting that the higher bio productivity may be related to warmer water rather than to human activities (Tarrats et al., 2014). This drop in lake levels along with the rise in water temperature may be linked to the global warming trend recognised over recent decades (IPCC, 2013), which, indeed, is having relevant effects in the Pyrenees such as decrease in snowpack depth, snow cover and direct precipitation (López-Moreno, 2005; López-Moreno and Stähli, 2008) and changes in the vegetation composition (Gottfried et al. 2012), pointing

## 5.3. TIMING AND DYNAMICS OF VEGETATION BELT CHANGES IN THE CENTRAL PYRENEES

A thorough multi-proxy study in Lake Basa de la Mora (BSM) (1914 m a.sl) and Estaña (EST) (670 m a.s.l) based on vegetation dynamics and lake level variations has reported changes in the amount and in the seasonality of the precipitation during the Holocene in an altitudinal transect in the Central Pyrenees. Given the key area where the Lake Basa de la Mora is placed, in the Central Pyrenees, halfway between the Mediterranean Sea and the Atlantic Ocean, the dynamics between the Mediterranean-like *Pinus* forest and the Atlantic-like deciduous forest has proven the succession of different precipitation patterns in the area. Additionally, the study of the sedimentary facies has displayed relative lake level changes and the analyses of the lake sediment properties have allowed distinguishing between two main water sources: direct rainfall and melting inputs. The integration of all these data have resulted in a precise reconstruction of the precipitation in the Central Pyrenees during the Holocene having recognized three main stages with different rainfall patterns. During the second part of Early Holocene (9.8-8.2 cal Ka BP) (the BSM lacks the onset of the Holocene) the annual water budget was very high but there was a dry season. During this period the snowpack melting played a relevant role providing water during the summer. During the Mid Holocene dominated an Atlantic-like precipitation patter with absence of a dry season and a very high annual water budget. Through the Late Holocene it established a drier climate, firstly with the installation of a dry season and later with an increasing trend to less annual precipitation.

Additionally, comparison of the vegetation dynamics between the BSM sequence, placed in the subalpine belt of the Pyrenees, and the Estanya sequence (EST), placed in the lowermost vegetation belt of the Pre-Pyrenean Range (670 m asl) has allowed to investigate the role of the seasonal temperature as main driver of the altitudinal vegetation belt shifts during the Holocene. Particularly cold winters and hot summers took place at the onset of the Holocene (11.7-9.8 cal ka BP) avoiding the development of the forest. An increase in winter temperatures led to the establishment of arboreal taxa in the area during the second part of the Early Holocene (9.8-8.2 cal ka BP). During the Mid Holocene (8.2-4.8 cal ka BP) the most mild winter temperatures of the Holocene favored the vegetation belts to rise to higher altitudes. Finally during the Late Holocene (4.8 cal yr BP-present), vegetation changes seems to more related to precipitation changes than to temperature shifts.

The integration of the precipitation and the temperature interpretations has resulted in an exhaustive regional climate reconstruction for the Pyrenees during the Holocene.

The onset of the Holocene (11.7-9.8 cal Ka BP) was characterized by the occurrence of cold winters as well as a likely shortage in water availability. These harsh climate conditions resulted in the dominance of steppe taxa and avoided the development of any short of tress in the lowlands. Though the BSM sequence lacks this period, other high altitude sequences in the Pyrenees have shown the existence of lowered treeline in agreement with cold winter conditions. These climate features are likely related to the characteristics of the solar insolation, which was minimum in winters and maximum in summers at this time. The maxima summer values of the solar insolation could result in high rates of evaporation what definitely hinder the spread of arboreal taxa in regions such as the lowlands of the Pyrenees where water is not a surplus.

The second part of the Early Holocene (9.8-8.2 cal Ka BP) was characterized by high continentality with a marked contrast between winters and summers as well as by the occurrence of a dry season but a high amount of water availability due to summer glacier and snowpack melting. This led to the development of a pine forest in the subalpine belt but the expansion of the deciduous taxa in the lowlands due to less harsh winters and high rates of water supply from the Pyrenean peaks. Higher altitude sequences in the Pyrenees show well-developed forests of pine in the case of the eastern records, and of deciduous taxa in the case of the western sequences. Overall it means a general increase of winter temperatures that allowed the upward expansion of the forest. Conversely the precipitation regimen contrasts significantly between the western and the eastern parts of the Pyrenees with Mediteranean-like precipitation pattern in the east and Atlantic-like precipitation pattern in the west. Given the similarity of the vegetation in the Central part (BSM sequence) and the eastern part of the Pyrenees, it seems that the Mediterranean pattern was prevailing at this time and also that the east-west humidity gradient was stonger than today since there are no presence of such dense deciduous forests currently in the subalpine belt of the western Pyrenees.

Besides, superimposed on these long-term climate conditions during the Early Holocene, the BSM sequence has proven the existence of at least four short-living and abrupt climate shifts centered at 9.7, 9.3, 8.8 and 8.3 cal ka BP.  These climate events are characterized by the occurrence of dry condition. They coincide with events recorded in the North Atlantic which origins are linked to perturbations of the Atlantic Overturning Meridional Circulation (AMOC) through meltwater pulses. Agreement between the climate events recorded in the North Atlantic and in the Pyrenees indicates that variations in the northern latitudes could trigger changes in the middle latitudes of Western Europe almost synchronously.

The Mid Holocene (8.2-6 cal Ka BP) was characterized by an increase in winter temperatures and the occurrence of an Atlantic-like precipitation pattern with high rates of rainfall and absence of a dry season, at least in the highlands, that resulted in the rise of the vegetation belts, with the establishment of a mixed Mediterranean forest in the lowlands and a deciduous forest at high altitudes reaching up to the treeline. As a result of these humid conditions both lakes reached their highest lake levels during this period. The humid conditions of the Mid Holocene have been recognized across the whole Mediterranean region through the spread of deciduous taxa and increase in lake levels. Reinforcement of the AMOC and warmer Atlantic waters in the middle latitudes could be responsible for increased evaporation and thus water-content in the air. Additionally, different atmospheric circulation pattern with stronger westerlies and a prevailing negative NAO-like mode in the North Atlantic resulted from the northward migration of the ITCZ and the shifts in the AMOC could be behind the arrival of abundant rainfall over the Mediterranean.

During the Late Holocene (6 cal Ka BP-present) it took place a progressive decrease in the water availability that led to the establishment of the modern-like precipitation pattern. This shift in the precipitation pattern took place in two main steps: firstly by the establishment of a dry season (6-4.8 cal ka BP) that resulted in the substitution of the deciduous forest by a pine forest in the subalpine belt and, secondly by an increasing trend toward drier conditions characterized by a drop in the annual water budget (4.8 cal Ka BP-present) that favored the expansion of evergreen *Quercus* at lowlands and that led to an increase in the heliophytes such as *Artemisia*.

## References


Alley, R., Agustsdottir, A., 2005. The 8k event: cause and consequences of a major Holocene abrupt climate change. Quat. Sci. Rev. 24, 1123–1149.

Alley, R.B., Mayewski, P.A., Sowers, T., Stuiver, M., Taylor, K.C., Clark, P.U., 1997. Holocene climatic instability: A prominent, widespread event 8200 yr ago. Geology 25, 483.

Allué, E., Martínez-Moreno, J., Alonso, N., Mora, R., 2012. Changes in the vegetation and human management of forest resources in mountain ecosystems at the beginning of MIS 1 (14.7–8 ka cal BP) in Balma Guilanyà (Southeastern Pre-Pyrenees, Spain). Comptes Rendus Palevol 11, 507–518.

Alt-Epping, U., Stuut, J.-B.W., Hebbeln, D., Schneider, R., 2009. Variations in sediment provenance during the past 3000 years off the Tagus River, Portugal. Mar. Geol. 261, 82–91.

Anderson, R.S., Jiménez-Moreno, G., Carrión, J.S., Pérez-Martínez, C., 2011. Postglacial history of alpine vegetation, fire, and climate from Laguna de Río Seco, Sierra Nevada, southern Spain. Quat. Sci. Rev. 30, 1615–1629.

Aranbarri, J., González-Sampériz, P., Valero-Garcés, B., Moreno, A., Gil-Romera, G., Sevilla-Callejo, M., García-Prieto, E., Di Rita, F., Mata, M.P., Morellón, M., Magri, D., Rodríguez-Lázaro, J., Carrión, J.S., 2014. Rapid climatic changes and resilient vegetation during the Lateglacial and Holocene in a continental region of south-western Europe. Glob. Planet. Change 114, 50–65.

Bal, M.-C., Pelachs, A., Perez-Obiol, R., Julia, R., Cunill, R., 2011. Fire history and human activities during the last 3300cal yr BP in Spain's Central Pyrenees: The case of the Estany de Burg. Palaeogeogr. Palaeoclimatol. Palaeoecol. 300, 179–190.

Barandiarán, I., Martí, B., del Rincón, M.A., Maya, J.L., 2012. Prehistoria de la Península Ibérica. Editorial Ariel, Barcelona.

Benito, G., Sopeña, A., Sánchez-Moya, Y., Machado, M.J., Pérez-González, A., 2003. Palaeoflood record of the Tagus River (Central Spain) during the Late Pleistocene and Holocene. Quat. Sci. Rev. 22, 1737–1756.

Björck, S., Rittenour, T., Rosén, P., França, Z., Möller, P., Snowball, I., Wastegård, S., Bennike, O., Kromer, B., 2006. A Holocene lacustrine record in the central North Atlantic: proxies for volcanic activity, short-term NAO mode variability, and long-term precipitation changes. Quat. Sci. Rev. 25, 9–32.

Bond, G., 1997. A Pervasive Millennial-Scale Cycle in North Atlantic Holocene and Glacial Climates. Science 278, 1257–1266.

Bond, G., Kromer, B., Beer, J., Muscheler, R., Evans, M.N., Showers, W., Hoffmann, S., Lotti-Bond, R., Hajdas, I., Bonani, G., 2001. Persistent Solar Influence on North Atlantic Climate During the Holocene. Science 294, 2130 –2136.

Braconnot, P., Otto-Bliesner, B., Harrison, S., Joussaume, S., Peterchmitt, J.-Y., Abe-Ouchi, A., Crucifix, M., Driesschaert, E., Fichefet, T., Hewitt, C.D., Kageyama, M., Kitoh, A., Loutre, M.-F., Marti, O., Merkel, U., Ramstein, G., Valdes, P., Weber, L., Yu, Y., Zhao, Y., 2007. Results of PMIP2 coupled simulations of the Mid-Holocene and Last Glacial Maximum – Part 2: feedbacks with emphasis on the location of the ITCZ and mid- and high latitudes heat budget. Clim. Past 3, 279–296.

Bradley, R.S., Hughes, M.K., Diaz, H.F., 2003. Climate in Medieval Time. Science 302, 404 –405.

Calò, C., Henne, P.D., Curry, B., Magny, M., Vescovi, E., La Mantia, T., Pasta, S., Vannière, B., Tinner, W., 2012. Spatio-temporal patterns of Holocene environmental change in southern Sicily. Palaeogeogr. Palaeoclimatol. Palaeoecol. 323-325, 110–122.

Cañellas-Boltà, N., Rull, V., Vigo, J., Mercadé, A., 2009. Modern pollen-vegetation relationships along an altitudinal transect in the central Pyrenees (southwestern Europe). The Holocene 19, 1185–1200.

Carbonell, E., Rodríguez, J.P., 2007. El Paleolítico Inferior en Cataluña. Veleia 24-25, 331–343.

Carreras Ares, J.J., 1996. Historia de Aragón II.: economía y sociedad: resumen de las lecciones impartidas en los cursos 1987-88 y 1988-89. Institución Fernando el Católico, Zaragoza.

Carrión, J.S., 2002. Patterns and processes of Late Quaternary environmental change in a montane region of southwestern Europe. Quat. Sci. Rev. 21, 2047–2066.

Carrión, J.S., Fernández, S., González-Sampériz, P., Gil-Romera, G., Badal, E., Carrión-Marco, Y., López-Merino, L., López-Sáez, J.A., Fierro, E., Burjachs, F., 2010. Expected trends and surprises in the Lateglacial and Holocene vegetation history of the Iberian Peninsula and Balearic Islands. Rev. Palaeobot. Palynol. 162, 458–475.

Carrión, J.S., Fuentes, N., González-Sampériz, P., Sánchez Quirante, L., Finlayson, J.C., Fernández, S., Andrade, A., 2007. Holocene environmental change in a montane region of southern Europe with a long history of human settlement. Quat. Sci. Rev. 26, 1455–1475.

Carrión, J.S., Sánchez-Gómez, P., Mota, J.F., Yll, R., Chaín, C., 2003. Holocene vegetation dynamics, fire and grazing in the Sierra de Gádor, southern Spain. The Holocene 13, 839–849.

Chueca-Cía, J., Julián-Andrés, A., Saz-Sánchez, M.A., Creus-Novau, J., López-Moreno, J.I., 2005. Responses to climatic changes since the Little Ice Age on Maladeta Glacier (Central Pyrenees). Geomorphology 68, 167–182.

Colombaroli, D., Marchetto, A., Tinner, W., 2007. Long-term interactions between Mediterranean climate, vegetation and fire regime at Lago di Massaciuccoli (Tuscany, Italy). J. Ecol. 95, 755–770.

Combourieu Nebout, N., Peyron, O., Dormoy, I., Desprat, S., Beaudouin, C., Kotthoff, U., Marret, F., 2009. Rapid climatic variability in the west Mediterranean during the last 25 000 years from high resolution pollen data. Clim. Past 5, 503–521.

Corella Aznar, J.P., 2011. Climate and human impact in Northern Spain since Mid-Holocene: the High Resolution records of lakes Arreo and Moncortès. Universidad de Zaragoza, Instituto Pirenaico de Ecología, Zaragoza.

Corella, J.P., Amrani, A.E., Sigró, J., Morellón, M., Rico, E., Valero-Garcés, B.L., 2011. Recent evolution of Lake Arreo, northern Spain: influences of land use change and climate. J. Paleolimnol. 46, 469–485.

Corella, J.P., Moreno, A., Morellón, M., Rull, V., Giralt, S., Rico, M.T., Pérez-Sanz, A., Valero-Garcés, B.L., 2010. Climate and human impact on a meromictic lake during the last 6,000 years (Montcortès Lake, Central Pyrenees, Spain). J. Paleolimnol. 46, 351–367.

Cunill, R., Soriano, J.-M., Bal, M.-C., Pèlachs, A., Pérez-Obiol, R., 2012. Holocene treeline changes on the south slope of the Pyrenees: a pedoanthracological analysis. Veg. Hist. Archaeobotany 21, 373–384.

Davis, B.A.S., Stevenson, A.C., 2007. The 8.2 ka event and Early–Mid Holocene forests, fires and flooding in the Central Ebro Desert, NE Spain. Quat. Sci. Rev. 26, 1695–1712.

deMenocal, P., Ortiz, J., Guilderson, T., Adkins, J., Sarnthein, M., Baker, L., Yarusinsky, M., 2000. Abrupt onset and termination of the African Humid Period: Quat. Sci. Rev. 19, 347–361.

Di Rita, F., Magri, D., 2009. Holocene drought, deforestation and evergreen vegetation development in the central Mediterranean: a 5500 year record from Lago Alimini Piccolo, Apulia, southeast Italy. The Holocene 19, 295–306.

Dormoy, I., Peyron, O., Nebout, N.C., Goring, S., Kotthoff, U., Magny, M., Pross, J., 2009. Terrestrial climate variability and seasonality changes in the Mediterranean region between 15 000 and 4000 years BP deduced from marine pollen records. Clim Past 5, 615–632.

Ejarque, A., Julià, R., Riera, S., Palet, J.M., Orengo, H.A., Miras, Y., Gascón, C., 2009. Tracing the history of highland human management in the eastern Pre-Pyrenees: an interdisciplinary palaeoenvironmental study at the Pradell fen, Spain. The Holocene 19, 1241 –1255.

Ejarque, A., Miras, Y., Riera, S., Palet, J.M., Orengo, H.A., 2010. Testing micro-regional variability in the Holocene shaping of high mountain cultural landscapes: a palaeoenvironmental case-study in the eastern Pyrenees. J. Archaeol. Sci. 37, 1468–1479.

Ejarque Montolio, A., 2011. Génesis y configuración microregional de un paisaje cultural pirenaico de alta montaña durante el holoceno: estudio polínico y de otros indicadores paleoambientales en el valle del Madriu-Perafita-Claror (Andorra) (info:eu-repo/semantics/doctoralThesis). Univesitat Roviar i Virgili, Tarragona.

El Kenawy, A., López-Moreno, J.I., Vicente-Serrano, S.M., 2012. Trend and variability of surface air temperature in northeastern Spain (1920–2006): Linkage to atmospheric circulation. Atmospheric Res. 106, 159–180.

Esteban-Amat, E., 2003. La humanización de las altas cuencas de la garona y las Nogueras (4500 AC-1955 DC). Ministerio de Medio Ambiente, Secretaría General de Medio Ambiente, Organismo Autónom de Parques Nacionales, Madrid.

Fletcher, W.J., Debret, M., Sanchez Goni, M.F., 2012. Mid-Holocene emergence of a low-frequency millennial oscillation in western Mediterranean climate: Implications for past dynamics of the North Atlantic atmospheric westerlies. The Holocene.

Fletcher, W.J., Sanchez Goñi, M.F., Peyron, O., Dormoy, I., 2010. Abrupt climate changes of the last deglaciation detected in a Western Mediterranean forest record. Clim Past 6, 245–264.

Frigola, J., Moreno, A., Cacho, I., Canals, M., Sierro, F.J., Flores, J.A., Grimalt, J.O., Hodell, D.A., Curtis, J.H., 2007. Holocene climate variability in the western Mediterranean region from a deepwater sediment record. Paleoceanography 22.

García-Ruiz, J.M., Lasanta, T., Valero-Garcés, B., Martí, C., Begueria, S., López-Moreno, J.I., Regües, D., Lana-Renault, N., 2005. Soil erosion and runoff generation related to land use changes in the Pyrenees, in: Global Change and Mountain Regions: An Overview of Current Knowledge, Advances in Global Change Research. Springer, Dordrecht.

García-Ruiz, J.M., Valero-Garcés, B.L., 1998. Historical Geomorphic Processes and Human Activities in the Central Spanish Pyrenees. Mt. Res. Dev. 18, 309–320.

Gasse, F., 2000. Hydrological changes in the African tropics since the Last Glacial Maximum. Quat. Sci. Rev. 19, 189–211.

Ghienne, J.-F., Schuster, M., Bernard, A., Duringer, P., Brunet, M., 2002. The Holocene giant Lake Chad revealed by digital elevation models. Quat. Int. 87, 81–85.

Gil-Romera, G., Carrión, J.S., Pausas, J.G., Sevilla-Callejo, M., Lamb, H.F., Fernández, S., Burjachs, F., 2010. Holocene fire activity and vegetation response in South-Eastern Iberia. Quat. Sci. Rev. 29, 1082–1092.

Gómez, D., Fillat, F., 1981. La cultura ganadera del fresno.

González-Sampériz, P., Utrilla, P., Mazo, C., Valero-Garcés, B., Sopena, M., Morellón, M., Sebastián, M., Moreno, A., Martínez-Bea, M., 2009. Patterns of human occupation during the early Holocene in the Central Ebro Basin (NE Spain) in response to the 8.2 ka climatic event. Quat. Res. 71, 121–132.

González-Sampériz, P., Valero-Garcés, B.L., Moreno, A., Morellón, M., Navas, A., Machín, J., Delgado-Huertas, A., 2008. Vegetation changes and hydrological fluctuations in the Central Ebro Basin (NE

Spain) since the Late Glacial period: Saline lake records. Palaeogeogr. Palaeoclimatol. Palaeoecol. 259, 157–181.

González-Trueba, J.J., Moreno, R.M., Martinez de Pison, E., Serrano, E., 2008. `Little Ice Age' glaciation and current glaciers in the Iberian Peninsula. The Holocene 18, 551–568.

Gottfried, M., Pauli, H., Futschik, A., Akhalkatsi, M., Barančok, P., Benito Alonso, J.L., Coldea, G., Dick, J., Erschbamer, B., Fernández Calzado, M.R., Kazakis, G., Krajči, J., Larsson, P., Mallaun, M., Michelsen, O., Moiseev, D., Moiseev, P., Molau, U., Merzouki, A., Nagy, L., Nakhutsrishvili, G., Pedersen, B., Pelino, G., Puscas, M., Rossi, G., Stanisci, A., Theurillat, J.-P., Tomaselli, M., Villar, L., Vittoz, P., Vogiatzakis, I., Grabherr, G., 2012. Continent-wide response of mountain vegetation to climate change. Nat. Clim. Change 2, 111–115.

Harrison, J., 1990. The Economic History of Spain Since 1800. Econ. Hist. Rev. 43, 79–89.

Hély, C., Braconnot, P., Watrin, J., Zheng, W., 2009. Climate and vegetation: Simulating the African humid period. Comptes Rendus Geosci. 341, 671–688.

Hoffman, J.S., Carlson, A.E., Winsor, K., Klinkhammer, G.P., LeGrande, A.N., Andrews, J.T., Strasser, J.C., 2012. Linking the 8.2 ka event and its freshwater forcing in the Labrador Sea: THE 8.2 ka EVENT IN THE LABRADOR SEA. Geophys. Res. Lett. 39, n/a–n/a.

Hoogakker, B.A.A., Chapman, M.R., McCave, I.N., Hillaire-Marcel, C., Ellison, C.R.W., Hall, I.R., Telford, R.J., 2011. Dynamics of North Atlantic Deep Water masses during the Holocene: HOLOCENE N ATLANTIC DEEP WATER DYNAMICS. Paleoceanography 26, n/a–n/a.

IPCC, 2007. Synthesis Report.Contribution of Woriking Groups I, II and II to the Fourth Assesment Report of the Intergovermental Panel on Climate Change, Pachauri, R.K and Reisinger, A. ed. Cambridge University Press, Geneva, Switzerland.

Iversen, J., 1944. Viscum, Hedera and Ilex as Climate Indicators: A Contribution to the Study of the Post-Glacial Temperature Climate. Geol. Foereningan Stockh. Foerhandlingar 66, 463–483.

Jalut, G., Dedoubat, J.J., Fontugne, M., Otto, T., 2009. Holocene circum-Mediterranean vegetation changes: Climate forcing and human impact. Quat. Int. 200, 4–18.

Jiménez-Moreno, G., Anderson, R.S., 2012. Holocene vegetation and climate change recorded in alpine bog sediments from the Borreguiles de la Virgen, Sierra Nevada, southern Spain. Quat. Res. 77, 44–53.

Joussaume, S., Taylor, K.E., Braconnot, P., Mitchell, J.F.B., Kutzbach, J.E., Harrison, S.P., Prentice, I.C., Broccoli, A.J., Abe-Ouchi, A., Bartlein, P.J., Bonfils, C., Dong, B., Guiot, J., Herterich, K., Hewitt, C.D., Jolly, D., Kim, J.W., Kislov, A., Kitoh, A., Loutre, M.F., Masson, V., McAvaney, B., McFarlane, N., de Noblet, N., Peltier, W.R., Peterschmitt, J.Y., Pollard, D., Rind, D., Royer, J.F., Schlesinger, M.E., Syktus, J., Thompson, S., Valdes, P., Vettoretti, G., Webb, R.S., Wyputta, U., 1999. Monsoon changes for 6000 years ago: Results of 18 simulations from the Paleoclimate Modeling Intercomparison Project (PMIP). Geophys. Res. Lett. 26, 859–862.

Kobashi, T., Severinghaus, J.P., Brook, E.J., Barnola, J.-M., Grachev, A.M., 2007. Precise timing and characterization of abrupt climate change 8200 years ago from air trapped in polar ice. Quat. Sci. Rev. 26, 1212–1222.

Kohfeld, K.E., Harrison, S.P., 2000. How well can we simulate past climates? Evaluating the models using global palaeoenvironmental datasets. Quat. Sci. Rev. 19, 321–346.

Kröpelin, S., Verschuren, D., Lézine, A.-M., Eggermont, H., Cocquyt, C., Francus, P., Cazet, J.-P., Fagot, M., Rumes, B., Russell, J.M., Darius, F., Conley, D.J., Schuster, M., von Suchodoletz, H., Engstrom, D.R., 2008. Climate-Driven Ecosystem Succession in the Sahara: The Past 6000 Years. Science 320, 765 –768.

Kutzbach, J., Bonan, G., Foley, J., Harrison, S.P., 1996. Vegetation and soil feedbacks on the response of the African monsoon to orbital forcing in the early to middle Holocene. Nature 384, 623–626.

Kutzbach, J.., Webb, T., 1993. Conceptual basis for understanding late-Quaternay climatess, in: Global Climates since the Last Glacial Maximum. University of Minnesota Press.

Lasanta, T., 1988. The process of desertion of cultivated areas in the Central Spanish Pyrenees. Pirineos 132, 15–36.

Lasanta-Martínez, T., Vicente-Serrano, S.M., Cuadrat-Prats, J.M., 2005. Mountain Mediterranean landscape evolution caused by the abandonment of traditional primary activities: a study of the Spanish Central Pyrenees. Appl. Geogr. 25, 47–65.

Lasheras-Álvarez, L., Pérez-Sanz, A., Gil-Romera, G., González-Sampériz, P., Sevilla-Callejo, M., Valero-Garcés, B.L., 2013. Historia del fuego y la vegetación en una secuencia holocena del Pirineo central: la Basa de la Mora. Cuad. Investig. Geográfica 39, 77–95.

Lawson, I., Frogley, M., Bryant, C., Preece, R., Tzedakis, P., 2004. The Lateglacial and Holocene environmental history of the Ioannina basin, north-west Greece. Quat. Sci. Rev. 23, 1599–1625.

Lebreiro, S.M., Voelker, A.H.L., Vizcaino, A., Abrantes, F.G., Alt-Epping, U., Jung, S., Thouveny, N., Gràcia, E., 2009. Sediment instability on the Portuguese continental margin under abrupt glacial climate changes (last 60kyr). Quat. Sci. Rev. 28, 3211–3223.

Leorri, E., Cearreta, A., Milne, G., 2012. Field observations and modelling of Holocene sea-level changes in the southern Bay of Biscay: implication for understanding current rates of relative sea-level change and vertical land motion along the Atlantic coast of SW Europe. Quat. Sci. Rev. 42, 59–73.

Levis, S., Bonan, G.B., Bonfils, C., 2004. Soil feedback drives the mid-Holocene North African monsoon northward in fully coupled CCSM2 simulations with a dynamic vegetation model. Clim. Dyn. 23, 791–802.

Lionello, P., 2012. The climate of the Mediterranean Region from the past to the future. Elsevier Science, Burlington.

Liu, Z., Wang, Y., Gallimore, R., Gasse, F., Johnson, T., deMenocal, P., Adkins, J., Notaro, M., Prentice, I.C., Kutzbach, J., Jacob, R., Behling, P., Wang, L., Ong, E., 2007. Simulating the transient evolution and abrupt change of Northern Africa atmosphere–ocean–terrestrial ecosystem in the Holocene. Quat. Sci. Rev. 26, 1818–1837.

López-Merino, L., Cortizas, A.M., López-Sáez, J.A., 2010. Early agriculture and palaeoenvironmental history in the North of the Iberian Peninsula: a multi-proxy analysis of the Monte Areo mire (Asturias, Spain). J. Archaeol. Sci. 37, 1978–1988.

López-Moreno, J.I., 2005. Recent variations of snowpack depth in the Central Spanish Pyrenees. Artic Antartic Alp. Res. 37, 253–260.

López-Moreno, J.I., Stähli, M., 2008. Statistical analysis of the snow cover variability in a subalpine watershed: Assessing the role of topography and forest interactions. J. Hydrol. 348, 379–394.

López-Sáez, J.A., López-Merino, L., Mateo, M.Á., Serrano, Ó., Pérez-Díaz, S., Serrano, L., 2009. Palaeoecological potential of the marine organic deposits of Posidonia oceanica: A case study in the NE Iberian Peninsula. Palaeogeogr. Palaeoclimatol. Palaeoecol. 271, 215–224.

Lucio, J.V., 1982. Estudio del Medio Físico del Sobrarbe. Aprovechamiento de los pastos estivales en el Valle de Gistain. Explotación actual y capacidad potencial.

Magny, M., Combourieu-Nebout, N., de Beaulieu, J.L., Bout-Roumazeilles, V., Colombaroli, D., Desprat, S., Francke, A., Joannin, S., Ortu, E., Peyron, O., Revel, M., Sadori, L., Siani, G., Sicre, M.A., Samartin, S., Simonneau, A., Tinner, W., Vannière, B., Wagner, B., Zanchetta, G., Anselmetti, F., Brugiapaglia, E., Chapron, E., Debret, M., Desmet, M., Didier, J., Essallami, L., Galop, D., Gilli, A., Haas, J.N., Kallel, N., Millet, L., Stock, A., Turon, J.L., Wirth, S., 2013. North-south palaeohydrological contrasts in the central Mediterranean during the Holocene: tentative synthesis and working hypotheses. Clim. Past 9, 2043–2071.

Magny, M., Miramont, C., Sivan, O., 2002. Assessment of the impact of climate and anthropogenic factors on Holocene Mediterranean vegetation in Europe on the basis of palaeohydrological records. Palaeogeogr. Palaeoclimatol. Palaeoecol. 186, 47–59.

Magny, M., Vannière, B., Calo, C., Millet, L., Leroux, A., Peyron, O., Zanchetta, G., La Mantia, T., Tinner, W., 2011. Holocene hydrological changes in south-western Mediterranean as recorded by lake-level fluctuations at Lago Preola, a coastal lake in southern Sicily, Italy. Quat. Sci. Rev. 30, 2459–2475.

Mann, M.E., Zhang, Z., Rutherford, S., Bradley, R.S., Hughes, M.K., Shindell, D., Ammann, C., Faluvegi, G., Ni, F., 2009. Global Signatures and Dynamical Origins of the Little Ice Age and Medieval Climate Anomaly. Science 326, 1256–1260.

Marcott, S.A., Shakun, J.D., Clark, P.U., Mix, A.C., 2013. A Reconstruction of Regional and Global Temperature for the Past 11,300 Years. Science 339, 1198–1201.

Marín, A.B., González-Morales, M.R., Estévez, J., 2011. Paleoclimatic inference of the mid-Holocene record of monk seal (Monachus monachus) in the Cantabrian Coast. Proc. Geol. Assoc. 122, 113–124.

Marshall, J., Kushnir, Y., Battisti, D., Chang, P., Czaja, A., Dickson, R., Hurrell, J., McCartney, M., Saravanan, R., Visbeck, M., 2001. North Atlantic climate variability: phenomena, impacts and mechanisms. Int. J. Climatol. 21, 1863–1898.

Martín-Puertas, C., Jiménez-Espejo, F., Martínez-Ruiz, F., Nieto-Moreno, V., Rodrigo, M., Mata, M.P., Valero-Garcés, B.L., 2010. Late Holocene climate variability in the southwestern Mediterranean region: an integrated marine and terrestrial geochemical approach. Clim. Past 6, 807–816.

Martín-Puertas, C., Valero-Garces, B.L., Pilar Mata, M., Gonzalez-Samperiz, P., Bao, R., Moreno, A., Stefanova, V., 2008. Arid and humid phases in southern Spain during the last 4000 years: the Zonar Lake record, Cordoba. The Holocene 18, 907–921.

Mayewski, P.A., 2004. Holocene climate variability. Quat. Res. 62, 243–255.

Mercuri, A.M., Sadori, L., Uzquiano Ollero, P., 2011. Mediterranean and north-African cultural adaptations to mid-Holocene environmental and climatic changes. The Holocene 21, 189 –206.

Miras, Y., Ejarque, A., Orengo, H., Mora, S.R., Palet, J.M., Poiraud, A., 2010. Prehistoric impact on landscape and vegetation at high altitudes: An integrated palaeoecological and archaeological approach in the eastern Pyrenees (Perafita valley, Andorra). Plant Biosyst. - Int. J. Deal. Asp. Plant Biol. 144, 924–939.

Miras, Y., Ejarque, A., Riera, S., Palet, J.M., Orengo, H., Eubab, I., 2007. Dynamique holocène de la végétation et occupation des Pyrénées andorranes depuis le Néolithique ancien, d'après l'analyse pollinique de la tourbière de Bosc dels Estanyons (2180 m, Vall del Madriu, Andorre). Comptes Rendus Palevol 6, 291–300.

Mojtahid, M., Jorissen, F.J., Garcia, J., Schiebel, R., Michel, E., Eynaud, F., Gillet, H., Cremer, M., Diz Ferreiro, P., Siccha, M., Howa, H., 2013. High resolution Holocene record in the southeastern Bay of Biscay: Global versus regional climate signals. Palaeogeogr. Palaeoclimatol. Palaeoecol. 377, 28–44.

Montes-Ramírez, L., Utrilla-Miranda, M.., Martínez-Bea, M., 2006. Trabajos recientes en yacimientos musterienses de Aragón: : una revisión de la transición Paleolítico Medio/Superior en el Valle del Ebro. Zona Arquelógica 7, 215–232.

Montserrat-Martí, J., 1992. Evolución glaciar y postglaciar del clima y la vegetación en la vertiente sur del Pirineo: estudio palinológico., Monografías del Instituto Pirenaico de Ecología-CSIC. Zaragoza.

Morales-Molino, C., 2013. Dinámica vegetal desde el Tadiglaciar en la cuenca del Duero: interacciones con el clima, fuego e impacto humano. Universidad Politécnica de Madrid, Madrid.

Morellón, M., Pérez-Sanz, A., Corella, J.P., Büntgen, U., Catalán, J., González-Sampériz, P., González-Trueba, J.J., López-Sáez, J.A., Moreno, A., Pla-Rabes, S., Saz-Sánchez, M. á., Scussolini, P., Serrano, E., Steinhilber, F., Stefanova, V., Vegas-Vilarrúbia, T., Valero-Garcés, B., 2012. A multi-proxy perspective on millennium-long climate variability in the Southern Pyrenees. Clim. Past 8, 683–700.

Morellón, M., Valero-Garcés, B., González-Sampériz, P., Vegas-Vilarrúbia, T., Rubio, E., Rieradevall, M., Delgado-Huertas, A., Mata, P., Romero, Ó., Engstrom, D.R., López-Vicente, M., Navas, A., Soto, J., 2011. Climate changes and human activities recorded in the sediments of Lake Estanya (NE Spain) during the Medieval Warm Period and Little Ice Age. J. Paleolimnol. 46, 423–452.

Morellón, M., Valero-Garcés, B., Vegas-Vilarrúbia, T., González-Sampériz, P., Romero, Ó., Delgado-Huertas, A., Mata, P., Moreno, A., Rico, M., Corella, J.P., 2009. Lateglacial and Holocene palaeohydrology in the western Mediterranean region: The Lake Estanya record (NE Spain). Quat. Sci. Rev. 28, 2582–2599.

Moreno, A., Valero-Garcés, B.L., González-Sampériz, P., Rico, M., 2008. Flood response to rainfall variability during the last 2000 years inferred from the Taravilla Lake record (Central Iberian Range, Spain). J. Paleolimnol. 40, 943–961.

Muñoz Sobrino, C., Ramil-rego, P., Gómez-orellana, L., Varela, R.A.D., 2005. Palynological data on major Holocene climatic events in NW Iberia. Boreas 34, 381–400.

Nesje, A., Lie, yvind, Dahl, S.O., 2000. Is the North Atlantic Oscillation reflected in Scandinavian glacier mass balance records? J. Quat. Sci. 15, 587–601.

O'Brien, S.R., Mayewski, P.A., Meeker, L.D., Meese, D.A., Twickler, M.S., Whitlow, S.I., 1995. Complexity of Holocene Climate as Reconstructed from a Greenland Ice Core. Science 270, 1962–1964.

Ocakoğlu, F., Kır, O., Yılmaz, İ.Ö., Açıkalın, S., Erayık, C., Tunoğlu, C., Leroy, S.A.G., 2013. Early to Mid-Holocene Lake level and temperature records from the terraces of Lake Sünnet in NW Turkey. Palaeogeogr. Palaeoclimatol. Palaeoecol. 369, 175–184.

Pascua Echegaray, E., 2012. Señores del paisaje: ganadería y recursos naturales en Aragón, siglos XIII-XVIII. Publicacions de la Universitat de València, Valencia.

Pèlachs, A., Soriano, J.M., Nadal, J., Esteban, A., 2007. Holocene environmental history and human impact in the Pyrenees. Contrib. Sci. 3, 421–429.

Pérez-Obiol, R., Bal, M.-C., Pèlachs, A., Cunill, R., Soriano, J.M., 2012. Vegetation dynamics and anthropogenically forced changes in the Estanilles peat bog (southern Pyrenees) during the last seven millennia. Veg. Hist. Archaeobotany 21, 385–396.

Pérez-Obiol, R., Jalut, G., Julia, R., Pelachs, A., Iriarte, M.J., Otto, T., Hernandez-Beloqui, B., 2011. Mid-Holocene vegetation and climatic history of the Iberian Peninsula. The Holocene 21, 75–93.

Pla, S., Catalan, J., 2005. Chrysophyte cysts from lake sediments reveal the submillennial winter/spring climate variability in the northwestern Mediterranean region throughout the Holocene. Clim. Dyn. 24, 263–278.

Pons, A., Reille, M., 1988. The holocene- and upper pleistocene pollen record from Padul (Granada, Spain): A new study. Palaeogeogr. Palaeoclimatol. Palaeoecol. 66, 243–263.

Prentice, C., Guiot, J., Huntley, B., Jolly, D., Cheddadi, R., 1996. Reconstructing biomes from palaeoecological data: a general method and its application to European pollen data at 0 and 6 ka. Clim. Dyn. 12, 185–194.

Rasmussen, S.O., Vinther, B.M., Clausen, H.B., Andersen, K.K., 2007. Early Holocene climate oscillations recorded in three Greenland ice cores. Quat. Sci. Rev. 26, 1907–1914.

Remie-Constable, O., 1996. Trade and traders in Muslim Spain: the commercial realignment of the Iberian peninsula, 900 - 1500. Cambridge Univ. Press, Cambridge.

Renssen, H., Goosse, H., Fichefet, T., Brovkin, V., Driesschaert, E., Wolk, F., 2005. Simulating the Holocene climate evolution at northern high latitudes using a coupled atmosphere-sea ice-ocean-vegetation model. Clim. Dyn. 24, 23–43.

Renssen, H., Seppä, H., Crosta, X., Goosse, H., Roche, D.M., 2012. Global characterization of the Holocene Thermal Maximum. Quat. Sci. Rev. 48, 7–19.

Renssen, H., Seppä, H., Heiri, O., Roche, D.M., Goosse, H., Fichefet, T., 2009. The spatial and temporal complexity of the Holocene thermal maximum. Nat. Geosci. 2, 411–414.

Riera, S., Wansard, G., Julià, R., 2004. 2000-year environmental history of a karstic lake in the Mediterranean Pre-Pyrenees: the Estanya lakes (Spain). CATENA 55, 293–324.

Rius, D., Vannière, B., Galop, D., 2012. Holocene history of fire, vegetation and land use from the central Pyrenees (France). Quat. Res. 77, 54–64.

Roberts, N., Eastwood, W.J., Kuzucuoglu, C., Fiorentino, G., Caracuta, V., 2011. Climatic, vegetation and cultural change in the eastern Mediterranean during the mid-Holocene environmental transition. The Holocene 21, 147–162.

Roberts, N., Stevenson, T., Davis, B., Cheddadi, R., Brewster, S., Rosen, A., 2004. Holocene climate, environment and cultural change in the circum-Mediterranean region, in: Battarbee, R.W., Gasse, F., Stickley, C.E. (Eds.), Past Climate Variability through Europe and Africa. Springer Netherlands, Dordrecht, pp. 343–362.

Rull, V., González-Sampériz, P., Corella, J.P., Morellón, M., Giralt, S., 2011. Vegetation changes in the southern Pyrenean flank during the last millennium in relation to climate and human activities: the Montcortès lacustrine record. J. Paleolimnol. 46, 387–404.

Sadori, L., Jahns, S., Peyron, O., 2011. Mid-Holocene vegetation history of the central Mediterranean. The Holocene 21, 117–129.

Sánchez Goñi, M.F., Hannon, G.E., 1999. High-altitude vegetational pattern on the Iberian Mountain Chain (north-central Spain) during the Holocene. The Holocene 9, 39–57.

Simonneau, A., Chapron, E., Vannière, B., Wirth, S.B., Gilli, A., Di Giovanni, C., Anselmetti, F.S., Desmet, M., Magny, M., 2013. Mass-movement and flood-induced deposits in Lake Ledro, southern Alps, Italy: implications for Holocene palaeohydrology and natural hazards. Clim. Past 9, 825–840.

Stevenson, A.C., 2000. The Holocene forest history of the Montes Universales, Teruel, Spain. The Holocene 10, 603–610.

Stika, H.-P., 2005. Early Neolithic agriculture in Ambrona, Provincia Soria, central Spain. Veg. Hist. Archaeobotany 14, 189–197.

Taylor, K.E., Stouffer, R.J., Meehl, G.A., 2012. An Overview of CMIP5 and the Experiment Design. Bull. Am. Meteorol. Soc. 93, 485–498.

Tarrats, P., Rieradevall, M., González-Sampériz, P., Pérez-Sanz, A., Valero-Garcés, B., Moreno, A., 2014. Relating actual with subfossil chironomid assemblages. Holocene habitat changes and paleoenvironmental reconstruction of Basa de la Mora Lake (Central Pyrenees). Presented at the Erupean Geoscience Union, Vienna.

Trigo, R., Osborn, T., Corte-Real, J., 2002. The North Atlantic Oscillation influence on Europe: climate impacts and associated physical mechanisms. Clim. Res. 20, 9–17.

Trouet, V., Esper, J., Graham, N.E., Baker, A., Scourse, J.D., Frank, D.C., 2009. Persistent Positive North Atlantic Oscillation Mode Dominated the Medieval Climate Anomaly. Science 324, 78–80.

Van Geel, B., 1978. A palaeoecological study of holocene peat bog sections in Germany and The Netherlands, based on the analysis of pollen, spores and macro- and microscopic remains of fungi, algae, cormophytes and animals. Rev. Palaeobot. Palynol. 25, 1–120.

Vannière, B., Magny, M., Joannin, S., Simonneau, A., Wirth, S.B., Hamann, Y., Chapron, E., Gilli, A., Desmet, M., Anselmetti, F.S., 2013. Orbital changes, variation in solar activity and increased anthropogenic activities: controls on the Holocene flood frequency in the Lake Ledro area, Northern Italy. Clim. Past 9, 1193–1209.

Wanner, H., Beer, J., Bütikofer, J., Crowley, T.J., Cubasch, U., Flückiger, J., Goosse, H., Grosjean, M., Joos, F., Kaplan, J.O., Küttel, M., Müller, S.A., Prentice, I.C., Solomina, O., Stocker, T.F., Tarasov, P., Wagner, M., Widmann, M., 2008. Mid- to Late Holocene climate change: an overview. Quat. Sci. Rev. 27, 1791–1828.

Zapata, L., Peña-Chocarro, L., Pérez-Jordá, G., Stika, H.-P., 2004. Early Neolithic Agriculture in the Iberian Peninsula. J. World Prehistory 18, 283–325.

# 6

# Conclusions

# CONCLUSIONS

## Climate dynamics in north-eastern Spain during the Holocene

The comparison between the multi-proxy study (including pollen, sedimentology, geochemistry, chironomids and charcoal) carried in lacustrine sequence of Lake Basa de la Mora and the vegetation reconstruction from the lacustrine sequence of Lake Estaña has allowed inferring seasonal changes in temperature and precipitation in north-eastern Spain during the Holocene.

i. The onset of the Holocene (11.7-9.8 cal Ka BP) was characterized by the occurrence of high seasonality, characterized by cold winters and hot summers, and low water availability. These climate conditions led to the expansion of steppe communities dominated by *Juniperus* and *Artemisia* in the lowlands (EST) and limited the expansion of the forest upwards.

ii. The second part of the Early Holocene (9.8-8.2 cal Ka BP) was characterized by still high continentality but increased water availability and likely milder winter temperatures that allowed the expansion of the arboreal taxa in the lowlands and favored the rise of the forest upwards.

   - However, the nature of the vegetation in Estaña and in Basa de la Mora points out different precipitation patterns during this period with steadily distributed rainfall, deduced from *Corylus*-dominated landscape, in the lowlands, and a Mediterranean-like pattern, with the occurrence of a dry season, deduced from a conifer-dominated landscape, in the highlands.
   - The multi-proxy study of Basa de la Mora indicates that great part of the water source during this period was related to the melting of glaciers and snowpack, contributing to the arrival of large amount of water into the lowlands during the summer.
   - Superimposed on these long-term climate conditions during the Early Holocene, the BSM sequence has proven the existence of at least four short-living and abrupt climate shifts centered at 9.7, 9.3, 8.8 and 8.3 cal ka BP and characterized by dry conditions.
   - These episodes coincide with climate events triggered in the North Atlantic and indicate the high sensibility of the Pyrenees to shifts in the northern latitudes.

iii. The Mid Holocene (8.2-6 cal Ka BP) was characterized by an increase in winter temperatures and in the precipitation with the occurrence of an Atlantic-like precipitation pattern with high rates of rainfall and absence of a dry season that led to the upward migration of the deciduous forest, which could establishes in the subalpine belt.

iv. At ca 6 cal Ka BP, it took place a change toward drier and similar-to-present conditions. This change took place in two main steps.

- Between 6 and 4.8 cal Ka BP, it established a Mediterranean-like pattern with the occurrence of a dry season that resulted in the substitution of the deciduous forest by a pine forest in the subalpine belt.
- From 4.8 cal Ka BP, it took place a progressive decline in the total amount of annual rainfall that led to a reduction in the presence of mesophytes and an expansion of semi-deciduous and evergreen *Quercus*.

v. During the last millennium, the imprints of the Medieval Climate Anomaly and the Little Ice Age can be recognized in both sequences by changes in the vegetation and in the lake levels.

**The impact of the anthropogenic activities in the Pyrenees**

vi. The first signs of agricultural activities took place in EST at 3.1 cal ka BP while the upper vegetation belt does not show important deforestation phases.

vii. From 3 to 1.2 cal ka BP (1050 BC- 750 AD) agriculture was the main activity and was mainly concentrated in the lowlands.

viii. Between 750 and 1150 AD (1.2 and 0.8 cal ka BP) took place the spread of the grazing activities along with the diversification of the agricultural practises in the lowlands and the anthropogenic pressure over the subalpine belt increased.

ix. The greatest impact of human activities over landscape took place between 1150 and 1650 AD (0.8 and 0.3 cal ka BP) and its effects could be noticed across the southern central Pyrenees regardless the altitude, but some zones were less modified than others.

x. Between 1650 and 1800 AD (0.3-0.15 cal ka BP), human activities were concentrated at low altitudes while high-lands were partially abandoned as a likely result of increasing colder conditions during the Little Ice Age.

xi. After 1800 AD (0.15 cal ka BP) the anthropogenic pressure increased in the higher vegetation belts as a result of the increasing population and the ameliorated climate conditions after the end of the LIA.

xii. The forest definitely recovered at all altitudes and the treeline ascended during the second half of the 20$^{th}$ century as a result of rural land abandonment and the recent increase in temperatures.

**PiControl and Mid-Holocene climate model simulations**

xiii. The CMIP5 models fail to reproduce key aspects of both the modern and MH climate of the northern Africa and Mediterranean region, including the correct geographical location of zonal precipitation regimes in the pre-industrial simulation and the magnitude of MH changes in these regimes.

xiv. In the Mediterranean region, the simulations show a tendency for increased growing-season precipitation. Such a shift is required to explain observed vegetation changes in this region in the MH. However the simulated shift is much too small to trigger those changes.

xv. The failure to simulate observed mid-Holocene changes in the Mediterranean raises concerns about the reliability of model projections of future climates in these regions.

## CONCLUSIONES

### Dinámica del clima en el noreste de España durante el Holoceno

La comparación entre el estudio multi-proxy (incluyendo polen, sedimentología, geoquímica, quironómidos y carbones) llevado a cabo en la secuencia lacustre de la Basa de la Mora y la reconstrucción de la vegetación realizada en el sondeo lacustre del lago de Estaña ha permitido inferir cambios en la estacionalidad de la precipitación y de la temperatura in el Noreste de España durante el Holoceno.

i. El comienzo del Holoceno (11.7-9.8 cal Ka BP) se caracterizó por la ocurrencia de una alta continentalidad, caracterizada por inviernos muy fríos y veranos muy cálidos, y una baja disponibilidad hídrica. Estas condiciones climáticas dieron lugar a la expansión de comunidades estépicas dominadas por *Juniperus* y *Artemisia* en Estaña y limitó la expansión del bosque en altitud.

ii. La segunda parte del Holoceno Temprano (9.8-8.2 cal Ka BP) se caracterizó por la existencia todavía de una alta continentalidad pero con un aumento de la disponibilidad hídrica y de las temperaturas de invierno que permitieron la expansión de los taxones arbóreos en Estaña y favorecieron es ascenso de los bosques en altitud.

   - Sin embargo, la naturaleza de la vegetación en Estaña y en la Basa de la Mora apuntan a la existencia de patrones de precipitación diferentes durante este periodo, con una distribución anual de la lluvia uniforme en Estaña, deducido de la dominancia de *Corylus*, y un patrón de precipitación de tipo mediterráneo con la ocurrencia de una estación seca en la Basa de la mora, deducido de la dominancia de *Pinus*.

   - El estudio multi-proxy de la Basa de la Mora indica que el origen de gran parte del agua de este periodo estaría relacionado con la fusión de los mantos de nieve y glaciares durante el verano, lo que contribuiría al aporte de gran cantidad de agua hacia las zonas más bajas de los Pirineo.

   - Superpuesta a estas condiciones climáticas durante el Holoceno Temprano, la secuencia de la Basa de la Mora ha mostrado la existencia de al menos cuatro eventos climáticos abruptos y de corta duración registrados en los años 9.7, 9.3, 8.8 y8.3 cal ka BP y caracterizados por condiciones climáticas áridas.

   - Estos episodios coinciden con eventos originados en el Atlántico Norte e indican la gran sensibilidad de los Pirineos a los cambios en latitudes septentrionales.

iii. El Holoceno Medio (8.2-6 cal Ka BP) se caracterizó por un aumento de las temperaturas y de la precipitación, con el establecimiento de un patrón de precipitación de tipo atlántico con tasas altas de lluvia y ausencia de una estación seca que dio lugar a la migración del bosque de caducifolios hacia cotas altitudinales mayores hasta su establecimiento en el piso subalpino de los Pirineos.

iv. Hacia el año 6 cal Ka BP tuvo lugar un cambio hacia condiciones más áridas, similares a las actuales. Este cambio tuvo lugar en los pasos principales.

- Entre 6 y 4.8 cal Ka BP se estableció un patrón de precipitación tipo mediterráneo con la ocurrencia de una estación seca que originó la substitución del bosque de caducifolios por un bosque de pino en el piso subalpino.
- A partir del año 4.8 cal Ka BP tuvo lugar una disminución progresiva de la precipitación anual total que resultó en l reducción de la presencia de árboles caducifolios y la expansión de *Quercus* marcescente y perennifolio.

v. Durante el último milenio, las huellas de la Anomalía Climática Medieval y de la Pequeña Edad de Hielo pueden reconocerse en ambas secuencias por cambios tanto en la vegetación como en los niveles de los lagos.

## El impacto de la actividad antrópogénica en los Pirineos

vi. Los primeras señales de actividad agrícola se reconocen en Estaña en el año 3.1 cal yr BP mientras que los pisos de vegetación más altos no muestras indicios de fases de deforestación.

vii. Entre los años 1050 AC y 750 DC (3-1.2 cal ka BP) la agricultura fue la principal actividad antrópica y se concentró principalmente en cotas bajas.

viii. Ente 750 y 1150 DC (1.2-0.8 cal ka BP) tuvo lugar la expansión de las actividades ganaderas junto con la diversificación de los cultivos en las cotas bajas y la presión antrópica en pisos de vegetación más altos aumentó.

ix. El mayor impacto humano sobre el paisaje tuvo lugar entre 1150 y 1650 AD (0.8-0.3 cal ka BP) cuando se produjo un procesos de deforestación masiva. Sus efectos pudieron notarse en todos los pisos de vegetación aunque algunas zonas fueron menos afectadas que otras.

x. Ente 1650 y 1800 AD (0.3-0.15 cal ka BP) la actividad antropogénica se concentró en cotas bajas mientras que el piso subalpino fue parcialmente abandonado como resultado probable de la ocurrencia de condiciones muy frías durante la Pequeña Edad de Hielo.

xi. Después de 1800 AD (0.15 cal yr BP) la presión antropogénica aumento en el piso subalpino como resultado de la creciente población en el área y las condiciones climáticas más suaves.

xii. El bosque se recuperó definitivamente en todos los pisos de vegetación durante la segunda parte del siglo XX como resultado del éxodo rural.

**Simulaciones de modelos climáticos para el periodo Pre-Industrial y el Holoceno-Medio**

xiii. Los modelos climáticos del CMIP5 fallan a la hora de reproducir aspectos claves del clima tanto del presente como del Holoceno Medio en la región del Mediterráneo y Norte de África. Estos fallos incluyen la correcta posición geográfica de las zonas de precipitación en las simulaciones del periodo Pre-Industrial y la magnitud de la precipitación en el Holoceno Medio.

xiv. En la región mediterránea, las simulaciones para el Holoceno-Medio muestran una tendencia al aumento de precipitación en primavera de acuerdo con el cambio de precipitación necesario para explicar la expansión de los caducifolios en el Mediterráneo durante el Holoceno Medio. Sin este aumento es extremadamente pequeño como para haber podido desencadenar tales cambios en la vegetación.

xv. El fallo a la hora de simular las condiciones de precipitación necesarias para explicar los cambios ambientales que tuvieron lugar en Mediterráneo durante el Holoceno Medio suscita preocupaciones sobre la fiabilidad de los modelos en las proyecciones climáticas futuras para la región.